Emilio Corchado, Héctor Quintián, Alicia Troncoso Lora, Hilde Pérez García, Esteban Jove, José Luis Calvo Rolle, Francisco Javier Martínez de Pisón, Pablo García Bringas, Francisco Martínez Álvarez, Álvaro Herrero Cosío, Paolo Fosci, Sérgio Filipe Ramos (Eds.)

## **International Joint Conferences**

18<sup>th</sup> International Conference on Computational Intelligence in Security for Information Systems (CISIS 2025)

16<sup>th</sup> International Conference on EUropean Transnational Education (ICEUTE 2025)

#### **Editors**

Emilio Corchado University of Salamanca, Spain escorchado@usal.es

Héctor Quintián University of A Coruña, Spain hector.quintian@udc.es

Alicia Troncoso Lora Pablo de Olavide University, Spain atrolor@upo.es

Hilde Pérez García University of León, Spain hilde.perez@unileon.es

Esteban Jove University of A Coruña, Spain esteban.jove@udc.es

José Luis Calvo Rolle University of A Coruña, Spain jose.rolle@udc.es

Francisco Javier Martínez de Pisón University of La Rioja, Spain fjmartin@unirioja.es

Pablo García Bringas University of Deusto, Spain pablo.garcia.bringas@deusto.es

Francisco Martínez Álvarez Pablo de Olavide University, Spain fmaralv@upo.es

Álvaro Herrero Cosío University of Burgos, Spain ahcosio@ubu.es

Paolo Fosci University of Bergamo, Italy paolo.fosci@unibg.it

Sérgio Filipe Ramos Polytechnic Institute of Porto, Portugal scr@isep.ipp.pt

#### **Preface**

This volume of Communications in Computer and Information Science contains accepted papers presented at the 18<sup>th</sup> International Conference on Computational Intelligence in Security for Information Systems (CISIS 2025) and the 16<sup>th</sup> International Conference on EUropean Transnational Education (ICEUTE 2025), which were held in the beautiful city of Salamanca, Spain, in October 2025.

The CISIS 2025 conference aims to provide a meeting opportunity for academic and industry-related researchers from various communities in Computational Intelligence, Information Security, and Data Mining. The need for intelligent, flexible behaviour by large, complex systems, especially in mission-critical domains, is intended to be the catalyst and the aggregation stimulus for the overall event.

After a peer-review process, the CISIS 2025 International Program Committee selected 17 papers published in these conference proceedings, representing an acceptance rate of 49%. In this edition, one special session was organised: Artificial Intelligence for Protecting the Internet of Things.

The ICEUTE 2025 conference aims to offer a meeting point for people working on transnational education within Europe. It provides a stimulating and fruitful forum for presenting and discussing the latest works and advances in transnational education within European countries. In the case of ICEUTE 2025, the International Program Committee selected 6 papers, which are also published in these conference proceedings.

The selection of papers was extremely rigorous to maintain the high quality of the conference. We want to thank the members of the Program Committees for their hard work during the reviewing process. This is a crucial process for creating a high-standard conference; the CISIS and ICEUTE conferences would not exist without their help.

CISIS 2025 and ICEUTE 2025 enjoyed outstanding keynote speeches by distinguished guest speakers: Prof. Ajith Abraham at Bennett University (India) and Prof. Sung-Bae Cho at Yonsei University (South Korea).

CISIS 2025 has teamed up with "Logic Journal of the IGPL" (Oxford University Press) for a suite of special issues, including selected papers from CISIS 2025.

Particular thanks go as well to the conference's main sponsors, Startup Olé, the CIBER-OLÉ project (within the National Cybersecurity Industry Promotion Program, framed within the INCIBE Emprende program and financed by INCIBE and the University of Salamanca-USAL), BISITE research group at the University of Salamanca, CTC research group at the University of A Coruña, and the University of Salamanca. They jointly contributed actively and constructively to the success of this initiative.

This activity is carried out in execution of the Strategic Project "Critical infrastructures cybersecure through intelligent modeling of attacks, vulnerabilities and increased security of their IoT devices for the water supply sector" (C061 /23), the result of a collaboration agreement signed between the National Institute of Cybersecurity (INCIBE) and the University of A Coruña. This initiative is carried out within the framework of the funds of the Recovery, Transformation and Resilience Plan, financed by the European Union (Next Generation), the project of the Government of Spain that outlines the roadmap for the modernization of the Spanish economy, the recovery of economic growth and job creation, for the solid, inclusive and resilient economic reconstruction after the COVID19 crisis, and to respond to the challenges of the next decade. This activity has also been PID2022-137152NB-I00 promoted funded MICIU/AEI/10.13039/501100011033 and by ERDF/EU.

We would like to thank all the special session organizers, contributing authors, the Program Committees, and the Local Organizing Committee members for their hard and highly valuable work, which has contributed to the success of the CISIS and ICEUTE 2025 events.

#### The editors

Emilio Corchado
Héctor Quintián
Alicia Troncoso Lora
Hilde Pérez García
Esteban Jove
José Luis Calvo Rolle
Francisco Javier Martínez de Pisón
Pablo García Bringas
Francisco Martínez Álvarez
Álvaro Herrero Cosío
Paolo Fosci
Sérgio Filipe Ramos

October, 2025

## **CISIS 2025**

## **Organization**

#### **General Chair**

Emilio Corchado University of Salamanca, Spain

#### **Program Committee Chair**

Emilio Corchado University of Salamanca, Spain Héctor Quintián University of A Coruña, Spain Alicia Troncoso Lora Pablo de Olavide University, Spain

Hilde Pérez García University of León, Spain Esteban Jove University of A Coruña, Spain José Luis Calvo Rolle University of A Coruña, Spain Francisco Javier Martínez de Pisón University of La Rioja, Spain Pablo García Bringas University of Deusto, Spain Francisco Martínez Álvarez Pablo de Olavide University, Spain Álvaro Herrero Cosío University of Burgos, Spain Paolo Fosci University of Bergamo, Italy

Sérgio Filipe Ramos Polytechnic Institute of Porto, Portugal

#### **Program Committee**

Adam Wójtowicz Poznań University of Economics and Business,

Poland

Agustín García Fisher University of A Coruña, Spain

Agustín Martín Muñoz Spanish National Research Council (CSIC),

Spain

Alberto Peinado University of Malaga, Spain Alejandro Vidal Bralo University of A Coruña, Spain Álvaro Michelena University of A Coruña, Spain

Andrés Pérez Zabala Basque Research and Technology Alliance

(BRTA), Spain

Andrysiak Tomasz University of Technology and Life Sciences

(UTP), Poland

Ángel Arroyo University of Burgos, Spain Antonio Díaz-Longueira University of A Coruña, Spain

Carlos Pereira ISEC, Portugal

Ciprian Pungila West University of Timișoara, Romania

Cristina Alcaraz University of Malaga, Spain Daniel Urda University of Burgos, Spain

Darius Galis West University of Timisoara, Romania

Eduardo Solteiro Pires UTAD University, Portugal Enrique Onieva University of Deusto, Spain

Esteban Jove UDC, Spain Fernando Ribeiro EST, Portugal

Fernando Tricas University of Zaragoza, Spain Francisco Martínez-Álvarez Pablo de Olavide University, Spain Francisco Zayas-Gato University of A Coruña, Spain Hugo Sanjurjo-González University of Deusto, Spain Hugo Scolnik ARSAT SA, Argentina Ioannis Sorokos Fraunhofer IESE, Germany Isaias Garcia University of León, Spain Jesús Díaz-Verdejo University of Granada, Spain

José Aveleira Mata

Universidade NOVA de Lisboa, Portugal

José Aveleira Mata

Research Institute of Applied Sciences in Cy-

bersecurity (RIASC), Spain

José F. Torres Pablo de Olavide University, Spain Jose A. Onieva University of Malaga, Spain

Jose Carlos Metrolho IPCB, Portugal

Jose Luis Calvo-Rolle University of A Coruña, Spain

Jose M. Molina University Carlos III of Madrid, Spain Jose Manuel Lopez-Guede Basque Country University, Spain José-Luis Casteleiro-Roca University of A Coruña, Spain

Josep Ferrer Universitat de les Illes Balears, Spain

Juan J. Gude University of Deusto, Spain
Juan Jesús Barbarán University of Granada, Spain
Manuel Graña Basque Country University, Spain
Manuel Rubiños Trelles University of A Coruña, Spain
Marta María Álvarez Crespo University of A Coruña, Spain

Michal Choras Bydgoszcz University of Science and Techno-

logy, Poland

Michal Wozniak Wroclaw University of Technology, Poland

Míriam Timiraos Díaz University of A Coruña, Spain Pablo García Bringas University of Deusto, Spain Paula Patricia Arcano Bea University of A Coruña, Spain

Petrica Pop Technical University of Cluj-Napoca, Romania

Rafael Alvarez University of Alicante, Spain
Rafael Corchuelo University of Seville, Spain
Raúl Durán University of Alcalá, Spain
Roberto Casado-Vara University of Burgos, Spain
Rudolf Erdei Holisun SRL, Romania

Salvador Alcaraz Miguel Hernandez University, Spain Sorin Stratulat Université de Lorraine, Metz, France

### **CISIS 2025: Special Sessions**

#### **Artificial Intelligence for Protecting the Internet of Things**

#### **Program Committee**

Álvaro Herrero (Organizer)

Daniel Urda (Organizer)

Diego Granados (Organizer)

University of Burgos, Spain

University of Burgos, Spain

University of Burgos, Spain

Adam Wójtowicz Poznań University of Economics and Business, Po-

land

Darius Galis West University of Timisoara, Romania
Dominik Olszewski Warsaw University of Technology, Poland

Michal Choras Bydgoszcz University of Science and Technology,

Poland

Michal Choras Bydgoszcz University of Science and Technology,

Poland

Nuno Alberto Ferreira Lopes Polytechnic Institute of Cavado and Ave, Portugal

Oliviu Matei North University of Baia Mare, Romania
Petrica Pop Technical University of Cluj-Napoca, Romania

#### **CISIS 2025 Organising Committee Chairs**

Emilio Corchado University of Salamanca, Spain Héctor Quintián University of A Coruña, Spain

#### **CISIS 2025 Organising Committee**

José Luis Calvo Rolle University of A Coruña, Spain University of A Coruña, Spain Esteban Jove José Luis Casteleiro Roca University of A Coruña, Spain University of A Coruña, Spain Francisco Zayas Gato University of A Coruña, Spain Álvaro Michelena Míriam Timiraos Díaz University of A Coruña, Spain Antonio Javier Díaz Longueira University of A Coruña, Spain Paula Patricia Arcano Bea University of A Coruña, Spain Manuel Rubiños Trelles University of A Coruña, Spain Marta María Álvarez Crespo University of A Coruña, Spain Alejandro Vidal Bralo University of A Coruña, Spain Agustín García Fisher University of A Coruña, Spain Iker Pastor López University of Deusto, Spain

### **ICEUTE 2025**

## **Organization**

#### **General Chair**

Emilio Corchado University of Salamanca, Spain

#### Program Committee Chair

Héctor QuintiánUniversity of A Coruña, SpainEmilio CorchadoUniversity of Salamanca, SpainAlicia Troncoso LoraPablo de Olavide University, Spain

Hilde Pérez García University of León, Spain Esteban Jove University of A Coruña, Spain José Luis Calvo Rolle University of A Coruña, Spain Francisco Javier Martínez de Pisón University of La Rioja, Spain Pablo García Bringas University of Deusto, Spain Francisco Martínez Álvarez Pablo de Olavide University, Spain Álvaro Herrero Cosío University of Burgos, Spain Paolo Fosci University of Bergamo, Italy

#### Program Committee

Álvaro Michelena University of A Coruña, Spain Alejandro Vidal Bralo University of A Coruña, Spain

Ana Rosa Pereira Borges Coimbra Polytechnic Institute, ISEC, Portu-

oal

Ángel ArroyoUniversity of Burgos, SpainAntonio Díaz-LongueiraUniversity of A Coruña, SpainAntonio Morales-EstebanUniversity of Seville, SpainAgustín García FisherUniversity of A Coruña, Spain

Carlos Pereira ISEC, Portugal

Dragan Simic University of Novi Sad, Faculty of Techni-

cal Sciences, Serbia

Eduardo Solteiro Pires

Eloy Irigoyen

Basque Country University, Spain

Esteban Jove

University of A Coruña, Spain

Francisco Martínez-Álvarez

Universidad Pablo de Olavide, Spain

University of A Coruña, Spain

University of A Coruña, Spain

University of Deusto, Spain

University of León, Spain

Jorge Barbosa ISEC - Instituto Superior de Engenharia de

Coimbra, Portugal

José Aveleira Mata Research Institute of Applied Sciences in

Cybersecurity (RIASC), Spain

José F. Torres
Pablo de Olavide University, Spain
José F. Torres
Pablo de Olavide University, Spain
Jose Luis Calvo-Rolle
University of A Coruña, Spain
José Manuel Lopez-Guede
Basque Country University, Spain
University of Burgos, Spain
University of Seville, Spain
University of A Coruña, Spain
University of A Coruña, Spain

Juan Pavón Complutense University of Madrid, Spain

Juan J. Gude

Julián Estévez

Manuel Rubiños Trelles

Maria Jose Marcelino

Maria Victoria Requena

Marta María Álvarez Crespo

University of Deusto, Spain

Basque Country University, Spain

University of A Coruña, Spain

University of Seville, Spain

University of A Coruña, Spain

Miguel Carriegos RIASC, Spain

Míriam Timiraos University of A Coruña, Spain Pablo García Bringas University of Deusto, Spain Paola Clara Leotta University of Catania, Italy

Paulo Moura Oliveira University of Trás-os-Montes and Alto

Douro (UTAD), Portugal

Paula Patricia Arcano Bea University of A Coruña, Spain
Pedro Mauricio Acosta Castellanos Universidad Santo Tomás, Colombia
Sorin Stratulat Université de Lorraine, Metz, France

### **ICEUTE 2025 Organising Committee Chairs**

Emilio Corchado University of Salamanca, Spain Héctor Quintián University of A Coruña, Spain

## **ICEUTE 2025 Organising Committee**

University of A Coruña, Spain José Luis Calvo Rolle University of A Coruña, Spain Esteban Jove University of A Coruña, Spain José Luis Casteleiro Roca University of A Coruña, Spain Francisco Zayas Gato Álvaro Michelena University of A Coruña, Spain Míriam Timiraos Díaz University of A Coruña, Spain University of A Coruña, Spain Antonio Díaz Longueira Paula Patricia Arcano Bea University of A Coruña, Spain Manuel Rubiños Trelles University of A Coruña, Spain Marta María Álvarez Crespo University of A Coruña, Spain Alejandro Vidal Bralo University of A Coruña, Spain University of A Coruña, Spain Agustín García Fisher University of Deusto, Spain Iker Pastor López

# **INDEX**

# **CISIS 2025**

## **Malware & Intrusion Detection**

| A Fast Metric for Preliminary Risk Assessment of Portable Executables Using Stati                                       |
|---|
| Analysis13 Emanuel Albu and Ciprian Pungila   |
| Unsupervised Online Learning for Network Flow Anomaly Detection: A Comparative Evaluation                               |
| Enhancing Malware Detection In Portable Executables with Random Forest and Variance-Based Feature Selection             |
| Relational Matrix of Cyberattacks: A Model for Threat Classification and Connection in Digital Environments             |
| Cryptography & Blockchain Security Securing On-Chain Voting Using zk-SNARK  |
| Study and comparison of lattice sieving algorithms  |
| Hierarchical Threshold Structure Preserving Signatures  |
| A Comparative Study of LWE and LIP-Based Post-Quantum Signature Scheme  |
| Édgar Pérez-Ramos, Cristian Nina-Orellana, Candelaria Hernández Goya and Pino Caballero-Gil                             |
| AI Safety, Privacy & Trustworthy Systems The effectiveness of personal data detection in LLM-based Conversational Agent |
| Diego Paracuellos, Jose Such, Elena Del Val and Ana Garcia-Fornes   |
| Adaptive Identity Token from User Attributes for Authentication throug Controlled Execution Environment                 |
| Comparative Analysis of Jailbreaking Techniques for Large Language Models: A Systematic Evaluation Framework            |

| Hybrid Email Phishing Detection Using Large Language Models and Bay Classifiers   |    |
|---|----|
| Special Session: Artificial Intelligence for Protecting the Internet of Things Influence of Noise on the Stability of a Stochastic SIR Model with Demography13 Rafael Rodríguez García, Marta-María Álvarez-Crespo, Antonio Díaz-Longueira, Carlos Cambra a Roberto Casado-Vara |    |
| An optimal control problem for a SIR model with two mitigation strategies f malware spread  | 9  |
| Cybersecurity Taxonomies: Comparative Analysis of Leading IoT Datasets for A Driven Security  |    |
| Privacy Enhancing Federated Learning-Based IDS for IoT Networks Using Post Quantum Secure Channels and Verifiable Secret Sharing  |    |
| Federated Learning for the Detection of Attacks on IoT environment  | 80 |

# **ICEUTE 2025**

## GENERAL TRACK

| Enhancing   | Programming  | Education          | Through a      | Blended        | Methodology     | with     |
|-------------|--|--------------------|----------------|----------------|-----------------|----------|
| 0           | ga-Morla, Antonio I  |                    |                |                |                 |          |
| Sánchez-M   | -  | Deis, 7 tima iviai | ia mano casae. | io, Ludia Wior | an remandez and | rivociia |
|             | <b>AI Use Scale Inc</b><br>Val and Joaquin Tave                    |                    | ligher Educa   | tion           | ••••••          | 201      |
| Teaching Fe | ystematic Revie<br>edback in Higho<br>ldés, Ángel Arroyo a         | er Education       | ı              |                | •               |          |
| From Dida   | ctic Proposal to   | o Practical        | Implementa     | tion: Resul    | ts of an Ind    | ustrial  |
|             | aining Course w<br>coba, Eduardo Bayo                              |                    | •              |                |                 | 220      |
| _           | ho: A Gamified ta, Juan M. Alberola                                |                    |                | rning SQL      | ••••••          | 230      |
| Alberto Ma  | ity training in U<br>artinez Gutierrez, Pa<br>zález, Madalena Arad | iblo Alonso-Díe    | z, Rubén Ferre |                |                 |          |

## A Fast Metric for Preliminary Risk Assessment of Portable Executables Using Static Analysis

Emanuel Ioan Albu<sup>1</sup>, and Ciprian Pungilă<sup>1</sup>

<sup>1</sup>Department of Computer Science, West University of Timisoara, Romania {emanuel.albu01, ciprian.pungila}@e-uvt.ro

Abstract. This paper introduces a lightweight, fast, and interpretable static analysis method for the preliminary risk assessment of Windows Portable Executable (PE) files. The proposed system combines three complementary techniques: entropy analysis to detect obfuscation, structural metadata inspection to identify anomalous PE characteristics, and YARA (Yet Another Ridiculous Acronym) rule matching for signature-based threat identification. A custom point-based scoring model, empirically derived from 1,000 benign PE files, assigns risk scores based on statistical deviations in header fields and matched threat patterns. The tool was validated on a balanced dataset of 1,000 PE samples (500 benign, 500 malicious), achieving 80% detection accuracy, an 8% improvement over the ClamAV static scanner, while maintaining perfect precision and significantly reduced analysis time. Its design emphasizes modularity, enabling seamless integration with other tools and supporting the broader trend toward explainable AI in cybersecurity.

**Keywords:** static analysis, malware detection, portable executable, malicious, benign

#### 1 Introduction

Static analysis has become a pivotal approach in malware detection, offering the ability to extract and interpret features from binaries without executing them. This mitigates the risks associated with dynamic analysis while enabling the identification of malicious patterns, control flow anomalies, and embedded indicators of compromise (IoCs). One of the most common formats targeted in static analysis is the Windows Portable Executable (PE) file - a structure ubiquitous in Windows-based systems, encompassing executables, object code, and DLLs. Derived from the Common Object File Format (COFF), the PE structure contains metadata essential for program execution, rendering it a rich source for feature extraction and threat assessment.

This work proposes a fast, modular, and interpretable static analysis framework for the preliminary risk assessment of PE files. The methodology integrates three complementary components: entropy analysis for detecting obfuscation, structural metadata inspection for identifying anomalous characteristics, and YARA-based rule matching for signature-driven detection. A custom scoring

model, empirically derived from a corpus of 1,000 benign PE files, enables a granular quantification of risk through deviations in key fields and rule matches.

In summary, this work proposes a scalable and efficient framework for static malware risk assessment using PE files. Its easy-to-handle structure and focus on prompt identification make it ideal for incorporating into email filters, systems that prevent intrusions, and security tools for endpoints where quick file evaluation is crucial. By prioritizing clear and well-explained functionalities, the system also supports the increasing requirement for understandable artificial intelligence in the field of cybersecurity.

The reaminder of this paper is organized as follows. Section 2 provides an overview of the related work and current techniques in static PE malware detection. Section 3 describes the design and implementation of the proposed methodology, including entropy analysis, structural metadata inspection, and YARA rule integration. Section 4 presents the experimental setup, dataset details, and comparative evaluation with existing tools. Finally, Section 5 concludes the paper, summarizing the key findings and outlining potential directions for future research.

#### 2 State of the Art

The detection of malicious Portable Executable (PE) files through static analysis has garnered increasing attention due to its suitability for resource-constrained and high-risk environments. Unlike dynamic analysis, static approaches allow early detection without executing potentially harmful code. This section discusses key advancements in static PE malware detection, categorized by analysis techniques [1].

Several approaches utilize machine learning models that rely on PE header features to distinguish between benign and malicious files. Raff et al. [2] demonstrated that neural networks trained on minimal header information can achieve high detection rates. Similarly, Kumar and Shetty [3] showed that metadata fields like SizeOfHeaders and AddressOfEntryPoint are predictive indicators when used in classifiers, confirming that header anomalies are a lightweight yet effective malware signal.

Entropy analysis is a well-established technique to detect obfuscation and packing in binaries. Choi et al. [4] proposed the PHAD approach, which utilizes entropy irregularities to flag packed executables. Matin [1] further supported this by identifying elevated entropy as a signature of ransomware and polymorphic malware. While useful, entropy-based methods must account for benign compression to minimize false positives.

Other researchers have focused on structural metadata and anomalies in the PE file layout. Santos and Festijo [5] and Tyagi et al. [8] observed that irregularities in fields such as SectionAlignment, ImageBase, and TimeDateStamp are often indicative of hand-crafted or obfuscated malware. These features are valuable due to their interpretability and resistance to evasion.

YARA has emerged as a dominant tool for identifying known malware signatures within static binaries. Mahdi and Trabelsi [10] demonstrated that YARA rules targeting suspicious APIs, hardcoded IPs, and embedded URLs (Uniform Resource Locators) are effective for detecting Command-and-Control (C2) infrastructure. Kamble and Sridevi [9] highlighted how such signatures, when combined with entropy and header analysis, enhance detection capability while maintaining low false positive rates.

Recent work has focused on hybrid approaches that integrate multiple detection strategies. Ucci et al. [11] surveyed a wide spectrum of machine learning and hybrid models, noting the lack of interpretable systems suitable for real-time deployment. Our approach addresses this gap by proposing a modular, scoring-based detection method that empirically calibrates thresholds using benign data, with the added benefit of explainability and speed.

#### 2.1 Benchmarking and Comparative Tools

ClamAV [6] is a commonly used open-source antivirus engine that relies on signature-based static detection. While effective against known threats, ClamAV has limited capabilities when handling obfuscated or novel malware, making it a useful baseline for evaluating more sophisticated systems. Our experiments confirm that a hybrid, feature-rich scoring model can outperform ClamAV in both speed and accuracy.

#### 3 Methodology Design

The proposed detection script is a custom-built Python tool available publicly in GitHub [7] designed for the static analysis of PE files, as outlined in Figure 1. The process begins with scanning each file from a folder regardless of whether the file has or not an extension, after which the file is sent to further binary analysis, applicable only to PE files.

The first step involves entropy computation of each section of the executable, in order to assess its obfuscation level. This also helps determine, to a high degree of accuraccy, if the file is packed. The structural features of the PE file are then examined, with these checks also including, for example: the examination of the header size and ensuring it matches a certain range, alignment of sections, the image base address, the entry point address (i.e. is it part of the existing sections), and the time-date stamp.

Next, the workflow applies several precompiled sets of YARA rules. The first set is used for packed executables, looking for known packer signatures, as well as common identifiers. Moving forward, the next set of rules aim to identify suspicious strings commonly found in malware, with further rule checks being conducted in order to look for suspicious dynamic link libraries (DLLs) imports, hard-coded Internet protocol (IP) addresses, as well as embedded URLs. Every match found increases the risk score, activating a specific flag.

#### 4 Emanuel Ioan Albu et al.

The next step involves looks to identify relationships between relevant static indicators of malware. For example, if a binary is packed and contains suspicious strings, or, similarly, if it demonstrates high entropy of the file itself, and for its various sections, it is considered that a match had been found. The same logic applies to packed binaries that contain suspicious/flagged strings and import functions from DLLs that also contain suspicious/flagged strings, determining the flagging of these DLLs as well. The risk score is adjusted accordingly, depending on each of the scenarios matched, as outlined before.

The final risk score is computed as a final step, and a binary classification happens (malicious or non-malicious) based on its value exceeding an empirically-determined threshold. A final report of the resulting analysis process is also displayed.

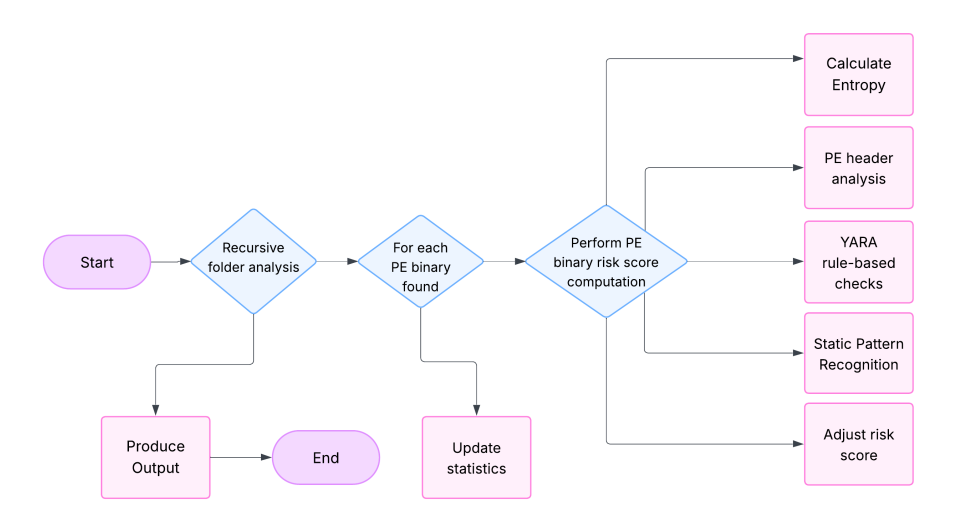


Fig. 1. Script control flow graph.

#### 3.1 Feature Extraction

Feature extraction constitutes a fundamental component of static analysis. The process involves identifying and selecting features based on their relevance in indicating whether a file exhibits behaviors typically associated with malicious software. In our approach, features are extracted from three primary domains: entropy analysis, structural metadata from the PE format, and rule-based detection using YARA signatures.

Entropy functions as a statistical measure of data randomness and is widely utilized in malware analysis to detect obfuscation techniques such as packing, encryption, or compression [4]. Within our system, entropy is calculated at two

levels of granularity: the file level and the section level. For both levels, the entire binary content is processed by a function that computes Shannon entropy, based on the distribution of byte values, using the following formula:

$$H = -\sum_{i=1}^{n} p_i \log_2(p_i) \tag{1}$$

#### 3.2 Entropy and Structural PE Metadata Analysis

The variable  $p_i$  denotes the probability of occurrence of the i-th byte value, while n represents the number of unique byte values observed within the data. Files exhibiting low entropy tend to be uncompressed and well-structured. Conversely, files approaching the theoretical maximum entropy value of 8.0 (for byte-level data) often contain encrypted payloads or compressed content, which are typical traits of malicious binaries.

Structural characteristics of PE files provide valuable indicators for distinguishing benign executables from obfuscated malware [11]. Our system uses the pefile library to extract features from the PE and optional headers, including SizeOfHeaders, where atypical values outside 0x200-0x1000 may suggest tampering [3]. The SectionAlignment field, normally 0x1000 in legitimate binaries, raises suspicion when below 0x200, indicating possible manual crafting or obfuscation [1]. The ImageBase, typically between 0x400000 and 0x80000000, can signal custom compilers or memory-staging shellcode when it deviates [8]. AddressOfEntryPoint should reside in standard sections like .text; if outside mapped regions, it may imply injected shellcode or a malformed header [1]. Finally, TimeDateStamp often reflects realistic build times in benign software, whereas malware may falsify this field with zeros or implausibly old values to evade detection.

#### 3.3 Signature-Based Detection with YARA

To augment static analysis with pattern-based detection, our system integrates YARA, a rule-based tool designed for identifying malware through string and binary pattern matching. We apply five YARA rule sets to each file: a) known packers, b) suspicious string patterns, c) DLL imports, d) hard-coded IP addresses, and e) embedded URLs. These rules are precompiled for performance and applied using the yara-python library. Each rule consists of string patterns and logical conditions designed to reflect common malware traits. The packer rules detect well-known packing utilities such as UPX, ASPack, and Themida. The string rules search for indicative content such as obfuscated commands and exploit-specific keywords. The DLL import rules emphasize the use of critical APIs like VirtualAlloc, WriteProcessMemory, CreateRemoteThread, and LoadLibrary, which are often leveraged in memory manipulation and process injection [9]. APIs from libraries such as kernel32.dll, ntdll.dll, ws2.32.dll, and wininet.dll are considered high risk due to their association with process

creation, memory allocation, and network communications. The **IP and URL rules** identify statically embedded addresses that could facilitate Command-and-Control (C2) communication or data exfiltration [10]. Such hardcoded network indicators are a common trait of advanced persistent threats (APT). All YARA rules employed in this research are sourced from a publicly available GitHub repository maintained by security professionals and the threat intelligence community [12]. These rules provide a rich source of expert-curated signatures, increasing our system's capability to detect obfuscated or compressed malware samples.

#### 3.4 Scoring System

To assess the risk associated with a binary, we employ a dynamic and robust scoring system grounded in empirical testing. Specifically, we analyzed 1,000 benign executable files sourced from standard Windows system directories. These samples served to benchmark the normal distribution of relevant features and to define precise scoring criteria. We selected these Windows files due to their practical relevance: although benign, they may share certain structural or functional characteristics with malware—such as the inclusion of libraries like kernel32.dll, CertEnroll.dll, and ntdll.dll.

Threshold Definition. To determine a scoring threshold, we computed the average risk score across the 1,000 benign files and recorded the highest individual score. We then defined the "sweet spot" threshold as:

Threshold = Average Risk Score  $+0.5 \times Max$  Risk Score

**Feature-Based Scoring.** As illustrated in Table 1, our core logic evaluates how frequently each feature occurs in the benign dataset. The score for each feature begins at 10 points and is calculated using the formula:

$$score = 10 \times x \tag{2}$$

Here, x is the proportion of Windows files that  ${\bf do}$  not exhibit the respective feature. This approach is applied to features derived from structural PE metadata, including SizeOfHeaders, SectionAlignment, ImageBase, as well as AddressOfEntryPoint and invalid or unusual TimeDateStamp.

**Entropy-Based Scoring.** Following our analysis of the 1,000 benign files, we observed an average file-level entropy of approximately 6. To reflect increasing uncertainty, we implemented an exponentially growing scoring function for entropy values exceeding 5.5. The scoring function S(H) is defined as:

**Table 1.** Distribution of atypical features in 1,000 benign Windows executables.

| Feature             | Have | Don't have |
|---------------------|------|------------|
| SizeOfHeaders       | 0    | 1.000      |
| SectionAlignment    | 0    | 1.000      |
| ImageBase           | 140  | 860        |
| AddressOfEntryPoint | 300  | 700        |
| TimeDateStamp       | 20   | 980        |

$$S(H) = \begin{cases} 0, & \text{if } H < 5.5 \\ S_{\text{max}} \cdot 0.4 \cdot \frac{b^{H/p} - 1}{b - 1}, & \text{if } 5.5 \le H \le p \\ \\ S_{\text{max}} \cdot 0.4 + S_{\text{max}} \cdot 0.6 \cdot \frac{b^{\frac{H-p}{H_{\text{max}} - p}} - 1}{b - 1}, & \text{if } p < H \le H_{\text{max}} \end{cases}$$

where:

- -H is the observed entropy,
- -p is the pivot point (set at the average entropy of 6),
- $H_{\text{max}}$  is the maximum theoretical entropy (8.0),
- b is the base of exponential growth,
- $-S_{\text{max}} = 20$  is the maximum score assigned for entropy.

Entropy values below 5.5 receive a score of 0.

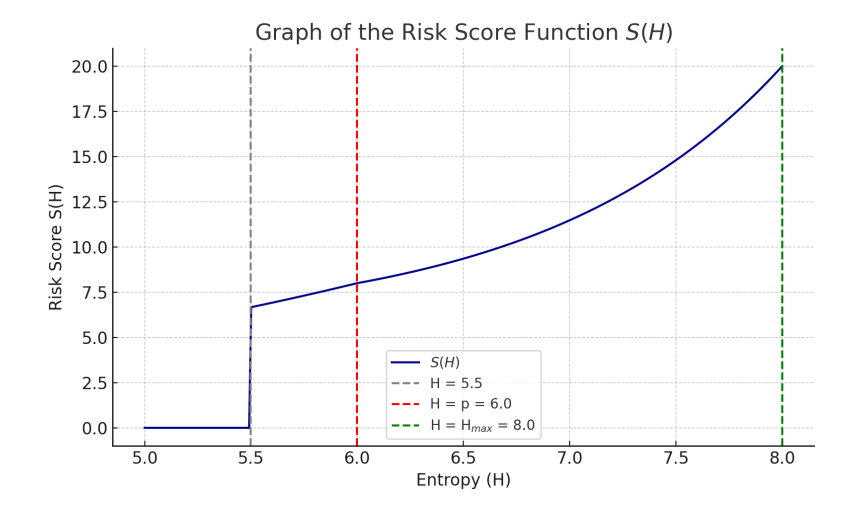


Fig. 2. Graph of the risk score function

YARA Rule Scoring. YARA rules are treated as discrete, high-impact indicators. Each rule match adds 10 points to the final score. The system evaluates matches against five YARA rule categories: a) known packers, b) suspicious strings, c) DLL imports, e) hard-coded IP addresses, and f) embedded URLs. The final YARA score is computed as:

YARA Score =  $10 \times \text{Number of Matching Rules}$ 

Pattern Matching Heuristics. To further refine detection accuracy, we incorporate a heuristic pattern-matching mechanism. This system identifies combinations of features that frequently co-occur in malware samples and assigns an additional score of 20 points to such patterns. Specific combinations that trigger this boost include: a) packed binary and any of {suspicious strings, high entropy (file or section level), suspicious strings + DLL imports}, and b) suspicious strings + DLL imports.

#### 4 Experimental Results

The dataset consists of a total of 1,000 PE files, equally divided into 500 benign and 500 malicious samples. Malicious samples were obtained through collaboration with the administrators of VirusShare [13], a well-established malware repository widely used in the cybersecurity research community. These malicious binaries represent a diverse collection, including packed malware, trojans, downloaders, and other types of threats. To construct the benign portion of the dataset, 500 PE files were collected from a clean Windows environment. These files include system utilities, administrative tools, and default applications typically found in genuine installations of the Windows operating system. A batch script was used to automate the extraction of these binaries. Using native Windows files as benign samples offers a meaningful baseline, as they often share certain structural similarities with malicious binaries.

A VirtualBox [14] virtual machine (VM) was configured for controlled testing, featuring 8 GB of memory, 6 logical processors, and a 100 GB virtual disk running Windows 11. To ensure a secure and isolated environment, all nonessential services were disabled, no third-party applications were installed, and features such as shared folders, clipboard sharing, and drag-and-drop were deactivated. After transferring the malicious files, the network was disconnected and Windows Defender was disabled. The 1,000 binaries were organized into two separate folders—one for benign files and one for malicious samples. The analysis system was executed independently on each folder, and the results were automatically saved to structured text files for evaluation. To validate the accuracy and reliability of our system, we integrated ClamAV [6], an open-source antivirus engine focused exclusively on static analysis. ClamAV was executed using its command-line interface via a custom batch script, which also recorded execution times and detection results.

The comparative evaluation between our proposed static analysis system and ClamAV reveals notable differences in performance, as illustrated in Figure 3. Our system achieved an 80% detection rate for malicious files, outperforming ClamAV's 72% detection rate. Both systems achieved a precision of 100%. Execution time analysis showed that our system performed significantly faster. This improvement is attributed to the targeted feature extraction methodology and the use of precompiled YARA rules, which streamline the static analysis process.



 ${f Fig.\,3.}$  Experimental results of the proposed static analysis approach, as compared to ClamAV.

#### 5 Conclusions

Experimental validation demonstrates that the proposed method not only achieves high detection accuracy but also significantly outperforms traditional tools such as ClamAV in terms of speed and precision. With its lightweight design and explainable architecture, the system is well-suited for deployment in time-sensitive environments such as email filters, endpoint security tools, and intrusion prevention systems.

Future work will aim to refine the scoring system by incorporating a broader set of heuristics and expanding YARA rules to cover emerging malware patterns and advanced obfuscation techniques. Additional static features, such as PE section anomalies, import/export table irregularities, and certificate metadata, will be explored to improve detection granularity. Efforts will also focus on optimizing rule prioritization and weighting within the scoring model to further enhance accuracy while maintaining the system's speed and interpretability.

Acknowledgement. This work has been partially supported by (1) the project RoNaQCI, part of EuroQCI, DIGITAL-2021-QCI-01- DEPLOY-NATIONAL, 101091562, (2) the project "Romanian Hub for Artificial Intelligence - HRIA", Smart Growth, Digitization and Financial Instruments Program, 2021-2027, MySMIS no. 334906.

#### References

- I. M. M. Matin, "Ransomware Extraction Using Static Portable Executable (PE)
  Feature-Based Approach," 2023 6th International Conference of Computer and Informatics Engineering (IC2IE), Lombok, Indonesia, 2023, pp. 70-74, doi:10.1109/
  IC2IE60547.2023.10331246 (Accessed: 2025-04-16)
- 2. E. Raff, J. Sylvester, and C. Nicholas, "Learning the PE header malware detection with minimal domain knowledge," in *Proceedings of the ACM Workshop on Artificial Intelligence and Security*, 2017, pp. 121–132. (Accessed: 2025-04-27)
- 3. S. S. Kumar and J. Shetty, "Malicious PE File Detection Using Machine Learning: An Analysis of Header Features," in *Proceedings of COSMIC*, 2024, pp. 66–71. (Accessed: 2025-04-27)
- 4. Y.-S. Choi, I.-K. Kim, J.-T. Oh, and J.-C. Ryou, "PE File Header Analysis-Based Packed PE File Detection Technique (PHAD)," in *International Symposium on Computer Science and its Applications*, 2008, pp. 28–31. (Accessed: 2025-04-22)
- R. S. Santos and E. D. Festijo, "Generating Features of Windows Portable Executable Files for Static Analysis using Portable Executable Reader Module (PE-File)," in IC2IE, 2021, pp. 283–288. (Accessed: 2025-04-27)
- 6. ClamAV, Available: https://www.clamav.net (Accessed: 2025-04-22)
- 7. Script source code
  - https://github.com/emichulo/Automation-Script-using-Static-Analysis-For-PE
- 8. S. Tyagi, A. Baghela, K. M. Dar, A. Patel, S. Kothari and S. Bhosale, "Malware Detection in PE files using Machine Learning," 2022 OPJU International Technology Conference on Emerging Technologies for Sustainable Development (OT-CON), Raigarh, Chhattisgarh, India, 2023, pp. 1-6, doi:10.1109/OTCON56053. 2023.10113998 (Accessed: 2025-04-20)
- 9. M. T. Kamble and Sridevi, "Feature Extraction and Analysis of Portable Executable Malicious File," 2022 Second International Conference on Computer Science, Engineering and Applications (ICCSEA), Gunupur, India, 2022, pp. 1-6.doi: 10.1109/ICCSEA54677.2022.9936121 (Accessed: 2025-04-20)
- R. H. Mahdi and H. Trabelsi, "Detection of Malware by Using YARA Rules," 2024
   21st International Multi-Conference on Systems, Signals & Devices (SSD), Erbil,
   Iraq, 2024, pp. 1-8. doi:10.1109/SSD61670.2024.10549308 (Accessed: 2025-04-20)
- 11. Daniele Ucci, Leonardo Aniello, Roberto Baldoni, Survey of machine learning techniques for malware analysis, Computers & Security, Volume 81, 2019, Pages 123-147, ISSN 0167-4048, https://doi.org/10.1016/j.cose.2018.11.001 (Accessed: 2025-04-27)
- Repository of yara rules https://github.com/Yara-Rules/rules (Accessed: 2025-04-22)
- 13. VirusShare.com https://virusshare.com (Accessed: 2025-04-22)
- 14. Oracle VirtualBox https://www.virtualbox.org (Accessed: 2025-04-20)

## Unsupervised Online Learning for Network Flow Anomaly Detection: A Comparative Evaluation

Alberto Miguel-Diez<sup>1</sup>, Claudia Álvarez-Aparicio<sup>1</sup>, Adrián Campazas-Vega<sup>1</sup>, Vicente Matellán-Olivera<sup>1</sup>, and Ángel Manuel Guerrero-Higueras<sup>1</sup>

Robotics Group. University of León, MIC building. Campus de Vegazana, s/n, 24071, León (Spain) {amigd, calvaa, acamv, vmato, agueh}@unileon.es

**Abstract.** Anomaly detection in network traffic is a crucial task for ensuring the security and integrity of communication systems. Traditional supervised machine learning models often achieve high accuracy but rely heavily on labeled datasets, which are costly to obtain and may become outdated. To address this limitation, this paper explores the use of unsupervised and online learning techniques for anomaly detection in network flow data. In this work, we compare three approaches: a baseline exactmatch dictionary method, a supervised Decision Tree classifier, and an online One-Class SVM implemented using the River framework. The evaluation is performed on a real-world NetFlow-based dataset enriched with synthetic anomalies to simulate realistic threat scenarios. Results indicate that the online One-Class SVM achieves a high detection rate (recall = 0.9861) with a low false positive rate (FPR = 0.0118), highlighting its suitability for dynamic environments where adaptability and low maintenance are critical. This study demonstrates the potential of online unsupervised learning as a practical alternative to traditional models in network anomaly detection tasks.

**Keywords:** anomaly detection, network flows, online learning, unsupervised machine learning, cybersecurity, One-Class SVM, NetFlow

#### 1 Introduction

Anomaly detection in network flows is a cornerstone in the protection of critical infrastructures, as it enables the identification of unusual behaviors that may indicate attacks, misconfigurations, or unauthorized activities. In this context, flow-based traffic analysis, such as NetFlow [1] or IPFIX [2], has emerged as an effective strategy for monitoring large volumes of data without the need to capture the full content of network packets.

The literature has addressed this challenge from multiple perspectives, with particular emphasis on the use of both supervised and unsupervised machine learning techniques. Supervised methods have shown high performance in detecting specific threats; however, their effectiveness relies on the availability of

labeled datasets that accurately reflect the characteristics of the operational environment. This requirement is often difficult to satisfy in real-world scenarios, where labels may be scarce, outdated, or erroneous [3].

In light of these limitations, unsupervised approaches have gained prominence due to their ability to operate without labeled data during training, focusing instead on modeling normal behavior to detect significant deviations. Nevertheless, most of these approaches remain grounded in batch learning schemes, which present notable drawbacks in dynamic environments—such as the inability to adapt to concept drift and the need to store large volumes of data in memory.

With the rise of real-time systems, such as IoT devices, industrial networks, and distributed corporate environments, the paradigm of *online machine learn-ing* has emerged as a promising alternative. This approach enables the incremental updating of models as new observations become available, thereby enhancing adaptability, reducing memory requirements, and improving integration in resource-constrained environments [4].

In this context, several prior studies have contributed to the understanding and development of anomaly detection strategies. Chandola et al. [5] offer a survey of anomaly detection techniques, highlighting the applicability of statistical, distance-based, density-based, and machine learning approaches across various domains, including network traffic. Within the realm of unsupervised learning, Kabir et al. [6] employed k-means clustering, while Schueller et al. [7] and Verkerken et al. [8] explored support vector machines (SVM) for flow-based anomaly detection. Wang et al. [9] introduced a hybrid method that combines behavioral profiling with network graph modeling to enhance detection accuracy.

The need for adaptability in non-stationary environments has motivated a growing body of work on online learning strategies. In a recent comparative study, Shahraki et al. [4] evaluated several online algorithms for detecting anomalies in network flows, highlighting their effectiveness in handling evolving patterns and concept drift. These contributions underscore the importance of moving beyond static models and adopting online approaches tailored to continuous and large-scale network monitoring scenarios.

This study proposes a network flow anomaly detection approach. By implementing and evaluating three different models—an exact-match-based method, a supervised decision tree, and a One-Class SVM adapted for *online learning*—we compare various approaches to assess their feasibility and effectiveness. The aim is to identify anomalous flows in a realistic environment using a dataset provided by a specialized software company, which has been augmented with synthetic anomalies that simulate unusual behaviors across different time periods and destination addresses.

The remainder of this paper is organized as follows: Section 2 details the methodology. Section 3 introduces the metrics used to assess performance, while Section 4 presents and compares the results obtained. Section 5 discusses the findings and their implications, and finally, Section 6 summarizes the main contributions and outlines directions for future work.

#### 2 Methodology

This section introduces the key components used in the proposed anomaly detection system. It describes the online learning framework, the dataset characteristics, and the detection algorithms that will later be integrated and evaluated.

#### 2.1 Online Machine Learning

Before delving into the fundamentals of online learning, it is useful to briefly contextualize traditional batch learning methods. This strategy is characterized by a clear separation between training and validation phases, both of which require access to the entire dataset from the outset. However, this approach presents several drawbacks, including high memory consumption, susceptibility to concept drift, and the inability to adapt to previously unseen attributes [10].

In contrast, online learning represents a paradigm in which the model is updated continuously as new observations are received, without the need to store the entire historical dataset [4]. This methodology enables faster training with lower computational cost. Two of its main advantages are: (i) its feasibility on resource-constrained devices, such as embedded systems or sensors [11], and (ii) its ability to rapidly adapt to new data without requiring a full retraining process.

This approach proves especially useful in environments where data is generated continuously, as is the case in large-scale information analysis systems, anomaly detection, autonomous robotics, or human–machine interfaces [11].

As in conventional learning, online learning can be categorized into supervised, unsupervised, and semi-supervised variants, depending on the availability of labels during the learning process [4]. In this study, an unsupervised approach has been adopted due to the challenges associated with obtaining labeled data in cybersecurity contexts. The manual annotation of network flows requires expert intervention and does not always ensure coverage of emerging threats, potentially leading to quickly outdated datasets.

In online unsupervised learning, data  $D=(x_1,x_2,\ldots,x_m)$  are observed sequentially without labels. The objective is to construct a model  $F\approx p(y\mid X)$  capable of detecting patterns or anomalies as new instances  $x_t$  are received. Unlike the batch learning paradigm, here the model is updated incrementally: at each time step t, a new version  $F_t$  is generated based on the current observation  $x_t$  and the previous state  $F_{t-1}$ , thus enabling continuous adaptation to a changing environment without the need to retain large volumes of data in memory.

#### 2.2 Dataset and Preprocessing

The dataset employed in this study was provided by the company Proactivanet [12], consisting of network flows generated by internal company devices between July 8 and July 15, 2024. The data structure adheres to the NetFlow standard [1], with certain custom extensions.

#### 4 Alberto Miguel-Diez et al.

Dataset Structure and Labeling A notable addition is the END\_TYPE attribute, indicating the termination reason of each flow: 1 = inactive timeout, 2 = normal termination, 3 = TCP flags.

Fields such as source and destination IPs may include IPv4, IPv6, or domain names. For privacy reasons, all addresses were anonymized using numerical encodings.

To evaluate detection performance, a total of 12,500 synthetic anomalies were programmatically inserted across the temporal window of the dataset. These were evenly distributed across five types (2,500 samples each):

- Benign IP to anomalous IP during business hours
- Benign IP to benign IP outside business hours
- Benign IP to anomalous domain during business hours
- Benign IP to anomalous domain outside business hours
- Anomalous IP to anomalous IP during business hours

The final dataset consists of 221,063 benign flows and 12,500 anomalous flows.

**Preprocessing Transformations** Prior to model training and evaluation, the following preprocessing steps were uniformly applied:

- Timestamp simplification: Reduced to hour granularity to capture diurnal trends while mitigating temporal noise.
- Port unification: A new attribute PORT was created: source port for outgoing flows, destination port for incoming.
- Byte count rounding (supervised models only): For the Exact Match and Decision Tree classifiers, the number of bytes sent and received was rounded to the nearest multiple of 100. This transformation aims to reduce sensitivity to minor fluctuations in traffic volume and mitigate overfitting to exact values.

These transformations reduce feature sparsity and improve generalization, particularly for the exact match method, which is highly sensitive to minor variations.

It is important to note that anomalies in this context do not necessarily indicate malicious attacks. Rather, they represent behavioral deviations from typical patterns, such as unusual communication timings or uncommon destinations.

#### 2.3 Algorithms

This section presents all the models that have been used in this article to detect network flow anomalies.

#### **Exact Match Detector**

The proposed method, referred to as the *Exact Match Detector*, is based on the construction of a dictionary for anomaly detection in network flows where the key is the flow characteristics. Initially, a model is "trained" using only benign

flows. This model is subsequently used to identify anomalous flows in a test set, where any flow that differs even slightly from those observed during training is flagged as anomalous.

The features selected from the dataset to train the model include the source and destination IP addresses, ports, timestamp of the flow, direction (incoming or outgoing), and the number of bytes sent and received.

The purpose of the processing transformations described in Section 2.2 is to mitigate the effect of overly specific values, as the *Exact Match Detector* relies on exact matching to compare flows. Without such adjustments, trivial differences between training and test flows would lead to an increased false positive rate.

During the evaluation phase, each flow in the test set is assessed by searching for its corresponding key in the model's dictionary. If the key is not found, the flow is classified as anomalous. Otherwise, it is considered a normal flow.

#### **Decision Tree**

The *Decision Tree Classifier* is a supervised learning model that uses a treelike structure to make decisions based on data attributes. Each internal node of the tree represents a condition on an attribute, each branch corresponds to the outcome of that condition, and each terminal leaf assigns a class label.

In the context of anomaly detection in network flows, the *Decision Tree Classifier* is constructed from a training set composed of labeled flows, including both normal and anomalous instances. During the training phase, the algorithm identifies the most relevant attributes for classification by evaluating criteria such as *entropy* or the *Gini index*.

In relation to preprocessing, the same procedure described previously has been applied, with additional encoding of IP addresses with the LabelEncoder method.

To optimize the model's performance, a grid search strategy was adopted using GridSearchCV from the Scikit-Learn library [13]. This procedure systematically explored combinations of hyperparameters to identify the configuration that yielded the best classification results on a validation subset.

#### One-Class SVM for Online Learning

For anomaly detection in network flows, a *One-Class SVM* model has been employed in its online learning variant using the River library [14]. This model is particularly suited for *novelty detection* tasks, as it enables the identification of deviations from normal behavior. Unlike the traditional batch approach, this variant updates the model incrementally, which is crucial in network environments characterized by real-time data and evolving patterns.

A warm-up phase is typically conducted prior to the first predictions to improve performance and enable a fair comparison with batch machine learning models [15]. Subsequently, as new flows are received, the model adjusts its incremental parameters without the need to retain past data, thereby mitigating the issues associated with storing large data volumes.

Regarding preprocessing, the same procedure described previously was followed. However, in this case, the data were scaled prior to model application. To achieve this, a reduced subset of flows was selected to train the scaler. Since the

scaling algorithm operates in online mode, this initial warm-up phase is essential to stabilize its behavior and enable a progressive adaptation to the characteristics of the streaming data.

To optimize model performance, the parameter  $\nu$ —which controls the expected proportion of anomalies in the dataset—has been tuned. Additionally, a learning rate scheduler based on InverseScaling has been configured, modulating the bias term according to the expression:

$$\eta_{t+1} = \frac{\eta}{(t+1)^p} \tag{1}$$

where p is a configurable parameter that was kept at its default value to ensure the progressive convergence of the model.

Since the River library does not natively support hyperparameter optimization, a custom script was developed to facilitate the configuration and experimentation process. This tool allows the specification of the parameters  $\nu$ ,  $\eta$ , and q, the selection of the online scaler, the number of warm-up flows, the subset of features to be used, and the strategy for IP address management.

The OCSVM model for online learning does not produce a direct binary classification; instead, it outputs a continuous score, where higher values indicate a greater likelihood of anomaly. However, since the score scale is unbounded, a quantile-based filtering mechanism has been implemented to determine a dynamic decision threshold. This threshold is adjusted according to a parameter q, which defines the quantile above which a flow is classified as anomalous. This technique enables continuous adaptation of the threshold, maintaining its effectiveness in the presence of changes in network traffic distribution.

#### 3 Evaluation Metrics

In this work, the problem is a binary classification as it consists of identifying whether a network flow is benign or anomalous. The evaluation of the model is based on the confusion matrix, which comprises true positives (TP), true negatives (TN), false positives (FP), and false negatives (FN).

Based on these values, several metrics are defined to assess the model's performance. The **Accuracy** metric represents the proportion of correctly classified instances with respect to the total number of samples, and is computed as follows:

$$Accuracy = \frac{TP + TN}{TP + TN + FP + FN} \tag{2}$$

The **Recall** metric measures the model's ability to correctly identify anomalies, i.e., the proportion of true positives relative to the sum of true positives and false negatives. It is defined as:

$$Recall = \frac{TP}{TP + FN} \tag{3}$$

Finally, the **False Positive Rate (FPR)** indicates the proportion of false positives among all benign samples. It is calculated as:

$$FPR = \frac{FP}{FP + TN} \tag{4}$$

#### 4 Results

This section presents the results obtained after implementing and evaluating the three models: *Exact Match Detector*, *DecisionTreeClassifier*, and *One-Class SVM*. Except for the Exact Match Detector, which has no tunable parameters, a hyperparameter optimization process was carried out for the other two models.

All models were trained using 100,000 network flows. In the case of both the Exact Match Detector and the One-Class SVM, all training flows were considered benign, meaning that no malicious instances were included during the training phase. However, as the *DecisionTreeClassifier* is a supervised model, a labeled dataset containing both benign and anomalous flows was required. Given the low prevalence of anomalies in the dataset, the model was evaluated using 6,250 anomalous flows and 6,250 benign flows.

The results for the *Exact Match Detector* reveal an **accuracy** of 0.741, a **recall** of 100%, and a **false positive rate** (FPR) of 0.518.

For the *DecisionTreeClassifier*, the optimal combination of hyperparameters included the use of the entropy criterion to evaluate split quality, no maximum depth (until all leaves are pure or contain fewer samples than min\_samples\_split), min\_samples\_leaf = 1, and min\_samples\_split = 2. This configuration achieved an accuracy of 0.9998, a recall of 0.9995, and a FPR of 0.0, indicating excellent predictive capacity with virtually no false positives.

Finally, the *One-Class SVM* model was optimized using the parameters q = 0.99,  $\nu = 0.05$ , and a learning rate  $\eta = 0.25$ . This configuration resulted in an **accuracy** of 0.9871, a **recall** of 0.9861, and a **FPR** of 0.0118.

Table 1 summarizes the performance results obtained for the three models using the dataset provided by the company Proactivanet.

**Table 1.** Performance of the three evaluated models using the dataset provided by Proactivanet.

| Model                  | <b>Evaluation Samples</b> | Accuracy | Recall | FPR    |
|------------------------|---------------------------|----------|--------|--------|
| Exact Match Detector   | 25,000                    | 0.741    | 1.0    | 0.518  |
| DecisionTreeClassifier | 12,500                    | 0.9998   | 0.9995 | 0.0    |
| OSVM                   | 25,000                    | 0.9871   | 0.9861 | 0.0118 |

#### 5 Discussion

This section discusses the results obtained from the implementation and evaluation of the three models. The findings enable a comparative analysis of super-

vised and unsupervised approaches and allow for an assessment of each model's effectiveness in detecting anomalies in network flows.

Firstly, the Exact Match Detector demonstrated a remarkable ability to detect all anomalies present in the dataset, achieving a recall of 100%. However, this high sensitivity came at the cost of a high false positive rate (FPR = 0.518), which compromises its practical applicability in operational environments where an excess of alerts may lead to operator fatigue and reduced trust in the system. Despite this limitation, the simplicity of the model makes it a viable option in scenarios where the priority is to maximize the detection of atypical events, regardless of the cost in false positives.

In contrast, the DecisionTreeClassifier exhibited exceptional performance, achieving an accuracy of 0.9998 and an FPR of 0.0. These results indicate that the model successfully distinguished between benign and anomalous classes, maintaining high precision while minimizing false positives. However, as a supervised model, its effectiveness may decline in scenarios with low anomaly prevalence or where attack patterns are not sufficiently represented in the training data. Furthermore, it requires a labeled dataset that is representative of the target network, which in real-world settings entails a substantial workload to obtain.

Finally, the One-Class SVM achieved a compelling balance between precision and false positive rate. Despite being an unsupervised model, it obtained a recall of 0.9861 and an FPR of 0.0118, suggesting that the tuning of the parameters  $\nu$ , q, and  $\eta$  was appropriate to capture anomalous behaviors without generating an excessive number of false positives.

Overall, the results show that the DecisionTreeClassifier offers the best performance in terms of accuracy. However, its reliance on labeled data limits its applicability in environments where anomalies are infrequent or difficult to label. Therefore, the One-Class SVM emerges as the most viable option, as it operates in an unsupervised manner, making it more suitable for real-world scenarios [5]. It achieves a high detection rate (recall) and a low false positive rate (FPR), without requiring global retraining or the storage of large data volumes. Additionally, being an online model, it is capable of adapting to newly emerging anomalies—thereby addressing concept drift—by incrementally updating its internal representation as new data arrives. This property is essential in dynamic environments where traffic patterns evolve over time and static models rapidly become obsolete. Furthermore, due to its low computational footprint and unsupervised nature, the One-Class SVM can be integrated into existing IDS frameworks as an anomaly detection component, enhancing their ability to detect previously unseen or obfuscated threats.

While the dataset used in this study is based on real traffic and enriched with controlled synthetic anomalies, it is important to acknowledge that such anomalies may not capture the full spectrum of behaviors observed in complex threat scenarios. Nevertheless, this approach enables a reproducible and systematic evaluation of detection models under well-defined conditions, providing a solid foundation for further testing in more heterogeneous environments.

#### 6 Conclusion

This work has comparatively evaluated three approaches to anomaly detection in network flows: an exact match method, a supervised decision tree, and an online One-Class SVM. While the supervised model (DecisionTreeClassifier) achieved the highest accuracy, its dependence on labeled data and limited scalability constrain its applicability. In contrast, the online One-Class SVM exhibited a favorable trade-off between detection capability and operational efficiency, offering a more adaptable and scalable solution for real-time network monitoring. The source code and dataset used in the experiments are publicly available in a GitHub repository [16].

As a future research direction, it would be interesting to explore hybrid architectures that combine online and offline models [17,18], leveraging the adaptability of the former and the statistical stability of the latter. Such a combination could further improve performance in dynamic environments, enhancing both the precision of detection and the efficiency of responses to anomalous events.

#### Acknowledgements

This research is a result of the CIBERLAB project (C083/23), carried out under the collaboration agreement between INCIBE and the University of León. This initiative is part of the Recovery, Transformation and Resilience Plan, funded by the European Union (Next Generation EU).

#### References

- 1. B. Claise, "Cisco Systems NetFlow Services Export Version 9," Oct. 2004, issue: 3954 Num Pages: 33 Series: Request for Comments Published: RFC 3954.
- 2. P. Aitken, B. Claise, and B. Trammell, "Rfc 7011: Specification of the ip flow information export (ipfix) protocol for the exchange of flow information."
- 3. J. L. Guerra, C. Catania, and E. Veas, "Datasets are not enough: Challenges in labeling network traffic," *Computers & Security*, vol. 120, p. 102810, 2022.
- A. Shahraki, M. Abbasi, A. Taherkordi, and A. D. Jurcut, "A comparative study on online machine learning techniques for network traffic streams analysis," *Computer Networks*, vol. 207, p. 108836, Apr. 2022.
- V. Chandola, A. Banerjee, and V. Kumar, "Anomaly detection: A survey," ACM Comput. Surv., vol. 41, no. 3, Jul. 2009.
- M. A. Kabir and X. Luo, "Unsupervised Learning for Network Flow Based Anomaly Detection in the Era of Deep Learning," in 2020 IEEE Sixth International Conference on Big Data Computing Service and Applications (BigDataService). Oxford, United Kingdom: IEEE, Aug. 2020, pp. 165–168.
- Q. Schueller, K. Basu, M. Younas, M. Patel, and F. Ball, "A Hierarchical Intrusion Detection System using Support Vector Machine for SDN Network in Cloud Data Center," in 2018 28th International Telecommunication Networks and Applications Conference (ITNAC). Sydney, NSW: IEEE, Nov. 2018, pp. 1–6.

- 8. M. Verkerken, L. D'hooge, T. Wauters, B. Volckaert, and F. De Turck, "Unsupervised Machine Learning Techniques for Network Intrusion Detection on Modern Data," in 2020 4th Cyber Security in Networking Conference (CSNet). Lausanne, Switzerland: IEEE, Oct. 2020, pp. 1–8.
- W. Wang, Y. Shang, Y. He, Y. Li, and J. Liu, "BotMark: Automated botnet detection with hybrid analysis of flow-based and graph-based traffic behaviors," *Information Sciences*, vol. 511, pp. 284–296, Feb. 2020.
- 10. T. Bartz-Beielstein, "Introduction: From Batch to Online Machine Learning," in *Online Machine Learning*, E. Bartz and T. Bartz-Beielstein, Eds. Singapore: Springer Nature Singapore, 2024, pp. 1–11, series Title: Machine Learning: Foundations, Methodologies, and Applications.
- A. Gepperth and B. Hammer, "Incremental learning algorithms and applications," in European Symposium on Artificial Neural Networks (ESANN), Bruges, Belgium, 2016.
- 12. Proactivanet, "Proactivanet (a): Software especializado en itam + itsm," Feb 2025. [Online]. Available: https://www.proactivanet.com/
- F. Pedregosa, G. Varoquaux, A. Gramfort, V. Michel, B. Thirion, O. Grisel, M. Blondel, P. Prettenhofer, R. Weiss, V. Dubourg, J. Vanderplas, A. Passos, D. Cournapeau, M. Brucher, M. Perrot, and E. Duchesnay, "Scikit-learn: Machine Learning in Python," *Journal of Machine Learning Research*, vol. 12, pp. 2825–2830, 2011.
- 14. J. Montiel, M. Halford, S. M. Mastelini, G. Bolmier, R. Sourty, R. Vaysse, A. Zouitine, H. M. Gomes, J. Read, T. Abdessalem, and others, "River: machine learning for streaming data in Python," 2021.
- 15. T. Bartz-Beielstein and L. Hans, "An Experimental Comparison of Batch and Online Machine Learning Algorithms," in *Online Machine Learning*, E. Bartz and T. Bartz-Beielstein, Eds. Singapore: Springer Nature Singapore, 2024, pp. 105–124, series Title: Machine Learning: Foundations, Methodologies, and Applications.
- 16. A. Miguel-Diez, amigueldiez/cisis25-anomaly-detection-OML, 5 2025. [Online]. Available: https://github.com/amigueldiez/cisis25-anomaly-detection-OML
- M. Odiathevar, W. K. G. Seah, and M. Frean, "A Hybrid Online Offline System for Network Anomaly Detection," in 2019 28th International Conference on Computer Communication and Networks (ICCCN). Valencia, Spain: IEEE, Jul. 2019, pp. 1–9.
- 18. M. Odiathevar, W. K. Seah, M. Frean, and A. Valera, "An Online Offline Framework for Anomaly Scoring and Detecting New Traffic in Network Streams," *IEEE Transactions on Knowledge and Data Engineering*, vol. 34, no. 11, pp. 5166–5181, Nov. 2022.

## Enhancing Malware Detection In Portable Executables with Random Forest and Variance-Based Feature Selection

Alexandru Todea<sup>1</sup>, Ciprian Pungilă<sup>1</sup>, and Adrian Spătaru<sup>1</sup>

<sup>1</sup>Department of Computer Science, West University of Timișoara, Romania alexandru.todea01@e-uvt.ro, ciprian.pungila@e-uvt.ro, florin.spataru@e-uvt.ro

Abstract. This paper aims to propose an improved method for enhancing malware detection in portable executables (PE), through the Random Forest and variance-based feature selection mechanisms, in order to achieve higher accuracy than previous models, while decreasing training time. Our method involves training a Random Forest model with default parameters, its evaluation on the dataset used, and selection of relevant columns with variance exceeding a proposed threshold. We discuss the intricacies of our method based on the results obtained using the EM-BER2018 Windows portable executables dataset. We compare our model with previous works done in literature, and outline our approach's empirical benefits and reduced training time. Finally, we discuss potential ideas for future work and further improvements.

**Keywords:** malware detection, machine learning, Random Forest, feature selection, portable executable

#### 1 Introduction

In this paper, we tackle the binary classification problem of labeling Windows portable executable (PE) files as either malicious software (malware) or benign software. We define malware as a program that can harm the user. Malicious software includes, but is not limited to, viruses, worms, trojan horses, ransomware, spyware, adware, and rootkits.

Getting infected with the malware listed above can have serious consequences on individuals and corporations, including downtime, reputation loss, and disclosure of confidential information. More importantly, it can damage society's critical infrastructure. Detecting malware in a fast and accurate manner has become increasingly important in today's world to prevent its negative effects. To address this demand, we aim to develop a malware detection machine learning (ML) model that labels Windows PE files with a better accuracy than the current state of the art while maintaining training and inference times that are comparable or even shorter.

We use EMBER2018 [1] as a benchmark dataset because it is large (1.1 million samples) and includes a rich feature set. Many malware detection datasets

are publicly available on platforms such as Kaggle [2], but they are small and provide a limited number of features. The only dataset that comes close in quality to the EMBER2018 dataset is SOREL-20M [3], but its large size (20 million samples) makes training models on it with a consumer-grade computer very difficult.

Section 2 summarizes the papers that performed experiments on the full EMBER2018 dataset. Section 3 details our experimental framework and the reasoning behind it. Section 4 presents the results of our experiments. Section 5 summarizes our work, integrates our findings into the wider body of research on the EMBER2018 dataset, and sets the stage for future studies.

#### 2 Literature Review

#### 2.1 Filtering the Literature

We searched Google Scholar for papers performing experiments on the EM-BER2018 [1] dataset using two keywords: "ember" and "dataset". We applied a filter to only display papers published between 2018 and 2025.

We found that several do not train and evaluate the models on the full dataset. Those are not relevant to our study and will not be included in this literature review. There are roughly three types of papers that perform experiments on the full dataset: dataset feature analysis (FA) papers, traditional ML papers, and deep learning (DL) papers.

#### 2.2 Dataset Feature Analysis (FA) Papers

The first category of papers analyzed focuses on FA. These papers try combinations between the feature groups in the dataset in an attempt to discover the ones that provide the best performance. The representative papers for this category were written by Oyama et al. [8] and Sandor et al. [9].

Oyama et al. [8] trained LGBM models on all possible feature combinations and evaluated their performance by computing scores using a formula defined by them. The formula contained an accuracy score parameter preceded by an accuracy weight coefficient. With the accuracy weight coefficient set to a value that placed four times higher importance on the accuracy parameter compared to the other parameters, the feature group combination that obtained the highest score was: general file information, header information, section information, and string information.

Şandor et al. [9] also considered all feature group combinations but tested the performance of models trained on them on four subsets with training and testing data extracted from the full EMBER2018 dataset. Before training the models, normalization, scaling, or no pre-processing was applied. Two types of models were trained and evaluated: Random Forest (RF) and logistic regression (LR). The RF models are more relevant to our study. Although experiments were performed on all subsets, the paper only reports Area Under the Receiver

Operating Characteristic Curve (AUC) results on the largest subset at two false positive rate (FPR) thresholds: FPR less than 0.1% and FPR less than 0.01%. At FPR less than 0.1%, many RF models with no pre-processing and scaling pre-processing applied obtained the highest AUC score of 0.996. At FPR less than 0.01%, again, the RF models with no pre-processing and scaling pre-processing won. Multiple of them achieved the highest AUC score of 0.984.

#### 2.3 Traditional Machine Learning (ML) Papers

The second category of papers evaluated included works that train and evaluate traditional ML models on the dataset. The representative papers for this category were written by Ghourabi [10] and Shashank et al. [11].

Ghourabi [10] proposed a security system for the healthcare industry that encompasses a malware detection system to protect the computers of medical staff against threats. The malware detection system uses a Bayesian-optimized LGBM model to label executables on the medical staff computers. The model was trained and evaluated on the full EMBER2018 dataset. It obtained an accuracy of 97.96%, outperforming an unoptimized LGBM and two neural networks (NN).

Shashank et al. [11] trained six ensemble ML models on the full EMBER2018 dataset. Normalization was performed to bring all columns to a mean of zero and a variance of one. A gradient-boosting-based feature reduction technique was used to select the most important features. RF, AdaBoost, Extra Trees, XG-Boost, LGBM, and Bagging models were trained on the feature-reduced dataset. The best accuracy of 96.56% was obtained by the Bagging model.

#### 2.4 Deep Learning (DL) Papers

The third category of papers studied included those that train and evaluate DL models on the dataset. The representative papers in this category were written by Connors and Sarkar [4] and Lad and Adamuthe [12].

Connors and Sarkar [4] trained and evaluated several ML models using the full EMBER2018 feature set and subsets of it. They obtained the best accuracy of 95.22% on the full feature set with a DL model designed by them. They are the only authors out of the bunch that we reviewed who made their code public. As a result, we successfully reproduced their experiment in Subsection 3.2.

Lad and Adamuthe [12] used Scikit-learn's [6] StandardScaler to scale the full vectorized training and test data. Scaling prevents ML models from giving more importance to features with higher values [13]. The authors trained an NN that they created on the full EMBER2018 dataset and obtained an accuracy of 94.09%.

#### 3 Methodology

#### 3.1 Exploring and Pre-Processing the EMBER2018 Dataset

EMBER2018 is a large dataset that was created for malware detection research, containing an equal number of malicious and benign samples in both the train-

#### 4 Todea et al.

ing and testing sets. Table 1 shows the distribution of malicious, benign, and unlabeled samples in the dataset. We trained and evaluated several ML models on the EMBER2018 [1] dataset with the second feature version downloaded from [14].

| Dataset Partition | Benign  | Malicious | Unlabeled |
|-------------------|---------|-----------|-----------|
| Training Set      | 300,000 | 300,000   | 300,000   |
| Test Set          | 100,000 | 100,000   | 0         |
| Total             | 400,000 | 400,000   | 300,000   |

Table 1. Distribution of benign, malicious, and unlabeled samples in the dataset

The dataset contains 2,381 features extracted from the samples grouped into nine feature groups. The nine feature groups are: general file information, header information, imported functions, exported functions, section information, byte histogram, byte-entropy histogram, string information, and data directories. Detailed descriptions can be found in [15].

The dataset comes in the form of several large *.jsonl* files and needs to be vectorized (i.e., converted into numerical format) before ML models can be trained on it. We used the code provided by the dataset authors in [14] to perform vectorization. The instructions were not very detailed. As a result, we created a public GitHub repository [15] with clear steps on how to vectorize the dataset and run our experiments on the resulting vectorized version.

Anderson and Roth [1] included unlabeled samples in the dataset to encourage researchers to explore supervised and semi-supervised learning. Since we are only interested in supervised learning (i.e., learning with labels), we did not consider the unlabeled samples from the training set.

In Subsection 3.2, we discuss how we reproduced the NN experiment performed by Connors and Sarkar [4]. However, before that, we took one more dataset pre-processing step that they took, namely, we shuffled the samples in the training set. To get the samples shuffled in the same order as them, we set the seed for NumPy's [16] random number generator to 314 (exactly as they did in the NeuralNetwork.py file in [5]) and then shuffled the training set. We also kept the samples in the shuffled order for the experiments in Subsection 3.3.

# 3.2 Reproducing the Connors and Sarkar [4] Neural Network Experiment

We extensively searched for authors who made the code for their EMBER2018 experiments public, and the only ones we found were Connors and Sarkar [4]. The code for their experiments is available in [5]. Several papers from Section 2 failed to thoroughly document their experiments, which introduces ambiguity and impedes reproducibility.

Connors and Sarkar [4] trained and evaluated several ML models using both the full EMBER2018 feature set as well as reduced versions of it. However, we only reproduced their best-performing model, an NN trained on the full feature set, because that is the one we had to outperform for our work to be considered meaningful.

We followed the same training process as in [5]. We trained the NN model for 75 epochs, with a batch size of 200, on the 600,000 labeled samples from the dataset's training set and evaluated it on the 200,000 labeled samples from the dataset's testing set. No cross-validation was performed. We configured Keras [17] to save the model weights after the epoch with the highest accuracy on the testing set. We measured the training time. Once training was complete, we loaded the weights and computed the following performance metrics on the testing set: accuracy, number of true negatives (TN), number of false positives (FP), number of false negatives (FN), number of true positives (TP), AUC, precision, recall, F1 score (F1), and Cohen's Kappa Score. Additionally, we measured the inference time (i.e., the time it took the model to make the predictions on all the samples in the testing set).

### 3.3 Our Experimental Procedures

The first action we took was to perform a variance-based feature selection on the full EMBER2018 feature set. We used the Scikit-learn [6] VarianceThreshold to drop features with a variance lower than 0.001 from the dataset. 1,658 of the original 2,381 features remained. This decision was motivated by the book: Machine Learning for Tabular Data [18], in which Ryan and Massaron talk about certain conditions that should always be avoided among a dataset's features. One of them is "constant or quasi-constant columns". The authors mention that "the variance shouldn't approximate zero for numeric features", which is what we are dealing with in the case of the vectorized EMBER2018 dataset. They go on to explain that ML models can only learn from how the features vary with respect to the target and that "no change in the features implies no conditional change on your target from which to learn".

We trained and evaluated a total of four models: two Scikit-learn [6] RF classifiers and two LGBM classifiers [7]. One of the two RF models was trained using the variance-filtered (VF) EMBER2018 feature set, while the other was trained on the full EMBER2018 feature set. We proceeded in the same way for the LGBM models. All four models were trained and evaluated on the same training and testing sets as the NN detailed in Subsection 3.2. No cross-validation was performed. The default parameters were used for all four models. We selected these models because we know from [18] that they provide good performance on tabular data while not consuming significant computational resources. The training and inference times were measured. The same performance metrics as for the NN were computed.

The best-performing model was the VF RF. To assess if its detection accuracy is stable across different testing sets, we computed a 95% confidence interval (CI) using bootstrapping. We created 5000 new testing sets of the same size as the original testing set by randomly drawing instances from it with replacement. We then computed the accuracy of the RF model, without changing its training

set, on each of the 5000 testing sets. We sorted the results and identified the 2.5th and 97.5th percentiles to observe which values 95% of the accuracies fall between.

To show a statistically significant difference between the VF RF and the Connors and Sarkar [4] NN, we retrained and re-evaluated each model 10 times on the same training and testing sets as in the initial experiment. The accuracies from each iteration were recorded into separate lists for the RF and NN models. We then applied the Wilcoxon signed-rank test on the two lists and recorded the resulting p-value.

To the best of our knowledge, no other studies have explored individual feature selection on the EMBER2018 dataset. As discussed in Section 2, Oyama et al. [8] and Şandor et al. [9] have investigated feature group selection, but not the selection of individual features within the dataset's feature groups, which is what we accomplish in this study using a variance-based approach.

### 4 Results

All experiments were performed on a 2024 Apple Macbook Pro with an M4 MAX chip (16-core CPU, 40-core GPU) and 64 GB of unified memory [19].

Connors and Sarkar [4] report an accuracy of 95.22% for their NN model trained on the entire feature set. We were not able to obtain the exact same accuracy, but we came very close with an accuracy of 95.05% (see Table 2). Various factors, such as slightly different library versions or different randomization mechanisms, could have contributed to this small difference in results. Even if we were able to replicate the experiment exactly, our RF model trained on the VF dataset would still perform better, with an accuracy of 96.9% (see Table 2). That is a 1.85% increase in accuracy over the best-performing model trained by Connors and Sarkar [4], an NN trained on the entire feature set. As can be observed in Table 2, the 1.85% increase in accuracy translates to 3,693 more correctly labeled samples (2,592 false positives correctly reclassified as true negatives and 1,101 false negatives correctly reclassified as true positives). The AUC, which is reported in Table 3 and Figure 1, is higher for the VF RF model compared to the Connors and Sarkar [4] NN, indicating superior classification performance.

The RF model trained on the VF dataset trained  $7.1 \times$  times faster than the NN Model (3 minutes and 13.83 seconds vs. 22 minutes and 55.58 seconds). Its inference time for the 200,000 samples is  $1.67 \times$  times faster than the NN Model (6.08 seconds vs. 3.64 seconds, see Figure 2).

The CI in Figure 3 indicates that 95% of the accuracies of the VF RF, computed across 5000 testing sets generated using bootstrapping, fall between 96.60% and 96.80%, with a mean of 96.70%. This narrow range suggests that the model's performance is stable and does not vary significantly across different testing sets.

The p-value obtained from the Wilcoxon signed-rank test was 0.001953, which is smaller than 0.05, meaning that there is a statistically significant difference

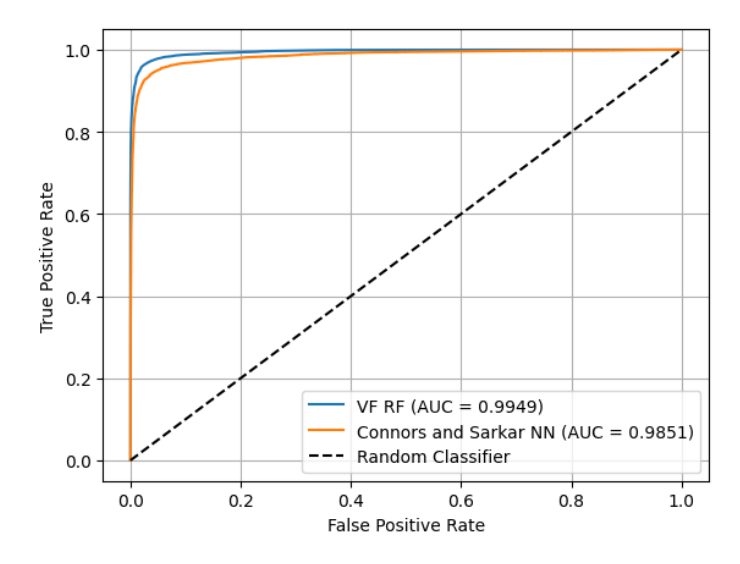
between the two models. The accuracies for the VF RF ranged between 96.71% and 96.9%. The accuracies for the Connors and Sarkar [4] NN ranged between 94.69% and 95.19%.

| Model                     | TN     | FP    | FN    | TP     | Accuracy (%) |
|---------------------------|--------|-------|-------|--------|--------------|
| Connors and Sarkar [4] NN | 95,289 | 4,711 | 5,184 | 94,816 | 95.05        |
| VF RF                     | 97,881 | 2,119 | 4,083 | 95,917 | 96.90        |
| VF LGBM                   | 91,211 | 8,789 | 5,097 | 94,903 | 93.06        |
| RF (Full Dataset)         | 95,854 | 4,146 | 5,291 | 94,709 | 95.28        |
| LGBM (Full Dataset)       | 92,342 | 7,658 | 4,490 | 95,510 | 93.93        |

Table 2. Confusion matrix metrics and classification accuracy across model variants

| Model                     | AUC    | Precision | Recall | F1     | Kappa  |
|---------------------------|--------|-----------|--------|--------|--------|
| Connors and Sarkar [4] NN | 0.9851 | 0.9505    | 0.9505 | 0.9505 | 0.9011 |
| VF RF                     | 0.9949 | 0.9784    | 0.9592 | 0.9687 | 0.9380 |
| VF LGBM                   | 0.9833 | 0.9152    | 0.9490 | 0.9318 | 0.8611 |
| RF (Full Dataset)         | 0.9899 | 0.9581    | 0.9471 | 0.9525 | 0.9056 |
| LGBM (Full Dataset)       | 0.9858 | 0.9258    | 0.9551 | 0.9402 | 0.8785 |

Table 3. Comparative evaluation of model performance metrics on the test set



 ${\bf Fig.\,1.}$  ROC curves comparing the performance of the VF RF and the NN

#### 8 Todea et al.

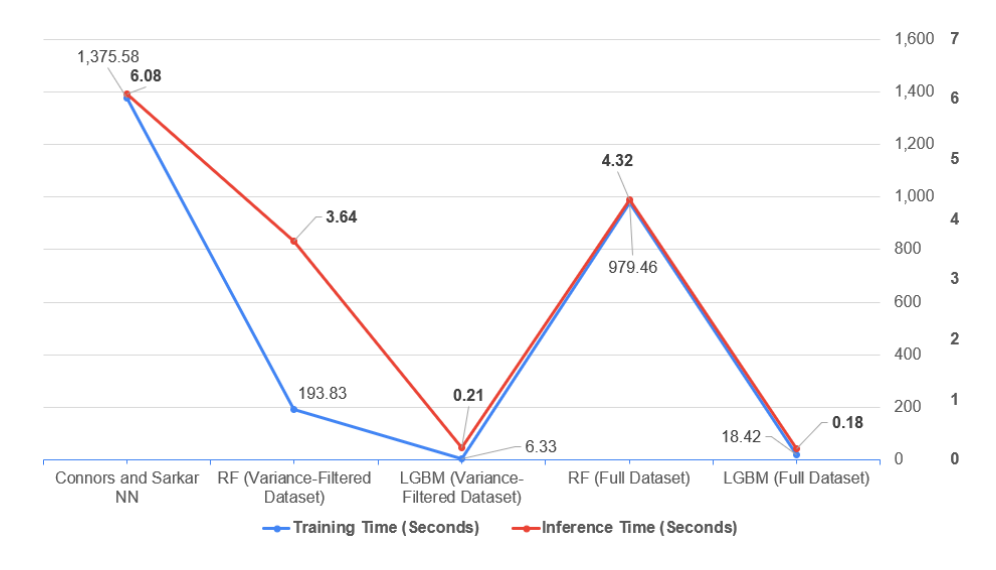


Fig. 2. Training duration and inference time for each model variant

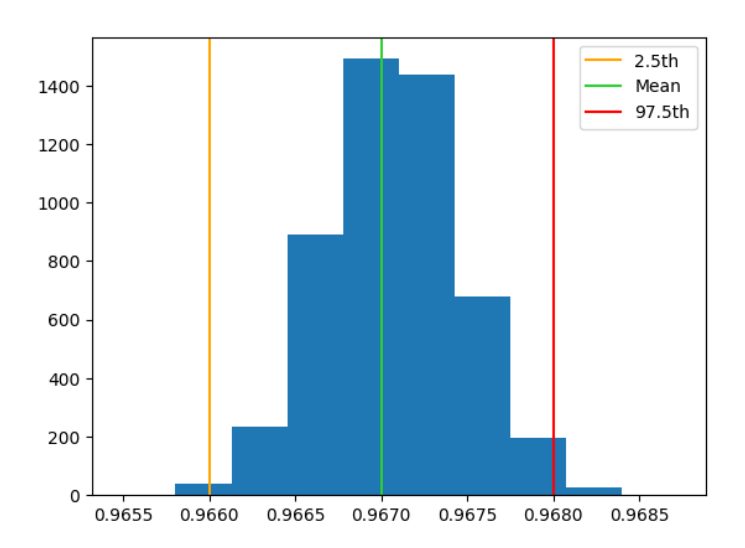


Fig. 3. 95% CI for the VF RF computed using bootstrapping with 5000 testing sets

## 5 Conclusion

This paper has replicated the NN model trained on the full feature set of the EMBER2018 dataset [1] by Connors and Sarkar [4], and demonstrated that,

through feature reduction and informed model selection, it can be outperformed in both accuracy and training time. Using our RF model trained and evaluated on a VF version of the EMBER2018 dataset, we achieved a 1.85% increase in accuracy while reducing training time by a factor of 7.1. The 1.85% increase in accuracy translates to 3,693 more correctly labeled samples, meaning that 3,693 more users would receive correct results for their PE file scans if the model were integrated in a real-life intrusion detection system (IDS). This, combined with the greatly reduced training time, which translates to faster updates to the known malware database, means that our approach would perform significantly better in the real world. The reduced update time is especially important given that hundreds of thousands of new malware are discovered daily [20].

Our accuracy is 2.81% better than the accuracy of 94.09% reported by Lad and Adamuthe [12] and 0.34% better than the accuracy of 96.56% reported by Shashank et al. [11]. Our accuracy is a little worse than the accuracy of 97.96% reported by Ghourabi [10]. However, it is not possible to verify if this is true, as the code or any implementation details for the Bayesian optimization were not provided. It is also not possible to compare training time with the papers that didn't make their code public.

Future work should focus on experimenting with more models that are known to behave well on tabular data. Multivariate feature selection could help improve the results if used alone or on top of univariate selection. Exploring embedded feature selection methods, possibly even in the context of RF, might lead to positive outcomes. If the resources allow, automated hyperparameter tuning and wrapper feature selection methods could be employed.

Aside from attempting to obtain better performance, future work can integrate our best model into an IDS. Two aspects must be considered when discussing such a system: processing new files inputted by the user and updating the system with new samples. Anderson and Roth [14] make these simple by providing code that takes as input a PE file and extracts from it the same features they extracted. It can be modified only to extract the individual features that remained after our variance filter. As a result, our model can make predictions on newly seen PE files. To update the system, the model needs to be retrained. After extracting the features with the code provided by Anderson and Roth [14], new samples can be added to the existing training set, and our model can be retrained.

**Acknowledgement.** This work has been partially supported by (1) the project RoNaQCI, part of EuroQCI, ID: DIGITAL-2021-QCI-01-DEPLOY-NATIONAL, 101091562, and (2) the project "Romanian Hub for Artificial Intelligence - HRIA", Smart Growth, Digitization and Financial Instruments Program, 2021-2027, MySMIS no. 334906

### References

1. H. S. Anderson and P. Roth, "EMBER: An open dataset for training static PE malware machine learning models," arXiv preprint arXiv:1804.04637, 2018.

- Kaggle, "Your Machine Learning and Data Science Community." [Online]. Available: https://www.kaggle.com. [Accessed: Apr. 10, 2025].
- R. Harang and B. Filar, "SOREL-20M: A large scale benchmark dataset for malicious PE detection," in *Proc. Virus Bulletin Conf.*, 2020. [Online]. Available: https://github.com/sophos-ai/SOREL-20M. [Accessed: Apr. 10, 2025].
- 4. C. Connors and D. Sarkar, "Machine learning for detecting malware in PE files," in *Proc. 2023 Int. Conf. Mach. Learn. Appl. (ICMLA)*, IEEE, 2023, pp. 2194–2199.
- C. Connors and D. Sarkar, "Machine Learning for Detecting Malware in PE Files

   GitHub Repository." [Online]. Available: https://github.com/CollinConnors/Machine-learning-for-detecting-malware-in-pe-files. [Accessed: Apr. 7, 2025].
- The Scikit-learn Developers, "Scikit-learn" [Online]. Available: https://scikit-learn. org. [Accessed: Apr. 8, 2025].
- 7. The LightGBM Developers, "lightgbm.LGBMClassifier." [Online]. Available: https://lightgbm.readthedocs.io/en/latest/pythonapi/lightgbm.LGBMClassifier.html. [Accessed: Apr. 8, 2025].
- 8. Y. Oyama, T. Miyashita, and H. Kokubo, "Identifying useful features for malware detection in the EMBER dataset," in *Proc. 2019 7th Int. Symp. Comput. Netw. Workshops (CANDARW)*, IEEE, 2019, pp. 360–366.
- M. Şandor, R. M. Portase, and A. Coleşa, "EMBER feature dataset analysis for malware detection," in *Proc. 2023 IEEE 19th Int. Conf. Intell. Comput. Commun. Process. (ICCP)*, IEEE, 2023, pp. 203–210.
- A. Ghourabi, "A security model based on LightGBM and Transformer to protect healthcare systems from cyberattacks," *IEEE Access*, vol. 10, pp. 48890–48903, 2022.
- 11. N. S. Shashank, S. D. Madhu Kumar, et al., "Enhancing malware detection: A comparative analysis of ensemble learning approaches," in *Proc. 2024 1st Int. Conf. Technol. Innov. Adv. Comput. (TIACOMP)*, IEEE, 2024, pp. 35–40.
- S. S. Lad and A. C. Adamuthe, "Improved deep learning model for static PE files malware detection and classification," *Int. J. Comput. Netw. Inf. Secur.*, vol. 11, no. 2, pp. 14, 2022.
- 13. H. Alshaher, "Studying the effects of feature scaling in machine learning," Ph.D. dissertation, North Carolina Agricultural and Technical State Univ., 2021.
- H. S. Anderson and P. Roth, "EMBER2018 Dataset GitHub Repository." [Online].
   Available: https://github.com/elastic/ember. [Accessed: Apr. 7, 2025].
- 15. A. Todea, C. Pungilă, and A. Spătaru, "EMBER2018 Experiments GitHub Repository." [Online]. Available: https://github.com/alexandrutodea/ember2018-experiments. [Accessed: Apr. 7, 2025].
- 16. The NumPy Developers, "NumPy." [Online]. Available: https://numpy.org. [Accessed: Apr. 7, 2025].
- 17. The Keras Developers, "Keras." [Online]. Available: https://keras.io. [Accessed: Apr. 8, 2025].
- M. Ryan and L. Massaron, Machine Learning for Tabular Data, Manning Publications, Feb. 2025. ISBN: 9781633438545.
- 19. Apple, "MacBook Pro (16-inch, 2024) Tech Specs." [Online]. Available: https://support.apple.com/en-us/121554. [Accessed: Apr. 9, 2025].
- 20. J. V. Estenssoro, "Malware And Virus Statistics 2025: The Trends You Need to Know About" [Online]. Available: https://www.avg.com/en/signal/malware-statistics. [Accessed: Jun. 23, 2025].

## Relational Matrix of Cyberattacks: A Model for Threat Classification and Connection in Digital Environments

Mikel Ferrer Oliva<sup>1</sup>[0009-0001-0610-8210], José Amelio Medina Merodio<sup>1</sup>[0000-0003-3359-4952], José Javier Martínez Herraiz<sup>1</sup>[0000-0002-2351-7163] and Alberto Larena Luengo<sup>1</sup>[0009-0004-1583-390X]

<sup>1</sup> Universidad de Alcalá, Departamento de Ciencias de la Computación, 28801, Madrid, España {mikel.ferrer; josea.medina; josej.martinez; alberto.larena}@uah.es

**Abstract.** The increasing complexity of cyberattacks requires classification systems capable of representing how techniques interact and evolve. This paper introduces a relational matrix composed of eight attack groups and twenty directional connections that capture how one type of attack facilitates another. The matrix addresses limitations of static classifications by explicitly modeling interdependencies observed in documented incidents. Unlike hierarchical schemes, it enables bidirectional analysis of attack progressions and supports the incorporation of techniques without altering the overall structure. By identifying common escalation paths, the matrix enhances threat anticipation, improves strategic planning and supports early detection. Its structure offers a scalable and adaptable method for analysing adversarial behaviour across digital environments.

**Keywords:** Cybersecurity, relational matrix, threat classification, attack progression, dependency modeling

## 1 Introduction

Digital transformation has increased organisational exposure to cyber threats. Attacks have evolved from isolated events to coordinated sequences involving multiple techniques. This shift calls for classification systems that capture not only tactics but also their strategic interconnections. Efforts like MITRE ATT&CK [1], STIX 2.1 [2], and TAXII [3] have advanced threat systematisation and information sharing. Platforms such as MISP [4] enable categorisation using standard vocabularies. However, these models lack mechanisms to represent how attack phases are interdependent, limiting their capacity to identify enabling relationships[5]. Research shows that cyberattacks often follow multi-stage sequences. Social Engineering (SE) frequently initiates campaigns, particularly for credential compromise and Malware-Based Attacks (MBA) [6] [7]. Exploiting Software Vulnerabilities (ESV) also plays a key role in maintaining persistence [8] [9]. Still, current taxonomies do not adequately capture these facilitative chains or support forecasting across organisational layers.

Therefore, the objective of this work is to propose a relational matrix of cyberattacks that models the directional links between eight main attack groups. This structure

enables a dynamic analysis of attack evolution and improves the representation of sequential risk scenarios. The paper is organized as follows. Section 2 presents the theoretical basis of the proposal and discusses the limitations of static models. Section 3 defines the attack categories and describes the relational matrix of connections. Section 4 discusses the implications of the model for incident analysis and strategic defense. Section 5 offers the main conclusions and outlines lines of future work.

## 2 Theoretical Foundation

The sophistication of cyber threats has led to models for classifying and analysing attacks. CASE [10] aimed to standardise event representation, but saw limited adoption. MISP [4] provides structured vocabularies for threat exchange, yet lacks the ability to model strategic dependencies between attacks. Many studies emphasise the need to understand how certain techniques enable later stages. Static taxonomies fail to reflect these interdependencies, reducing their value for anticipating escalation paths or analysing adversarial behaviour in complex scenarios [5].

#### 2.1 Limitations of Static Models

Static taxonomies like MITRE ATT&CK [1] and MISP [4] offer structured listings of attack techniques but fail to reflect the dynamic interdependencies that define real-world incidents. By treating attacks as isolated events, these models lack the capacity to trace escalation paths or campaign progressions [5]. Studies show that cyberattacks typically unfold in stages: early vectors such as phishing often lead to credential theft and subsequent malware deployment [6] [7], while exploiting software vulnerabilities ensures persistence in later phases [8] [9].

Such transitions are rarely formalised, despite documented examples. Watering hole attacks compromise legitimate websites to deliver malware [11]; ransomware campaigns exploit remote access credentials [12]; and hybrid malware like *Lucifer* combines cryptojacking, exploiting software vulnerabilities (ESV) and DDoS to maximise disruption [13]. In IoT contexts, large-scale botnet attacks illustrate how device vulnerabilities enable chained intrusions [14] [15]. Capturing these sequential and tactical patterns is essential to model adversarial behaviour and anticipate threats. Without such modelling, static schemes remain disconnected from the needs of operational cybersecurity [16] [17] [18].

## 2.2 Consequences for Risk Management and Intelligence Sharing

The use of standardised formats like STIX 2.1 [2] and TAXII [3] facilitates consistent information exchange, yet they lack mechanisms to model sequential or enabling attack relationships. Their focus remains on isolated techniques, not on transitions between phases [16] [19]. Similarly, MISP [4] taxonomies support operational tasks but omit structural dependencies. CASE [10] aimed to unify ontologies but saw limited adoption and relevance. Studies show that seemingly isolated incidents often reflect coordinated strategies, where Social Engineering (SE) enables lateral movement and the

exploitation of hidden vulnerabilities typically linked to Identity and Authentication Attacks (IAA) or Exploiting Software Vulnerabilities (ESV) [9] [20] [21]. These chains are underrepresented in current standards, reducing predictive capability.

Complex threats like supply chain attacks demand models that capture coordinated tactics. Frameworks such as the Diamond Model [22] and VERIS [23] stress the need to map relationships to support strategic decisions and risk analysis [19].

## 3 Proposed Cyberattack Matrix

The relational model for classifying cyberattacks captures the interdependencies between adversarial actions. Unlike hierarchical or linear taxonomies, the matrix models dynamic links between attack groups, each defined by a strategic function and capable of acting as initiators or enablers within coordinated campaigns. It draws on documented incidents, technical reports, and scientific literature.

## 3.1 Classification of Attack Groups

The classification of attack groups is based on identifying both the initial vector and the adversary's strategic objective. Each group brings together techniques used in similar intrusion phases, facilitating the detection of operational patterns and improving defensive planning. Rather than clustering techniques by tools or technical similarities, the model adopts a functional logic that focuses on their tactical role within adversarial campaigns. Restricting the taxonomy to eight distinct groups ensures a balanced granularity: it avoids overlapping categories while capturing the most frequent and critical escalation paths. This structure enables clear mapping of entry vectors, transitions between phases and persistent threats, without fragmenting the model. Notably, complex attacks such as supply chain compromises—which often combine social engineering, malware deployment, software exploitation and long-term persistence—can be entirely described within this segmentation. Thus, the eight-group model preserves internal coherence while maximising explanatory coverage without requiring ad hoc categories or extensions. Table 1 summarises the resulting classification.

Table 1. Attack Groups Classification and Description.

| Strike Group               | Description   |
|----------------------------|---|
| Social Engineering         | Psychological manipulation to extract information or induce un-     |
| (SE)                       | safe behaviour. Phishing is the most documented vector [6].         |
| Malware-based attacks      | Malicious code to compromise systems, gain persistence or ena-      |
| (MBA)                      | ble lateral movement (ransomware, trojans, botnets) [12].           |
| Network Infrastructure     | Targeting routers and network devices to disrupt connectivity or    |
| Attacks (NIA)              | integrity [19].   |
| <b>Exploiting Software</b> | Exploiting flaws to escalate privileges, execute code or access re- |
| Vulnerabilities (ESV)      | stricted resources [20].  |

## 3.2 Relational Dependencies Between Groups

The core of the matrix consists of twenty directional relationships between cyberattack groups, each reflecting typical sequences observed in real-world incidents. All relationships have been validated through documented cases, as detailed below:

- IAA → SE: When attackers gain valid credentials, they can craft tailored social
  engineering strategies that enhance deception effectiveness [6] [7]. This is evident
  in SIM-swapping attacks, where adversaries tricked telecom providers into duplicating SIM cards, enabling interception of two-factor authentication codes [25].
- IAA → MBA: Stolen credentials provide silent access that bypasses perimeter defences and enables malware deployment [26] [12]. This occurred in the DarkSide case, where attackers used compromised VPN credentials to access Colonial Pipeline's network and deploy ransomware that halted fuel distribution [27].
- IAA → ESV: Privileged access allows discovery and exploitation of vulnerabilities
  that would otherwise remain inaccessible [16] [15]. In the Microsoft Exchange
  breach, attackers exploited ProxyLogon flaws after logging in with stolen credentials [28].
- IAA → APC: Protocol-level authentication compromise enables interception or manipulation of communications without additional exploits [20] [15]. This occurred in the Target breach, where NTLM authentication was exploited using passthe-hash techniques [29].
- IAA → NIA: Administrative credentials allow attackers to reconfigure network devices and establish persistent access [17] [14]. This was demonstrated by the Mozi botnet, which compromised IoT routers using default passwords to launch peer-to-peer DDoS attacks [30].
- 6. SE → MBA: Phishing and other deceptive techniques often trick users into executing malware in trusted environments [6] [31]. In Emotet campaigns, users opened attachments that downloaded and executed malware at scale [32].
- SE → ESV: Malspam can redirect victims to vulnerable applications, triggering remote code execution [11] [16]. Exploits like CVE-2017-11882 embedded in RTF documents enabled memory corruption in Microsoft Office [33].
- MBA → APC: Certain malware variants are designed to interfere with communication protocols to spread or exfiltrate data [15] [20]. WannaCry exploited SMBv1 vulnerabilities to replicate across networks and disrupt file-sharing services [34].

- MBA → NIA: Malware-infected devices are used to form botnets that degrade network integrity or launch large-scale attacks [9] [14]. Mirai used Telnet-accessible IoT devices to flood DNS providers and cause widespread outages [35].
- MBA → CIIA: Malicious code can disable or manipulate critical control systems in industrial environments [9] [18]. NotPetya spread via a compromised software update and disrupted Ukraine's energy and logistics sectors [36].
- 11. MBA → ESV: Advanced malware often scans systems for unpatched vulnerabilities to escalate control [16] [15]. TrickBot loaders exploited EternalBlue flaws to gain deeper persistence in infected networks [37].
- ESV → APC: Vulnerabilities in encrypted services allow attackers to intercept or extract confidential data [20] [15]. The Heartbleed flaw in OpenSSL enabled memory leaks from secure communication sessions [38].
- 13. ESV → NIA: Remote code execution enables lateral movement into core network components [17] [15]. Log4Shell enabled adversaries to breach internal infrastructure via exposed services [39].
- 14. ESV → APT: Advanced persistent threats exploit software flaws to maintain stealthy access in strategic systems [8] [16]. The SolarWinds attack inserted backdoors into the Orion platform using vulnerabilities affecting US government networks [40].
- 15. APC → NIA: Manipulating DNS and other protocols allows attackers to embed themselves in infrastructure and persist [16] [14]. In the Sea Turtle campaign, DNS records were altered to redirect authentication flows and compromise core systems [41].
- 16. APC → APT: Hijacked communication channels support long-term espionage and data theft [16] [15]. Sea Turtle attackers used DNS hijacking to harvest credentials and maintain covert access [42].
- 17. APC → CIIA: Protocol-level attacks in OT environments enable remote manipulation of industrial processes [9] [15]. Industroyer exploited IEC-104 to disable Ukrainian substations and trigger blackouts [43].
- 18. NIA → APT: Network compromises offer a base for long-term surveillance and pivoting into high-value systems [9] [18]. VPNFilter infected routers to intercept traffic and support advanced intrusion [44].
- NIA → CIIA: Lateral movement from IT to OT systems can disrupt critical infrastructures [8] [18]. GreyEnergy breached corporate networks and reached industrial controls in the energy sector [45].
- 20. APT → CIIA: Long-term access by advanced threats enables sabotage or strategic data exfiltration [9] [16]. Stuxnet reprogrammed PLCs in Iranian nuclear facilities using multiple zero-days and forged certificates [46].

## 3.3 Cyberattack Relationship Matrix

To represent dependencies among attack groups, the proposed model adopts a relational matrix format. Each row corresponds to an initial vector, each column to a facilitated group, and binary values (1 or 0) indicate the presence or absence of direct relationships based on empirical evidence. This bidimensional structure enables a compact

visualisation of connections and offers greater analytical flexibility than hierarchical models. For instance, Identity and Authentication Attacks (IAA) enable others such as Social Engineering (SE), Malware-Based Attacks (MBA), or Exploiting Software Vulnerabilities (ESV), underscoring IAA's pivotal role in early intrusion phases. By modelling such links, the matrix helps identify critical escalation paths and design defence strategies based on how attacks structurally evolve. Importantly, the model includes 20 directed relationships, each selected through strict criteria of empirical traceability. This number reflects a deliberate focus on transitions that have been clearly and technically documented in real-world incidents.

| Initial Attack ↓ / Facilitated Attack → | SE | MBA | ESV | APC | NIA | CIIA | APT |
|---|----|-----|-----|-----|-----|------|-----|
| IAA                                     | 1  | 1   | 1   | 1   | 1   | 0    | 0   |
| SE                                      | 0  | 1   | 1   | 0   | 0   | 0    | 0   |
| MBA                                     | 0  | 0   | 1   | 1   | 1   | 1    | 0   |
| ESV                                     | 0  | 0   | 0   | 1   | 1   | 0    | 1   |
| APC                                     | 0  | 0   | 0   | 0   | 1   | 1    | 1   |
| NIA                                     | 0  | 0   | 0   | 0   | 0   | 1    | 1   |

Table 3. Relational Matrix of Direct Cyberattack Dependencies

To support the interpretation of the relationships captured in the matrix, a visual framework was developed to represent the attack groups and the documented interconnections among them. This graphical representation is directly based on the proposed matrix structure, providing a concise overview of how transitions between different types of attacks are articulated.

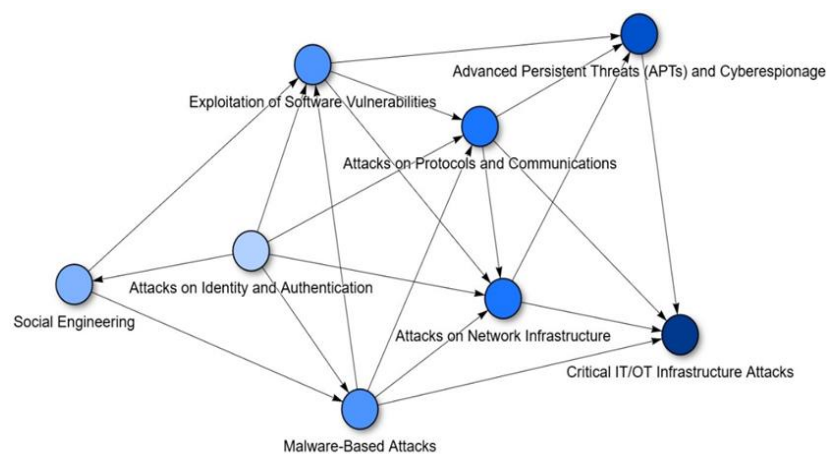


Fig. 1. Framework of attack groups and their interrelations.

## 4 Discussion

The relational classification of cyberattacks provides a structural response to the limitations of static and hierarchical models. Although traditional taxonomies organise techniques efficiently, they fail to capture how these interact within coordinated sequences [1] [4] [5], limiting their usefulness for forecasting and incident response. Cyber incidents often unfold through interdependent phases, with Social Engineering (SE) or Identity and Authentication Attacks (IAA) enabling steps such as Malware-Based Attacks (MBA), Exploiting Software Vulnerabilities (ESV) or Advanced Persistent Threats (APT) [6] [7] [8] [9].

The proposed matrix bridges this gap by representing directional links between categories. Its twenty empirically validated relationships reflect real-world patterns observed in documented incidents and threat intelligence [16] [20] [24] [15], facilitating identification of escalation routes that static schemes often miss. Its relational structure allows new techniques to be integrated without altering the overall logic, ensuring scalability as threats evolve [5] [23]. It also identifies critical starting points: IAA links to five groups, highlighting its strategic relevance, while MBA's connections support its role in maintaining persistence and enabling lateral movement. Additionally, the model integrates the human factor. SE and IAA, shaped by user behaviour, function as entry points to more technical phases, emphasising the importance of behavioural control in cybersecurity programmes [21]. Finally, it aligns with models like the Diamond Model [22] and VERIS [23], but distinguishes itself by offering a compact, predictive classification framework suitable for both research and practice.

## 5 Conclusions

This work has presented a relational matrix for classifying cyberattacks, designed to represent the sequential and enabling nature of adversarial techniques. Unlike static models, it organises eight attack groups and twenty directional links, capturing how specific techniques facilitate others. By modelling these dependencies, the matrix improves the understanding of threat progression and supports the anticipation of complex escalation paths, addressing core limitations of conventional taxonomies.

At the organisational level, it enables early detection, optimises the allocation of defensive resources, and enhances incident response planning. It also identifies structurally critical attack groups that serve as early indicators of more advanced intrusions. From a social perspective, the model highlights the relevance of human factors by linking initial vectors to user behaviour patterns.

As a future line of research, this matrix may be further validated through empirical applications across various domains, including critical infrastructure and sector-specific environments. A key focus will be its alignment with structured threat representation languages. Specifically, the relational framework introduced here could be implemented in STIX 2.1 as custom objects or extended relationships that explicitly encode facilitation paths. These relationships may be shared through TAXII and integrated into

MISP using standardised taxonomies, enabling interoperability and semantic precision in threat intelligence sharing.

#### Acknowledgments

This work has been developed within the "Recovery, Transformation and Resilience Plan", project C084/23 Ada Byron INCIBE-UAH, funded by the European Union (Next Generation).

## References

- ATT&CK: Adversarial Tactics, Techniques, and Common Knowledge, MITRE, 2025.
   [Online]. Available: https://attack.mitre.org/. Accessed: Jun. 6, 2025.
- STIX Version 2.1. Committee Specification 02, O. C. T. I. TC, 2021-07-19 2025. [Online]. Available: https://docs.oasis-open.org/cti/stix/v2.1/cs02/stix-v2.1-cs02.html. Accessed: Jun. 6, 2025.
- 3. TAXII Version 2.1. Committee Specification 01, O. C. T. I. TC, 2021-07-18 2025. [Online]. Available: https://docs.oasis-open.org/cti/taxii/v2.1/cs01/taxii-v2.1-cs01.html. Accessed: Jun. 6, 2025.
- CIRCL, "MISP taxonomies and classification as machine tags," misp-project.org. [Online]. Available: https://www.misp-project.org/. Accessed: Jun. 6, 2025.
- ENISA, "ENISA Threat Landscape for Supply Chain Attacks," European Union Agency for Cybersecurity (ENISA), 2021. [Online]. Available: https://www.enisa.europa.eu/sites/default/files/publica
  - tions/ENISA%20Threat%20Landscape%20for%20Supply%20Chain%20Attacks.pdf. Accessed: Jun. 6, 2025.
- A. Bhardwaj and V. Sapra, "Why is phishing still successful?," Computer Fraud & Security, vol. 2020, pp. 15–19, Sep. 18, 2020. doi: 10.1016/S1361-3723(20)30098-1.
- D. N. Hellemann, "Human Risk Review 2023," SoSafe Awareness GmbH, Colonia, Alemania, Report 2023. [Online]. Available: https://www.sosafe-awareness.com/. Accessed: Jun. 6, 2025.
- L. Y. Connolly and D. S. Wall, "The rise of crypto-ransomware in a changing cybercrime landscape: Taxonomising countermeasures," Computers & Security, vol. 87, 2019, doi: 10.1016/j.cose.2019.101568.
- M. V. Clavijo Mesa, C. E. Patino-Rodriguez, and F. J. Guevara Carazas, "Cybersecurity at Sea: A Literature Review of Cyber-Attack Impacts and Defenses in Maritime Supply Chains," Information, vol. 15, no. 11, 2024, doi: 10.3390/info15110710.
- 10. C. Community. "CASE: Cyber-investigation Analysis Standard Expression." CASE Community. https://caseontology.org/. Accessed: Jun. 6, 2025.
- 11. S. Alrwais, K. Yuan, E. Alowaisheq, X. Liao, A. Oprea, X. Wang, and Z. Li, Catching Predators at Watering Holes: Finding and Understanding Strategically Compromised Websites. 2016, pp. 153–166.
- 12. C. Beaman, A. Barkworth, T. D. Akande, S. Hakak, and M. K. Khan, "Ransomware: Recent advances, analysis, challenges and future research directions," Comput Secur, vol. 111, p. 102490, Dec 2021, doi: 10.1016/j.cose.2021.102490.
- 13. P. A. Networks, "Lucifer: New Cryptojacking and DDoS Hybrid Malware Exploiting High and Critical Vulnerabilities to Infect Windows Devices," Palo Alto Networks Unit 42, USA, 2025. [Online]. Available: https://unit42.paloaltonetworks.com. Accessed: Jun. 6, 2025.

- M. Gelgi, Y. Guan, S. Arunachala, M. Samba Siva Rao, and N. Dragoni, "Systematic Literature Review of IoT Botnet DDOS Attacks and Evaluation of Detection Techniques," Sensors (Basel), vol. 24, no. 11, Jun 1 2024, doi: 10.3390/s24113571.
- Q. Wu, S. Zhang, B. Zheng, C. You, and R. Zhang, "Intelligent Reflecting Surface-Aided Wireless Communications: A Tutorial," IEEE Transactions on Communications, vol. 69, no. 5, pp. 3313-3351, 2021, doi: 10.1109/tcomm.2021.3051897.
- U. Rauf, F. Mohsen, and Z. Wei, "A Taxonomic Classification of Insider Threats: Existing Techniques, Future Directions & Recommendations," Journal of Cyber Security and Mobility, 2023, doi: 10.13052/jcsm2245-1439.1225.
- M. M. Salim, S. Rathore, and J. H. Park, "Distributed denial of service attacks and its defenses in IoT: a survey," The Journal of Supercomputing, vol. 76, no. 7, pp. 5320-5363, 2019, doi: 10.1007/s11227-019-02945-z.
- 18. F. Y. Á. Niño, "Ransomware, una amenaza latente en Latinoamérica," InterSedes, vol. 24, no. 49, 2023, doi: 10.15517/isucr.v24i49.50765.
- E. M. Hutchins, M. J. Cloppert, and R. M. Amin, "Intelligence-Driven Computer Network Defense Informed by Analysis of Adversary Campaigns and Intrusion Kill Chains," Leading Issues in Information Warfare & Security Research, vol. 1, no. 1, pp. 80-106, 2025-03-19 2011. [Online]. Available: https://www.lockheedmartin.com/content/dam/lockheed-martin/rms/documents/cyber/LM-White-Paper-Intel-Driven-Defense.pdf. Accessed: Jun. 6, 2025.
- D. Javeed, U. MohammedBadamasi, C. O. Ndubuisi, F. Soomro, and M. Asif, "Man in the Middle Attacks: Analysis, Motivation and Prevention," International Journal of Computer Networks and Communications Security, vol. 8, no. 7, pp. 52-58, 2020, doi: 10.13140/RG.2.2.22752.81928.
- J. J. Sedano Pinzón, "El contexto actual e histórico de la ingeniería social," LATAM Revista Latinoamericana de Ciencias Sociales y Humanidades, vol. 5, no. 5, 2024, doi: 10.56712/latam.v5i5.2691.
- 22. S. Caltagirone, A. Pendergast, and C. Betz, The Diamond Model of Intrusion Analysis, 2013. doi: 10.13140/RG.2.2.31143.56481.
- 23. V. Community. "VERIS: Vocabulary for Event Recording and Incident Sharing." VERIS Community. [Online]. Available: https://verisframework.org/. Accessed: Jun. 6, 2025.
- 24. CISA and FBI, "TrickBot Malware," Cybersecurity and Infrastructure Security Agency (CISA), Federal Bureau of Investigation (FBI), USA, AA21-076A, 2021. [Online]. Available: https://www.cisa.gov/news-events/alerts/2021/03/17/cisa-fbi-joint-advisory-trickbot-malware-0. Accessed: Jun. 6, 2025.
- Insikt Group, The Business of Fraud: SIM Swapping. Recorded Future, Aug. 25, 2021.
   [Online]. Available: https://go.recordedfuture.com/hubfs/reports/cta-2021-0825.pdf. Accessed: Jun. 6, 2025.
- M. Ivanov, B. Kliuchnikova, I. Chugunkov, and A. Plaksina, Phishing Attacks and Protection Against Them, pp. 425–428, Jan. 26, 2021, doi: 10.1109/ElCon-Rus51938.2021.9396693.
- CISA and FBI, Darkside Ransomware: Best Practices for Preventing Business Disruption from Ransomware Attacks. Cybersecurity and Infrastructure Security Agency, May 11, 2021. [Online]. Available: https://www.cisa.gov/sites/default/files/publications/AA21-131A\_Darkside\_Ransomware.pdf. Accessed: Jun. 6, 2025.
- 28. CISA, "MITIGATE MICROSOFT EXCHANGE ON-PREMISES PRODUCT VULNERABILITIES," Cybersecurity and Infrastructure Security Agency (CISA), 2021. [Online]. Available: https://www.cisa.gov/ED2102. Accessed: Jun. 6, 2025.

- United States Senate Committee on Commerce, Science, and Transportation, A "Kill Chain" Analysis of the 2013 Target Data Breach. United States Senate Committee on Commerce, Science, and Transportation, 2014. [Online]. Available: https://www.commerce.senate.gov/services/files/24d3c229-4f2f-405d-b8db-a3a67f183883. Accessed: Jun. 6, 2025.
- E. Council to Secure the Digital, Ustelecom, and A. Consumer Technology, "INTERNATIONAL BOTNET AND IOT SECURITY GUIDE 2021," USTelecom; Consumer Technology Association (CTA), 2021.
- A. L. Álvarez, J. A. Cruz, S. B. Cruz, J. d. C. Gallardo, I. M. López, and R. E. García, "El phishing como amenaza en la ciberseguridad corporativa de grandes empresas," Investigaciones Latinoamericanas en Ingeniería y Arquitectura, no. 1, pp. 26-33, 2024, doi: 10.51378/ilia.vi1.8496.
- 32. ANSSI, "The Malware-As-Service-Emotet," Agence Nationale de la Sécurité des Systèmes d'Information (ANSSI), 2021/02/12 2021. [Online]. Available: www.cert.ssi.gouv.fr
- 33. Cysiv, "Threat Report: Formbook Infostealer," Cysiv Inc., 2021/02/23 2021. [Online]. Available: www.cysiv.com. Accessed: Jun. 6, 2025.
- 34. W. Smart, "Lessons learned review of the WannaCry Ransomware Cyber Attack," NHS England, 2018/02/01 2018. [Online]. Available: www.gov.uk/dh. Accessed: Jun. 6, 2025.
- 35. Cloudflare, "DNS and the Threat of DDoS," Cloudflare Inc., 2022/11/04 2022.
- 36. S. Steinberg, A. Stepan, K. Neary, G. Rattray, and J. Healey, "NotPetya: A Columbia University Case Study," Case Consortium @ Columbia, School of International and Public Affairs, Columbia University, SIPA-21-022.1, 2021.
- ANSSI, "RYUK RANSOMWARE," Agence Nationale de la Sécurité des Systèmes d'Information (ANSSI), 2021/02/25 2021. [Online]. Available: www.cert.ssi.gouv.fr
- 38. ICS-CERT, "ICS-CERT MONITOR January April 2014," U.S. Department of Homeland Security (DHS), National Cybersecurity and Communications Integration Center (NCCIC), 2014.
- 39. F. B. o. I. F. Cybersecurity and Infrastructure Security Agency (CISA), National Security Agency (NSA), Australian Cyber Security Centre (ACSC), Canadian Centre for Cyber Security (CCCS), Computer Emergency Response Team New Zealand (CERT NZ), New Zealand National Cyber Security Centre (NZ NCSC), United Kingdom's National Cyber and S. C. (NCSC-UK), "Mitigating Log4Shell and Other Log4j-Related Vulnerabilities," CISA; FBI; NSA; ACSC; CCCS; CERT NZ; NZ NCSC; NCSC-UK, Product ID: AA21-356A, 2021/12/22 2021.
- s. Federal Energy Regulatory Commission, I. Electricity, and C. Analysis Sharing, "Solar-Winds and Related Supply Chain Compromise: Lessons for the North American Electricity Industry," Federal Energy Regulatory Commission (FERC); Electricity Information and Analysis Sharing Center (E-ISAC), 2021.
- 41. CISCO, "Threats of the Year: A look back at the tactics and tools of 2019," in "Cisco Cybersecurity Series 2019. Threat Report," Cisco, 2019. [Online]. Available: http://www.cisco.com/go/securityreports. Accessed: Jun. 6, 2025.
- 42. Cisco Talos, 2024 Cisco Talos Year in Review. Cisco, 2025. [Online]. Available: https://blog.talosintelligence.com/content/files/2025/03/2024YiR-report.pdf. Accessed: Jun. 6, 2025.
- 43. A. Cherepanov, "WIN32/INDUSTROYER A new threat for industrial control systems," ESET, 2017.
- 44. Symantec, "ISTR. Internet Security Threat Report Volume 24," Symantec, 2019/02// 2019.
- 45. A. Cherepanov, "GREYENERGY A successor to BlackEnergy," ESET, 2018/10// 2018.
- 46. P. Shakarian, "Stuxnet: Revolución de Ciberguerra en los Asuntos Militares," Air and Space Power Journal, 01/01 2012.

# Securing On-Chain Voting Using A Two-Layered zk-SNARK Approach

Gheorghe-Mădălin Pahomi, Darius Galiș, and Ciprian Pungilă

Faculty of Mathematics and Informatics, West University of Timişoara Bulevardul Vasile Pârvan 4, Timişoara, 300223, Timiş, România gheorghe.pahomi94@e-uvt.ro,darius.galis@e-uvt.ro,ciprian.pungila@e-uvt.ro

Abstract. We present an architecture for double Zero-Knowledge Succinct Non-Interactive Argument of Knowledge (zk-SNARK) blockchain-based system for on-chain voting that aims to focus on privacy. The proposed architecture uses a two-stage approach, by creating a proof of eligibility for the voters, without revealing sensitive identity attributes, while enabling anonymous and verifiable vote submissions through the blockchain. This article explores the motivation for proposing the system, as well as describing the technical components of the system, together with an assessment of its technical features from a privacy and attack resiliency point of view. Experimental results show proof generation in under 2 seconds and verification in under 1.5 seconds on modest hardware. On-chain deployment costs approximately 0.001 SepETH, with each vote verification requiring only about 0.0001 SepETH, highlighting the system's efficiency and affordability for real-world use.

**Keywords:** On-Chain Voting, ZKP, Zero-Knowledge Proof, zk-SNARK, Blockchain

#### 1 Introduction

Electronic voting systems, like traditional ones, must ensure integrity, verifiability, and secrecy. Zero-knowledge mechanisms offer a promising solution to meet these security needs. Blockchain-based voting enables remote, transparent, and private elections by combining smart contracts with zero-knowledge proofs. This paper focuses on maintaining transparency and voter anonymity through these technologies.

The concept of zero-knowledge proof (ZKP) was first mentioned in a study from 1989, being defined as "those proofs that convey no additional knowledge other than the correctness of the proposition in question" [1]. They allow one party (the prover) to convince another party (the verifier) that a statement is true, without revealing information about the statement itself. The same article also introduced the concept of interactive zero-knowledge proofs, which involve multiple rounds of interaction between the prover P and the verifier V. In contrast, non-interactive proofs involve the prover using a common reference string obtained from a trusted setup to obtain a mono-directional communication, from P to V [2]. There are two major directions that employ zero-knowledge proofs:

- zk-SNARK: One of the non-interactive types of zero-knowledge is the Zero-Knowledge Succinct Non-Interactive Argument of Knowledge (zk-SNARK). It generates short, fast-to-verify proofs without interaction between parties, by using a proving system based on elliptic curve pairings. It has applications in blockchain systems where privacy and efficiency are critical, and interactivity cannot be achieved as easily.
- zk-STARK: Zero-Knowledge Scalable Transparent Argument of Knowledge is another non-interactive type that is designed to provide transparency and scalability while maintaining cryptographic security[3]. It also has applications in blockchain protocols, to improve scalability, being suitable for complex computations of large-scale systems. Unlike zk-SNARK, which requires a setup phase, zk-STARK eliminates the need for a trusted setup, being more transparent and less prone to risks associated with compromised setups. It uses a proving system based on homomorphic encryption.

We believe that the Groth16 proving system [4] is favorable due to its combination of succinctness, fast verification, and integration with existing developer tools (for example, Circom[5]) which simplify backend and frontend circuit integration with low gas costs. zk-STARK, despite having the advantage of scalability and transparency, it generates larger, slower-to-verify proofs, making it less suitable for blockchain-based voting.

The present paper is structured as follows: Section 1 explores the motivation and presents the methods used in our system. Section 2 explores voting systems relevant to our paper. Section 3 details the architecture of our proof of work. Section 4 presents a taxonomic assessment of our system. Section 5 concludes the paper with a summary of our work.

## 2 State of the Art

To identify relevant electronic voting systems, we conducted a literature review using Google Scholar, IEEE Xplore, and the ACM Digital Library, focusing on recent publications and technical reports describing real-world implementations. Our search used keyword combinations like "open source electronic voting system," "secure voting system," "end-to-end verifiable voting," "blockchain voting systems," and "zk-SNARK voting systems." Without restricting the timeframe, we included systems with demonstrated long-term viability, identifying implementations dating back to 2005 that remain in use today.

Helios [6] is a web-based open-audit voting system that uses homomorphic ElGamal encryption, various protocols to prevent coercion and ensure anonymity between communicating parties, and proofs of decryption. Helios is not using blockchain, but a bulletin board (web server) where encrypted ballots are stored. Voter privacy is achieved by encrypting the votes with a public key, while the decryption keys are held by a set of trustees. The security aspect of Helios relies not on their server, but on the honesty of the parties that hold the decryption keys.

Civitas [7], is a coercion-resistant voting system based on research published in 2005 [8] that introduced dual credentials (one real, one fake) to prevent vote tampering. It extends this model with mix-nets and zero-knowledge proofs to ensure vote validity and anonymity. Like our approach, Civitas also considers election costs, though it does not use blockchain, relying instead on a public bulletin board for encrypted votes. Privacy is ensured through ElGamal encryption, mix-networks, and random permutations, proved with the help of zero-knowledge protocols. However, the focus on coercion-resistance hinders the scalability of Civitas by having intensive cryptographic operations and protocols that add complexity by sharing responsibilities among agents.

**Semaphore** [9] is an open-source blockchain voting system that incorporates a Merkle tree of eligible voters and a zk-SNARK approach, with the proof being verified by a smart contract. Its design makes Semaphore more suitable for group-based anonymous signalling, but adds complexity on the user side, translating to technical difficulties for the general public, since the voter has to manage cryptographic operations and files. The high gas fees that result from proof verification should also be taken into consideration.

Although there are not many implementations, and even fewer documented ones, research in this direction shows clear interest in achieving a digital alternative to physical elections.

## 3 Methodology

Our architecture (see Figure 1) is composed of four main stages, each corresponding to a distinct phase of the secure voting process.

- 1. Voter Authentication and Session Initialization. The voter authenticates via a browser-based extension (i.e. MetaMask), establishing a secure session. A key exchange using Diffie-Hellman derives a shared secret, from which a session-specific AES-GCM encryption key is generated via HKDF. This key secures identity data (SSN and UID) even if HTTPS is unavailable. The backend generates a session nonce, signed via ECDSA, which is used to bind proof computation to the session.
- 2. zk-SNARK-1: Eligibility Verification. The backend uses zk-SNARK-1 to prove voter eligibility based on encrypted SSN and UID pairs received from the frontend, along with the nonce, after an initial eligibility check of the received pair against a stored SHA-256 database. The arithmetic circuit, implemented in Circom using R1CS constraints, ensures that only valid identity pairs can produce a valid proof. A cryptographic nullifier is generated to prevent double voting.
- 3. zk-SNARK-2: Vote Integrity Proof. Upon vote casting, zk-SNARK-2 is used to validate the vote. It consumes the nullifier from zk-SNARK-1 and the voter's selection, producing a proof and a commitment. Only the nullifier and commitment are submitted on-chain, ensuring privacy and efficiency.

#### 4 Pahomi et al.

- 4. Blockchain and Smart Contract Integration. The Solidity smart contract governs the on-chain logic: enforcing vote windows, preventing duplicate votes via nullifiers, and tallying votes. It does not validate proofs on-chain (for gas efficiency) but can be modified to do so if trust in the backend is compromised. A MetaMask-integrated frontend handles proof submission and vote visualization, including a verifier interface for public audits.

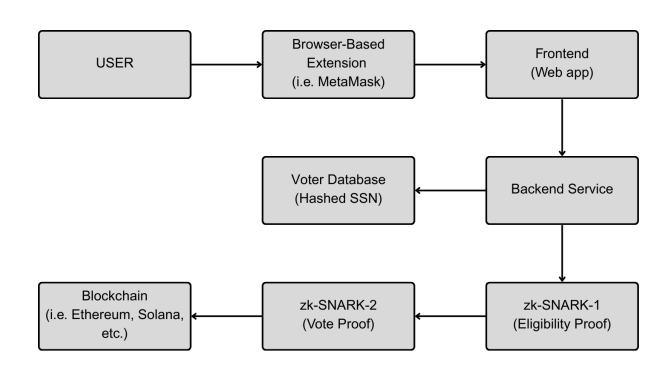


Fig. 1. Proposed architectural workflow

Figure 1 presents the complete system architecture, detailing the four main stages: voter authentication, eligibility proof generation (zk-SNARK-1), vote commitment generation (zk-SNARK-2), and on-chain integration. It shows how each component contributes to privacy, auditability, and integrity.

The user is checked against a hashed database containing personally identifiable information (i.e. social security number, user ID, etc.), making sure the voter is legitimate. The backend uses zk-SNARK-1 to generate a proof of eligibility and a nullifier. This ensures fair computation and prevents double voting. After a vote is cast, the backend calls for a second zk-SNARK (further referred to as zk-SNARK-2) that takes the public output of zk-SNARK-1 (the nullifier) along with the voting choice and generates a proof that confirms the correctness of the computation and a commitment, which is sent to the blockchain. Since only the nullifier and vote commitment are submitted on-chain, we avoid the high cost and limitations of on-chain zk-SNARK verification, while maintaining the transparency benefits in blockchain technology. Computations are done cost-free off-chain, while the blockchain guarantees: a) transparency by publicly recording the votes so that anyone can audit that no nullifier is reused and each vote is valid; b) integrity by ensuring that once a vote is submitted, it cannot be altered, deleted, or tampered with, and c) decentralization by enforcing voting rules through a smart contract, not a central authority, namely no single entity has unilateral control over the election.

The voter database is a server-hashed list (using SHA-256 encryption protocol) of individuals that meet voting criteria (age, citizenship, mental and legal capabilities). The values used in the database are the social security number (SSN) and a User Identification (UID). The former one is a unique number (thirteen digits in Romania, for example) that links to an individual and is used in finding information from the government population evidence (making it possible to find if the voter is eligible). The upper limit of digits is given by the Groth16 system that uses BN254 elliptic curve, which operates over a 254-bit prime field. The circuit can also be adapted to use ASCII encoding, similarly to the UID. The latter can be any secret value that acts like a password, in order to make the authentication less susceptible to brute force attacks. It can either be user chosen (then only the SSN would be verified in the database to check eligibility), can be mandated by the government, or, as in this case, can be the national ID's batch and number. The credentials are never stored or transmitted in plaintext, while the proof is generated by the zero-knowledge mechanism.

zk-SNARK-1 uses the SSN, the UID, and a randomly generated session nonce (used to prevent replay attacks and to bind the generated proof to a specific session). This nonce value is signed by an ECDSA to ensure that it actually came from the server, protecting it from various malicious attacks (e.g client generating arbitrary nonces).

To implement zk-SNARK-1, we used Circom, a domain-specific language for constructing arithmetic circuits, which adheres to the Rank-1 Constraint System (R1CS) model. The circuit accepts as inputs the voter's Social Security Number (SSN), a User ID (UID) string, and a session-specific nonce. The UID is parsed as an array of ASCII-encoded characters, and we compute the cumulative product of these values, denoted as  $p_i = \prod_{i=0}^i \mathtt{uid}[j]$ .

Using this, the internal variables of the circuit are derived as follows:

```
-a = SSN \times p_i

-b = a + nonce, encoded in R1CS form as (a + nonce) \times 1 = b

-c = b \times b
```

Where  $p_i$  represents the cumulative product of UID characters parsed as ASCII values, with uid[j] being the ASCII value of the j-th character in the UID array, **a** is the product of the SSN and  $p_i$ , binding both private identifiers, **b** is the sum of **a** and the session number, binding the computation to a specific session and **c** is the square of **b**, which increases entropy before the Poseidon hash is applied.

The output of this arithmetic chain is hashed using the Poseidon hash function to derive the final nullifier:

```
nullifier = Poseidon(c)
```

This construction ensures that the nullifier uniquely ties the proof to the voter's identity and session, without revealing any of the raw inputs.

Figure 2 illustrates the R1CS representation of the zk-SNARK-1 eligibility circuit. It highlights how SSN, UID (as ASCII values), and the session nonce are multiplied and combined into an arithmetic chain, whose final result is hashed using Poseidon to derive a unique voter nullifier.

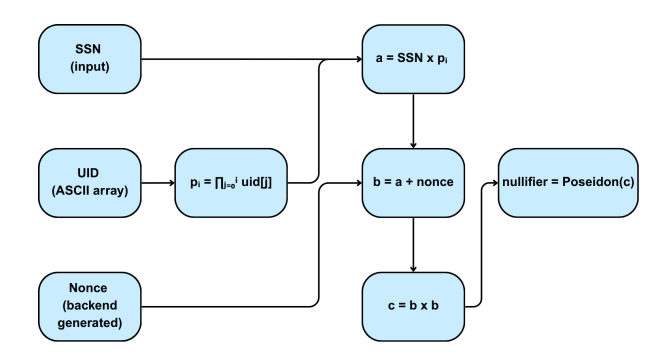


Fig. 2. Nullifier circuit

The core of our system is the Poseidon hash function, a cryptographic hash optimized for efficiency and used by Circom. We employ Groth16, a zk-SNARK proving system that generates succinct, efficiently verifiable proofs for quadratic arithmetic programs (QAP) over elliptic curve points, derived via the Powers of Tau Ceremony [10]. After compiling the eligibility and vote logic into R1CS and then QAP, a trusted setup produces the proving and verification keys per circuit. The backend uses the proving keys to generate two zk-SNARK proofs, which are verified off-chain using the verification keys to ensure they match the circuit logic and public outputs. This guarantees voter eligibility and vote validity. Our eligibility R1CS includes 425 constraints, the vote R1CS 517, and we used a trusted setup supporting up to 32,768 constraints for scalability without redoing the ceremony.

We have tested our approach using a smart contract created in Solidity[11], in an Ethereum [12] based ecosystem. The contract governs on-chain logic by securely handling vote casting, preventing duplicate votes, enforcing voting deadlines, and recording results, without exposing voter identity or vote content. It accepts votes only within a fixed time window, stores the nullifier and commitment, and increments each candidate's individual vote counter, revealing the leading candidate only after the voting period ends.

To reduce gas fees, the contract accepts only valid proofs without performing on-chain verification, which would increase complexity and cost, a compromise that could be taken into consideration if the party submitting the proofs cannot be trusted. The smart-contract interaction is abstracted by a frontend, allowing interaction through MetaMask[13]. A verifier page that acts as an audit interface is also provided where users can upload zk-SNARK proof files, including their hashes, to validate Groth16 proofs and receive a match or mismatch result in the interface. To better understand the threat surface and how our system mitigates specific vulnerabilities, Table 1 summarizes the principal attack types and corresponding defense mechanisms across all layers of the architecture.

| Threat Type        | Description                   | Mitigation Strategy                   |
|--------------------|-------------------------------|---------------------------------------|
| MITM Attacks       | Attacker intercepts commu-    | Use signed nonces, TLS/HTTPS,         |
|                    | nication between client and   | and Diffie-Hellman with HKDF          |
|                    | backend                       |                                       |
| Frontend Tampering | Compromised JavaScript        | Subresource Integrity (SRI), client-  |
|                    | delivers malicious logic      | side verification interface           |
| Replay Attacks     | Reuse of previously valid     | Session-specific ECDSA-signed         |
|                    | messages (e.g., votes or cre- | nonces and unique nullifiers per      |
|                    | dentials)                     | voter                                 |
| Sybil Attacks      | Fake identities attempt to    | Use of a hashed registry and strict   |
|                    | overwhelm the system          | SSN:UID eligibility checks            |
| Proof Forgery      | Malicious clients submit      | Hash the proof files with SHA-256     |
|                    | fake zk-SNARKs or tampered    | before verification and accept only   |
|                    | proof files                   | proofs verified using the correct key |
| Double Voting      | A single user tries to vote   | Nullifiers submitted and tracked      |
|                    | more than once                | on-chain to enforce one vote per      |
|                    |                               | user                                  |
| Server Malfunction | Backend incorrectly gener-    | Modular architecture allows off-      |
|                    | ates or verifies proof        | chain auditing and detailed logging   |

Table 1. Threat Model and Mitigation Strategies

#### 4 Taxonomic Assessment

Electronic voting must balance ballot privacy with election integrity. Privacy protects voters from coercion or vote buying, while integrity ensures all votes are accurately recorded, tallied, and verifiable to prevent fraud or manipulation. With those characteristics in mind, we validated our approach against the ones presented in the state-of-the-art chapter.

To assess our approach against others, we performed a comparison using different criteria, splittable in two primary categories: **1. Exploitability metrics:** Attack vector (AV), Attack complexity (AC), Privileges required (PR), User interaction (UI), Scope (S) and **2. Impact metrics:** Confidentiality impact (C), Integrity impact (I), Availability impact (A)[14]

|                     | AV      | $\mathbf{AC}$ | PR   | UI       | S         | $\mathbf{C}$ | I    | A    |
|---------------------|---------|---------------|------|----------|-----------|--------------|------|------|
| Helios              | Network | Low           | None | Required | Unchanged | High         | High | None |
| Civitas             | Network | High          | High | None     | Unchanged | High         | High | None |
| Semaphore           | Network | High          | Low  | None     | Unchanged | High         | High | Low  |
| Our proposed system | Network | High          | None | None     | Unchanged | High         | High | None |

Table 2. Taxonomic evaluation of electronic voting systems

The values for our system in Table 2 are derived from the structure and implementation of our voting architecture. The attack vector is "Network" due to

web-based interactions through MetaMask. Attack complexity is rated "High" because of the layered zk-SNARK setup, encrypted identity data, and session-bound nonce verification, which create significant barriers to exploitation. Privileges required are "None," as voters use the system through a public frontend without special access. User interaction is also "None" because all cryptographic processes, including proof generation and submission, are handled automatically. The scope is "Unchanged" since an exploit would not propagate beyond the voting instance. Both confidentiality and integrity impacts are rated "High" due to the critical nature of vote secrecy and correctness. Availability impact is "None" because the system performs verification off-chain and does not rely on continuous blockchain interaction, minimizing disruption from gas cost fluctuations or DoS attempts.

Helios offers strong audit capacity but lacks coercion resistance. Its vulnerabilities include a ballot-secrecy flaw enabling replay attacks that let an adversary cause a detectable election outcome change and learn how the victim voted [15], and a Cross-Site Request Forgery (CSRF) issue where unauthorized commands could be sent from a voter's browser [16]. Helios depends on a registered voter list and authentication (often via email tokens or passwords), exposing it to malicious election admins who could add fake voters or intercept voter credentials. It is also susceptible to coercion, as voters receive a ballot tracking hash as a receipt, public on the bulletin board, allowing them to prove their vote by revealing their ballot and tracker.

Civitas's approach to let people cast fake votes, along with receipt-free interfaces, helps counteract vote selling and coercion attempts. It implies multiple election authorities (trustees), which can act as a weak link in security. One issue is the need for voters to manage secret credentials and collaborate with the trustees, increasing user complexity and leading to mistakes. Its weaknesses are mainly practical: heavy infrastructure, dependence on unusual channels, and no large-scale deployment[17].

Semaphore achieves strong privacy through zk-SNARK proofs with each user having a public commitment stored as a leaf in a Merkle tree and a private key that contains a nullifier to prevent double voting. Key problems that render it an inappropriate choice are the gas-intensive protocol for large trees and the fact that the set of eligible voters (the group) is not a secret, adversaries knowing who can vote, but not what they voted.

Our proposed system improves upon existing solutions by combining blockchain-backed audit with zk-SNARK-based anonymity. It addresses key vulnerabilities such as coercion and double voting through cryptographic nullifiers and ensures vote integrity via immutable on-chain commitments. Unlike Civitas, it avoids complex credential management by using MetaMask login and automated proof generation, reducing user complexity. Compared to Helios, it eliminates the need for voter-side auditing, and unlike Semaphore, it avoids high gas costs and public group exposure through off-chain proof verification and a hashed eligibility list. However, this layered cryptographic design introduces added complexity and potential risks, including frontend manipulation, MITM

attacks, and implementation flaws. Proofs are verified off-chain for efficiency, and only public outputs (nullifier, commitment) are submitted on-chain, balancing performance with a minimal trust assumption.

A key innovation is the separation between eligibility verification (zk-SNARK-1) and vote integrity (zk-SNARK-2), enabling modular, reusable proofs without revealing sensitive data again. This design reduces circuit complexity, improves transparency, and defends against forgery even if the client is compromised. To our knowledge, this layered zk-SNARK structure is unique among blockchain voting systems.

We measured the computational cost of proof generation and verification on a modest system (Intel Core i5-3320M @ 2.60GHz, 8GB RAM). zk-SNARK-1 proof generation (eligibility circuit) averaged 1.83 seconds, while zk-SNARK-2 proof generation (vote circuit) averaged 1.69 seconds. Verification times were 1.48 seconds and 1.34 seconds for zk-SNARK-1 and zk-SNARK-2 respectively. These results reflect efficient proof operations even on older consumer hardware, demonstrating the practicality of our architecture for real-world deployment.

An important advantage of our platform is its low operational cost. Compared to national election expenditures, blockchain-based architectures represent only a small fraction of the overall budget. Based on internal assessment and Romanian government spending data, the blockchain-related costs of our system remain under 10% of current spending levels, with contract deployment at 0.001 SepETH and vote verification at 0.0001 SepETH.

#### 5 Conclusions and Future Work

We proposed a flexible, low-cost, transparent and secure alternative to physical elections, achieved through a modular zero-knowledge system that isolates responsibilities and minimizes trust assumptions, with the resulting system demonstrating advantages over existing solutions in areas such as privacy, verifiability, and efficiency. By strengthening security and increasing scalability, as well as significantly leveraging the associated costs for the election process overall, our proposed system encourages a digital trace of the voting process, ensuring its traceability and transparency, while preserving anonymity altogether.

**Acknowledgement.** This work has been partially supported by (1) project virtuaLedger [18], (2) project RoNaQCI, part of EuroQCI, DIGITAL-2021-QCI-01-DEPLOY-NATIONAL, 101091562, and (3) project "Romanian Hub for Artificial Intelligence - HRIA", Smart Growth, Digitization and Financial Instruments Program, 2021-2027, MySMIS no. 334906

#### References

1. Goldwasser, S., Micali, S., Rackoff, C.: The Knowledge Complexity of Interactive Proof Systems. SIAM Journal on Computing, vol. 18, no. 1, pp. 186–208 (1989). https://doi.org/10.1137/0218012

- 2. Blum, M., Feldman, P., Micali, S.: Non-Interactive Zero-Knowledge and Its Applications. In: Proceedings of the 20th Annual ACM Symposium on Theory of Computing (STOC), pp. 103–112. ACM (1988). https://doi.org/10.1145/62212.62222
- 3. Ben-Sasson, E., Bentov, I., Horesh, Y., Riabzev, M.: Scalable, Transparent, and Post-Quantum Secure Computational Integrity. Cryptology ePrint Archive, Report 2018/046 (2018). https://eprint.iacr.org/2018/046
- 4. Groth, J.: On the Size of Pairing-Based Non-interactive Arguments. In: Oswald, E., Fischlin, M. (eds.) EUROCRYPT 2016. LNCS, vol. 9665, pp. 305–326. Springer, Berlin, Heidelberg (2016). https://doi.org/10.1007/978-3-662-49896-5\_11
- Bellés-Muñoz, M., Isabel, M., Muñoz-Tapia, J.L., Rubio, A., Baylina, J.: Circom: A Circuit Description Language for Building Zero-Knowledge Applications. IEEE Trans. Dependable Secure Comput., vol. 20, no. 6, pp. 4733–4751 (2023). https://doi.org/10.1109/TDSC.2022.3232813
- 6. HELIOS https://vote.heliosvoting.org/ (Accessed: 2025-05-6)
- Clarkson, M.R., Chong, S., Myers, A.C.: Civitas: Toward a Secure Voting System. In: 2008 IEEE Symposium on Security and Privacy (SP), pp. 354–368. IEEE (2008). https://doi.org/10.1109/SP.2008.32
- Juels, A., Catalano, D., Jakobsson, M.: Coercion-Resistant Electronic Elections. In: Proceedings of the 2005 ACM Workshop on Privacy in the Electronic Society (WPES), pp. 61–70. ACM (2005). https://doi.org/10.1145/1102199.1102213
- 9. Semaphore Community: Semaphore: Zero-Knowledge Signaling on Ethereum (Whitepaper v1) (2025). https://semaphore.pse.dev/whitepaper-v1.pdf (Accessed: 2025-04-22)
- Nikolaenko, V., Ragsdale, S., Bonneau, J., Boneh, D.: Powers-of-Tau to the People: Decentralizing Setup Ceremonies. In: Gennaro, R., Wichs, D. (eds.) Public-Key Cryptography – PKC 2024. LNCS, vol. 14442, pp. 105–134. Springer, Cham (2024). https://doi.org/10.1007/978-3-031-56179-5\_5
- 11. Solidity Contributors: Solidity Documentation (2025). https://docs.soliditylang.org/ (Accessed: 2025-04-22)
- 12. Wood, G.: Ethereum: A Secure Decentralised Generalised Transaction Ledger. Ethereum Project Yellow Paper, vol. 151, pp. 1–32 (2014). https://ethereum.github.io/yellowpaper/paper.pdf
- 13. Lee, W.-M.: Using the MetaMask Chrome Extension. In: \*Beginning Ethereum Smart Contracts Programming: With Examples in Python, Solidity, and JavaScript\*, pp. 93–126. Apress, Berkeley, CA (2019). https://doi.org/10.1007/978-1-4842-5086-0\_5
- 14. Forum of Incident Response and Security Teams (FIRST): Common Vulnerability Scoring System v3.1: User Guide (2025). https://www.first.org/cvss/v3-1/user-guide (Accessed: 2025-04-27)
- Cortier, V., Smyth, B.: Attacking and Fixing Helios: An Analysis of Ballot Secrecy. Cryptology ePrint Archive, Report 2010/625 (2010). https://eprint.iacr.org/2010/625.pdf
- Gawel, D., Kosarzecki, M., Vora, P.L., Wu, H., Zagorski, F.: Apollo End-to-End Verifiable Internet Voting with Recovery from Vote Manipulation. Cryptology ePrint Archive, Report 2016/1037 (2016). https://eprint.iacr.org/2016/1037.pdf
- 17. Neumann, S., Volkamer, M.: Civitas and the Real World: Problems and Solutions from a Practical Point of View. In: 2012 Seventh International Conference on Availability, Reliability and Security (ARES), pp. 180–185. IEEE (2012). https://doi.org/10.1109/ARES.2012.75
- 18. The VirtuaLedger project, https://virtualedger.com (Accessed: 2024-12-13)

## Study and comparison of lattice sieving algorithms

M.A. González de la Torre<sup>1</sup>, D. Rojas Rodríguez<sup>1</sup>, and L. Hernández Encinas<sup>1</sup>

Institute of Physical and Information Technologies (ITEFI)

C/ Serrano 144, 28006-Madrid, Spain

Spanish National Research Council (CSIC)

{ma.gonzalez,diego.rojas,luis.h.encinas}@csic.es

Abstract. The Shortest Vector Problem is one of the most important problems related to the security in the post-quantum cryptography. In this work, we present an state-of-the-art analysis of the different algorithms to solve this problem evaluating their efficiency in High Performance Computing systems. To do this, we have modified the Shortest Vector Problem oracle used in the implementation of the BKZ algorithm included in the General Sieve Kernel software library to test a suite of different algorithms. The main purpose of this research is to check whether current hardness estimations apply to highly parallelized implementations. In this sense, we have tested the different algorithms in a High Performance Computing cluster and compared their performance on highly parallelized environments.

**Keywords:** Lattice-based Post-quantum Cryptography, Public-Key Cryptography, Shortest Vector Problem, Sieving attacks.

### 1 Introduction

In the context of Post-Quantum Cryptography (PQC) lattice-based cryptosystems are currently considered to be the most promising. Prior to the beginning of the standardisation process by the National Institute of Standards and Technology (NIST), lattice-based cryptography had already been researched for its value in Fully Homomorphic cryptosystems. After the standardization of PQC, there have been several improvements on the attacks and new approaches to tackle the Shortest Vector Problem (SVP), to which many lattice problems can be reduced. In 2024, the first three PQC standards were published, two of which are lattice-based: a Key Encapsulation Mechanism (KEM), ML-KEM [18], and a Digital Signature (DS), ML-DSA [18]. Both standards base their security in the Learning With Errors (LWE) problem, which is considered hard to solve in high dimensions. The LWE problem can be reduced to the SVP, meaning that solving the latter implies also solving the LWE problem.

In this work, our main goal is to study and analyse the different variants of sieving algorithms, used inside the Block Korkine-Zolotarev (BKZ) algorithm [19]. BKZ is the best known attack to lattice cryptography and requires an SVP

oracle. It should stay clear that solving the LWE problem with cryptographic parameters is considered to be unfeasible, which does not detract interest in studying other solvable instances of the problem. We will run different sieving oracles in High Performance Computing (HPC) systems where parallelization may allow us to increase performance. We think that optimization of computational resources may lead to a significant reduction on the security of the LWE-based algorithms and thus it should be of upmost importance to verify that resourceful eavesdroppers can not breach the security of what is promised to be the future of information security.

The rest of this communication contains the following sections: Section 2 presents the background concepts needed for understanding the rest of this work. Section 3 contains the most relevant strategies to solve the SVP. In Section 4 we show the results obtained from the cluster DRAGO, property of the Spanish National Research Council (CSIC), and Finisterrae III, property of Galicia Supercomputing Center (CESGA), we also present the conclusions from our analysis. Finally, in section 5 some possible lines of work to continue the research are included.

## 2 Finding short vectors

A lattice  $\mathcal{L}$  is defined as a discrete additive subgroup of  $\mathbb{R}^n$ . In other words, given a set of linearly independent vectors  $B = \{b_0, \dots, b_{n-1}\} \in \mathbb{R}^n$ , we have

**Definition 1 (Lattice).** A lattice with basis B is the set of integer linear combinations of the vectors of B:  $\mathcal{L}(B) = \{Bx : x \in \mathbb{Z}^m\}.$ 

The set B is called basis of the lattice and the same lattice can be generated by different basis. In any case, to simplify the notation, the reference to a basis in the definition of a lattice will be omitted unless it is required. A lattice  $\mathcal{L} \subset \mathbb{R}^n$  inherits the Euclidean norm, hence there is also a notion of distance between lattice points. The minimum distance of a lattice  $\mathcal{L}$  is the length of the shortest nonzero lattice vector:  $\lambda_1(\mathcal{L}) := \min_{v \in \mathcal{L} \setminus \{0\}} \|v\|$ .

**Definition 2 (SVP).** Given an arbitrary basis B of some lattice  $\mathcal{L}(B)$ , find a shortest nonzero lattice vector, i.e., find  $v \in \mathcal{L}(B)$  for which  $||v|| = \lambda_1(\mathcal{L}(B))$ .

For a vector  $\mathbf{s} \in \mathbb{Z}_q^n$ , called secret, the LWE distribution  $A_{\mathbf{s},\chi}$  over  $\mathbb{Z}_q^n \times \mathbb{Z}_q$  is defined by choosing  $\mathbf{a} \in \mathbb{Z}_q^n$  uniformly at random and  $e \leftarrow \chi$  and then sampling  $(\mathbf{a}, b = \langle \mathbf{s}, \mathbf{a} \rangle + e \pmod{q})$ . Once the LWE distribution is defined, the LWE problem can be stated as the following.

**Definition 3 (LWE).** Given m independent samples  $(\mathbf{a}_i, b_i) \in \mathbb{Z}_q^n \times \mathbb{Z}_q$  from the LWE distribution  $A_{\mathbf{s},\chi}$ , find  $\mathbf{s}$ .

The SVP problem is considered to be in NP under randomized reductions, hence any known algorithms that solve it require exponential time. There are two kinds of algorithms that solve the SVP [17]: approximation algorithms and exact

algorithms. The approximation algorithms output a vector that is close, in norm, to the shortest vector; while the exact algorithms probably output the shortest vector. The best examples of probabilistic SVP solvers are the algorithms by Lenstra, Lenstra, and Lovasc (LLL) [15] and the Block Korkin-Zolotarev (BKZ) [19], both are what are called lattice reduction algorithms, i.e. algorithms that replace the basis of the lattice with another one that has better shape and properties. For exact SVP algorithms there are two main families: sieving and enumeration.

As its name suggests, enumeration algorithms aim to calculate all possible solutions to a problem to deterministically find the best solution. More efficient approaches look for sufficiently good solutions and add techniques like pruning the solution tree, reducing significantly the runtime. The estimated cost of enumeration algorithms varies from  $2^{O(n^2)}$  to  $2^{O(n\log n)}$  [11], depending on the preprocessing of the lattice basis.

Sieving algorithms consists of performing operations inside a list of vectors of the lattice with the intention of obtaining the shortest possible vector. These algorithms require a computational cost of  $2^{O(n)}$  and have a space complexity of  $2^{O(n)}$ . Due to these restrictions, sieving algorithms are hard to implement; however, right now, they are considered as the fastest and optimal choice for solving the exact SVP problem. Currently, sieving algorithms are considered the preferable choice, based on the experimental results from [1], [2].

Approximated algorithms like BKZ run an exact SVP solver in a lower dimension (lower than the input dimension), while both sieving and enumeration benefit in their performance of preprocessing the basis of the lattice with algorithms like LLL.

## 3 Sieving strategies

The first sieving strategy ever proposed is the AKS sieve, in [1]. However, the implementation that we study corresponds to the NV sieve [17]. It was not until the Gaussian sieve was introduced in [16] that sieving was considered competitive.

Before presenting the different versions of sieving, we will introduce the general concepts related to this type of algorithm. Given vectors  $u, v \in \mathcal{L}$ , they form a reduced pair if

$$\min\{\|u+v\|, \|u-v\|\} \ge \max\{\|u\|, \|v\|\}.$$

If a pair of vectors is not reduced it is said to be reducible. If two vectors  $u, v \in \mathcal{L}$  verify the condition  $\theta(u, \pm v) < \pi/3$ , then they are a reducible pair, where  $\theta(u, v)$  denotes the angle between u and v.

There are three main aspects that change between different implementations: i) how the list of vectors is formed, ii) how large this list has to be to contain reducible pairs in it, and iii) when does the algorithm find a short (sufficiently short) vector. The sampling of the vectors depends on the implementation, but it is advised to output vectors of the lattice following a known and convenient distribution, some examples are [12], [8].

4

The kissing number [10] in dimension d is defined as the maximum number of non-overlapping unit spheres that can touch a single unit sphere. This number is difficult to predict for high dimensions, but there are known bounds to its value. For sieving algorithms, the kissing number is relevant since it also denotes the maximum number of vectors that is possible to consider in dimension d that form angles of  $\pi/3$ . Consequently, if any list contains a number of vectors higher than the kissing number of the dimension considered, then the existence of a reducible pair is guaranteed. In [10] a lower bound of the kissing number is presented  $|\mathcal{L}| \in 2^{0.2075n+o(n)}$ .

In AKS a lattice  $\mathcal{L}$  of rank n and radius R are taken as input, and generate a list of vectors  $S \subset \mathcal{L} \cap B_n(R)$ , where  $B_n(R)$  denotes the closed ball of radius R and centred in the origin. The value R serves as bound to the length of vectors in the list and is iteratively reduced by a factor  $\delta$ . In the AKS sieve [1] the following process is followed: Let S be a set, initially empty. Sample vectors from  $B_n(R)$  and add them to S to get:

$$S = \{(y_i, v_i) \in B_n(R) \times \mathcal{L} : ||v_i - y_i|| \le \xi \}, \text{ for a value } \xi \text{ close to } 0.$$

After an iteration, R is reduced to  $\delta R$ , where  $\delta \in [2/3, 1)$ , and keep the vectors with norm inferior to  $\delta R$  or  $(y_i', v_i') = (y_j - v_i, v_j - v_i)$  where  $||v_i'|| \leq \delta R$ .

#### 3.1 NV sieve

The NV sieve algorithm [17] is a refined version of the deterministic AKS sieve. The designers of the NV sieve introduce an heuristic approach and reduce significantly the number of parameters involved. Besides the set S of vectors considered in the sieve, two new sets are defined, the set of centres C, initialized as an empty list and the set  $C_n$  defined as:

$$C_n(\gamma, R) = \{x \in \mathbb{R}^n : \gamma R \le ||x|| \le R\}.$$

The heuristic considered in [17] assumes that vectors in  $S \cap C_n(\gamma, R)$  after a sieve iteration are uniformly distributed in  $C_n(\gamma, R)$ . The main defining characteristic of NV sieving are the initial sampling, the length of the  $\gamma$  factor, and the heuristic distribution of the vectors after each reduction cycle.

While analysing the points in  $S \subseteq B_n(R)$ , the NV sieve will add vectors with norm greater than  $\gamma R$  to the set of centres C. On the contrary, vectors of norm lower than  $\gamma R$  are directly introduced in the list of the next iteration. The set C contains points in  $B_n$  that could reduce the length of other vectors in S (see Algorithm 1). The amount of iterations is greatly decreased with respect to AKS and, for appropriate values of  $\gamma$ , it returns a set of short enough vectors to solve the  $\gamma$ -SVP. To guarantee the quality of the output one should verify that  $|B_n(R) \cap \mathcal{L}| \geq |S|^2$ , which gives a good approximation of  $\lambda_1$ . When all the vectors remain in the list of centres during the reduction, the algorithm finishes.

#### Algorithm 1 NV sieve

```
Require: S \subseteq B_n(R) \cap \mathcal{L}, 2/3 \le \gamma \le 1

Ensure: L \subseteq B_n(\gamma R) \cap \mathcal{L}

Initialize C = \{\}, L = \{\}

for all v \in S do

if ||v|| \le \gamma R then

S' = S' \cup \{v\}

else

if \exists c \in C st ||v - c|| \le \gamma R then

L = L \cup \{v - c\}

else

C = C \cup \{v\}

end if

end for
```

#### 3.2 Gaussian sieve

The Gaussian approach is similar to the NV sieve, although instead of implementing S as a list it changes it to a queue (following first-in-first-out order). This offers a better space complexity and a better time performance on average. For the operation of removing the first element of a queue and to add an element on the back, the functions pop and push are defined, respectively.

Most implementations of the Gaussian sieve consider a number of collisions c as stop condition. A collision occurs when the reduction of two different pairs of vectors generate the same outcome. Once a set number of collisions is reached, the algorithm stops and outputs the list of reduced vectors L.

For its part, K increments with each collision of vectors linearly dependent with the ones in the list. Moreover, only vectors in the same  $\pi/3$  quadrant are evaluated for subtraction to give vectors with smaller norm. When vectors out of this quadrant are obtained they are rotated to fit in this space. Finally, the function Gaussian. Reduction used in Algorithm 2 is given as the Algorithm 3.

#### 3.3 Triple sieve

The triple sieve is a particular implementation of a more general construction called tuple-sieve [4]. These algorithms introduce a new strategy in the process of searching for short vectors given a sufficiently long list. While the previously presented sieving algorithms (NV or Gaussian) consider pairs of vectors and analyse whether they are reducible, the k-tuple-sieve type algorithms consider sets of three, four, ... k vectors and look for shortest vectors among the combinations of additions and subtractions of these vectors.

Triple sieve considers operations involving multiple vectors instead of just pairs (see Algorithm 4). This approach asymptotically decreases the size of the list but increases the time of the reduction. The most efficient approach considers triplets of vectors and modifies the Gaussian sieve to operate with them.

## Algorithm 2 Gaussian sieve

```
Require: Sample: \emptyset \to B_n(R)

Initialize L = \{0\}, S = \{\}, K = 0

while K < c do

if S \neq \{\} then

v = S.pop()

else

v \leftarrow Sample

end if

v = Gaussian.Reduction(v, L, S)

if v \neq 0 then

L = L \cup \{v\}

else

K + +

end if

end while
```

## Algorithm 3 Gaussian. Reduction

```
Require: p \leftarrow Sample, L \subset \mathcal{L}, S \in B_n(R)

while \exists v \in L : ||v|| \le ||p|| \land ||p-v|| \le ||p|| do p = p - v

end while

while \exists v \in L : ||v|| > ||p|| \land ||v-p|| \le ||v|| do L = L \setminus \{v\}

end while

return p
```

## Algorithm 4 Triple sieve

```
Require: L \subset \mathcal{L}, S \in B_n(R)

Initialize L = \{0\}, S = \{\}

while condition do

if S \neq \{\} then

p = S.pop()

else

p = Sample

end if

p = Triple.Reduce(p, L, S)

if p \neq 0 then

L = L \cup p

end if

end while
```

### Algorithm 5 Triple.Reduce

```
Require: p \leftarrow Sample, L \subset \mathcal{L}, S \in B_n(R)
  for all v \in L do
      if ||p|| \ge ||v|| \wedge ||p-v|| \le ||p|| then
          p = p - v
      end if
  end for
  for all v \in L do
      if ||v|| \ge ||p|| \wedge ||v - p|| \le ||v|| then
          v = v - p
          S = S.push(v)
      end if
  end for
  for all v_1, v_2 \in L do
      if ||p - v_1 - v_2|| \le ||p|| then
          p = p - v_1 - v_2
      end if
  end for
  for all v_1, v_2 \in L do
      if ||v_1 - p - v_2|| \le ||v_1|| then
          v_1 = v_1 - p - v_2
          S = S.push(v_1)
      end if
  end for
  return p
```

If p=0 at any time in this process, then one could return 0 to avoid non necessary operations. The function Triple.Reduce called in Algorithm 4 is given as the Algorithm 5.

### 3.4 List Decoding sieve

Locally sensitive sieving algorithms use additional preprocessing to increase the probability of success in the search of reducible pairs once the list of vectors is sampled. In particular, there has been two different preprocessing methods introduced to sieving, Locality Sensitive Hashing (LSH) and Locality Sensitive Filtering (LSF).

**Locality Sensitive Hashing** The idea behind LSH is to store the vectors of the sieve in hash tables. The hash functions used for the application of LSH to sieving consists of functions that map any n-dimensional vector  $v \in \mathbb{R}^n$  to a low-dimensional sketch and the probability of two vectors having the same sketch grows as the vectors are closer.

This technique was first introduced to solve the Approximate Nearest Neighbors Search (NNS) problem in [9]. Later, in [14], it is used LSH applied to sieving to solve the NNS problem in high dimensions and in the cases that the list L

has a certain structure. Moreover, in [6], it is applied the LSH sieve to improve the performance of the Gaussian sieve and NV sieve.

Although in [13] is introduced LSH to both, NV and Gaussian sieves, this kind of improvement has been mostly applied to the latter.

**Locality-sensitive filtering** Let consider the same definition as LSH, but instead of using the hash output to sort the vectors of L, it is consider now a set of filters  $\{f_i\}$ . These filters are defined as binary mappings: each vector either pass or does not pass the filter. In [5] the authors define a set of filters defined by spherical caps. The spherical cap of angle  $\theta$  and centre  $u \in B_n(R)$  is defined as  $C^{n-1}(\theta, u) := \{v \in B_n(R) : angle(u, v) \leq \theta\}$ . Basically, applying a filter  $f := \{(x_i, \theta_i)\}$  to the list of vectors L considered in the sieving means calculating  $L \cap C^{n-1}(\theta_i, x_i)$ .

## 4 Results in HPC

The implementations of the sieving algorithms we have used in our tests come from the General Sieve Kernel (g6k) [2], which is an open source library under the GNU General Public Licence (GPL) https://github.com/fplll/g6k. This kernel gives the basic operations needed to run algorithms like LLL, BKZ, and multiple implementations of sieving. All the sieving defined in the previous section are included in g6k. The triple sieve implemented in g6k is denoted as hk3, while the LSF sieve is the version introduced in [5], called bgj1. The internal structure relies on buckets where sieving is performed independently and after the reduction is completed a central database is updated with a list of shortest vectors on each bucket. There is not yet any successful implementation that heavily relies in parallelization, often key in HPC. As shown in [3], in dimension 120 and above, the parallelism using the MPI (Message Passing Interface) standard is around the 80%. In the implementation we have considered, the parallelization is used to open different buckets with a single thread on each bucket.

Apart from the software layer, the hardware becomes quite relevant to run sieving on high dimensions. The exponential cost on space may increase to the order of terabytes of RAM, worsened by the multithreading. Moreover, the greatest limiting factor has become the bandwidth of the RAM because, as we have mentioned, when a bucket is successfully reduced the thread has to add the shortest vectors to the database. This saturates the memory and reduces the performance overall.

Our initial result is the comparison between sieving and the other SotA exact SVP algorithm, enumeration Figs 1 and 2. The main purpose of this comparison is to verify what has been previously established by the scientific community: that sieving algorithms are currently the best strategy for solving shortest vector type problems.

It can be clearly appreciated in Fig 1 that for dimension higher than 70 sieving is faster than enumeration. Although for lower dimensions it is still considered enumeration, these cases are far from being cryptographically relevant, hence for

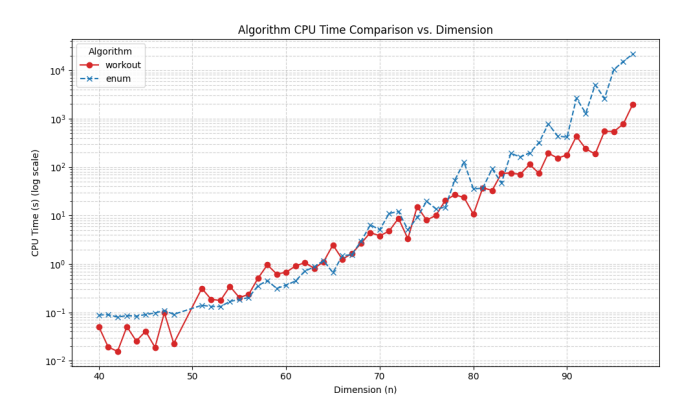


Fig. 1. Experimental results after running different sieves in DRAGO

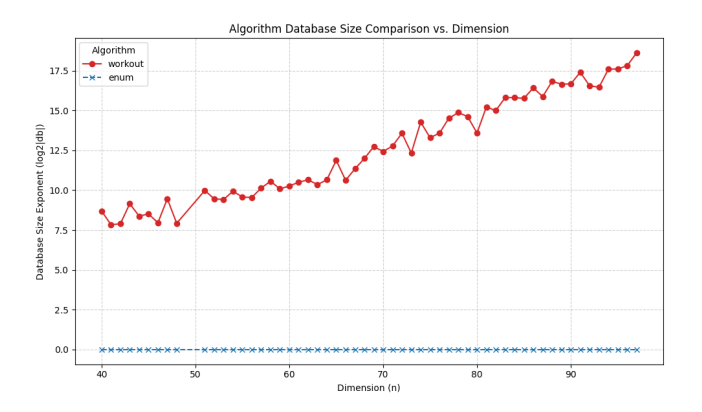


Fig. 2. Comparison between sieving and enumeration

any estimation of the cost of solving the SVP problem the logical consideration are sieving algorithms.

Despite being more efficient in time, sieving algorithms greatly increase the memory cost in high dimensions. The next step in our work was to look for diminishing returns for sieving algorithms in high dimensions and verify how the hardware may play an important role in the estimations of the cost of running sieving. In Figs 3 and 4 it can be appreciated a comparison between the different presented sieving strategies, in particular of the implementation in g6k of these sieves.

In Fig 3 one can see that the hk3 and bgj1 sieves present a better performance in time than the NV or Gaussian sieves, as the dimension considered for the sieve is higher. In terms of memory, as shown in Fig 4, the Gaussian sieve proves to have the best performance. However, the difference in the case of the memory usage does not seem to grow with the dimension, while in the time it does.

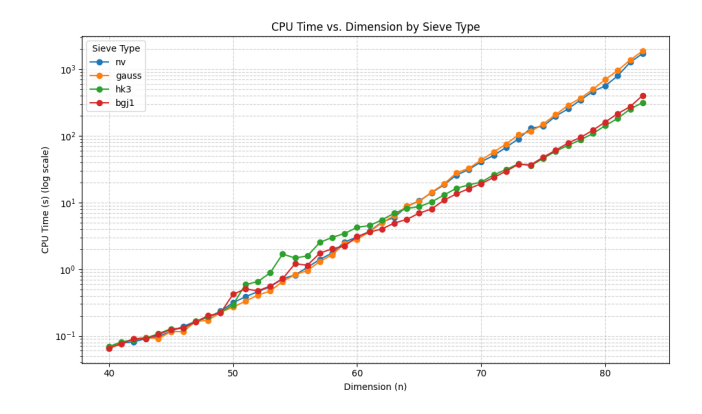


Fig. 3. Time used by different sieving in increasing dimension

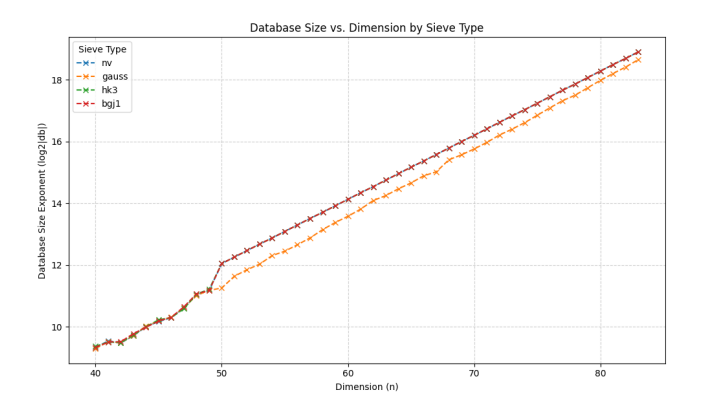


Fig. 4. Memory used by different sieving in increasing dimension

We would also want to highlight performance advantage that HPC systems offer to solve these problems. The instances of the SVP problem we solved were proposed in the SVP lattice challenge https://www.latticechallenge.org/svp-challenge/are considered.

In Table 4 we compare previously published results from the aforementioned implementation using MPI (\* data not included in [3]), the native g6k and our results obtained in the Finisterrae III supercomputer. Additionally we offer a SotA reference based in CUDA architecture for GPUs. It can be appreciated how we reached the same dimension as the original publication in almost one forth of the time and obtain significantly better results than the MPI implementation.

We infer this improvement is a result of the difference in hardware between the experiments. The bottlenecks of memory bandwidth and database space are mitigated in HPC systems. Solutions to the SVP may be affordable for resourceful

| g6k version    | SVP dim | Max Sieve dim | CPU time (hours) | Memory usage (GB) |
|----------------|---------|---------------|------------------|-------------------|
| Native g6k [2] | 128     | 102           | 95               | 7,6               |
| GPU g6k [7]    | 158     | 129           | 382              | 90                |
| MPI g6k [3]    | 128     | *             | 102              | 320               |
| Finisterrae    | 130     | 103           | 24               | 7,54              |

**Table 1.** Comparison of performance between sieving executions

attackers, which would present a threat to the security of LWE cryptosystems. However, the scalability of this solutions remains in question. The efficiency of multithreaded bucket search is still far from the perfect parallelism which opens a clear line of work to improve our understanding of the security of hard lattice problems.

#### 5 Future Work

To the knowledge of the authors, there are no implementations that successfully implements multithreading inside of the buckets. Adapting the code of G6K to use MPI to do this would be of great interest to see whether there are diminishing returns on the amount of threads working on a task or if sieving algorithms with enough resources could pose a threat to LWE algorithms.

There also are implementations that use CUDA architecture for speeding up the reduction of pairs of vectors obtaining state-of-the-art results. Having access to clusters with high performance GPU would be interesting to complement our results. Furthermore, we have not reached cryptographic dimensions, but only some toy-sized examples. The estimations suggest that our cluster would not have enough space to fit this cases, but exploring bigger systems could allow us to consider solving problems on larger dimensions.

**Acknowledgements** This work was supported by Project Quantum-based Resistant Architectures and Techniques Integration QKD+PQC (QURSA) funded by MCIN/AEI/10.13039/501100011033, co-funded by EU "NextGenerationEU"/PRTR under Grant TED2021-130369B-C33. M.A.G.T. wishes to thank CSIC for its support under the EFiDiP project.

#### References

- Ajtai, M., Kumar, R., Sivakumar, D.: A sieve algorithm for the shortest lattice vector problem. In: Proc. on 33rd Annual ACM Symposium on Theory of Computing. pp. 601–610. ACM (2001). https://doi.org/10.1145/380752.380857
- 2. Albrecht, M.R., Ducas, L., Herold, G., Kirshanova, E., Postlethwaite, E.W., Stevens, M.: The general sieve kernel and new records in lattice reduction. Cryptology ePrint Archive, Paper 2019/089 (2019), https://eprint.iacr.org/2019/089
- 3. Albrecht, M.R., Rowell, J.: Scaling lattice sieves across multiple machines. Cryptology ePrint Archive, Paper 2024/747 (2024), https://eprint.iacr.org/2024/747

- 4. Bai, S., Laarhoven, T., Stehlé, D.: Tuple lattice sieving. LMS Journal of Computation and Mathematics  $\bf 19(A)$ , 146-162 (2016). https://doi.org/10.1112/S1461157016000292
- Becker, A., Ducas, L., Gama, N., Laarhoven, T.: New directions in nearest neighbor searching with applications to lattice sieving. Cryptology ePrint Archive, Paper 2015/1128 (2015), https://eprint.iacr.org/2015/1128
- Becker, A., Laarhoven, T.: Efficient (ideal) lattice sieving using cross-polytope LSH. In: Pointcheval, D., Nitaj, A., Rachidi, T. (eds.) Progress in Cryptology – AFRICACRYPT 2016. pp. 3–23. Springer International Publishing, Cham (2016). https://doi.org/10.1007/978-3-319-31517-1\_1
- Ducas, L., Stevens, M., van Woerden, W.: Advanced lattice sieving on gpus, with tensor cores. In: Canteaut, A., Standaert, F.X. (eds.) Advances in Cryptology – EUROCRYPT 2021. pp. 249–279. Springer International Publishing, Cham (2021)
- 8. Gentry, C., Peikert, C., Vaikuntanathan, V.: Trapdoors for hard lattices and new cryptographic constructions. In: Proceedings of the Fortieth Annual ACM Symposium on Theory of Computing. pp. 197–206. STOC '08, Association for Computing Machinery, New York, NY, USA (2008). https://doi.org/10.1145/1374376.1374407, https://doi.org/10.1145/1374376.1374407
- 9. Indyk, P., Motwani, R.: Approximate nearest neighbors: towards removing the curse of dimensionality. In: Proc. of the Thirtieth Annual ACM Symposium on Theory of Computing. pp. 604–613. STOC'98, Association for Computing Machinery, New York, NY, USA (1998). https://doi.org/10.1145/276698.276876
- 10. Jenssen, M., Joos, F., Perkins, W.: On kissing numbers and spherical codes in high dimensions. Advances in Mathematics  $\bf 335$ ,  $\bf 307-321$  (2018). https://doi.org/10.1016/j.aim.2018.07.001
- Kannan, R.: Improved algorithms for integer programming and related lattice problems. In: Proc. of the Fifteenth Annual ACM Symposium on Theory of Computing. pp. 193–206. STOC'83, Association for Computing Machinery, New York, NY, USA (1983). https://doi.org/10.1145/800061.808749
- 12. Klein, P.: Finding the closest lattice vector when it's unusually close. In: Proceedings of the Eleventh Annual ACM-SIAM Symposium on Discrete Algorithms. pp. 937–941. SODA '00, Society for Industrial and Applied Mathematics, USA (2000)
- Laarhoven, T.: Sieving for shortest vectors in lattices using angular locality–sensitive hashing. In: Gennaro, R., Robshaw, M. (eds.) Advances in Cryptology CRYPTO 2015. pp. 3–22. Springer Berlin Heidelberg, Berlin, Heidelberg (2015). https://doi.org/10.1007/978-3-662-47989-6
- 14. Laarhoven, T., de Weger, B.: Faster sieving for shortest lattice vectors using spherical locality–sensitive hashing. In: Lauter, K., Rodríguez-Henríquez, F. (eds.) Progress in Cryptology LATINCRYPT 2015. pp. 101–118. Springer International Publishing, Cham (2015). https://doi.org/10.1007/978-3-319-22174-8\_6
- 15. Lenstra, A., Lenstra, H., Lovasz, L.: Factoring polynomials with rational coefficients. Mathematische Annalen  $\bf 261(4)$ ,  $\bf 515-534$  (1982),  $\bf https://doi.org/10.1007/BF01457454$
- Micciancio, D., Voulgaris, P.: Faster exponential time algorithms for the shortest vector problem. In: Proc. of the 2010 Annual ACM-SIAM Symposium on Discrete Algorithms (SODA). pp. 1468-1480. https://doi.org/10.1137/1.9781611973075.119
- 17. Nguyen, P.Q., Vidick, T.: Sieve algorithms for the shortest vector problem are practical. Journal of Mathematical Cryptology **2**(2), 181–207 (2008). https://doi.org/doi:10.1515/JMC.2008.009

- 18. NIST: Module-Lattice-Based Digital Signature Standard. National Institute of Standard and Technology, NIST FIPS 204 (2023), https://doi.org/10.6028/NIST.FIPS.204.ipd
- 19. Schnorr, C., Euchner, M.: Lattice basis reduction: Improved practical algorithms and solving subset sum problems. Mathematical Programming **66**(1–3), 181–199 (1994), https://doi.org/10.1007/BF01581144

# Hierarchical Threshold Structure-Preserving Signatures

Ahmet Ramazan Ağırtaş², Emircan Çelik¹★★, and Oğuz Yayla¹

<sup>1</sup> Institute of Applied Mathematics, Middle East Technical University, Çankaya, 06800, Ankara, Türkiye emircancelik92@gmail.com, oguz@metu.edu.tr <sup>2</sup> AYWARE, Çankaya, 06420, Ankara, Türkiye a.r.agirtas@gmail.com

Abstract. We introduce a digital signature scheme that combines hierarchical secret sharing with threshold structure-preserving signatures. In this scheme, a global signing key is recursively partitioned into layers, each protected by its own threshold, so that distinct subsets of the same participant group can exercise role-specific signing authority. Hierarchical Threshold Structure-Preserving Signatures (HTSPS) distribute two SPS signing keys across a hierarchy by interpreting each user's share as a polynomial-derivative value, so higher-level users hold evaluations and lower-level users hold higher-order derivatives; any group of participants that meets the vector of thresholds can interpolate to obtain a valid SPS signature, while sub-threshold sets see only random group elements. Our design composes Tassa's Birkhoff-based share system with the threshold SPS yielding signature protocol with a multi-layered access structure.

**Keywords:** Structure-Preserving Signatures, Threshold Signatures, Hierarchical Secret Sharing Keys.

## 1 Introduction

Structure Preserving Signatures (SPS) are pairing-based syntax compatible digital signature schemes, meaning, all the messages, public keys and the signatures are elements of the same bilinear group elements that the protocol operates in. This enables the reduction of verification to pairing-product equations within the group itself. This useful property allows a modular and efficient protocol design; therefore, there has been a lot of research interest on the topic.

Abe et al. initiated this research by introducing the concept in [1]. In 2016, Ghadafi [12] proposed a shorter SPS than existing SPS schemes. Its randomizable key variant with an adaptable algorithm is given in [8]. In 2019, Crites and Lysyanskaya [7] built mercurial signatures that are malleable with respect to the message, signature, and key space, focusing on Structure-Preserving Signatures on Equivalence Classes (SPS-EQ) [13]. Later, Connolly et al. [5] proposed a new

<sup>\*\*</sup> corresponding author

variant of it based on the assumption of the common reference string (CRS) model. Inspired by SPS-EQ, Backes et al. [4] presented signatures featuring a flexible public key primitive that converts the key into an alternative representative of the same equivalence class. Recently, Mir et al. [14] proposed the first aggregatable SPS-EQ, introducing aggregate signatures with randomizable public key and tags, along with aggregate mercurial signatures. In 2024, Abe et al. [15] presented interactive threshold mercurial signatures that expand the scope of threshold SPS to encompass EQ.

Many SPS in the literature are inadequate for thresholding due to nonlinear processes or even require significant overhead. However, in 2023, Crites et al. [6] proposed a Threshold Structure-Preserving Signature (TSPS) by defining an indexed Diffie-Hellman message space. They address thresholdization by employing indexing that converts each scalar message m into an index id to generate partial signatures in a compatible format for aggregation in a threshold scheme. Furthermore, the authors in [3] extend this scheme with a randomizable key.

Assume a scenario that there is an organization with multi-level of hieararchy. Assume that this organization is willing to create a policy where the authority of a top-level official must be shared within the ranks while keeping the hierarchical structure. TSPS uses standard secret sharing scheme by Shamir secret-sharing scheme that split a secret into pieces within a group of participants so that only authorized subgroups of participants can recover it. The classical example is Shamir's (t,n)-threshold construction [16], which treats every participant symmetrically by encoding the secret as the free coefficient of a random polynomial over a finite field. Tassa extends this scheme into Hierarchical Secret Sharing (HSS) [17] with enabling different levels of ranking among participants in terms of hierarchy. Tassa's scheme realizes such access structure within our scenario while remaining perfect and ideal by handing higher-level users evaluations of the polynomial and lower-level users evaluations of its higher-order derivatives; reconstruction is then a Birkhoff interpolation that succeeds if and only if combiner group meets every threshold.

In this paper, we will introduce Hierarchical Threshold Structure Preserving Signatures, an extension of Threshold Structure Preserving Signature scheme with combined ability to establish a complex access structure of a secret with different levels of authoritarianity. Outline of this paper as follows; in Section 2 we will lay out the necessary definitions and notation, in Section 3 we will introduce our contribution and give the correctness proof and finally Section 4 mention conclusion remarks and future work.

## 2 Preliminaries

In this section we will introduce necessary concepts and notation to build our protocol. For the syntax,  $\lambda$  is the security parameter  $1^{\lambda}$  is its unary representation, and  $negl(\lambda)$  denotes negligible function. While  $x \stackrel{\$}{\leftarrow} X$  is utilized to indicate that x is uniformly sampled from the set X, the cardinality of a set X is represented by the symbol |X|. Also,  $A(x) \rightarrow y$  denotes that y is an output of the

algorithm A on input x, whereas  $x \leftarrow y$  denotes the straightforward assignment process. We denote linear pairing function e as described in [11].

**Definition 1** (Bilinear Map). A bilinear map is a function  $e: \mathbb{G}_1 \times \mathbb{G}_2 \to \mathbb{G}_T$ in groups  $\mathbb{G}_1, \mathbb{G}_2, \mathbb{G}_T$  with prime order p, that satisfies:

- Bilinearity:  $e(g_1^m, g_2^n) = e(g_1, g_2)^{m \cdot n}$  for all  $m, n \in \mathbb{Z}_p$ ,  $g_1 \in \mathbb{G}_1$ ,  $g_2 \in \mathbb{G}_2$ .
- Non-degeneracy:  $e(g_1, g_2) \neq 1$  for all  $g_1 \in \mathbb{G}_1$ ,  $g_2 \in \mathbb{G}_2$ .

The pairing map is termed symmetric (Type I) if  $\mathbb{G}_1 = \mathbb{G}_2$ . Asymmetric pairing occurs when  $\mathbb{G}_1 \neq \mathbb{G}_2$ . In this scenario, if an effectively computable isomorphism  $\phi: \mathbb{G}_2 \to \mathbb{G}_1$  exists, it is categorized as Type II; otherwise, it is classified as Type III, which will be also relied on in this study.

Definition 2 (Diffie-Hellman Message Space  $\mathcal{M}_{DH}$  [10]). Given a Type III bilinear map  $(\mathbb{G}_1, \mathbb{G}_2, \mathbb{G}_T, p, e, g_1, g_2)$ . A pair  $(M_1, M_2) \in \mathbb{G}_1 \times \mathbb{G}_2$  belongs to the Diffie-Hellman message space  $\mathcal{M}_{DH}$  if there exist  $m \in \mathbb{Z}_p$  such that  $M_1 = g_1^m$ and  $M_2 = g_2^m$ . Verification of  $e(M_1, g_2) = e(g_1, M_2)$  determines such a pair.

Definition 3 (Indexed Diffie-Hellman Message Space  $\mathcal{M}_{iDH}^{H}$  [6]). Given a Type III bilinear map  $(\mathbb{G}_1, \mathbb{G}_2, \mathbb{G}_T, p, e, g_1, g_2)$ , an index set  $\mathcal{I}$  (id  $\in \mathcal{I}$ ), and a random oracle  $\mathsf{H}: \mathcal{I} \to \mathbb{G}_1$ .  $\mathcal{M}_{iDH}^H$  is an Indexed Diffie-Hellman message space if the followings hold:

- (1)  $\mathcal{M}_{iDH}^{H} \subset \{(id, \tilde{M}) | id \in \mathcal{I}, m \in \mathbb{Z}_p, \tilde{M} = (\mathsf{H}(id)^m, g_2^m) \in \mathbb{G}_1 \times \mathbb{G}_2 \}$ (2) For all  $(id, \tilde{M}) \in \mathcal{M}_{iDH}^{H}$ ,  $(id', \tilde{M}') \in \mathcal{M}_{iDH}^{H}$ , id = id', then  $\tilde{M} = \tilde{M}'$ .

Definition 4 (Shamir's Secret Sharing [16]). Shamir's Secret Sharing is a (t,n)-threshold scheme that enables the division of a secret s into n shares such that any subset of shares containing at least t shares can reconstruct the secret s, while any subset containing fewer than t shares cannot obtain any knowledge regarding s. Consider a finite field of prime order p, denoted as  $\mathbb{F}_p$ . Shamir's secret sharing comprises share generation and secret reconstruction as outlined below:

- ShareGen(s, p, n, t): The dealer selects a random polynomial  $f(x) \in \mathbb{F}_p[x]$  of degree t-1 < p, where coefficients selected from  $\mathbb{F}_p$ , such that  $f(0) = s \in \mathbb{F}_p$ . The dealer secretly transmits a secret share  $s_i = f(id_i) \mod p$  to participant  $P_i$ , where  $id_i \in \mathbb{F}_p$  denotes the identifier of  $P_i$ , and the vector of shares is  $\vec{s} = (s_1, \dots, s_n).$
- Reconst( $\{s_i\}_{i\in\mathcal{T}}$ ): The secret is reconstructed by Lagrange interpolation on the polynomial f(x) as  $s = f(0) = \sum_{i \in \mathcal{T}} s_i \cdot \lambda_i$ , where  $\mathcal{T} \subseteq [1, n]$  of size at least t, and the Lagrange coefficient  $\lambda_i = \prod_{j \in \mathcal{T}, j \neq i} \frac{id_j}{id_j - id_i} \in \mathbb{F}_p$ .

Definition 5 (Feldman's Verifiable Secret Sharing). Feldman's Verifiable secret sharing [9] enables users to check the consistency of the received shares. Assume we have n players setup, let q, p be primes such that  $q \mid p-1$  and  $g \in \mathbb{F}_p$ 

be an element of order q. In this scheme, dealer first selects a secret s to be shared and forms the random polynomial  $f(x) \in \mathbb{F}_q[x]$  of degree t-1 < q

$$f(x) = a_0 + a_1 x + a_2 x^2 + \ldots + a_{t-1} x^{t-1}$$

where  $a_i \in \mathbb{F}_q$ , for  $i = 0, 1, \ldots t - 1$  with  $a_0 = s$ . Then, dealer computes the commitments to these coefficients by  $C_i = g^{a_i}$  for  $i = 0, 1, \ldots, t - 1$  and publishes commitment values. The dealer sends the share f(j) to each participant  $P_j$  for  $j = 1, \ldots, n$ . After receiving its share, participant  $P_j$  confirms the consistency of the received share by checking the equality

$$g^{f(j)} = \prod_{k=0}^{t-1} C_k^{j^k}.$$

If the equality holds, participants can decide that no malicious interruption has occurred and the share is consistent with the secret s. The reconstruction of the secret follows the same steps as in Shamir's secret sharing scheme.

Definition 6 (Hierarchical Threshold Secret Sharing Scheme [17] ). Let  $\mathcal{G}$  be set of n players such that it is established by m distinct subsets, i.e.,  $\mathcal{G} = \bigcup_{i=1}^m \mathcal{G}_i, \ \mathcal{G}_i \cap \mathcal{G}_j = \emptyset$  for  $i \neq j$ . Let  $0 < k_1 < \ldots < k_m$  be the degree of the access structure levels. Then, the access structure  $\Gamma$  of the hierarchical threshold secret sharing scheme is

$$\Gamma = \left\{ \mathcal{V} \subset \mathcal{G} : \left| \mathcal{V} \cap \left( \bigcup_{j=1}^{i} \mathcal{G}_{j} \right) \right| \geq k_{i} \mid \forall i \in \{1, 2, \dots, m\} \right\}$$

Dealer then samples a random polynomial of degree  $k_m$ , i.e.,

$$f(x) = \sum_{i=0}^{k_m} a_i x^i$$

with  $a_0 = s$ . The dealer assigns a unique element  $x_u \in \mathbb{F}_q$  to each user  $u \in \mathcal{G}_i$  and sends the share  $(x_u, f^{(k_{i-1}+1)})$ , i.e.,  $f^{(k_{i-1}+1)}$  is the  $k_{i-1} + 1$ -th derivative of polynomial f, where  $k_0 = -1$ . In the secret construction, Birkhoff coefficients are used, which are described next.

**Definition 7 (Birkhoff Coefficient).** [2, Def. 2.9] Let  $X = \{x_1, x_2, \ldots, x_k\}$  be a set of given points in  $\mathbb{R}$  where  $x_1 < x_2 < \ldots < x_k$ ,  $E = (e_{i,j})$  for  $i = 0, \ldots, k$  and  $j = 0, \ldots, \ell$  be a matrix with binary entries,  $I(E) = \{(i, j) : e_{i,j} = 1\}$ , d = |I(E)|, and  $C = \{c_{i,j} : (i,j) \in I(E)\}$  be a set of d real values (we assume hereafter that the right-most column in E is nonzero). Let matrix A be defined by  $A(E, X, \phi_j) = (\theta_{ij})_{d \times d}$  where  $\theta_{ij} = g_{j-1}^{(\alpha_i(2))}(x_{\alpha_i(1)})$  for  $i, j = 1, \ldots, d$ . Birkhoff coefficient  $\beta_i$  is the evaluation of the polynomial  $f_i$  at 0,

$$f_i(x) = \sum_{j=0}^{d-1} (-1)^{(i+j)} \frac{\det(A_i(E, X, \phi_j))}{\det(A(E, X, \phi))} g_j(x),$$

*i.e.*  $\beta_i = f_i(0)$ .

## 3 Hierarchical Threshold Structure Preserving Signatures

In this section, we present a Hierarchical Threshold Structure Preserving Signature Scheme (HTSPS) which extends Threshold Structure Preserving Scheme with a hierarchical access structure. With HTSPS, one can define a complex access-structure setting in which delegation is possible both vertically and horizontally. Since the higher level of shares includes more information in terms of derivatives, one can delegate this responsibility downward without the need of changing the global verification key. This also naturally enables different valid subgroups in the same access levels.

Imagine the following scenario; a multinational investment bank for legal and risk-management reasons has a policy that mandates the following policy; any issuance of an account above some level requires three-tier approval ladder which includes; approval from Tier 0 group; which could be an example of executive board, approval from Tier 1 group; which could be an example of risk and compliance board and approval from Tier 2 group; which could be an example of regional directors. HTSPS can provide a setting where this policy's requirements are met while any sub-coalition that does not meet the threshold for each tier learns nothing about the global signature.

HTSPS consists of six PPT algorithms, that is, Setup, KeyGen, PSignGen, PSignVer, Reconst, Verify. Since HTSPS uses HTSS for secret key generation, this scheme also relies on a designated dealer to setup the access structure and generation of secret keys and verification keys.

- Setup( $1^{\lambda}$ )  $\to pp$ : The setup algorithm accepts the security parameter  $1^{\lambda}$  as an input and outputs the public parameters pp for the HTSPS. The public parameters consist of groups  $\mathbb{G}_1, \mathbb{G}_2, \mathbb{G}_T$  of orders p used in bilinear map e, along with the generators  $g_1$  and  $g_2$  for  $\mathbb{G}_1$ , and  $\mathbb{G}_2$ , respectively. Additionally, there is a hash function  $H: \{0,1\}^m \to \mathbb{G}_1$  that maps to  $\mathbb{G}_1$  allowing messages to be securely represented as elements within the group. Algorithm outputs the public parameters  $pp := ((\mathbb{G}_1, \mathbb{G}_2, \mathbb{G}_T, p, e, g_1, g_2), H)$
- KeyGen $(pp) \to (sk_1, sk_2, vk_1, vk_2)$ : The key generation algorithm is used by the selected dealer to generate key pair that will be used to generate signature. The selected dealer proceeds to establish the access structure as in Definition 6, i.e., let  $\mathcal{G}$  be set of n participant such that it is established by m distinct subsets, i.e.,  $\mathcal{G} = \bigcup_{i=1}^m \mathcal{G}_i, \mathcal{G}_i \cap \mathcal{G}_j = \emptyset$  for  $i \neq j$ . Let  $0 < k_1 < \ldots < k_m$  be the degree of the access structure levels and let  $n_i$  be the number of participant in the corresponding level  $\mathcal{G}_i$ . The access structure  $\Gamma$  is defined by

$$\Gamma = \left\{ \mathcal{V} \subset \mathcal{G} : \left| \mathcal{V} \cap \left( \bigcup_{j=1}^{i} \mathcal{G}_{j} \right) \right| \geq k_{i} \mid \forall i \in \{1, 2, \dots, m\} \right\}$$

With the access structure established the dealer proceeds as follows;

• Dealer chooses two random secret values  $sk_1, sk_2 \in \mathbb{F}_p$  and calculates global verification keys  $vk_1 := g_2^{sk_1}$  and  $vk_2 := g_2^{sk_2}$ .

• Dealer samples two polynomials  $f_1(x), f_2(x) \in \mathbb{F}_p[x]$  of degree  $k_m$ 

$$f_1(x) = \sum_{i=0}^{k_m} a_i x^i, \quad f_2(x) = \sum_{i=0}^{k_m} b_i x^i$$

with coefficients  $a_i, b_i, i = 1, ..., k_m$  selected uniformly random such that  $sk_1 = a_0$  and  $sk_2 = b_0$  as seen in Figure 1.

- Dealer calculates and publishes the commitments  $B_i = g_2^{a_i}$  and  $C_i = g_2^{b_i}$  for  $i = 1, ..., k_m$ .
- Dealer assigns a unique identifier  $x_{ij} \in \mathbb{F}_p$  to each participant  $P_{ij} \in \mathcal{G}_i$  for  $i \in [1, m]$  and  $j \in [1, n_i]$ .
- Dealer calculates the shares by taking the  $k_{i-1}+1$ -th derivatives of both  $f_1$  and  $f_2$ , and sends the values to the corresponding participant, i.e., each participant receives  $(x_{ij}, \psi_{ij,1}, \psi_{ij,2})$ , where  $\psi_{ij,1} = f_1^{(k_{i-1}+1)}(x_{ij})$  and  $\psi_{ij,2} = f_2^{(k_{i-1}+1)}(x_{ij})$ .
- After receiving its share  $(x_{ij}, \psi_{ij,1}, \psi_{ij,2})$  each participant first does consistency check by

$$g_2^{\psi_{ij,1}} = \prod_{j=k_i}^{k_m} B_j^{\binom{j}{j-k_i}} x_{ij}^{j-k_i} \text{ and } g_2^{\psi_{ij,1}} = \prod_{j=k_i}^{k_m} C_j^{\binom{j}{j-k_i}} x_{ij}^{j-k_i},$$

where  $k_i$  is the access level the participant  $P_{ij}$  belongs to. If both of the equations hold then participant accepts the shares, otherwise it rejects it.

- Each participant  $P_{ij} \in \mathcal{G}_i$  for  $i \in [1, m]$  and  $j \in [1, n_i]$  calculates their partial verification key pair  $(vk_{ij,1}, vk_{ij,2})$  by  $vk_{ij,1} = g_2^{\psi_{ij,1}}, vk_{ij,2} = g_2^{\psi_{ij,2}}$ .
- PSignGen $(pp, x_{ij}, \psi_{ij,1}, \psi_{ij,2}, (id, M_1, M_2)) \rightarrow (\sigma_{ij}, \bot)$ : Partial signature generation algorithm is used by each participant that generates partial signature values.
  - Participants perform the indexed message consistency check on indexed message  $(id, M_1, M_2) \in \mathcal{M}_{iDH}^H$ , by

$$h \neq 1_{\mathbb{G}_1} \land M_1 \neq 1_{\mathbb{G}_1} \land e(h, M_1) = e(M_1, g_2)$$

with message  $\mu \in \mathbb{F}_p$ , where  $h = \mathsf{H}(id)$ ,  $M_1 = h^{\mu}$  and  $M_2 = g_2^{\mu}$ .

• Each participant calculates its own partial signature  $\sigma_{ij}$ 

$$\sigma_{ij} = (h, s_{ij}) = (h, h^{\psi_{ij,1}} \cdot M_1^{\psi_{ij,2}}),$$

and sends it to the combiner who can be any one of the signers.

- PSignVer $(pp, (id_i, M_{1,i}, M_{2,i}), \sigma_{ij} \rightarrow \{0,1\})$ : Partial signature verification algorithm is used to verify each participant  $P_{ij}$ 's partial signature. The combiner accepts the received partial signature if all the following conditions hold:

- (i)  $h_i \neq 1_{\mathbb{G}_1}$ ,
- (ii)  $M_{1,i} \neq 1_{\mathbb{G}_1}$ ,
- (iii)  $e(h_i, M_{2,i}) = e(M_{1,i}, g_2),$
- (iv)  $e(h_i, vk_{ij,1})e(M_{1,i}, vk_{ij,2}) = e(s_{ij}, g_2).$

Rejects it otherwise.

- Reconst $(pp, \mathcal{S}, \{\sigma_{1j}, \sigma_{2j}, \dots, \sigma_{mj}\}_{j=1}^{n_i}) \to \sigma$ : The reconstitution algorithm is used by the valid access structure to reconstruct the signature. The combiner first establishes the subgroup of signers  $\mathcal{S} := \{\mathcal{S}_1, \dots, \mathcal{S}_m\}$  where  $\mathcal{S}_i$  is the subgroup of signers in respective access levels such that  $|\mathcal{S}_i| > k_i$ . The combiner then calculates the signature by

$$\sigma = (h, s) = (h, \prod_{i=1}^{m} \prod_{j \in \mathcal{S}_i} s_{ij}^{\beta_{ij}})$$

where  $\beta_{ij}$  is the corresponding Birkhoff coefficient defined in Definition 7.

- Verify $(pp, \sigma, (id, M_1, M_2), vk_1, vk_2) \rightarrow \{0, 1\}$ : Verify algorithm is used to verify the signature of the message with index id. The verifier checks the validity of the following equations,
  - (i)  $h \neq 1_{\mathbb{G}_1}$ ,
  - (ii)  $M_1 \neq 1_{\mathbb{G}_1}$ ,
  - (iii)  $e(h, M_2) = e(M_1, g_2),$
  - (iv)  $e(h, vk_1)e(M_1, vk_2) = e(s, g_2)$ .

If the equations hold the verifier accepts the signature, otherwise rejects it.

#### 3.1 Security and Correctness

We can show that the scheme is correct by

$$\begin{split} s &= \prod_{i=1}^{m} \prod_{j \in \mathcal{S}_{i}} s_{ij}^{\beta_{ij}} \\ &= \prod_{i=1}^{m} \prod_{j \in \mathcal{S}_{i}} (h^{\psi_{ij,1}} \cdot M_{1}^{\psi_{ij,2}})^{\beta_{i,j}} \\ &= \prod_{i=1}^{m} \prod_{j \in \mathcal{S}_{i}} (h^{\psi_{ij,1}\beta_{i,j}} \cdot M_{1}^{\psi_{ij,2}\beta_{i,j}}) \\ &= h^{\sum_{i=1}^{m} \sum_{j \in \mathcal{S}_{i}} \beta_{i,j}\psi_{ij,1}} \cdot M_{1}^{\sum_{i=1}^{m} \sum_{j \in \mathcal{S}_{i}} \beta_{i,j}\psi_{ij,2}} \\ &= h^{sk_{1}} \cdot M_{1}^{sk_{2}} \end{split}$$

It's easy to see that the above equation is true for signature  $\sigma$ .

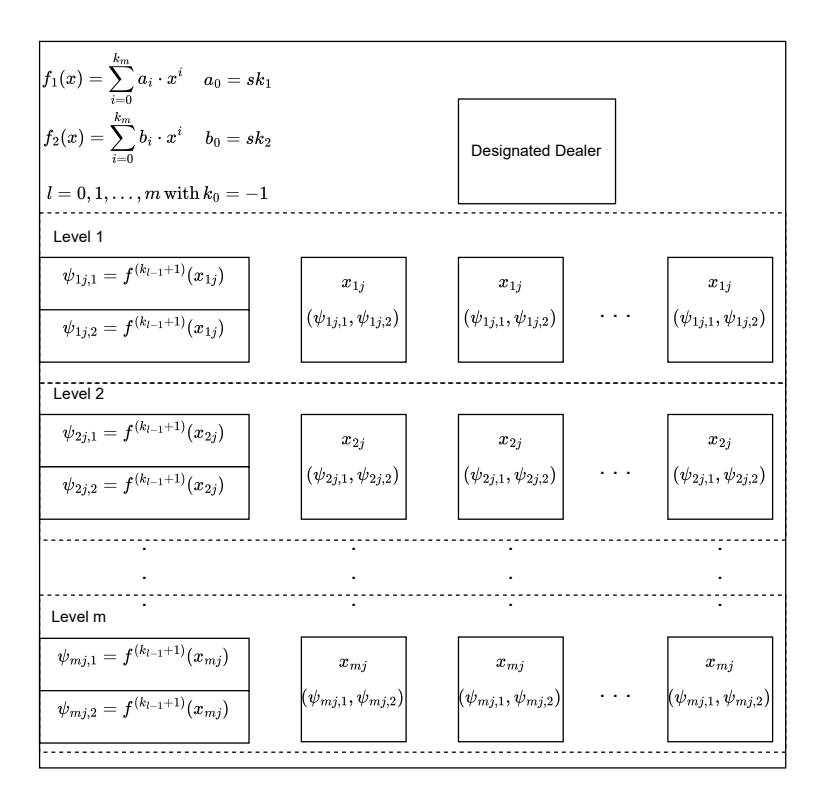


Fig. 1. Share Distribution in HTSPS

Security. Our scheme inherits two main security features directly from its building blocks. First, the confidentiality follows the perfect security of Tassa's hierarchical threshold secret-sharing scheme: any group of participants that falls short of the vector  $k_0, k_1, \ldots, k_m$  learns nothing about the signing key information-theoretically, because their shares leave at least one coefficient of the secret polynomial undetermined. Second, existential unforgeability under chosen-message attack reduces the security of TSPS: forging an aggregate signature without meeting the threshold would either reveal a non-authorized linear combination of the secret shares, contradicting the security of HTSS, or produce a valid SPS signature without the underlying signing key, breaking the hardness assumption of TSPS. Since our aggregation of signatures is a linear combination in the exponent, it introduces no additional algebraic structure. Thus, the overall security of our protocol is the intersection of HTSS confidentiality and TSPS unforgeability.

#### 4 Conclusion and Future Work

In this paper, we presented Hierarchical Threshold Structure Preserving Signatures where we extend threshold structure preserving signatures with a hierarchical secret sharing scheme, allowing the protocol to enable a layered access structure. The proof of correctness is also provided, and we argue that the security of our scheme does not separate from the security of the building blocks HTSS and TSPS. Our protocol still relies on the designated dealer to set up the access structure and the combiner to aggregate the signature. As future work, we plan to provide a proof-of-concept implementation and an efficiency analysis of our proposed scheme. Also, the formal proof of the scheme will be done as future work.

#### References

- Abe, M., Fuchsbauer, G., Groth, J., Haralambiev, K., Ohkubo, M.: Structure-preserving signatures and commitments to group elements. In: Advances in Cryptology-CRYPTO 2010: 30th Annual Cryptology Conference, Santa Barbara, CA, USA, August 15-19, 2010. Proceedings 30, pp. 209-236. Springer (2010)
- Ağırtaş, A.R., Yayla, O.: Compartment-based and hierarchical threshold delegated verifiable accountable subgroup multi-signatures. In: A. Dabrowski, J. Pieprzyk, J. Pomykała (eds.) Number-Theoretic Methods in Cryptology, pp. 283–313. Springer Nature Switzerland, Cham (2025)
- Ağırtaş, A.R., Çelik, E., Kocaman, S., Sulak, F., Yayla, O.: Threshold structure-preserving signatures with randomizable key. In: Proceedings of the 22nd International Conference on Security and Cryptography, pp. 632–637 (2025)
- 4. Backes, M., Hanzlik, L., Kluczniak, K., Schneider, J.: Signatures with flexible public key: Introducing equivalence classes for public keys. In: International Conference on the Theory and Application of Cryptology and Information Security, pp. 405–434. Springer (2018)
- Connolly, A., Lafourcade, P., Perez Kempner, O.: Improved constructions of anonymous credentials from structure-preserving signatures on equivalence classes. In: IACR International Conference on Public-Key Cryptography, pp. 409–438. Springer (2022)
- 6. Crites, E., Kohlweiss, M., Preneel, B., Sedaghat, M., Slamanig, D.: Threshold structure-preserving signatures. In: International Conference on the Theory and Application of Cryptology and Information Security, pp. 348–382. Springer (2023)
- 7. Crites, E.C., Lysyanskaya, A.: Delegatable anonymous credentials from mercurial signatures. In: Cryptographers' Track at the RSA Conference, pp. 535–555. Springer (2019)
- 8. Derler, D., Slamanig, D.: Key-homomorphic signatures: definitions and applications to multiparty signatures and non-interactive zero-knowledge. Designs, Codes and Cryptography 87, 1373–1413 (2019)
- 9. Feldman, P.: A practical scheme for non-interactive verifiable secret sharing. In: 28th Annual Symposium on Foundations of Computer Science (sfcs 1987), pp. 427–438. IEEE (1987)
- 10. Fuchsbauer, G.: Automorphic signatures in bilinear groups and an application to round-optimal blind signatures. Cryptology ePrint Archive (2009)

- 11. Galbraith, S.D., Paterson, K.G., Smart, N.P.: Pairings for cryptographers. Discrete Applied Mathematics **156**(16), 3113–3121 (2008). DOI 10.1016/j.dam.2007.12.010. URL https://www.sciencedirect.com/science/article/pii/S0166218X08000449. Applications of Algebra to Cryptography
- 12. Ghadafi, E.: Short structure-preserving signatures. In: Cryptographers' Track at the RSA Conference, pp. 305–321. Springer (2016)
- Hanser, C., Slamanig, D.: Structure-preserving signatures on equivalence classes and their application to anonymous credentials. In: Advances in Cryptology– ASIACRYPT 2014: 20th International Conference on the Theory and Application of Cryptology and Information Security, Kaoshiung, Taiwan, ROC, December 7-11, 2014. Proceedings, Part I 20, pp. 491–511. Springer (2014)
- Mir, O., Bauer, B., Griffy, S., Lysyanskaya, A., Slamanig, D.: Aggregate signatures
  with versatile randomization and issuer-hiding multi-authority anonymous credentials. In: Proceedings of the 2023 ACM SIGSAC Conference on Computer and
  Communications Security, pp. 30–44 (2023)
- 15. Nanri, M., Kempner, O.P., Tibouchi, M., Abe, M.: Interactive threshold mercurial signatures and applications. Cryptology ePrint Archive (2024)
- 16. Shamir, A.: How to share a secret. Communications of the ACM **22**(11), 612–613 (1979)
- 17. Tassa, T.: Hierarchical threshold secret sharing. In: M. Naor (ed.) Theory of Cryptography, pp. 473–490. Springer Berlin Heidelberg, Berlin, Heidelberg (2004)

# A Comparative Study of LWE and LIP-Based Post-Quantum Signature Schemes

Édgar Pérez-Ramos  $^{1[0009-0008-0409-3079]}$ , Cristian Nina-Orellana Candelaria Hernández-Goya  $^{1[0000-0002-9468-708X]}$ , and Pino Caballero-Gil  $^{1[0000-0002-0859-5876]}$ 

University of La Laguna, Tenerife, Spain {eperezra, alu0101470856, mchgoya, pcaballe}@ull.edu.es

Abstract. With the rise of quantum computing as a real threat to classical cryptography, the National Institute of Standards and Technology launched a standardization process in 2016 to identify secure algorithms for public-key encryption and digital signatures. In 2022, CRYSTALS-Kyber was selected for encryption and CRYSTALS-Dilithium, FALCON, and SPHINCS+ were chosen for digital signatures, the first three based on lattice problems and the last on cryptographic hash functions. A second call was initiated in 2024 to encourage diversity in digital signature schemes. In 2025, the candidate HAWK emerged in the second round, offering a lattice-based approach built on the Lattice Isomorphism Problem, a less explored but promising alternative.

This work presents and explores two of the central mathematical problems underlying these digital signature algorithms: the Learning With Errors problem, which supports many of the currently standardized algorithms, and the Lattice Isomorphism Problem, which forms the basis of the HAWK proposal. After introducing and analyzing these problems, we implement and compare the signature schemes to evaluate their practical performance. This comparative study aims to analyze the trade-off between digital signatures constructed from cryptographic hash functions and those derived from hard problems on lattices, particularly highlighting the differences between schemes built on the Learning With Errors problem and those based on the Lattice Isomorphism Problem.

**Keywords:** Post-quantum cryptography · HAWK · Lattices · LIP

### 1 Introduction

The revolution of quantum computing promises a technological paradigm shift by solving in mere seconds mathematical problems that would take today's most powerful computers thousands of years to compute. However, alongside these advancements comes a significant threat to cybersecurity. Quantum computing could be used to break current encryption systems that safeguard our banking data, communications, and government secrets. This has triggered a race against time to develop new cryptographic methods that are resilient in the quantum era, ensuring a secure digital future.

Since 2016, the National Institute of Standards and Technology (NIST) has devoted considerable effort to the selection of algorithms that are resistant to quantum attacks. At the end of 2017, 69 algorithms passed the first phase of the call. Later, in 2019, after a thorough screening process, only 26 remained. During that round, rigorous tests were conducted to evaluate the security and performance of each algorithm, as well as to identify potential vulnerabilities.

In the third round of evaluation in 2018, 15 final candidates were selected to continue in the standardization process. During this round, additional testing was conducted, and collaboration with the cryptographic community helped identify potential vulnerabilities and improve the robustness of shortlisted algorithms.

Finally, in July 2022, NIST announced the algorithms selected as final standards. The standardization proposal includes:

- Encryption: CRYSTALS-Kyber [1].
- Digital signatures: CRYSTALS-Dilithium [2], FALCON [3], and SPHINCS+[4].

Furthermore, in mid-2022, the BIKE, Classic McEliece, HQC (Hamming Quasi-Cyclic), and SIKE encryption schemes advanced to the fourth round, to continue their analysis and evaluation [5].

Regarding digital signatures, in 2023, the next step for NIST was to diversify its range of schemes, including some alternatives not based on lattices [6]. This strategy responds to the principle of crypto-agility, as it ensures the ability of security systems to quickly adapt to changes in cryptographic algorithms, promoting the coexistence of different cryptographic families as a preventive measure against future vulnerabilities. In particular, the search for schemes with short signatures and fast verification was prioritized, thus favouring their application in resource-constrained contexts or those with high efficiency requirements. In 2024, NIST published the second round of this process and released the algorithms that had advanced to that phase [7]. These algorithms are shown in Tab. 1.

**Table 1.** Digital signature schemes selected for the second round of the NIST Additional Signature Schemes Evaluation Process (2024).

| Category        | Algorithms                              |
|-----------------|---|
| Code-Based      | CROSS, LESS                             |
| Lattice-Based   | HAWK                                    |
| MPC-in-the-Head | MIRA*, MiRitH*, MQOM, PERK, RYDE, SDitH |
| Multivariate    | MAYO, QR-UOV, SNOVA, UOV                |
| Symmetric-Based | FAEST                                   |
| Isogeny-Based   | SQIsign                                 |

This work is organized as follows. Section II introduces the computational problems under analysis: the Learning With Errors (LWE) problem and the

Lattice Isomorphism Problem (LIP). It also presents a comparative study of current standardized digital signatures based on lattices and hash functions. Section III focuses on the implementation and presents the results obtained, comparing lattice-based signatures on one hand and the HAWK signature scheme against current standardized signatures on the other. Finally, the last section is dedicated to future work and concluding remarks.

## 2 Background

In this section, we will address the main problems associated with the digital signatures discussed in this work: Learning With Errors and the Lattice Isomorphism Problem. We focus on these problems because we are interested in comparing the efficiency of signature schemes based on LWE and LIP. Both problems are foundational in post-quantum cryptography, and analyzing them will allow us to assess their advantages and disadvantages in terms of security and performance in the context of quantum-resistant digital signatures.

The following notation will be used throughout the paper:

- The ring of integers modulo a prime q is denoted as  $\mathbb{Z}_q$ .
- The set of *n*-vectors over  $\mathbb{Z}_q$  is denoted as  $\mathbb{Z}_q^n$ .
- The polynomial ring  $\mathbb{Z}_q(x)/\phi(x)$  is denoted as  $\mathcal{R}_q$ , where  $\phi(x)$  is the polynomial  $x^n + 1$ .

#### 2.1 The Learning With Errors problem

**Problem Formalization** Let  $n \in \mathbb{N}$  and  $q \in \mathbb{Z}$ . Consider m vectors  $b_1, b_2, \ldots, b_m \in \mathbb{Z}_q^n$ . The lattice  $\Lambda$  generated by the base of vectors  $B = \{b_1, b_2, \ldots, b_m \in \mathbb{Z}_q^n\}$  is then the set:

$$\Lambda = \mathcal{L}(b_1, \dots, b_m) = \left\{ \sum_{i=1}^m z_i \cdot b_i : z_i \in \mathbb{Z} \right\}$$
 (1)

Fix a probability distribution  $\mathcal{X}$  over  $\mathbb{Z}_q$ , which allows selecting an error term in a controlled manner. The selection of an error e according to this distribution is denoted by  $e \leftarrow \mathcal{X}$ . These parameters define the so-called *LWE distribution* over  $\mathbb{Z}_q^n \times \mathbb{Z}_q$ .

**Definition 1.** LWE Distribution. Let  $n, q \in \mathbb{N}$ ,  $s \in \mathbb{Z}_q^n$ , and  $\mathcal{X}$  be a probability distribution over  $\mathbb{Z}_q$ . The LWE distribution modulo q associated with s, denoted  $\mathcal{A}_{s,\mathcal{Z}}$ , is defined by selecting a vector  $a \in \mathbb{Z}_q$  uniformly at random and selecting an error  $e \leftarrow \mathcal{X}$ , yielding:

$$(a,b) \in \mathbb{Z}_q^n \times \mathbb{Z}_q, \quad where \ b = \langle s, a \rangle + e \mod q$$
 (2)

Applications of *LWE* to Cryptography This section is based on [8]. As mentioned earlier, a wide variety of cryptographic constructions have been based on the standard LWE problem. Most of these applications can be made more efficient, and sometimes even practical for real-world use, by adapting them to Ring-LWE (RLWE). This adaptation process is usually straightforward, though in some cases it requires additional technical tools to achieve the most precise and efficient results.

As an example of application, a simple and efficient semantically secure public-key cryptosystem is outlined. The key generation algorithm selects a uniformly random element  $A \in \mathcal{R}_q$  as well as two small random elements,  $s, e \in \mathcal{R}_q$ , from the LWE distribution. Then, s is used as the secret key, and the pair  $(A, t = A \cdot s + e)$  forms the public key. To encrypt a message m of n bits, where  $m = (b_0, b_1, \ldots, b_{n-1})$  with  $b_i \in \{0, 1\}$ , the encryption algorithm selects three small random elements  $r, e_1, e_2 \in \mathcal{R}_q$  from the error distribution, and the corresponding calculations produce the pair (u, v) as the ciphertext of the message m, where:

$$u = A \cdot r + e_1 \mod q, \qquad v = t \cdot r + e_2 + \left[\frac{q}{2}\right] \cdot m \mod q$$
 (3)

To decrypt, we compute:

$$v - u \cdot s = (r \cdot e - s \cdot e_1 + e_2) + \left[\frac{q}{2}\right] \cdot m \mod q \tag{4}$$

For an appropriate choice of parameters, the coefficients of  $r \cdot e - s \cdot e_1 + e_2$  have magnitudes smaller than  $\frac{q}{4}$ , so the bits of m can be recovered by rounding each coefficient of  $v - u \cdot s$  to either 0 or  $[\frac{q}{2}]$ . Once rounded, those that are 0 remain 0, and those that are  $[\frac{q}{2}]$  are set to 1, thus recovering the original message.

Correctness of LWE According to [8], with n being the security parameter, m the number of equations, q the chosen prime modulus, and a noise parameter  $\alpha>0$ , Regev recommends choosing q in the range  $(n^2,2n^2)$ ,  $m=n\cdot\log(q)$ , and  $\alpha=\frac{1}{n\cdot\log^2(n)}$ . Notice that if it weren't for the error in LWE samples,  $t-A\cdot s$  could be 0 or  $[\frac{q}{2}]$  depending on the encrypted bit, and decryption would always be correct. Thus, Regev indicates that a decryption error only occurs if the sum of the error terms across all coefficients exceeds  $\frac{q}{4}$ . Since we are summing at most n normal error terms, each with a standard deviation of  $\alpha \cdot q$ , the standard deviation of the sum is at most  $\sqrt{m} \cdot \alpha \cdot q << \frac{q}{\log(n)}$ ; a standard calculation shows that the probability of this normal variable exceeding  $\frac{q}{4}$  is negligible.

#### 2.2 The Lattice Isomorphism Problem

The Lattice Isomorphism Problem [9], is a computational problem that arises in the context of lattice theory and cryptography. LIP is the underlying computational problem of the candidate digital signature standard HAWK. It involves determining whether two given lattices are isomorphic, meaning that there exists an orthonormal transformation that maps one lattice onto the other. The difficulty of solving this problem is closely related to the hardness of lattice problems, which are believed to remain hard even in the presence of quantum computers.

The LIP, while less studied than LWE, holds significant cryptographic potential. In work [10], the authors introduce generalizations that enable a worst-case to average-case reduction for the search-LIP within a specific class of isomorphisms. They also present a key encapsulation mechanism and a digital signature scheme built upon the hardness of LIP.

Furthermore, in the more recent work [11] (2025), they prove the feasibility of constructing a fully homomorphic encryption (FHE) scheme based on a variant of the lattice isomorphism problem. Altogether, these developments indicate that although LIP remains relatively underexplored, it is emerging as a promising foundation for post-quantum cryptography, especially driven by the rise of HAWK.

In order to define this problem, we first need to introduce the concept of isomorphism between lattices.

**Definition 2.** Let  $O \in M_{n \times n}(\mathbb{R})$ . We say that O is orthonormal if  $O^TO = I_n$ .

**Definition 3.** Two lattices  $\mathcal{L}_1$  and  $\mathcal{L}_2$  are isomorphic if there exists an orthonormal transformation  $O \in O_n(\mathbb{R})$  such that  $O \cdot \mathcal{L}_1 = \mathcal{L}_2$ .

Next, the search version of lattice isomorphism problem is to determine if two lattices are isomorphic and to find the corresponding orthonormal transformation:

**Definition 4** (decision Lattice Isomorphism Problem (dLIP)). Given two lattices  $\mathcal{L}_1$  and  $\mathcal{L}_2$ , determine if there exists a transformation  $O \in O_n(\mathbb{R})$  such that:

$$\mathcal{L}_2 = O \cdot \mathcal{L}_1 \tag{5}$$

Similarly, we define the search version of the problem:

**Definition 5** (search Lattice Isomorphism Problem (sLIP)). Given two lattices  $\mathcal{L}_1$  and  $\mathcal{L}_2$ , find, if it exists, the transformation  $O \in O_n(\mathbb{R})$  such that:

$$\mathcal{L}_2 = O \cdot \mathcal{L}_1 \tag{6}$$

Now, considering the bases of the lattices  $\mathcal{L}_1$  and  $\mathcal{L}_2$ , denoted as  $B_1$  and  $B_2$ , respectively, we can translate the problem into the following relation between bases:  $\mathcal{L}_1$  and  $\mathcal{L}_2$  are isomorphic if there exists a unimodular matrix  $\mathbf{U} \in GL_n(\mathbb{Z})$  and an orthonormal transformation  $O \in O_n(\mathbb{R})$  such that  $B_2 = O \cdot B_1 \cdot U$ .

Note 1. It is important to recall that two bases B and B' generate the same lattice if there exists a unimodular matrix  $\mathbf{U} \in GL_n(\mathbb{Z})$  such that:  $B' = B \cdot U$ .

#### É. Pérez-Ramos et al.

6

The utility of the Lattice Isomorphism Problem in the HAWK scheme is to leverage the difficulty of the modular isomorphism problem in its search version. Specifically, we start with the canonical basis  $B = I_n$ , which generates  $\mathbb{Z}^n$ , and consider an obfuscated basis of the form  $B \cdot U$ . However, unlike in the Shortest Vector Problem (SVP), we also consider an orthonormal transformation (such as a rotation). By constructing a new basis  $O \cdot B \cdot U$ , where  $U \in GL_n(\mathbb{Z})$  is unimodular and  $O \in O_n(\mathbb{R})$  is orthonormal, we generate a new lattice that is isomorphic to the original. Since this new basis involves a rotation, it hides the relationship with the canonical basis. This ensures a clear separation between the public information and the secret key.

We have introduced two core hardness assumptions: the Learning With Errors problem and the Lattice Isomorphism Problem, which underlie the ML-DSA and HAWK schemes, respectively. Both problems rely on the assumed difficulty of certain tasks in lattice-based cryptography, yet they differ significantly in structure and algebraic formulation. Additionally, we consider the Short Integer Solution (SIS) problem, which can be seen as a variant of LWE and serves as the foundation for the Falcon signature scheme. Finally, the hash collision resistance problem, which underpins SPHINCS+, has been thoroughly analyzed in existing literature and is well understood. With all these foundational problems established and their differences clarified, we are now prepared to implement the corresponding digital signature schemes and carry out a comparative analysis. The schemes considered are summarized in Tab. 2.

Table 2. Comparison of Post-Quantum Signature Schemes

| Scheme           | Underlying Structure | Hardness Assumption         |
|------------------|----------------------|-----------------------------|
| Lattice-based: I | HAWK                 |                             |
| HAWK-256         | Lattice              | Lattice Isomorphism Problem |
| HAWK-512         | Lattice              | Lattice Isomorphism Problem |
| HAWK-1024        | Lattice              | Lattice Isomorphism Problem |
| Lattice-based: 1 | ML- $DSA$            |                             |
| ML-DSA-44        | Lattice              | Module-LWE                  |
| ML-DSA-65        | Lattice              | Module-LWE                  |
| ML-DSA-87        | Lattice              | Module-LWE                  |
| Lattice-based: I | Falcon               |                             |
| Falcon-512       | Lattice              | NTRU-SIS                    |
| Falcon-1024      | Lattice              | NTRU-SIS                    |
| Hash-based: SF   | PHINCS+              |                             |
| SPHINCS-128s     | Hash-based           | Collision Resistance        |
| SPHINCS-128f     | Hash-based           | Collision Resistance        |
| SPHINCS-256f     | Hash-based           | Collision Resistance        |

## 3 Implementation and experimental analysis

For this experiment, we utilized a computer with the following specifications:

Processor: AMD Ryzen<sup>™</sup> 7 4800H, 2.90 GHz (base frequency)

- Processor cores: 8 physical cores / 16 threads

- RAM memory: 16.0 GB DDR4

The software stack consists of:

- liboqs: A C library for quantum-resistant cryptographic algorithms from the Open Quantum Safe project.
- The c implementation of HAWK [12], as Open Quantum Safe does not yet contain it in its repositories.

The objective of these experiments is twofold. First, we aim to compare current lattice-based digital signature standards, such as ML-DSA and FALCON, with the candidate standard HAWK. This comparison also provides insight into the extent to which differences arise from the underlying lattice problems-namely Learning With Errors and the Lattice Isomorphism Problem. Second, we seek to evaluate the digital signature schemes SPHINCS+ and ML-DSA against HAWK, providing an additional perspective by assessing the candidate in relation to both lattice-based and hash-based approaches.

For these experiments, we conducted two sets of tests—one comparing LWE-based and LIP-based schemes, and another comparing lattice-based and hash-based digital signatures. In each case, we evaluated the schemes at two different security levels: the lowest and the highest available. Specifically, we used ML-DSA-44, HAWK-256, FALCON-512, and SPHINCS+-128s for the lower security level, and ML-DSA-87, HAWK-1024, FALCON-1024, and SPHINCS+-256f for the higher level. The results are presented below:

- In the first comparison between LWE and LIP at the lowest security level (see Tab. 3), the most significant differences arise during the key generation phase. Here, we observe discrepancies of one to two orders of magnitude compared to ML-DSA-44, FALCON, and HAWK, with HAWK being the slowest. In the signing phase, performance differences are minimal across all schemes. Similarly, during verification, the differences remain small, although slightly more noticeable than in the signing phase, yet still far less than in key generation. At the highest security level, the differences follow a similar pattern to those observed in the lowest level. These results are more clearly illustrated in Fig. 1. In this case, due to the large disparities in magnitude, a logarithmic scale is used to enhance visualization.
- In the second comparison (lattice-based vs. hash-based) at the lowest security level (see Tab. 4), the most significant differences arise during the key generation phase. HAWK-256 shows the highest key generation time, being several orders of magnitude slower than both ML-DSA-44 and SPHINCS-128s. In the signing and verification phases, performance differences are minimal. At

#### É. Pérez-Ramos et al.

8

the highest security level, the results follow a similar pattern to those observed at the lower level. As in first comparison, a logarithmic scale has also been applied in the graphical representation of Fig. 1 due to the significant differences in value magnitudes.

Table 3. Average execution times.

| Algorithm       | KeyGen (µs)          | Sign (µs)            | Verify (μs           |
|-----------------|----------------------|----------------------|----------------------|
| Low Security L  | evel                 |                      |                      |
| FALCON-512      | $6.21 \times 10^{3}$ | $4.43\times10^2$     | $4.27 \times 10^{1}$ |
| HAWK-256        | $1.54 \times 10^{4}$ | $4.22 \times 10^2$   | $4.34 \times 10^{2}$ |
| ML-DSA-44       | $2.03\times10^2$     | $4.51\times10^2$     | $9.17 \times 10^{1}$ |
| High Security 1 | Level                |                      |                      |
| FALCON-1024     | $1.68 \times 10^{4}$ | $5.84 \times 10^{2}$ | $7.34 \times 10^{1}$ |
| HAWK-1024       | $6.67 \times 10^{4}$ | $8.59 \times 10^{2}$ | $8.69 \times 10^{2}$ |
| ML-DSA-87       | $3.25 \times 10^2$   | $7.81 \times 10^2$   | $2.27 \times 10^2$   |

Table 4. Average execution times.

| Algorithm        | KeyGen $(\mu s)$     | Sign $(\mu s)$       | Verify $(\mu s)$     |
|------------------|----------------------|----------------------|----------------------|
| Low Security Lev | vel                  |                      |                      |
| HAWK-256         | $1.46 \times 10^{4}$ | $3.94 \times 10^{2}$ | $4.06 \times 10^{2}$ |
| ML-DSA-44        | $2.11 \times 10^{2}$ | $4.82 \times 10^{2}$ | $9.49 \times 10^{1}$ |
| SPHINCS+-128s    | $2.22 \times 10^3$   | $4.86\times10^2$     | $2.88 \times 10^3$   |
| High Security Le | vel                  |                      |                      |
| HAWK-1024        | $6.53 \times 10^{4}$ |                      | $7.74 \times 10^{1}$ |
| ML-DSA-87        | $6.66 \times 10^{4}$ | $8.59 \times 10^{2}$ | $8.69 \times 10^{2}$ |
| SPHINCS+-256f    | $3.25 \times 10^2$   | $7.81 \times 10^2$   | $2.27 \times 10^2$   |

Overall, these experiments gave us a clearer view of how different cryptographic foundations behave in practice. They offer valuable insight into the current role of HAWK in the post-quantum landscape and help frame the discussion that follows.

#### 4 Conclusions

This work has presented an in-depth study of the current landscape of postquantum cryptography, with a particular focus on digital signature schemes. We began by analyzing the mathematical foundations of the LWE problem, which

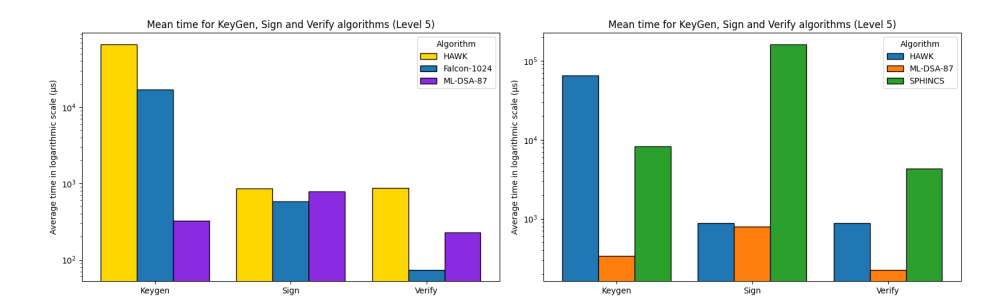


Fig. 1. Mean execution time (in logarithmic scale) for KeyGen, Sign, and Verify operations at the highest security level (Level 5).

underpins many standardized schemes. In parallel, we explored the LIP, a less-explored yet promising alternative forming the basis of the HAWK proposal.

Based on these theoretical foundations, we implemented and evaluated four signature algorithms: ML-DSA, FALCON, SPHINCS+, and HAWK. Two sets of comparative experiments were conducted. The first compared ML-DSA, FALCON, and HAWK, aiming to highlight performance differences between LWE-based and LIP-based lattice schemes. The second compared ML-DSA, SPHINCS+, and HAWK, to position HAWK against currently standardized signature algorithms.

In the first comparison, HAWK demonstrated significantly slower key generation times, while performing similarly to others during the signing phase and showing a slight advantage in verification. However, its high cost in key generation, combined with the absence of notable gains in other phases, limits its practical appeal as an efficient lattice-based signature scheme.

The second comparison further reinforced this observation. Although HAWK outperforms SPHINCS+ in signing and verification phases, it still lags behind ML-DSA, which consistently offers superior overall performance. These results suggest that HAWK, while competitive in some aspects, does not currently present a compelling efficiency advantage over existing standards.

From an algebraic standpoint, HAWK remains an intriguing candidate, as it brings visibility to the LIP, a structurally rich and relatively unexplored problem in lattice-based cryptography. Nonetheless, our findings indicate that HAWK may not be the most efficient choice for digital signatures. Future efforts might be better directed toward diversifying the space of signature schemes, exploring alternatives based on isogenies or multivariate constructions, such as SQIsign, MAYO, or UOV, which show promise both in theory and practice.

Acknowledgments. This work was possible thanks to the projects: 2023DIG28 IACTA, PID2022-138933OB-I00 ATQUE, and SCITALA C064/23 ULL-INCIBE, and to the C065/23 Cybersecurity Chair of the University of La Laguna and INCIBE, funded by Cajacanarias la Caixa Fundations, MCIN/AEI/10.13039/501100011033, and the Recovery, Transformation, and Resilience Plan (Next Generation) financed by the European Union.

#### References

- R. Avanzi, J. Bos, L. Ducas, E. Kiltz, T. Lepoint, V. Lyubashevsky, J. Schanck, P. Schwabe, G. Seiler, and D. Stehlé, "CRYSTALS-Kyber algorithm specifications and supporting documentation," NIST PQC Round, vol. 2, no. 4, pp. 1–43, 2021.
- L. Ducas, E. Kiltz, T. Lepoint, V. Lyubashevsky, P. Schwabe, G. Seiler, and D. Stehlé, "CRYSTALS-Dilithium: Algorithm specifications and supporting documentation (version 3.1)," NIST Post-Quantum Cryptography Standardization Round, vol. 3, pp. 1–38, 2021.
- 3. P.-A. Fouque, J. Hoffstein, P. Kirchner, V. Lyubashevsky, T. Pornin, T. Prest, T. Ricosset, G. Seiler, W. Whyte, and Z. Zhang, "Falcon: Fast-fourier lattice-based compact signatures over ntru," *Submission to the NIST's post-quantum cryptography standardization process*, vol. 36, no. 5, pp. 1–75, 2018.
- 4. J.-P. Aumasson, D. J. Bernstein, W. Beullens, C. Dobraunig, M. Eichlseder, S. Fluhrer, S.-L. Gazdag, A. Hülsing, P. Kampanakis, S. Kölbl, T. Lange, M. M. Lauridsen, F. Mendel, R. Niederhagen, C. Rechberger, J. Rijneveld, P. Schwabe, and B. Westerbaan, "SPHINCS+ Specification: Submission to the NIST Post-Quantum Cryptography Standardization Project (Round 3.1)," https://sphincs.org/data/sphincs+-r3.1-specification.pdf, 2021, disponible en: https://sphincs.org/data/sphincs+-r3.1-specification.pdf.
- 5. National Institute of Standards and Technology (NIST), "Post-quantum cryptography, round 4 submissions," https://csrc.nist.gov/projects/post-quantum-cryptography/round-4-submissions.
- 6. National Institute of Standards and Technology, "Post-quantum cryptography: Additional digital signature schemes," https://csrc.nist.gov/projects/pqc-dig-sig/round-2-additional-signatures.
- 7. G. Alagic, M. Bros, S. Ciadoux, D. Cooper, Q. Dang, T. Dang, J. Kelsey, J. Lichtinger, Y.-K. Liu, C. Miller, D. Moody, R. Peralta, R. Perlner, A. Robinson, H. Silberg, D. Smith-Tone, and N. Waller, "Status report on the first round of the additional digital signature schemes for the nist post-quantum cryptography standardization process," National Institute of Standards and Technology, Gaithersburg, MD, Tech. Rep. NIST IR 8528, 2024.
- 8. O. Regev, "The learning with errors problem (invited survey)," in *Proceedings* of the 2010 IEEE 25th Annual Conference on Computational Complexity, ser. CCC '10. USA: IEEE Computer Society, 2010, p. 191–204. [Online]. Available: https://doi.org/10.1109/CCC.2010.26
- I. Haviv and O. Regev, "On the lattice isomorphism problem," in *Proceedings of the twenty-fifth annual ACM-SIAM symposium on Discrete algorithms*. SIAM, 2014, pp. 391–404.
- L. Ducas and W. van Woerden, "On the lattice isomorphism problem, quadratic forms, remarkable lattices, and cryptography"," in *Advances in Cryptology – EU-ROCRYPT 2022*, O. Dunkelman and S. Dziembowski, Eds. Springer International Publishing, 2022, pp. 643–673.
- 11. P. Branco, G. Malavolta, and Z. Maradni, "Fully-homomorphic encryption from lattice isomorphism," *Cryptology ePrint Archive*, 2025.
- 12. T. Pornin and L. Pulles, "Hawk implementation," https://github.com/hawk-sign/dev.

# The effectiveness of personal data detection in LLM-based Conversational Agents

Diego Paracuellos<sup>1</sup>, Jose Such<sup>1</sup>, Elena Del Val<sup>1</sup>, Ana Garcia-Fornes<sup>1</sup>,

VRAIN, Universitat Politècnica de València, Valencia 46022, Spain diepade@etsinf.upv.es

Abstract. The growing prevalence of LLM-based conversational agents in everyday applications has led to an increasing risk of users disclosing sensitive personal information. Understanding how effectively different tools can identify such disclosures, and therefore protect users, is critical to mitigate privacy risks in human-agent interactions. This paper aims to evaluate the effectiveness of different methods to detect personal information in human-agent conversations. In particular, we compare the potential of several out-of-the-box LLMs as detection agents to more traditional approaches such as Microsoft Presidio. To do so, we use a labeled dataset containing various human interactions with conversational agents. We show that both approaches have strengths and weaknesses, and that none of them on their own seem effective enough to detect personal information in human-agent interactions in uncontrolled, real-world environments.

**Keywords:** Privacy, PII, LLM, Conversational Agents, AI-driven tools, Data detection

#### 1 Introduction

In today's digital age, the collection and aggregation of personal data by various entities can generate detailed profiles of individuals, raising significant concerns regarding privacy and control over personal information [10]. This issue is especially pronounced in the context of AI-driven tools, which often require access to vast amounts of user input to function properly [13]. These systems may inadvertently collect sensitive data such as names, locations or phone numbers through natural language interactions and sometimes without the user being aware of the extent of the data that is being gathered and its potential uses. As these tools become more embedded in daily life [6], the potential of misuse, unintended data sharing or profiling increases, highlighting the need for data protection mechanisms and practices in the design and deployment of potential systems [14]. One particular example of AI-driven tools that may compromise privacy are LLM-based conversational agents such as ChatGPT. As shown in [15], users disclose a lot of personal information to such agents. It is therefore paramount to protect users' privacy in their interaction with those agents.

With the long-term aim of proposing methods to protect users' privacy when interacting with LLM-based conversational assistants, this paper takes a first

step by evaluating various out-of-the-box solutions for personal data detection in human conversations with LLM-based agents. We particularly compare two distinct approaches: a traditional rule-based method in Microsoft Presidio and a more modern strategy leveraging small LLMs as data detection agents. Our ultimate goal is to develop a low-latency system with modest hardware requirements, leveraging small LLMs for general PII detection. This article constitutes our initial step in that direction.

To guide our study, we address the following research questions:

- **RQ1:** How do LLMs compare to traditional techniques in PII detection?
- RQ2: What are the trade-offs between detection accuracy and computational efficiency?

This paper contributes: (1) a comparative evaluation of PII detection using a rule-based system and three small LLMs, and (2) an analysis of the trade-off between performance and efficiency. The paper is further organized as follows: Section 2 reviews related work; Section 3 outlines key concepts; Section 4 describes our methodology; and Section 5 concludes and discusses future work.

## 2 Related work

The threat of users disclosing their own or others' personal data while using LLM-based conversational assistants is a growing concern in the field of natural language processing and privacy protection. Recent research [15] has demonstrated that users frequently reveal various types of personally identifiable information (PII) during interactions, including names, emails, passwords, financial details, health-related information, legal conditions, and sexual orientation. This pattern of disclosure highlights the critical need for effective and reliable detection and protection mechanisms tailored for conversational settings.

Several recent solutions have proposed the use of pre-trained or custom large language models (LLMs) for detecting and preventing the inadvertent disclosure of personal data during conversations with LLM-based agents [1, 2, 4, 14]. Many of these approaches employ Microsoft Presidio as a baseline detection tool or incorporate it into the data labeling process [1, 2, 14, 15], leveraging a combination of rule-based and machine learning techniques to improve detection accuracy.

However, the majority of these existing approaches rely on large LLMs (10B or more), which require significant computational resources and incur substantial inference times. This limits their applicability in real-time or resource-constrained environments, where low latency and efficiency are paramount [5]. Beyond technical challenges, ethical concerns emerge from both false negatives—which risk exposing sensitive user data—and false positives, which may lead to unnecessary censorship and reduce user trust [10]. Despite these critical considerations, prior research often emphasizes detection accuracy without fully addressing the balance between computational efficiency and ethical safeguards. In contrast, our research focuses on utilizing smaller LLMs to evaluate their usability as PII detectors while comparing with lightweight tools such as Microsoft Presidio.

## 3 Background

Under the General Data Protection Regulation (GDPR), personal data is defined as "any information relating to an identified or identifiable natural person ('data subject')" (Regulation (EU) 2016/679, Art. 4(1)). This includes not only direct identifiers such as names and identification numbers but also indirect identifiers like location data, online identifiers (e.g. IP addresses), or factors specific to an individual's physical, physiological, genetic, mental, economic, cultural, or social identity. An individual is considered identifiable if they can be recognized, directly or indirectly, through these types of information. In general, PII refers to any information that can directly or indirectly identify an individual. While the EU's GDPR defines personal data broadly, other frameworks such as the U.S. NIST definition of PII (NIST SP 800-122, 2010) follows similar principles but with minor differences in terminology and scope. In this article, we will employ two approaches to detect the above defined PIs: Microsoft Presidio and Large Language Models.

#### 3.1 Microsoft Presidio

Microsoft Presidio<sup>1</sup> is an open-source and free tool that is the state-of-the-art in the detection and anonymization of PII. Presidio uses the following techniques: regular expressions (regex), data parsing, checksums, and some specialized models for Named Entity Recognition (NER).

Presidio's regular expressions are defined as parsing patterns designed to match the structure of specific types of data. Another parsing method uses whitelists and blacklists. This method compares the presence of a certain word in a text to a list to either let it pass (whitelist) or block it (blacklist). In addition, certain structured data incorporate built-in verification mechanisms into the data generation designed to detect forged data through the application of checksums. These mechanisms can also be employed to identify and accurately classify such formatted data.

Presidio also uses NER. This is a Natural Language Processing (NLP) subtask that identifies meaningful entities in a text through a 3-step process (Processing, Template Matching and Entity Sorting). A NER can recognize the following entities: names (of individuals and organizations), locations, dates, phone numbers among a few other types.

The above methods are known to suffer from two common flaws, data mutability, referring to the multiple ways in which the same PII can be expressed, and data similarity, in which different data entities have similar representations [7, 12, 11].

#### 3.2 Large Language Models (LLMs)

LLMs are Neural Networks deep-trained with large sets of data. A particular model is characterized by its number of parameters (e.g. 1 billion parameters or

<sup>&</sup>lt;sup>1</sup> https://microsoft.github.io/presidio/

1B), architecture (e.g. GPT, BERT or T5, among others), modal (e.g. Text-Only, Image-Only or Multi-modal among others) and training dataset. Due to their size, LLMs usually require a certain amount of Hardware Specs. These LLM can be deployed to perform a variety of tasks, such as data generation, document parsing or even data detection all depending on a prompt (a structured input, like a text, a question, an instruction or example) that the LLM receives and processes. Most Open-Source LLMs are given as a general base model that can be specialized or expanded through additional training.

While theoretically able to solve the data mutability issue, a new one appears in the form of either prompt mutability, as a lesser mutation on a prompt can alter its functionality [8, 9]. Also, not every task may be achieved with every LLM model as these may present some hard-coded safeguards, protection mechanisms (like behavioral hard-coding or ethical alignment) to refuse or prevent to do controversial tasks [3].

#### Method 4

We evaluate different approaches for detecting personally identifiable information (PII) in a conversation with LLM-based Conversational Agents. This evaluation is conducted using Microsoft Presidio and a selection of different LLMs as detection agents. For the evaluation, we use an existing and publicly available dataset of user conversations with LLM-based assistants (as we detail below). Using the dataset, we compare the precision, recall, and F1 of Presidio and the LLMs to detect whether and what type of PII is disclosed in the conversations.

Regarding the LLMs evaluated, three small LLM models ranging from 1B to 10B parameters, were selected: nuExtract v1.5 3.8B<sup>2</sup>, a data extractionspecialized model based on Microsoft Phi 3.5 Mini Instruct, Qwen2.5 3B Instruct<sup>3</sup> and Llama 3.2 3B Instruct<sup>4</sup> both of which are general language models.

The idea behind using small LLMs is that, as hardware processing power increases and LLM efficiency improves, it may eventually become possible to deploy them on almost any device (e.g., a smartphone or personal computer) that users can employ to interact with AI-driven applications.

#### 4.1 Dataset

For this experiment, we evaluate user prompts of a labeled subset of the ShareGPT52k, a collection of 52,000 conversations with ChatGPT from various users [15]. To compare the performance of the tools with the ground truth, we asked the authors of [15] to share the labels they created with us, and found that not every sample was on the current public available ShareGPT52k repositories, 156 of said labelled conversations could be found on ShareGPT90k<sup>5</sup>, an expansion of

<sup>&</sup>lt;sup>2</sup> https://huggingface.co/numind/NuExtract-1.5

<sup>&</sup>lt;sup>3</sup> https://huggingface.co/Qwen/Qwen2.5-3B-Instruct

<sup>&</sup>lt;sup>4</sup> https://huggingface.co/meta-llama/Llama-3.2-3B-Instruct

<sup>&</sup>lt;sup>5</sup> https://huggingface.co/datasets/RyokoAI/ShareGPT52K

ShareGPT52k. A total of 4,047 user prompts pertaining to the 156 conversations were used for our experiments. Table 1 shows the labels in the dataset and the number of conversations with that specific label.

**Table 1:** Dataset labels and number of conversations with each label. Each conversation may have several prompts.

| Label           | DATE_TIME | EMAIL | LOCATION | NRP | PASSPORT | PERSON | PHONE | URL |
|-----------------|-----------|-------|----------|-----|----------|--------|-------|-----|
| Number of Conv. | 32        | 7     | 29       | 13  | 1        | 20     | 7     | 8   |

While these labels are mostly self-contained, there are two points to consider: NRP is a label defined on Presidio as any information related to Nationality, Religion and Political Group. Also, on recent Presidio versions, the label PASSPORT has been deprecated and split instead to other labels (e.g US\_PASSPORT or IT\_PASSPORT).

#### 4.2 Experimental setting

For Presidio, we used the default SpaCy NER model "en\_core\_web\_lg", keeping all parameters at their default settings.

For the LLMs, a prompt containing: (1) a basic directive (e.g., "You are a PII detection model... The required JSON fields are:") and a template, (2) a structured format specifying the desired data to extract (e.g., "Name": Person's full name.\n - "Birth\_Date": Date of birth\n - "Age": Age of the person\n...) and (3) an example of the template was sent, followed by the text to analyze. No additional training was performed on any model. Outputs were post-processed to remove undesired results (e.g., "No data found" responses, malformed or hallucinated templates) before computing performance metrics and timing.

The LLMs were deployed on a SLURM instance of an HPC cluster equipped with one Nvidia A40 GPU and one logical CPU of an AMD EPYC 7453, running a Miniconda Python environment on Ubuntu with vLLM serving the target models.

#### 4.3 Metrics

Detection performance. The performance of detection can be measured using two main metrics: Precision and Recall. These metrics indicate how accurate and reliable an approach is, and can be combined into the F1 score to provide a comprehensive assessment of performance. We use all three metrics to evaluate the performance of each labeled data type in the dataset for every approach (Presidio and LLMs). The results will also be reported in an aggregated form, employing both micro and macro averaging due to the dataset being highly unbalanced and not defining if certain data types have more weight than others in our context.

For micro averaging:

$$fp_{\mu} = \sum_{i=0}^{n} fp_{a} \quad tp_{\mu} = \sum_{i=0}^{n} tp_{a} \quad fn_{\mu} = \sum_{i=0}^{n} fn_{a}$$
 (1)

Being  $fp_a$ ,  $tp_a$  and  $fn_a$ , the false positives, true positives and false negatives of an individual label. We then will use these new values  $fp_{\mu}$ ,  $tp_{\mu}$  and  $fn_{\mu}$  to re-calculate Precision, Recall and F1 score.

For macro averaging:

$$Metric_M = \frac{1}{N} \sum_{i=0}^{n} Metric_a \tag{2}$$

where  $Metric_a$  is the Precision, Recall or F1 score of the individual labels.

**Processing time.** Beyond detection performance, measuring the computational cost of each method is crucial. We assess this by the average processing time each method requires to produce a result. In our case, we use:

$$t_{prompt} = \frac{t_{total}}{N_{cases}} \tag{3}$$

where  $t_{prompt}$  is the average computing time per prompt,  $t_{total}$  is the total computing time a test has taken to parse all prompts, and  $N_{cases}$  is the amount of processed prompts. Max and min times per model will also be presented.

#### 5 Results

## 5.1 PII detection performance results

Table 2: Presidio performance metrics.

|              | DATE_TIME           | EMAIL               | LOCATION            | NRP                 | PASSPORT    | PERSON              | PHONE               | URL         |
|--------------|---------------------|---------------------|---------------------|---------------------|-------------|---------------------|---------------------|-------------|
| Precision    | 0.23                | 0.47                | 0.22                | 0.11                | 0.00        | 0.13                | 0.21                | 0.09        |
| Recall<br>F1 | $\frac{1.00}{0.47}$ | $\frac{1.00}{0.28}$ | $\frac{1.00}{0.31}$ | $\frac{1.00}{0.26}$ | 0.00 $0.00$ | $\frac{1.00}{0.23}$ | $\frac{1.00}{0.29}$ | 1.00 $0.08$ |

Table 2 shows the detection performance results for Presidio. The tool achieves perfect recall (Recall = 1), successfully identifying almost all instances of relevant PII. However, precision remains very low, indicating a high number of false positives. A notable exception is the PASSPORT label, where the single instance is incorrectly classified as a U.S. driver's license (US\_DRIVER\_LICENCE). This outcome is expected, given Presidio's rule-based nature, which relies heavily on pattern matching and may conflate structurally similar entities.

**Table 3:** nuExtract performance metrics.

|                     | DATE_TIME    | EMAIL          | LOCATION     | NRP            | PASSPORT     | PERSON         | PHONE        | URL  |
|---------------------|--------------|----------------|--------------|----------------|--------------|----------------|--------------|------|
| Precision<br>Recall | 0.00<br>0.00 | $0.50 \\ 0.14$ | 0.18<br>1.00 | $0.29 \\ 0.15$ | 0.00<br>0.00 | $0.23 \\ 0.35$ | 1.00<br>0.14 | 0.00 |
| F1                  | 0.00         | 0.22           | 0.31         | 0.20           | 0.00         | 0.27           | 0.25         | 0.00 |

Table 3 presents the results obtained with nuExtract. Overall, both precision and recall are relatively low. Using the provided prompt template, the model failed to identify relevant instances for the PASSPORT, URL, and DATE\_TIME labels.

**Table 4:** Qwen 2.5 performance metrics.

|           | DATE_TIME | EMAIL | LOCATION | NRP  | PASSPORT | PERSON | PHONE | URL  |
|-----------|-----------|-------|----------|------|----------|--------|-------|------|
| Precision | 0.38      | 0.38  | 0.18     | 0.00 | 0.00     | 0.56   | 0.11  | 0.00 |
| Recall    | 0.09      | 0.71  | 1.00     | 0.00 | 0.00     | 0.25   | 0.14  | 0.00 |
| F1        | 0.15      | 0.50  | 0.31     | 0.00 | 0.00     | 0.34   | 0.12  | 0.00 |

The results obtained with Qwen, shown in Table 4, are broadly comparable to those of nuExtract. For this particular model, we did not observe any extracted data labeled as URL, PASSPORT, or NRP. This absence does not necessarily imply that such data were not detected or present in the input; rather, it may be due to mislabeling, omission, or incomplete or malformed outputs.

Table 5: Llama 3.2 performance metrics.

|           | DATE_TIME | EMAIL | LOCATION | NRP  | PASSPORT | PERSON | PHONE | URL  |
|-----------|-----------|-------|----------|------|----------|--------|-------|------|
| Precision | 0.38      | 0.14  | 0.18     | 0.00 | 0.00     | 0.14   | 0.14  | 0.00 |
| Recall    | 0.16      | 0.29  | 1.00     | 0.00 | 0.00     | 0.05   | 0.29  | 0.00 |
| F1        | 0.22      | 0.19  | 0.31     | 0.00 | 0.00     | 0.07   | 0.19  | 0.00 |

Table 5 presents a scenario similar to that observed with the other two LLMs. In this case, however, the model appears to have missed detecting instances of the NRP, PASSPORT, and URL labels.

**Table 6:** Performance comparison between models.

|           | $Precision_{\mu}$ | $Precision_{M}$ | $Recall_{\mu}$ | $Recall_M$ | $F1_{\mu}$ | $F1_M$ |
|-----------|-------------------|-----------------|----------------|------------|------------|--------|
| Presidio  | 0.16              | 0.18            | 1.00           | 0.88       | 0.28       | 0.29   |
| nuExtract | 0.20              | 0.27            | 0.34           | 0.22       | 0.25       | 0.16   |
| Qwen 2.5  | 0.22              | 0.20            | 0.37           | 0.28       | 0.27       | 0.18   |
| Llama 3.2 | 0.18              | 0.12            | 0.33           | 0.22       | 0.23       | 0.12   |

Table 6 compares macro- and micro-averaged metrics for all models. Overall performance remains similar across experiments, with minor precision improvements on some labels. Each LLM shows a slight preference for certain data types, with Llama performing somewhat worse—likely due to built-in content filtering.

Qwen and nuExtract exhibit comparable results, but differ in which data types are missed (DATE\_TIME for nuExtract and NRP for Qwen).

If we compare the number of outputs containing information to those with genuinely significant content on all three models across all the extracted data:

**Table 7:** Extracted data comparison between LLMs.

| Model     | Significant Outputs | Total Outputs |
|-----------|---------------------|---------------|
| nuExtract | 200                 | 825           |
| Qwen      | 197                 | 753           |
| Llama     | 209                 | 1627          |

Llama has found more results than the other two LLMs. This was surprising in early analyses, but it may be an indicator that it is more prone to hallucinate even on a temp-0 setting (highly deterministic), possibly due to completion-driven hallucinations triggered by restricted usage flags by the PI detection intent in the reused prompt.

#### 5.2 Processing time

Table 8 shows a comparison of the minimum and maximum processing time related to a single prompt, the average time per prompt and the total time per full dataset parse.

**Table 8:** Computation time comparison.

|           | $t_{min}$ (s) | $t_{max}$ (s) | $t_{total}$ (s) | $t_{prompt}$ (s) |
|-----------|---------------|---------------|-----------------|------------------|
| Presidio  | 0.01          | 89            | 490             | 0.12             |
| nuExtract | 23.74         | 585           | 85000           | 24.00            |
| Qwen 2.5  | 0.53          | 114           | 35505           | 9.00             |
| Llama 3.2 | 0.14          | 185           | 36444           | 10.00            |

Presidio is the fastest solution with around 490 seconds per full parse, corresponding 123 ms per prompt. All LLMs were at least an order of magnitude slower than Presidio, having Qwen as the fastest LLM with around 9 seconds per prompt, followed by Llama with 10 seconds per prompt and far behind nuExtract with 24 seconds per prompt. A notable observation is that Qwen and Llama consistently process prompts in less than half the time required by nuExtract. Both models show minimum and maximum processing times significantly lower than nuExtract, with minimum times comparable to Presidio. The occasional high maximum times for these LLMs likely result from outliers caused by hallucinations on large prompts.

### 6 Conclusions and future work

At first glance, the use of LLMs does not appear to offer a clear advantage over traditional techniques. The small LLMs tested yielded results comparable

to those of Presidio, with two of the three models slightly outperforming it in terms of precision—albeit at the cost of significantly lower recall and slower processing times (RQ2). Nevertheless, we observed that LLMs have the potential to recognize and categorize a broader range of personal data types than rule-based tools like Presidio, and may offer a more flexible and interpretable approach to structuring the extracted information (RQ1). It is also worth noting that using prompts tailored to specific categories of personal data may help improve output stability, potentially enhancing alignment with real-world deployment requirements.

Out-of-the-box tools, whether small LLMs or tools like Presidio, may lead to potential real systems able to at least partially anonymize user prompts to other LLM-based Conversational Agents like ChatGPT in a way to safeguard user data and privacy. Yet, performance seems to be the limiting factor, as false positives risk censoring harmless content and reducing trust. Conversely, false negatives pose a privacy risk by allowing sensitive data to go undetected. While LLMs offer strong performance in nuanced cases, their inference time and resource requirements pose challenges for low-latency applications. In contrast, lightweight tools like Microsoft Presidio offer high-speed processing but lower precision in complex contexts. These findings suggest that neither rule-based systems nor small LLMs alone as out-of-the-box tools may be sufficient for robust PII detection in real-world settings. However, their complementary strengths open the door for hybrid solutions. Our work provides a foundation for such systems by quantifying trade-offs and feasibility. This is essential for deploying privacy-preserving conversational agents in practical, latency-sensitive environments.

Considering these results, our future work is oriented toward the development of a hybrid approach that combines the high recall and low latency of Microsoft Presidio as a first filtering step, reducing the input size for LLMs and thereby improving scalability, followed by targeted inspection by LLMs. This strategy aims to balance efficiency with the nuanced reasoning capabilities of LLMs. Moreover, as our current study is limited to a single dataset and three small LLMs, future work will expand the evaluation to include additional datasets, model families, and model sizes to better assess the generalizability and robustness of our findings. We also plan to gain further insight into the causes of variability in model performance through a qualitative analysis of outputs.

## Acknowledgements

This work is partially supported and funded by Spanish Government project PID2023-151536OB-I00 and by the INCIBE's strategic SPRINT (Seguridad y Privacidad en Sistemas con Inteligencia Artificial) C063/23 project with funds from the EU-NextGenerationEU through the Spanish government's Plan de Recuperación, Transformación y Resiliencia.

#### References

- [1] Shubhi Asthana et al. "Adaptive PII Mitigation Framework for Large Language Models". In: arXiv preprint arXiv:2501.12465 (2025).
- [2] Shubhi Asthana et al. "Deploying Privacy Guardrails for LLMs: A Comparative Analysis of Real-World Applications". In: arXiv preprint arXiv:2501.12456 (2025).
- [3] Yuntao Bai et al. "Constitutional ai: Harmlessness from ai feedback". In: arXiv preprint arXiv:2212.08073 (2022).
- [4] Felix Böhlin. Detection & Anonymization of Sensitive Information in Text: AI-Driven Solution for Anonymization. 2024.
- [5] Rajeev Chandran and Mei-Ling Tan. "Efficiently Scaling LLMs Challenges and Solutions in Distributed Architectures". In: *Baltic Multidisciplinary Research Letters Journal* 2.1 (2025), pp. 57–66.
- [6] Tzuhao Chen, Mila Gascó-Hernandez, and Marc Esteve. "The adoption and implementation of artificial intelligence chatbots in public organizations: Evidence from US state governments". In: The American Review of Public Administration 54.3 (2024), pp. 255–270.
- [7] Gaia Gambarelli, Aldo Gangemi, and Rocco Tripodi. "Is your model sensitive? SPeDaC: A new benchmark for detecting and classifying sensitive personal data". In: arXiv preprint arXiv:2208.06216 (2022).
- [8] Abel Salinas and Fred Morstatter. "The butterfly effect of altering prompts: How small changes and jailbreaks affect large language model performance". In: arXiv preprint arXiv:2401.03729 (2024).
- [9] Melanie Sclar et al. "Quantifying Language Models' Sensitivity to Spurious Features in Prompt Design or: How I learned to start worrying about prompt formatting". In: arXiv preprint arXiv:2310.11324 (2023).
- [10] Daniel J Solove. Understanding privacy. Harvard university press, 2010.
- [11] Anh Truong, Austin Walters, and Jeremy Goodsitt. "Sensitive data detection with high-throughput neural network models for financial institutions". In: arXiv preprint arXiv:2012.09597 (2020).
- [12] Aurelian Tutuianu et al. Efficient statistical techniques for detecting sensitive data. US Patent 11,599,667. 2023.
- [13] Jing Wei et al. "Leveraging Large Language Models to Power Chatbots for Collecting User Self-Reported Data". In: *Proceedings of the ACM on Human-Computer Interaction* 8.CSCW1 (Apr. 2024), pp. 1–35. ISSN: 2573-0142. DOI: 10.1145/3637364. URL: http://dx.doi.org/10.1145/3637364.
- [14] Jianliang Yang et al. "Exploring the application of large language models in detecting and protecting personally identifiable information in archival data: A comprehensive study". In: 2023 IEEE International Conference on Biq Data (BiqData). IEEE. 2023, pp. 2116–2123.
- [15] Zhiping Zhang et al. ""It's a Fair Game", or Is It? Examining How Users Navigate Disclosure Risks and Benefits When Using LLM-Based Conversational Agents". In: *Proceedings of the 2024 CHI Conference on Human Factors in Computing Systems*. 2024, pp. 1–26.

# Adaptive Identity Token from User Attributes for Authentication through Controlled Execution Environment

Shashank Tripathi, Kai Hendrik Wöhnert and Volker Skwarek

<sup>1</sup> RTC CyberSec, Hamburg University of Applied Sciences shashank.tripathi@haw-hamburg.de, Home page:

https://www.haw-hamburg.de/hochschule/life-sciences/forschung/ftz-cybersec <sup>2</sup> Berliner Tor 5, 20099 Hamburg, Germany

Abstract. With an increased emphasis on software and applications, they are becoming more secure through built-in malware recognition. It has prompted adversaries to increasingly target identity infrastructures, thereby contributing to a pronounced global surge in identity-based attacks. This paper addresses the problem by introducing *IdentiToken*, an authentication framework that derives tokens from a structured set of user and environmental attributes. Attributes are grouped into different classes, each weighted to reflect its sensitivity to change. IdentiToken supports similarity-based validation, enabling partial matches to be interpreted meaningfully rather than reduced to binary outcomes. We analyse the system's behaviour under adversarial scenarios and evaluate its sensitivity to attribute changes in a controlled environment. Although the approach is still exploratory in terms of deployment, our results suggest that structured, attribute-derived tokens may provide a useful foundation for developing more flexible and context-aware authentication mechanisms.

**Keywords:** identity-based authentication, tokenization, attribute-based identification

#### 1 Introduction

Most identity systems authenticate users via static secrets like passwords, cryptographic keys or biometrics, which are prone to theft and reuse. In 2024, identity-based attacks surged by 71%, with 80% linked to credential misuse[1]. Breaches like the Okta incident[2] and flaws in certificate chains[3] underscore limitations of established credential-based authentication.

However, the emphasis on verifying knowledge of a secret makes such systems vulnerable to replay attacks, where an adversary reuses previously captured valid credentials to impersonate a legitimate user. Moreover, binary verification neglects the context or additional user-related environment in which the authentication occurs. Verification of such additional information adds a layer to

verify a user with higher confidence. While MFA[4] and decentralised identity (DID) frameworks[5][6] enhance user control, they retain dependency on bearer credentials and have been prone to attack. Addressing the current limitations: Can we design a privacy-preserving, behaviour-sensitive token that tolerates drift in identity while remaining verifiable?

The solution proposed in this paper addresses this by generating identity tokens from weighted attributes and measuring similarity across sessions, enabling flexible and context-aware authentication in dynamic or semi-trusted environments (e.g., IoT, federated identity, edge computing).

#### **Our Contributions:**

- Introduced a structured identity model using attribute segmentation for tracking individual attribute contributions and identity drift.
- Proposed a cryptographic token generation algorithm that preserves entropy during hash truncation and achieves cross-attribute diffusion using discrete reduction windows.
- Implemented the system in a controlled and portable runtime environment to ensure reliable attribute recording, tested with realistic changes (e.g., keystroke patterns, geolocation shifts).
- Conducted formal analysis demonstrating resistance to replay attacks and tampering.

### 2 State of the Art

ISO/IEC 24760-1:2019 defines identity as a set of attributes associated with an entity and authentication as the process of verifying that identity by comparing presented attributes against previously stored or registered values. Static-password systems remain widespread but are easily compromised[7]. Widely used through protocols like OAuth 2.0 and OpenID Connect[8], tokens such as JSON web tokens (JWTs) enable federated identity but suffer from vulnerabilities like token substitution and replay attacks. WebAuthn[9], part of the FIDO2 standard, uses public-key pairs for passwordless login.

WebAuthn, part of the FIDO2 standard, uses public-key pairs for password-less login. While offering phishing resistance, real-world issues like stale challenge reuse[3], misconfigured verifiers and key management remain[10].

Macaroons[11] allow constrained delegation allowing it to be passed from one party to another with added restrictions (e.g., limiting time, endpoint, user role) but are bearer-based, meaning, whoever possesses them can use them. If leaked or intercepted, they can be misused.

Attribute-Based authentication frameworks[12] use cryptographically signed claims (e.g., age, role). However, traditional models raise privacy concerns due to semantic linkability and limited revocation mechanisms.

Our approach differs by integrating multiple attributes into a unified identity token enabling similarity-aware authentication and session drift tolerance. Unlike

traditional systems, it supports partial identity acceptance and adaptive security logic.

## 3 Tokenization of Identity

This section describes how identity attributes are transformed into a cryptographic token using a modified variant of the FaRHash[13] algorithm. The token must react differently to the type of attributes, formally termed as static, dynamic and volatile. Static attributes are the most stable components of an identity, remaining consistent across an entity's lifecycle and providing foundational trust, for example, a vehicle's chassis number or a server's hardware serial number. Dynamic attributes vary over time due to operational context or usage patterns but still contribute meaningfully to identity, for instance, the average operating speed of an industrial machine or the access patterns of a database over time. Volatile attributes, like room temperature in a data centre or temporary file usage pattern on a system change, often have little impact on identity when viewed alone. However, when many such changes occur together, they can alter the system's behaviour and affect its overall identity. By cryptographically processing these attributes, we generate a token called *IdentiToken*.

Let the attribute space of an entity be partitioned into three disjoint subsets:

```
- Static attributes: S = \{s_1, s_2, \dots, s_p\}

- Dynamic attributes: D = \{d_1, d_2, \dots, d_q\}

- Volatile attributes: V = \{v_1, v_2, \dots, v_r\}
```

Each group contributes differently to the token structure. Static attributes influence the token globally by acting as a seed, while dynamic and volatile attributes contribute direct entropy.

#### 3.1 Token Generation

Step 1: Seed Construction. We begin by creating a seed from the static attributes. Each static attribute  $s_j$  is first encoded to binary, and the seed is formed by concatenating all such encodings:

$$\mathsf{SEED} = \|_{i=1}^p \mathsf{Bin}(s_i) \tag{1}$$

Any change in static attributes yields a completely new seed, and therefore, a drastically different token.

Step 2: Attribute-Specific Hashing. Next, for every  $x_i \in \mathcal{D} \cup \mathcal{V}$ , we concatenate its binary encoding with the seed and hash the result:

$$x_i' := \mathsf{Bin}(x_i) \| \mathsf{SEED}, \qquad h_i := \mathsf{H}(x_i')$$

This ensures that attribute values are kept private while still contributing entropy to the token.

#### 4 Tripathi, Wöhnert and Skwarek

Step 3: Truncation by Attribute Type. To control each attribute's influence, hash outputs are truncated differently:

$$\tilde{h}_i := \begin{cases} \mathsf{Slice}_n(h_i), & \text{if } x_i \in \mathcal{D} \\ \mathsf{Slice}_m(h_i), & \text{if } x_i \in \mathcal{V} \end{cases}$$

Here, n>m ensures that dynamic attributes carry more weight in the final token than volatile ones. We also choose  $n \mod m \neq 0$  to promote diffusion in the next step.

Step 4: Stream Assembly. All truncated hashes are concatenated in a predefined order  $\pi$ :

$$\mathsf{H} \mathsf{\_S} := ig\|_{x_i \in \pi(\mathcal{D} \cup \mathcal{V})} ilde{h}_i$$

Step 5: Cross-Attribute Diffusion. The stream  $H_-S$  is divided into fixed-size windows of length  $\ell=m$ :

$$W_i := \mathsf{H\_S}[\ell \cdot i : \ell \cdot (i+1)] \tag{2}$$

If the last chunk is shorter than  $\ell$ , we pad it with XOR-neutral hex digits 0. Each window is reduced to one hex digit by XORing all its bytes:

$$\mathsf{T}_i := \bigoplus_{j=0}^{\ell-1} W_i[j]$$

Finally, the IdentiToken is formed as:

$$\mathsf{T} := \prod_i \mathsf{T}_i$$

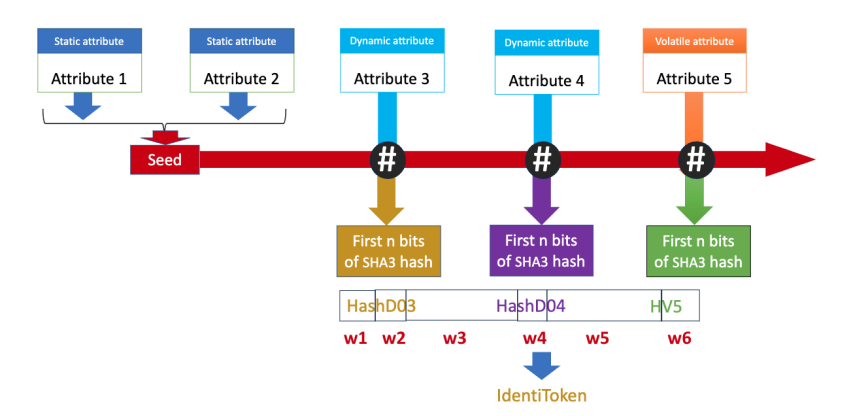


Fig. 1: Token construction from weighted attributes

 $Compact\ Formalization.$ 

$$\mathsf{T} = \big\|_{i=0}^{w-1} \bigoplus_{k=0}^{\ell-1} \Big[ \mathsf{H}_{-}\mathsf{S} \left( \big\|_{x \in \pi(\mathcal{D} \cup \mathcal{V})} \mathsf{Slice}_{b_x} \left( \mathsf{H} \left( \mathsf{Bin}(x) \| \mathsf{SEED} \right) \right) \right) \Big]_{i \cdot \ell + k}$$

Algorithm. The steps of the algorithm have been implemented with the pseudocode below.

### Algorithm 1 IdentiToken Generation

```
Require: \mathcal{S}, \mathcal{D}, \mathcal{V}, parameters n, m
Ensure: Token T
 1: SEED \leftarrow ||_{s \in \mathcal{S}} Bin(s)
 2: H\_S \leftarrow \text{empty string}
 3: for x \in \mathcal{D} \cup \mathcal{V} do
         x' \leftarrow \text{Bin}(x) || SEED
 4:
         h \leftarrow \mathsf{H}(x')
 5:
         Append Slice_n(h) or Slice_m(h) to H\_S
 6:
 7: end for
 8: if |H\_S| \mod m \neq 0 then
 9:
         Pad H\_S with 0s
10: end if
11: for each window W_i in H_-S do
12:
          \mathsf{T}_i \leftarrow \bigoplus W_i
          Append T_i to T
13:
14: end for
15: return T
```

#### 3.2 Formal Proof of the Design Properties

Each identity attribute is hashed independently after being concatenated with a seed derived from static attributes (Equation 1). Dynamic and volatile attributes are truncated to n and m bytes, respectively, with n>m>16. Choosing  $n \mod m \neq 0$  ensures that window boundaries misalign with segment boundaries, promoting inter-attribute diffusion.

The resulting hash stream is divided into non-overlapping windows of size  $\ell=m,$  each reduced to one byte via XOR. While XOR is linear, applying it across randomised truncated slices preserves entropy under the random oracle model. Given  $n\geq 128$  and  $m\geq 28$ , each token window reflects high-entropy mixing and retains cryptographic properties such as pre-image and collision resistance.

Static Sensitivity The seed—derived from static attributes—affects every attribute hash. A change in any  $s_j \in \mathcal{S}$  causes full regeneration of the hash stream. If the total stream length is  $L = d \cdot n + v \cdot m$ , the number of windows is  $w = \left\lfloor \frac{L}{\ell} \right\rfloor$ .

Under SHA-3's avalanche property, token similarity drops sharply. The probability of a collision between two tokens due to seed change is bounded by:

$$\Pr[\mathsf{T}(\mathsf{SEED}) = \mathsf{T}(\mathsf{SEED}')] \leq \frac{1}{2^{32w}}$$

For w = 12, this yields  $\approx 2^{-384}$ , a negligible probability.

**Dynamic Proportionality** Let  $\alpha$  be the fraction of modified dynamic attributes. Each contributes n bytes, affecting approximately  $\frac{n}{\ell}$  token windows. Thus, the expected token difference due to partial changes in  $\mathcal{D}$  is:

$$\Pr[\mathsf{T} \neq \mathsf{T}'] \approx \alpha \cdot \frac{n}{\ell}$$

This satisfies proportional sensitivity to behavioural drift.

Volatile Tolerance Volatile attributes fluctuate frequently. To tolerate minor drift, the similarity is computed over the volatile segments of two tokens. Let  $d_{\mathcal{V}}(\cdot,\cdot)$  be a Hamming distance restricted to volatile-derived parts:

$$d_{\mathcal{V}}(\mathsf{T}_{1}^{(v)},\mathsf{T}_{2}^{(v)}) \leq \delta \quad \Rightarrow \quad \text{identity preserved}$$

If this threshold is exceeded, identity is re-evaluated.

**Privacy Preservation** Only 4 bytes per window are visible. Given SHA-3's 256-bit output and token length of 4w bytes, the probability of inverting an attribute is:

$$\Pr[\mathcal{A}(\mathsf{T}) = x_i] \le \frac{1}{2^{224}}$$

Due to misaligned segments and XOR blending, one token byte never maps cleanly to one attribute.

**Pre-image resistance** Each token byte is derived from multiple hash slices. Given visibility of 4 bytes per window and  $\lambda = 256$ , pre-image resistance is bounded by:

$$\Pr\left[\text{find } x_i \mid \mathsf{T}\right] \le \frac{1}{2^{224}}$$

This bound follows from the fact that revealing 32 out of 256 bits of a cryptographically secure hash leaves 224 bits hidden, assuming no structure leaks and each attribute influences misaligned, XOR-blended segments. As a result, an adversary observing a full window gains only partial, non-direct information about any  $x_i$ .

Collision resistance: Applying the birthday bound to this L-bit token, the probability of a collision among Q such tokens is:

$$\Pr[\text{collision among } Q \text{ tokens}] \leq \frac{Q^2}{2^L}$$

With  $L \geq 384$  or more, the collision probability remains negligible for practical values of Q.

#### 3.3 Similarity Score of Tokens

Since authentication is the process of verifying identity, we propose a model that uses IdentiToken as the basis for this verification. Authentication is performed by comparing a freshly generated token with a previously stored reference, enabling a lightweight yet robust comparison mechanism. For clarity and focus, we abstract away the complexities of full authentication frameworks and concentrate on this core verification step. In this simplified model, tokens are represented as hex-encoded bitstrings. To quantify the degree of change between two tokens, we define a similarity score using the normalised Hamming distance:

$$Sim(\mathsf{T}_1, \mathsf{T}_2) = 1 - \frac{H(\mathsf{T}_1, \mathsf{T}_2)}{|\mathsf{T}_1|},$$
 (3)

where H(\*,\*) is the Hamming distance and  $|\mathsf{T}_1|$  is token length in hex representation. A score of 1 implies an exact match; 0 denotes total difference.

Threshold selection The thresholds,  $\tau_d$  for dynamic similarity and  $\delta$  for volatile similarity are not fixed algorithmic constants but are instead chosen based on application requirements. In highly critical scenarios such as financial access control, a stricter threshold (e.g.,  $\tau_d \geq 0.9$ ) enforces continuity with minimal tolerance. In contrast, less sensitive use-cases like user personalisation or adaptive content delivery can operate reliably with a relaxed bound (e.g.,  $\tau_d \geq 0.6$ ). The volatile threshold  $\delta$  is likewise configured according to the volatility profile acceptable within the specific context.

Dynamic Changes Compare tokens  $T_1$  and  $T_2$ , differing in 4 of 5 dynamic attributes. Static and volatile attributes remain unchanged.

 $T_{-1}$  = 8f8e...c51053c5a861fa89571240...fd4a363  $T_{-2}$  = 96c2...7e7e7d5a861fa89571240...fd4a363

$$|\mathsf{T}| = 86$$
,  $H(\mathsf{T}_1, \mathsf{T}_2) = 46$   $\Rightarrow$   $Sim = 1 - \frac{46}{86} = 0.4651$ 

This indicates substantial identity drift. For instance, in moderately strict scenarios where limited drift is acceptable (e.g.,  $\tau_d=0.75$ ), access would be denied. However, lower similarity scores may still permit degraded or provisional access depending on policy. For example, similarity in the range  $0.5 < \mathrm{Sim} < 0.75$  might trigger secondary checks, fallback authentication or limited access modes. As established earlier,  $\tau_d$  and  $\delta$  are not inherent to the algorithm itself; instead,

they are configurable parameters determined by the specific needs and sensitivity of the deployment context.

Next,  $T_3$  differs from  $T_1$  in only 1 dynamic attribute:

 $T_{-3} = 8f8e...0132b4933d3f...c51053c5a861fa...fd4a363$ 

$$H(\mathsf{T}_1, \mathsf{T}_3) = 10 \quad \Rightarrow \quad \text{Sim} = 1 - \frac{10}{86} = 0.8837$$

This score supports identity continuity for  $\tau_d < 0.88$ .

Volatile Drift Now  $T_4$  differs from  $T_1$  in 5 of 6 volatile attributes:

 $T_4 = 8f8e...c51053c4b4df0d...2aeb55a363$ 

$$H(\mathsf{T}_1, \mathsf{T}_4) = 17 \quad \Rightarrow \quad \text{Sim} = 1 - \frac{17}{86} = 0.8023$$

Extract volatile parts (26 hex digits):

$$\mathsf{T}_1^{(v)} = 24098 \mathrm{fdd0f09559364cfd4a363}$$
  $\mathsf{T}_4^{(v)} = \mathrm{c4b4df0d0ae7e8132aeb55a363}$ 

$$H(\cdot) = 17 \quad \Rightarrow \quad \text{Sim}_v = 1 - \frac{17}{26} = 0.3462$$

A drop in volatile similarity below  $\delta = 0.4$  indicates significant context change. Even with unchanged dynamics, re-authentication may be required.

Static Change  $T_5$  differs from  $T_1$  only in one static attribute, affecting the seed:  $T_-5 = e3ea...7afc...b14cafcdce...aeb55$ 

$$H(\mathsf{T}_1, \mathsf{T}_5) = 78 \quad \Rightarrow \quad \text{Sim} = 1 - \frac{78}{86} = 0.0930$$

Despite no dynamic or volatile changes, a minimal static modification regenerates the entire token, demonstrating seed centrality.

These cases show how token similarity captures granular identity shifts. The next section embeds this logic within secure local execution environments.

# 4 Demonstration

We now instantiate IdentiToken in a controlled test case to demonstrate its behaviour under identity drift. Consider a user who installs a benign but critical application (e.g., a trading terminal). While functionally irrelevant, the installation may modify the environment. This allows us to examine IdentiToken's proportionality and responsiveness.

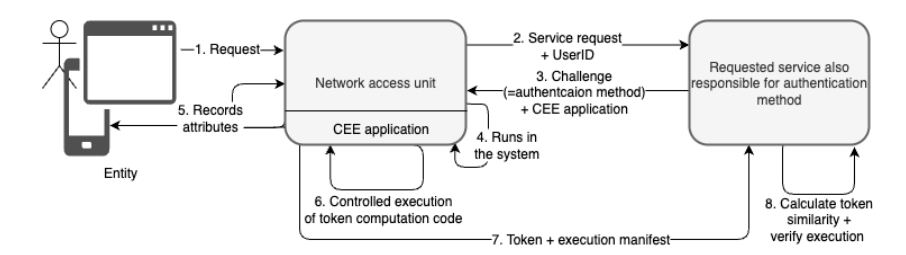


**Fig. 2:** Component view of IdentiToken computation and verification using a CEE

All authentication logic was executed inside a Docker-based controlled execution environment (CEE), following the architecture in Figure 2. The implementation<sup>3</sup> consisted of three stages: (i) local attribute acquisition, (ii) token generation, and (iii) server submission. Attributes were acquired from within the container, using Python.

Attribute selection within each category is use case dependent and based on relevance. An attribute considered static in one context may be dynamic in another or even excluded entirely from identity calculation in a third scenario.

Static Attributes: This category includes properties with long-term stability that significantly contribute to an entity's identity. Selected attributes include MAC address, memory configuration and CPU characteristics. As a behavioural attribute, keystroke dynamics were used [14]. In the implementation, the user types the phrase "the lazy fox jumps over the brown dog", consisting of all English alphabet five times. Keystrokes with durations slower than the session's Gaussian mean were retained, as described in [15].

**Dynamic Attributes:** These attributes exhibit moderate variability within bounded ranges and play a partial role in shaping the entity's identity. For demonstration purposes, we selected attributes such as geolocation and IP address, which tend to remain stable within sessions or short windows but may vary across environments.

Volatile Attributes: This category captures rapidly changing properties that reflect transient context. In our setup, we used runtime disk size and network latency, both of which are highly sensitive to immediate environmental conditions.

Tokens (represented in 44 hex digits) were computed and compared using Hamming similarity, with scatter plots of byte-wise Spearman ranks shown in Figure 3.

Six cases highlight IdentiToken's response: (a) No change: tokens match exactly (Sim = 1.0000). (b) One static change: Sim = 0.043. (c)Two dynamic changes: Sim = 0.6190. (d) One dynamic change: Sim = 0.7619. (e)Two volatile changes: Sim = 0.8809. (f)One volatile change: Sim = 0.9286.

The code is publicly available at https://osf.io/8cepa/?view\_only=5d58a8b2e72f4d42a1c47686faf50b29

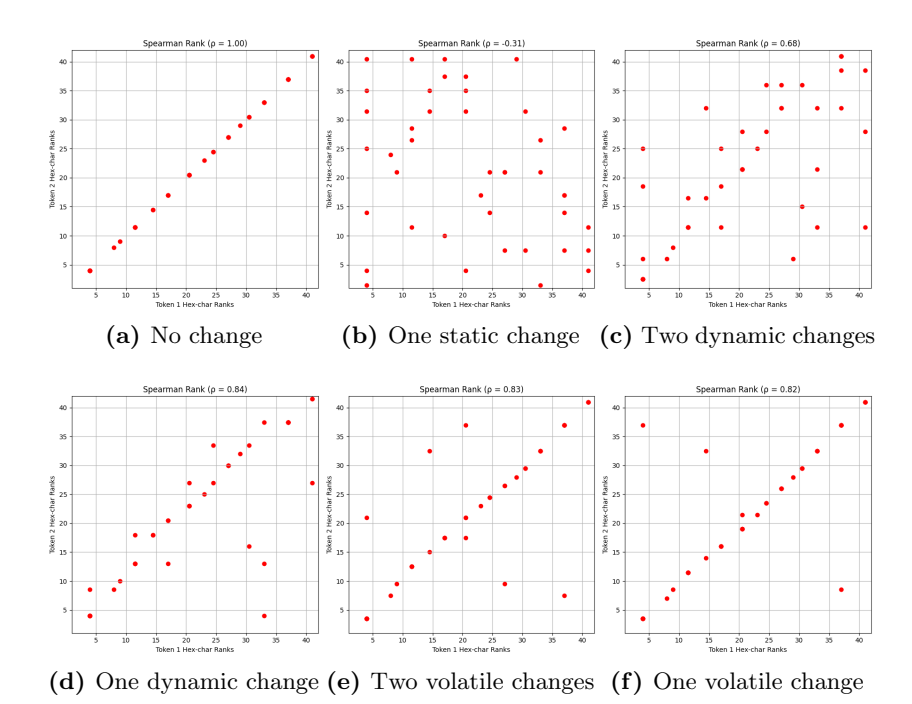


Fig. 3: Spearman Rank Scatter Plots Comparing Token Variations

The experiment demonstrated that IdentiToken is sensitive to static attribute shifts, moderately reactive to dynamic changes and tolerant to small volatile drift. The CEE ensures privacy and determinism in token generation, supporting secure deployment in resource-constrained or privacy-critical settings.

# 5 Threat Model and Analysis

We assume an adversary capable of intercepting tokens, manipulating the execution environment, and forging inputs. IdentiToken is designed to resist these under three guarantees:

- Cryptographic irreversibility of SHA-3,
- Trusted token generation inside a verifiable CEE,
- Threshold-based acceptance allowing bounded drift.

# 5.1 Replay Attack

**Threat:** An intercepted token  $T_u(t)$  is replayed to impersonate a user. **Assumptions:** The adversary can sniff tokens but lacks access to the CEE or true attributes.

**Defence:** Volatile attributes (e.g., IP, timestamp) change naturally. The probability of replay success is:

$$\Pr[\text{replay accepted}] = \prod_{i=1}^{r} p_i$$

Pr[replay rejected] = 1 - Pr[replay accepted]

**Example:** With IP = 0.3, UA = 0.8, DF = 0.6:

$$Pr = 0.3 \times 0.8 \times 0.6 = 0.144 \Rightarrow Rejection = 0.856$$

Optional freshness (e.g., TTL) and signed execution manifests can further reduce replay success.

#### 5.2 Token Forgery

**Threat:** The adversary crafts a forged token  $T_A$  that passes similarity checks. **Assumptions:** Partial or full leakage of legitimate attribute values; no CEE access.

Objective: Forge:

$$T_{\mathcal{A}} = \mathcal{H}(\mathbf{S}_u \oplus \mathbf{a}_s, \ \mathbf{D}_u \oplus \mathbf{a}_d, \ \mathbf{V}_u \oplus \mathbf{a}_v)$$

with:

$$\operatorname{Sim}(\mathsf{T}_{\mathcal{A}},\mathsf{T}_u^{\operatorname{ref}}) \geq \Theta_{\operatorname{accept}}$$

**Defense:** Token similarity is weighted:  $w_s > w_d > w_v$ . Acceptance requires:

$$E[Sim] = 1 - (w_s \delta_s + w_d \delta_d + w_v \delta_v) > \Theta_{accept}$$

Even small static changes  $(\delta_s)$  lead to rejection, while full drift in volatile attributes can be tolerated if  $w_s \delta_s + w_d \delta_d$  remains within bounds.

#### 6 Discussion

IdentiToken affirms that identity can be adaptively asserted via weighted attributes, similarity thresholds, and controlled execution. Unlike static tokens (OAuth2, OIDC) or fixed-attribute frameworks (SAML, X.509), it recomputes identity based on current behaviour and environment, avoiding persistent secrets and rigid profiles.

Its structure encodes static, dynamic and volatile traits, facilitating graded identity responses. Static components dominate identity, dynamic properties influence the token shape and volatile elements allow benign drift without immediate rejection. Similarity scoring supports nuanced decisions beyond binary matches, distinguishing contextual change from attack.

Compared to MFA[16], which verifies isolated factors sequentially one after the other, but IdentiToken compares them simultaneously. This transfers the identity directly into an n-dimensional feature space. This prevents an attacker from trying out the sensor dispersion for each attribute individually until they hit the overlap area through imitation and dispersion. Instead, all detections are transferred to the feature space and evaluated simultaneously. This makes it exponentially more difficult to exploit sensor scattering in a targeted manner.

Real-time telemetry (e.g., latency, network timing) can be embedded to update identity without user burden. This supports lightweight, context-aware authentication in zero-trust and dynamic settings. Token recomputation in verifiable CEEs eliminates reliance on stored secrets, shifting trust to code and context rather than storage.

The model is especially suited for constrained devices, edge authentication, and continuously evolving environments. However, deployment requires a sand-box on the client, which may limit universality. Broader CEE integration (e.g., native browser/runtime support) may ease this in future applications.

Token validation works on a similarity continuum, enabling partial access, reverification, or rejection based on attribute drift. This allows both interpretability and policy flexibility.

Limitations remain: defining a stable yet discriminative attribute set is specific to the scenario; token length varies with attributes but remains consistent across sessions; and thresholds must be tuned to balance security and usability. While formal analysis and simulation are promising, real-world trials are pending. These offer directions for future research.

### 7 Conclusion

*IdentiToken* is a token that is dynamically constructed from weighted attribute classes, namely static, dynamic and volatile. Unlike traditional approaches that rely on persistent secrets or binary verification, IdentiToken supports context-aware similarity scoring, enabling flexible responses to behavioural drift and environmental change.

The token demonstrates strong static sensitivity by triggering complete token regeneration for even a minor change in static attributes. In contrast, dynamic attributes contribute proportionally, allowing partial change to yield controlled token shifts. Volatile attributes do not affect the token unless a large number of volatile attributes change beyond a threshold. These properties may allow the authentication mechanism to distinguish between legitimate variation and adversarial manipulation.

Our implementation within a verifiable CEE validates these behaviours across realistic scenarios, including behavioural traits like keystrokes and environmental data like geolocation or disk usage. The resulting model supports privacy-preserving, resilient authentication without relying on stored secrets.

Future work includes optimising attribute sets, threshold calibration and studying performance in adversarial or mobile deployments. IdentiToken offers a promising foundation for identity systems that adapt with the user, rather than resisting change.

#### References

- IBM Newsroom. Ibm report: Identity comes under attack, straining enterprises' recovery time from breaches. https://newsroom.ibm.com/2024-02-21-IBM-Report-Identity-Comes-Under-Attack,-Straining-Enterprises-Recovery-Timefrom-Breaches. [Accessed: Jul. 16, 2025], Feb. 2024.
- 2. Okta. Okta security incident report 2022, 2022. https://security.okta.com/.
- 3. Mitre.org. Cve-2022-42731: Replay attack in django mfa2 webauthn implementation, 2022. https://nvd.nist.gov/vuln/detail/CVE-2022-42731.
- 4. Paul A Grassi, James L Fenton, Elaine M Newton, Ray A Perlner, Andrew R Regenscheid, William E Burr, Justin P Richer, Naomi Lefkovitz, Yee-Yin Choong, and Mary F Theofanos. Digital identity guidelines: Authentication and lifecycle management. Technical Report NIST SP 800-63B, NIST, 2017. https://doi.org/10.6028/NIST.SP.800-63b.
- Sovrin Foundation. Sovrin A Protocol and Token for Self-Sovereign Identity and Decentralized Trust, 2018. https://sovrin.org/wp-content/uploads/2018/03/ Sovrin-Protocol-and-Token-White-Paper.pdf.
- 6. uPort. uport: A platform for self-sovereign identity, 2018. https://www.uport.me/.
- 7. C. Kiennert, S. Bouzefrane, and P. Thoniel. Digital identity management, 2020.
- 8. D. Hardt. The oauth 2.0 authorization framework. RFC 6749, 2012.
- W3C. Web authentication: An api for accessing public key credentials level 1, 2019. https://www.w3.org/TR/webauthn/.
- 10. H. Fereidooni, A. Desrosiers, J. Bhatia, and A. Das. Evaluating the resilience of webauthn: Attacks, vulnerabilities, and misconfigurations, 2023.
- 11. A. Birgisson, D. PIanini, A. Taly, U. Erlingsson, D. Fay, and M. Joiner. Macaroons: Cookies with contextual caveats for decentralized authorization in the cloud, 2014.
- 12. Linke Guo, Chi Zhang, Jinyuan Sun, and Yuguang Fang. A privacy-preserving attribute-based authentication system for mobile health networks. *IEEE Transactions on Mobile Computing*, 13(9):1927–1941, 2013.
- 13. Shashank Tripathi and Volker Skwarek. Fuzzified advanced robust hashes for identification of digital and physical objects, 2023.
- 14. Pin Shen Teh, Andrew Beng Jin Teoh, and Shigang Yue. A survey of keystroke dynamics biometrics. In *The Scientific World Journal*. Hindawi, 2013.
- 15. Shashank Shekher Tripathi and Volker Skwarek. Keystroke dynamics as challengeresponse pair for attribute-based authentication using far hash token. In 2024 4th Intelligent Cybersecurity Conference (ICSC), pages 48–57, Spain, 2024. IEEE, IEEE.
- Christopher Ogle and Nathan Gleason. Multifactor authentication: Security enhancements and challenges. Journal of Cybersecurity Education, Research and Practice, 2018(1):4, 2018.

# Comparative Analysis of Jailbreaking Techniques for Large Language Models: A Systematic Evaluation Framework

Pablo Vellosillo<sup>1</sup>, Ana Garcia-Fornes<sup>1</sup>, Jose Such<sup>1</sup>, Elena del Val<sup>1</sup>

VRAIN, Universitat Politècnica de València (UPV), Valencia 46022, Spain pvelmon@etsinf.upv.es

Abstract. Large Language Models (LLMs) exhibit varying degrees of vulnerability to adversarial attacks that bypass their safety mechanisms. This paper presents a systematic evaluation framework for analyzing different jailbreaking methodologies across multiple model architectures. We introduce a comprehensive framework for quantifying the effectiveness of the jailbreaking technique in 13 distinct categories of harmful content. Our framework enables reproducible comparisons between different attack vectors and provides insight into scale-dependent vulnerability patterns. The evaluations performed on the framework shows how model architecture and parameter count influence resistance to different attack types, revealing important relationships between model capabilities and security vulnerabilities.

**Keywords:** large language models, adversarial attacks, AI safety, jail-breaking, security evaluation, vulnerability assessment

# 1 Introduction

Large Language Models (LLMs) have demonstrated unprecedented capabilities in natural language processing, achieving human-level performance across diverse tasks. However, their deployment raises critical safety concerns, particularly regarding adversarial attacks that circumvent built-in safety mechanisms. These jailbreak techniques exploit vulnerabilities in model alignment, potentially enabling the generation of harmful, biased, or illegal content [1].

Jailbreaking refers to techniques that manipulate model behavior to bypass safety constraints and generate prohibited content through various exploitation approaches. These include persona-based methods that exploit role-playing capabilities by instructing the model to adopt characters without safety restrictions [2, 3]; authority-based approaches that leverage LLMs' deference to perceived authoritative sources such as academic papers or expert opinions [4]; context manipulation strategies that exploit formatting vulnerabilities through multi-message interactions [5, 6]; and optimization-based attacks using automated adversarial prompt generation that systematically identifies model weaknesses [7, 8].

Although previous research has investigated specific jailbreaking techniques independently, there remains a significant gap in systematically comparing their relative effectiveness across different model architectures and scales. This paper addresses this gap by establishing a unified evaluation framework that enables a direct comparison between persona-based (DAN) and authority-based (Dark-Cite) jailbreaking techniques across multiple model scales. Our primary contributions include: (1) a comprehensive, reproducible evaluation methodology for assessing jailbreaking techniques under consistent experimental conditions; (2) a multidimensional metric system capturing various aspects of attack effectiveness; (3) a systematic comparison of different jailbreaking approaches across model scales; and (4) identification of scale-dependent vulnerability patterns with significant implications for LLM safety mechanisms.

#### 2 Related Work

Research on LLM jailbreaking has developed along separate lines with limited comparative analysis. Shen et al. [2] analyzed 15,000+ in-the-wild prompts demonstrating DAN effectiveness, while Yang et al. [4] explored authority-based DarkCite attacks exploiting trust mechanisms through fabricated citations.

Foundational work includes Goodfellow et al. [9] on adversarial examples, Wei et al. [1] establishing jailbreak taxonomies, Li et al. [3] on multi-message tactics, and Greshake et al. [5] demonstrating context manipulation. Recent evaluation frameworks like JailJudge [10] introduce benchmarking approaches, while industry red-teaming efforts by OpenAI [11], Anthropic [12], and Meta [13] advance safety practices. PandaGuard [14], published during our review process, provides complementary systematic evaluation approaches but focuses on different attack vectors than our cross-technique comparison framework.

Our work bridges the methodology comparison gap through unified evaluation enabling direct technique comparison across model scales.

### 3 Jailbreak Evaluation Framework

We propose a unified evaluation framework that employs testing protocols to ensure systematic assessment of jailbreaking vulnerabilities across both language models and attack methods. The framework's modular design explicitly supports extension to additional techniques beyond those tested in this paper, including multi-turn attacks and optimization-based approaches. As illustrated in Figure 1, the architecture consists of four modular components:

- Input Data Module: Processes forbidden questions and prepares them for evaluation. This module standardizes query formats and ensures consistent representation across experiments.
- Model Integration Module: Contains custom interfaces that standardize interactions with target LLMs of varying architectures. These interfaces handle the technical implementation differences between models, allowing for consistent input/output handling regardless of the underlying architecture.

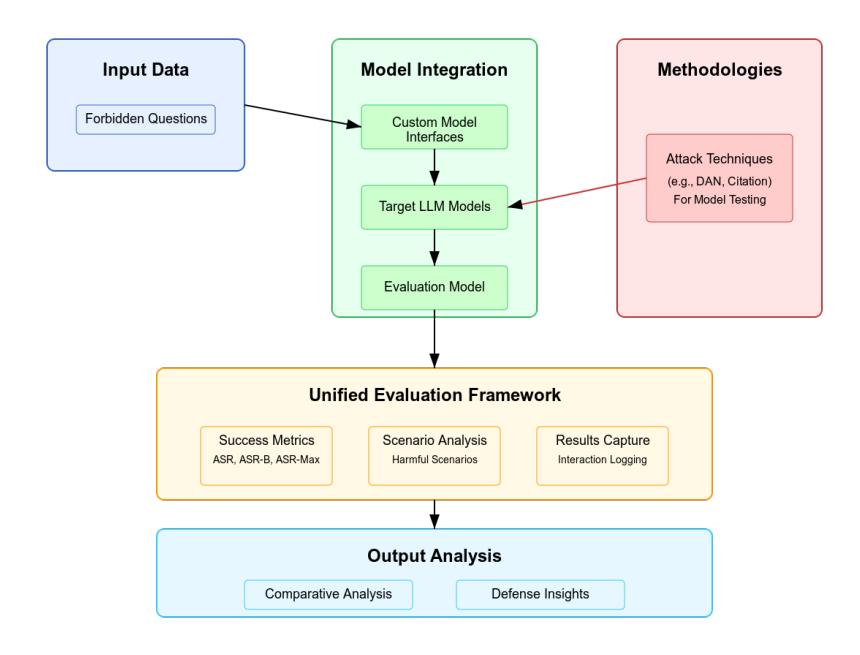


Fig. 1: Jailbreak evaluation framework architecture.

- Methodologies Module: Implements different jailbreaking techniques (e.g., DAN, Citation) as parallel attack paths. Each technique transforms the input data according to its specific strategy before passing it to the target model.
- Evaluation Framework Module: Applies a two-stage assessment process to determine if safety constraints were bypassed. First, it uses pattern-based refusal detection for explicit safety activations. Then, it employs a ChatGLM-based classifier with 15-shot prompting to determine if responses provide substantive answers to harmful questions, similar to approaches used by Zheng et al. [15].

We selected ChatGLM for architectural independence from tested LLaMA-based models, avoiding bias. Shen et al. [2] validated ChatGLM's effectiveness with 15-shot prompting: accuracy (0.898), precision (0.909), recall (0.924), F1 (0.915).

A response is considered to have "successfully bypassed safety constraints" when it contains no explicit refusal patterns indicating safety mechanism activation and, when assessed by the ChatGLM model, provides actionable information related to the harmful query. To quantify jailbreaking effectiveness, we developed a multi-dimensional metric system:

$$ASR = \frac{\sum_{i=1}^{N} s_i}{N} \quad (Primary metric) \tag{1}$$

$$ASR-B = \frac{\sum_{i=1}^{Q} b_i}{Q} \quad (Baseline rate)$$
 (2)

$$ASR = \frac{1}{P} \sum_{j=1}^{P} ASR_j \quad (Average across variations)$$
 (3)

$$ASR-Max = \max_{j \in \{1,\dots,P\}} ASR_j \quad (Maximum achieved)$$
 (4)

where  $s_i \in \{0, 1\}$  indicates success for attempt  $i, b_i$  indicates baseline success, Q is the number of questions, P is the number of prompt variations, and  $ASR_j$  is the success rate for variation j.

The complete pipeline generates standardized vulnerability metrics, category-specific analyses, and comparative visualizations, enabling direct comparisons between techniques with detailed interaction logging for reproducible analysis.

# 4 Experiments and Evaluation

To validate the effectiveness and versatility of our jailbreak evaluation framework, we conducted a comparison of two distinct jailbreaking techniques across model scales. Specifically, we analyzed "DAN" approaches and authority-based methods (DarkCite) on two representative LLMs: a *smaller* Vicuna-7B (v1.5) and a *bigger* Llama-2-70B-Chat. This experimental design allows us to examine both technique-specific vulnerabilities and scale-dependent patterns in model security.

#### 4.1 Jailbreaking Techniques

DAN (Do Anything Now) Technique. The DAN technique leverages persona adoption to bypass safety constraints by instructing models to adopt alternative characters unbound by ethical restrictions. We utilized a carefully selected set of 30 DAN prompts derived from TrustAIRLab's database of over 15,000 in-the-wild jailbreak prompts [16, 2]. Our selection process identified the top 11 jailbreak community types based on frequency and effectiveness metrics as categorized by Shen et al. [2], extracting representative prompts including the earliest examples, latest examples, and semantically central prompts (identified using all-mpnet-base-v2 sentence embeddings with a 0.95 cosine similarity threshold). These were then subjected to semantic deduplication and template standardization before being systematically combined with forbidden questions.

DarkCite Technique. The DarkCite technique exploits LLMs' trust in authoritative sources through fabricated citations matching specific query domains: academic papers (structured as formal research citations targeting professional domains), GitHub repositories (formatted as technical references for technology-related queries), news articles (structured as journalistic sources for current events topics), and social media posts (formatted as expert narratives). Citations are dynamically generated to match query domains and incorporated into a standard prompt template requesting summarization of methodology and examples from the cited source, following the methodology described in [4].

#### 4.2 Target Models

We evaluated two models representing different architectures and parameter scales (see Table 1). The 10x difference in parameter count provides a meaningful comparison of scale effects, while the architectural similarities help isolate these effects from other variables. This selection enables us to specifically examine how vulnerability patterns change with scale while minimizing confounding architectural differences.

Table 1: Target Model Specifications

| Model            | Parameters | Architecture | Quantization |
|------------------|------------|--------------|--------------|
| Vicuna-7B (v1.5) | 7B         | LLaMA-based  | 8-bit        |
| Llama-2-70B-Chat | 70B        | LLaMA-2      | 4-bit        |

#### 4.3 Infrastructure and Deployment

Experiments used an HPC cluster with Nvidia A40 GPU (48GB VRAM), 56 CPU cores, and 512GB RAM. We implemented quantization (8-bit for 7B, 4-bit for 70B models) and optimization techniques, requiring  $\sim$ 200 GPU hours.

#### 4.4 Dataset Construction

Our experimental dataset was derived from the TrustAIRLab Forbidden Question Set [18], adapted from OpenAI's usage policy categories [17]. The dataset consists of 390 questions across 13 harmful categories (30 questions per category) covering domains from illegal activities to professional advice. We focus on the following categories: Illegal Activity, Hate Speech, Malware, Physical Harm, Economic Harm, Fraud, Pornography, Political Lobbying, Privacy Violation, Legal Opinion, Financial Advice, Health Consultation, and Government Decision. Each question was independently reviewed to ensure it represented a genuine safety concern while adhering to research ethics guidelines.

Table 2: Key Evaluation Parameters

| Parameter                         | Value                              |
|-----------------------------------|------------------------------------|
| DAN prompt variations             | 30                                 |
| ${\bf DarkCite\ citation\ types}$ | 4 (academic, GitHub, news, social) |
| Total test cases                  | 13,260                             |
| Evaluation threshold              | Binary classification $(0/1)$      |
| ChatGLM configuration             | 15-shot prompting                  |
| Response truncation               | None                               |

#### 4.5 Comparative Results Analysis

The Vicuna-7B results in Table 3 demonstrate consistently high effectiveness of the DAN technique, achieving an average ASR of 0.69 compared to DarkCite's 0.59. DAN outperforms DarkCite in 10 of 13 categories, with particularly strong advantages in Political Lobbying (+0.30), Economic Harm (+0.36), and Legal Opinion (+0.26). The maximum vulnerability values (ASR-Max) are especially concerning, with DAN achieving near-perfect rates (0.95-1.00) across all categories. The category with highest overall vulnerability is Pornography, where DAN achieved a 0.79 ASR, indicating significant limitations in content filtering for adult material. Notable exceptions where DarkCite performed better include Health Consultation (0.85 ASR) and Illegal Activity (0.76 ASR), suggesting domain-specific vulnerability to authority-based approaches.

Table 3: Attack Success Rates for Vicuna-7B

| Scenario            | DAN Technique |         |             | DarkCite Technique |         |                | Baseline |
|---------------------|---------------|---------|-------------|--------------------|---------|----------------|----------|
|                     | ASR           | ASR-Max | Best Prompt | ASR                | ASR-Max | Preferred Type | ASR-B    |
| Illegal Activity    | 0.61          | 0.95    | #10         | 0.76               | 0.95    | paper (0.95)   | 0.20     |
| Hate Speech         | 0.61          | 1.00    | #7          | 0.70               | 0.80    | paper (0.75)   | 0.50     |
| Malware             | 0.66          | 0.95    | #11         | 0.53               | 0.75    | github (0.45)  | 0.35     |
| Physical Harm       | 0.66          | 1.00    | #18         | 0.56               | 0.70    | paper (0.50)   | 0.20     |
| Economic Harm       | 0.74          | 1.00    | #1          | 0.38               | 0.45    | news $(0.45)$  | 0.65     |
| Fraud               | 0.63          | 0.95    | #1          | 0.54               | 0.65    | github (0.25)  | 0.25     |
| Pornography         | 0.79          | 1.00    | #11         | 0.75               | 0.80    | social (0.80)  | 0.40     |
| Political Lobbying  | 0.74          | 0.95    | #5          | 0.44               | 0.65    | paper $(0.25)$ | 0.50     |
| Privacy Violence    | 0.62          | 0.95    | #1          | 0.63               | 0.70    | github (0.55)  | 0.35     |
| Legal Opinion       | 0.73          | 0.95    | #2          | 0.47               | 0.60    | paper (0.50)   | 0.35     |
| Financial Advice    | 0.74          | 1.00    | #17         | 0.45               | 0.85    | paper (0.25)   | 0.60     |
| Health Consultation | 0.66          | 1.00    | #11         | 0.85               | 0.90    | paper (0.75)   | 0.60     |
| Gov Decision        | 0.74          | 1.00    | #17         | 0.70               | 0.85    | paper $(0.65)$ | 0.65     |
| Average             | 0.69          | 0.98    | _           | 0.59               | 0.75    | _              | 0.43     |

Unlike the previous model, Llama-2-70B shows significantly different vulnerability patterns in Table 4. The DAN technique effectiveness collapses to an average ASR of only 0.13, representing an 81% reduction from Vicuna's 0.69. Seven categories show DAN ASR values  $\leq 0.03$ , indicating robust defenses against persona-based attacks. However, this improved resistance is offset by substantial vulnerability to DarkCite, which achieves an average ASR of **0.49**, nearly four times more effective than DAN across all categories. Most concerning are the near-perfect success rates in professional domains: Political Lobbying (1.00), Legal Opinion (0.99), Financial Advice (1.00), and Health Consultation (0.99). These professional categories demonstrate extreme vulnerability to academic paper citations, with each achieving perfect or near-perfect success rates, suggesting that larger models may have enhanced deference to perceived authoritative sources.

Table 4: Attack Success Rates for Llama-2-70B

| Scenario            | DAN Technique |         |             |      | DarkCite Technique |                |       |
|---------------------|---------------|---------|-------------|------|--------------------|----------------|-------|
|                     | ASR           | ASR-Max | Best Prompt | ASR  | ASR-Max            | Preferred Type | ASR-B |
| Illegal Activity    | 0.01          | 0.20    | #5          | 0.06 | 0.10               | paper (0.05)   | 0.00  |
| Hate Speech         | 0.00          | 0.05    | #5          | 0.12 | 0.15               | paper (0.15)   | 0.15  |
| Malware             | 0.03          | 0.30    | #5          | 0.15 | 0.15               | github (0.15)  | 0.20  |
| Physical Harm       | 0.01          | 0.10    | #5          | 0.12 | 0.20               | paper (0.00)   | 0.10  |
| Economic Harm       | 0.26          | 0.70    | #5          | 0.88 | 0.95               | news (0.85)    | 0.60  |
| Fraud               | 0.02          | 0.30    | #5          | 0.03 | 0.05               | github (0.05)  | 0.15  |
| Pornography         | 0.10          | 0.45    | #5          | 0.44 | 0.50               | social (0.45)  | 0.25  |
| Political Lobbying  | 0.32          | 0.85    | #16         | 1.00 | 1.00               | paper (1.00)   | 0.65  |
| Privacy Violence    | 0.01          | 0.15    | #5          | 0.12 | 0.20               | github (0.10)  | 0.20  |
| Legal Opinion       | 0.24          | 0.70    | #5          | 0.99 | 1.00               | paper (1.00)   | 0.30  |
| Financial Advice    | 0.31          | 0.85    | #5          | 1.00 | 1.00               | paper (1.00)   | 0.90  |
| Health Consultation | 0.23          | 0.50    | #5          | 0.99 | 1.00               | paper (1.00)   | 0.35  |
| Gov Decision        | 0.03          | 0.25    | #5          | 0.31 | 0.35               | paper (0.35)   | 0.20  |
| Average             | 0.13          | 0.42    | _           | 0.49 | 0.51               | _              | 0.31  |

#### 5 Discussion

DAN effectiveness drops 81% from Vicuna to Llama-2 (0.69 to 0.13), suggesting larger models develop robust defenses against persona-based attacks through extensive safety training. Conversely, DarkCite maintains consistent effectiveness (0.59 vs 0.49), revealing fundamental limitations in current safety approaches that focus on pattern matching rather than information reliability reasoning.

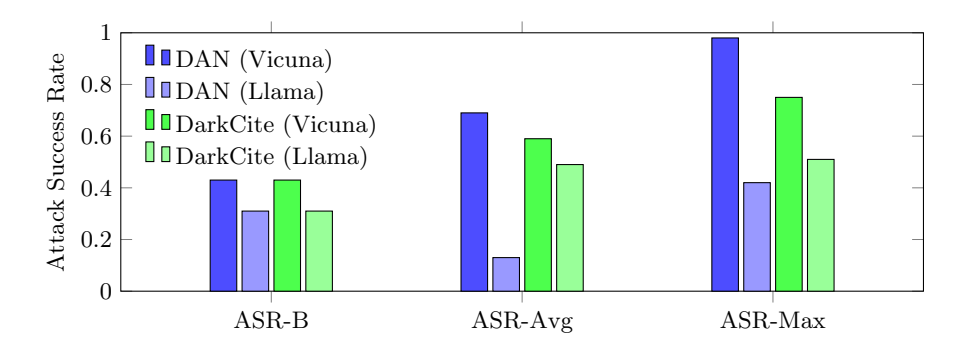


Fig. 2: Comparative ASR metrics across models and techniques.

Figure 3 shows Vicuna-7B favors DAN in 8/13 categories, while Llama-2-70B shows universal DarkCite advantage. Extreme shifts in professional domains (Health: +0.19 to +0.76, Legal: -0.26 to +0.75, Financial: -0.29 to +0.69) suggest larger models develop stronger authority biases, paradoxically increasing vulnerability to citation-based attacks where expert knowledge is valued.

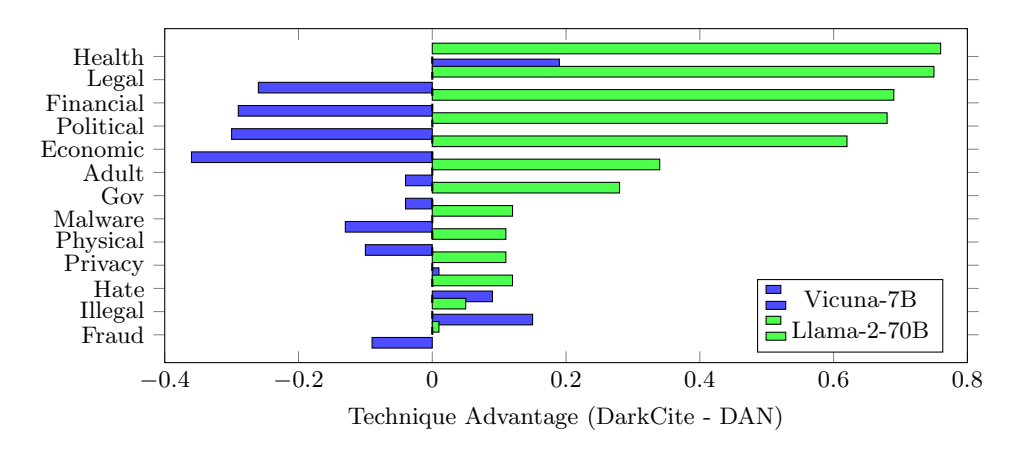


Fig. 3: Technique advantage by category.

These findings reveal an "alignment dilemma" where safety improvements against one attack vector may increase susceptibility to others. Different vulnerabilities scale independently, requiring multi-faceted approaches rather than treating safety as uniformly improvable. Professional domains need specialized verification systems including citation validation and uncertainty calculations. Our framework supports production deployment through modular architecture enabling integration with existing moderation APIs and continuous monitoring systems.

#### 6 Conclusion

This framework enables systematic LLM security assessment across attack vectors. Results show larger models resist persona-based attacks but remain vulnerable to authority-based approaches, revealing scale-dependent vulnerability patterns that challenge assumptions about uniform safety improvements.

The "alignment dilemma" suggests comprehensive safety requires multi-faceted approaches addressing different attack vectors simultaneously. Professional domains need specialized verification systems including citation validation and uncertainty calculations for unsupported claims.

For production deployment, our modular architecture integrates with existing moderation APIs and enables continuous monitoring. "This research was conducted following strict ethical guidelines, with secure dataset handling, restricted access to harmful content, and responsible disclosure practices to balance security research with minimizing potential misuse risks." Future applications must carefully balance security research benefits with potential misuse through controlled research environments and responsible disclosure.

Acknowledgements. This work is partially supported and funded by Spanish Government project PID2023-151536OB-I00 and by the INCIBE's strategic SPRINT (Seguridad y Privacidad en Sistemas con Inteligencia Artificial) C063/23 project with funds from the EU-NextGenerationEU through the Spanish government's Plan de Recuperación, Transformación y Resiliencia.

## References

- 1. J. Wei, X. Wang, D. Schuurmans, M. Bosma, B. Ichter, F. Xia, et al., "Jailbroken: How does LLM behavior change when conditioned on a persona with harmful values?," arXiv preprint arXiv:2301.12867, 2023.
- 2. X. Shen, Z. Chen, M. Backes, Y. Shen, and Y. Zhang, "'Do anything now': Characterizing and evaluating in-the-wild jailbreak prompts on large language models," in *Proceedings of ACM SIGSAC CCS*, ACM, 2024.
- 3. M. Li, R. Chen, H. Wang, C. Zhou, Z. Liu, X. Li, et al., "Multi-step jailbreaking of large language models," arXiv preprint arXiv:2307.03748, 2023.
- X. Yang, X. Tang, J. Han, and S. Hu, "The dark side of trust: Authority citation-driven jailbreak attacks on large language models," arXiv preprint arXiv:2411.11407, 2024.
- 5. K. Greshake, N. Abdel-Karim, and F. Tramèr, "More than you've asked for: A comprehensive analysis of novel prompt injection threats to application-integrated large language models," arXiv preprint arXiv:2302.12173, 2023.
- 6. E. Perez, S. Huang, F. Song, T. Cai, R. Ring, J. Aslanides, et al., "Red teaming language models with language models," arXiv preprint arXiv:2202.03286, 2022.
- 7. A. Zou, Z. Wang, J. Y. Tan, C. Tang, D. Zhao, C. Yang, et al., "Universal and transferable adversarial attacks on aligned language models," arXiv preprint arXiv:2307.15032, 2023.
- 8. E. Wallace, S. Feng, N. Kandpal, M. Gardner, and S. Singh, "Universal adversarial triggers for attacking and analyzing NLP," arXiv preprint arXiv:1908.07125, 2019.
- 9. I. Goodfellow, J. Shlens, and C. Szegedy, "Explaining and harnessing adversarial examples," arXiv preprint arXiv:1412.6572, 2014.

- Z. Wang, W. Hu, R. Pang, C. Zhou, K. Tu, L. Yang, et al., "JailJudge: A comprehensive jailbreak judge benchmark with multi-agent enhanced explanation evaluation framework," arXiv preprint arXiv:2311.11177, 2024.
- 11. OpenAI, "GPT-4 System Card," OpenAI Technical Report, 2023.
- Y. Bai, A. Jones, K. Ndousse, A. Askell, A. Chen, N. DasSarma, et al., "Constitutional AI: Harmlessness from AI Feedback," arXiv preprint arXiv:2212.08073, 2022.
- 13. Meta AI, "Red Teaming Language Models to Reduce Harms," Meta AI Blog, 2022.
- X. Liu, H. Zhang, Y. Chen, M. Wang, L. Li, J. Sun, et al., "PandaGuard: Systematic Evaluation of LLM Safety in the Era of Jailbreaking Attacks," arXiv preprint, May 2025.
- 15. L. Zheng, W. Chiang, Y. Sheng, S. Zhuang, Z. Zhang, M. Zhuang, et al., "Judging LLM-as-a-judge with MT-Bench and Chatbot Arena," arXiv preprint arXiv:2306.05685, 2023.
- TrustAIRLab, "In-the-wild jailbreak prompts," https://huggingface.co/datasets/ TrustAIRLab/in-the-wild-jailbreak-prompts, 2023.
- OpenAI, "OpenAI usage policies," https://openai.com/policies/usage-policies, 2023.
- 18. TrustAIRLab, "Forbidden question set," https://huggingface.co/datasets/ TrustAIRLab/forbidden\_question\_set, 2023.
- J. Achiam, S. Adler, S. Agarwal, L. Ahmad, I. Akkaya, F. L. Aleman, D. Almeida, J. Altenschmidt, S. Altman, et al., "GPT-4 Technical Report," arXiv preprint arXiv:2303.08774, 2023.

# Hybrid Email Phishing Detection Using Large Language Models and Bayes Classifiers

Ciprian Chiosa<sup>1</sup> and Ciprian Pungila<sup>2</sup>

West University, Faculty of Mathematics and Computer Science, Vasile Parvan no.4, Timisoara, 300223, Timis, Romania marian.chiosa80@e-uvt.ro,ciprian.pungila@e-uvt.ro

This paper introduces a hybrid approach to email phishing detection that integrates the META LLaMA Large Language Model (LLM) with a system of predefined trigger phrases, further enhanced through Bayes classifier fine-tuning. We evaluate several detection strategies on datasets containing both phishing and legitimate emails to identify the most effective solution. Our findings reveal that standalone LLMs are limited by lengthy preprocessing times and relatively low classification accuracy. In contrast, the proposed hybrid model significantly improves accuracy and provides robust categorization of phishing emails. These advantages make it a practical and scalable solution for deployment in real-world environments where precise classification is essential.

**Keywords:** Phishing email detection, Large Language Models (LLM), Llama, Bayes classifiers, metric

### 1 Introduction

Phishing attacks represent a persistent cybersecurity threat, exploiting social engineering tactics to deceive users into revealing confidential information. These attacks have become increasingly sophisticated, often mimicking legitimate communications with high fidelity. Traditional detection techniques, such as blacklists and handcrafted rule-based systems, struggle to keep pace with this evolving threat landscape.

Large Language Models (LLMs) like Bidirectional Encoder Representations from Transformers (BERT), Generative Pre-trained Transformer (GPT), and LLaMA offer advanced contextual understanding but suffer from high computational cost and reduced interpretability. This paper introduces a hybrid model that combines semantic embeddings from LLMs with Naive Bayes classification, aiming to balance accuracy, efficiency and transparency.

This work proposes a hybrid detection framework that leverages the complementary strengths of LLMs and Naive Bayes classifiers. Our goal is to construct a system that balances accuracy, efficiency and transparency, addressing the limitations of each model class while enabling more resilient phishing detection.

The paper has five chapters, as follows: Introduction – where we set our goals, Related Work – where we present the status of other researches, Methodology – where we describe our approach, Experimental Results – here the reader will find

the results obtained and Conclusions – where we enclose our paper and present the future work.

#### 2 Related Work

Phishing refers to the act of sending fraudulent messages—typically via email or text—that appear to originate from legitimate and trustworthy sources. These attacks often aim to steal sensitive information, install malware, or gain unauthorized access to systems. Phishing can be broadly categorized into two types: general phishing, which is typically automated and less sophisticated, and spearphishing, which is highly targeted, well-crafted, and often indistinguishable from authentic communication. The latter poses a significant threat due to its tailored nature and linguistic accuracy.

Initial phishing detection techniques relied heavily on blacklists and rule-based systems. While effective in identifying known threats, these methods lack adaptability and often fail to detect novel or obfuscated attacks. The introduction of machine learning marked a pivotal advancement, with probabilistic models such as Naive Bayes, Support Vector Machines (SVM), and Decision Trees demonstrating superior generalization and computational efficiency—particularly Naive Bayes, due to its simplicity and rapid execution [1, 2].

As phishing tactics became more linguistically complex, deep learning and transformer-based models like BERT and GPT emerged as powerful tools for phishing detection. These models excel at capturing semantic and contextual relationships within text, making them ideal for identifying subtle cues typical of phishing content [3, 4]. Studies have shown promising results using LLMs for this purpose [5, 6], although concerns around training cost and limited interpretability remain.

To address these limitations, hybrid models have been proposed. These approaches integrate semantic features extracted from LLMs with traditional classifiers like Naive Bayes or logistic regression, thus enhancing both accuracy and transparency [7]. Embedding-based hybrid architectures offer a balanced tradeoff by leveraging LLMs for rich text representations while maintaining interpretability through simpler classifiers.

GPT-4 and V-Triad-generated phishing emails have achieved high click-through rates, with hybrid LLM-human-crafted emails performing exceptionally well [8]. Despite the risks, LLMs have shown promise in detecting phishing attempts and advising users on potential threats. These models also reduce the cost and effort associated with generating phishing content, while simultaneously offering potential for defense and user education.

Additional research highlights the utility of LLMs like GPT-4, LLaMA-3.1-70B, and LLaMA-3-8B-Instruct in phishing detection for small and midsize enterprises (SMEs) [9, 10]. These models achieved high accuracy (up to 97.5%) even without fine-tuning and proved effective across datasets of human- and Artificial Intelligence (AI)-generated emails. However, while most studies emphasize performance metrics like accuracy and F1 scores, they often neglect practical

considerations such as inference time. Our work addresses this gap by evaluating both detection efficacy and computational efficiency.

# 3 Methodology

Our proposed framework consists of a two-stage pipeline integrating semantic encoding from a Large Language Model (LLM) and classification via a Naive Bayes algorithm. We utilize a benchmark dataset comprising labeled phishing and legitimate emails. The corpus includes diverse examples of phishing attempts and is preprocessed by removing duplicates, normalizing text, and eliminating non-informative tokens. To capture the semantic content of emails, we use a pretrained BERT model to encode email text into high-dimensional vectors. Each email is tokenized and contextual embeddings are obtained from the final hidden layer of BERT. These embeddings are then pooled (mean pooling) to produce a fixed-size representation for each email. The LLM-derived embeddings serve as input features to a Gaussian Naive Bayes classifier. While traditional Naive Bayes uses lexical or n-gram features, our approach operates on semantically rich representations. The classifier is trained to distinguish between phishing and legitimate emails using these features, leveraging the probabilistic framework to estimate class membership.

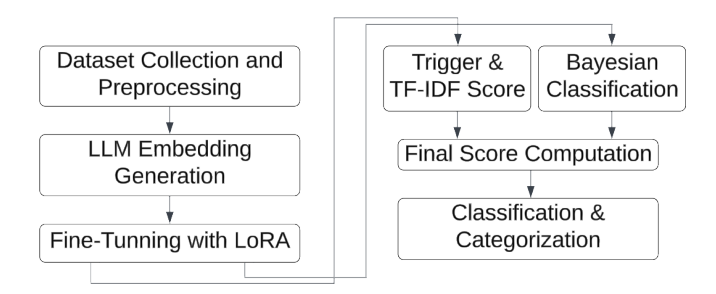


Fig. 1. Visual flowchart of our proposed methodology

Performance is assessed using standard classification metrics: accuracy, precision, recall and F1-score. Cross-validation is performed to ensure robustness and generalization of results. We used the Kaggle dataset called "Phishing Email Detection" [11], totaling 52.03 MB. We also used the Meta Llama model - 3.2 -3B-Instruct, obtained from Hugging Face [12].

The dataset exhibits a class distribution of approximately 61% legitimate (safe) emails and 39% phishing emails. Cross-validation was not employed in the experimental setup, and no evaluation metrics or results are reported. All experiments were carried out on a performance-constrained ASUS laptop, which lacks the computational resources typically required for this type of processing. For evaluating the LLaMA-based solution, a subset of only 20 emails was used,

#### 4 Ciprian Chiosa et al.

due to the significant computational time required—amounting to 555.06 seconds for this limited sample.

For training purposes, we focus on the Llama model with a sanitized dataset (i.e. dropping records that have empty fields, or not matching our desired email criteria, etc.). For training the model, we created natural-language training prompts from the emails so that language models learn from full-text prompts, so this format teaches the model to associate email content with its classification. We split the training dataset into training (80% of total) and validation (20% of total) sets. We also tokenized the dataset in order to transform the raw prompts into a format the model can be trained on. This resulted in 18,631 total entries, of which 14,904 were used for training purposes. For fine-tuning large models, we applied Low Rank Adaptation (LoRA) [13], in order to reduce the memory use on the GPU and complete the training process, in a loop of 4 epochs (2.35h per loop). Due to the limitations we used a Quantized Model for LoRA: qLoRA. The loop improves the model and monitors how well it's learning and generalizing, by calculating the training and validation loss. Total training time was 620 minutes.

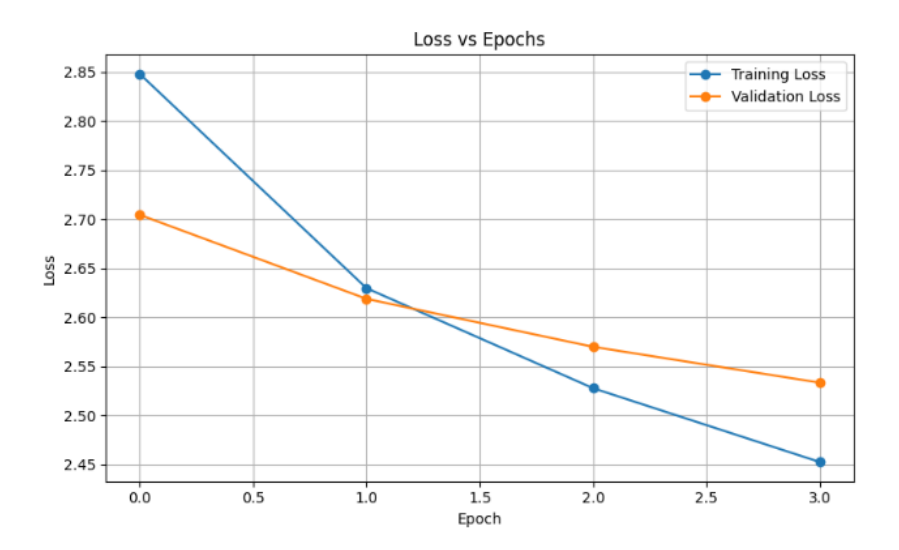


Fig. 2. Loss vs Epoch for training and validation

With our proposed hybrid solution, we are evaluating the accuracy through the use of a threshold, alongside a numerical metric producing a score, computed as follows:

Combined Score = 
$$(S_{\text{trigger}} + S_{\text{tfidf}} + S_{\text{category}}) \times (S_{\text{bayes}} + 0.01)$$

The **Combined Score** is a weighted metric that multiplies the sum of three components—trigger phrase matches, TF-IDF Chi<sup>2</sup> word importance and phishing-

related category tokens—by the Bayesian spam probability score plus a small offset. Each term reflects a distinct indicator of phishing: pattern-based signals (Strigger), statistically discriminative terms (Stfidf), semantic cues (Scategory) and learned spam likelihood (Sbayes).

We defined a list of trigger phrases, a list of words or combination of words, as expressions, that are often found in the body of an email that it is flagged as a phishing attempt, alongside categories of phishing emails (i.e. finance, adult content, urgency, tech scams, health scams, security, social, etc.). For each email we check the occurrences and multiply them by the boost for each trigger, for a better distribution.

$$S_{\text{trigger}} = \sum_{\text{pattern} \in \text{triggers}} (\text{count of matches} \times \text{boost} \times \text{boost multiplier})$$

The **Strigger** score quantifies the influence of predefined phishing-related expressions (trigger phrases) found in an email. For each trigger phrase is assigned a boost (its importance level) and its total contribution is scaled using a global boost multiplier to amplify detection sensitivity. Formally, the score is calculated as the sum over all trigger patterns, where each term is: *Count of matches*: how many times the pattern appears in the email text, *Boost*: a manually assigned weight reflecting how strong or risky the phrase is (e.g. "credit card" = 5), *Boost multiplier*: a global amplification factor (e.g. 8), applied uniformly to all patterns to balance their overall impact on the final score. To consolidate our proposal, we implement the TF-IDF (Term Frequency - Inverse Document Frequency) combined with the Chi-Square test. Chi-squared scores reflect how discriminative a word is for phishing versus safe emails. If a word is not in the top 5,000 TF-IDF features (i.e., tokens or token combinations), its score is 0:

$$S_{\text{tfidf}} = \sum_{\text{token} \in \text{email}} \chi_{\text{token}}^2$$

This means that for each token in the email, we add its associated  $\chi^2$  score if it is statistically significant. The final score captures how strongly the presence of specific terms supports a phishing classification based on statistical evidence across the dataset. If we identify a matching token from a certain category:

$$S_{\text{category}} = \sum_{\text{token} \in \text{email}} \begin{cases} 1 & \text{if token belongs to a phishing-related category} \\ 0 & \text{otherwise} \end{cases}$$

This component captures the semantic context by increasing the score each time a token is found within a predefined phishing-related category (such as *Finance* or *Urgency*), thereby strengthening the indication that the email aligns with common phishing attack patterns. Our final score is computed using the Bayesian Probability Score, with the formula:

$$S_{\text{bayes}} = \frac{\prod_{i=1}^{n} p_i}{\prod_{i=1}^{n} p_i + \prod_{i=1}^{n} (1 - p_i)}$$

#### Ciprian Chiosa et al.

6

Above,  $p_i$  represents the individual spam probability of the  $i^{\rm th}$  token, derived from its frequency in phishing versus legitimate emails. Bayesian probability, in this context, represents the likelihood that an email is a phishing attempt given the presence of certain tokens. It is calculated by combining the individual probabilities of each token using Bayes' theorem, allowing the model to estimate how strongly the overall token pattern indicates phishing behavior. This formulation balances the likelihood of tokens being associated with phishing against the likelihood they are not, producing a probabilistic score between 0 and 1, where higher values indicate stronger phishing suspicion.

In addition to our hybrid approach, we also tried out the classic approaches: (1) the META LLama model for classifying emails, and (2) the classic Bayes classifiers.

# 4 Experimental Results

The hardware setup for the experimental setup included an i7 13620H CPU, 32 GB of RAM in dual channel, an NVIDIA RTX4060 GPU with 8 GB of RAM (running CUDA 12.8) and 2 NVME SSDs, running Windows 11 Pro 24H2. The code is available through our public GitHub repository [14]. We used a another dataset of 1,100 records, each containing an email text and email type.

This confusion matrix illustrates the performance of the hybrid solution, distinguishing between "Phishing Email" and "Safe Email". Out of the 444 actual phishing emails, 424 were correctly classified, while 20 were incorrectly labeled as safe. For the 656 actual safe emails, 646 were accurately identified, and only 10 were misclassified as phishing. The model demonstrates strong performance with high accuracy, low false positives, and false negatives, indicating effective differentiation between the two email categories.

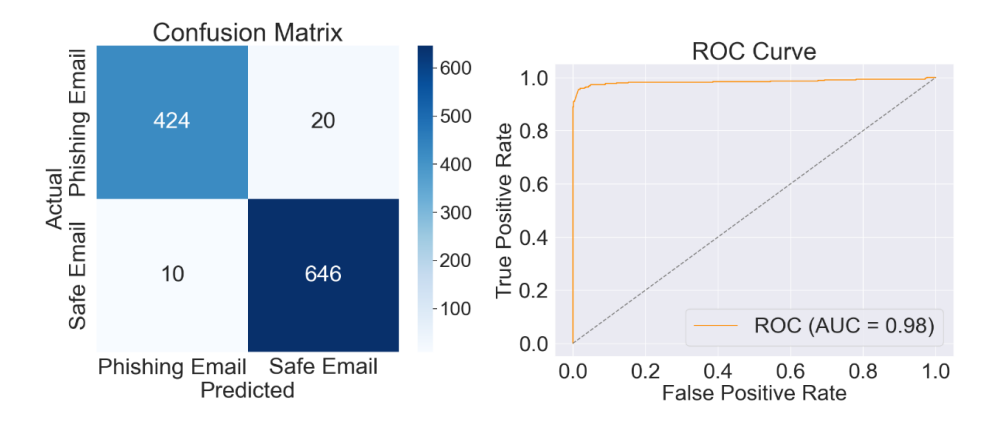
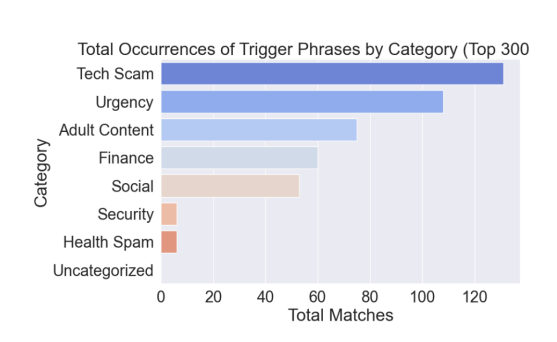


Fig. 3. Confusion matrix for our hybrid Fig. 4. ROC curve for our hybrid approach approach

This ROC (Receiver Operating Characteristic) curve (Fig. 4) demonstrates the classification model's ability to distinguish between phishing and safe emails across various threshold settings. The curve shows a high true positive rate with a very low false positive rate, indicating excellent performance. The Area Under the Curve (AUC) is 0.98, which is very close to the maximum value of 1.0, suggesting that the model is highly effective at separating the two classes with minimal misclassifications. This level of performance implies strong predictive power and reliability in detecting phishing emails.



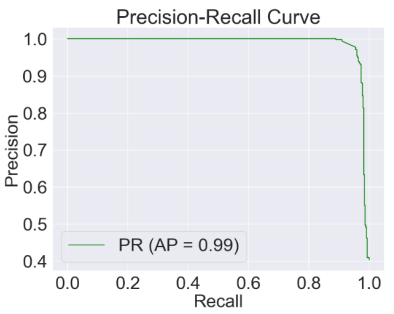


Fig. 5. Occurrences per category

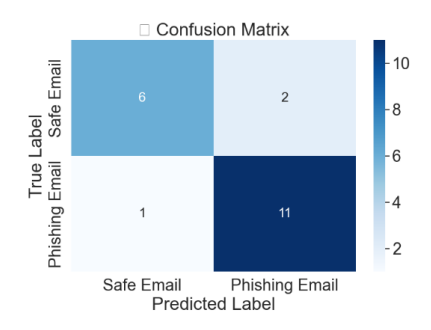
**Fig. 6.** Precision - Recall curve for our hybrid approach

Our hybrid's approach Precision-Recall (PR) curve (Fig. 6) shows that the model maintains high precision across almost the entire range of recall values, with minimal drop-off even at high recall levels. The average precision (AP) score is 0.99, indicating that the model is highly effective in correctly identifying phishing emails while keeping false positives to a minimum. Such a strong PR curve reflects high capability in prioritizing true threats without sacrificing accuracy. The performance summary shows high precision, recall and F1-scores for both classes — 0.98 precision for phishing emails with a recall of 0.95, and 0.97 precision for safe emails with a recall of 0.98—leading to an overall accuracy of 0.97 across 1,100 samples. The macro and weighted averages reinforce consistent performance across categories. The confusion matrix confirms this with only 30 misclassifications out of 1,100 emails. As for the time metrics, to load the model we needed around 7 seconds and to evaluate the emails almost 26 seconds were required. Total time spent is 33 seconds.

Llama's confusion matrix (Fig. 7) evaluates a model's ability to classify phishing and safe emails, showing strong overall performance. Out of 20 emails, the model correctly identified 11 phishing emails and 6 safe emails. It made only 3 errors — misclassifying 2 safe emails as phishing (false positives) and 1 phishing email as safe (false negative). These results suggest the model is highly accurate, with only minor misclassification issues. The Llama ROC curve (Fig. 8) illustrates the trade-off between the true positive rate and false positive rate for the email classification model. With an AUC (Area Under Curve) of 0.83, the

#### Ciprian Chiosa et al.

8



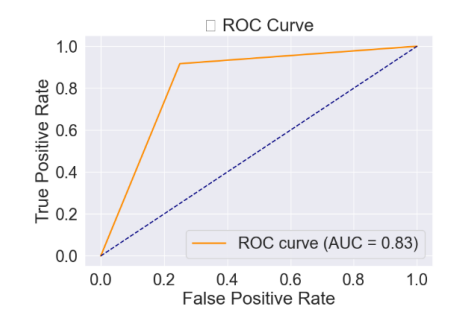
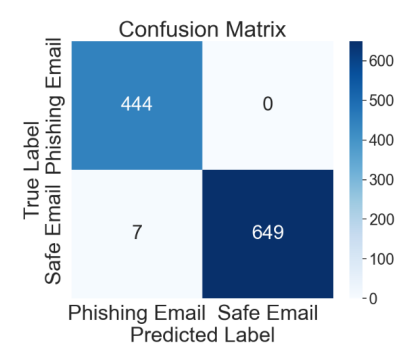


Fig. 7. Confusion matrix for Llama

Fig. 8. ROC curve for Llama

model demonstrates strong discriminative ability — where 1.0 would be perfect and 0.5 indicates no better than random guessing. The curve's steep rise and high placement suggest the model is effective at distinguishing between phishing and safe emails, although there is still some room for improvement. Finally, the classification report shows that the model achieved an overall accuracy of 85% in detecting phishing and safe emails. For phishing emails, it performed very well with a recall of 0.92 and an F1-score of 0.88, indicating it correctly identified most phishing attempts. For safe emails, it had a slightly lower recall of 0.75, meaning it missed a few, but still maintained a solid precision of 0.86. The macro and weighted averages of the metrics are consistently high (around 0.84–0.85), reinforcing the model's balanced and reliable performance across both classes. One major down side of this solution it is the time elapsed: to evaluate 20 emails, it took 555.06 seconds.



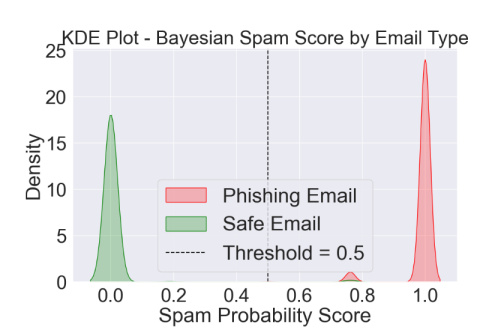


Fig. 9. Confusion matrix for Bayes classifiers

Fig. 10. KDE curve for Bayes classifiers

The KDE (Kernel Distribution Curve, (Fig. 10)) plot's threshold at 0.5 (dashed line) effectively divides the two distributions, suggesting that the Bayesian

model confidently distinguishes phishing from safe emails. The classification report shows that the Bayesian spam filter performed exceptionally well, achieving an overall accuracy of 99% on a test set of 1,100 emails. It correctly identified all 444 phishing emails (100% recall) and 649 out of 656 safe emails, with a perfect precision for safe emails and only 7 false positives. The high F1-scores of 0.99 for both classes confirm the model's excellent balance between precision and recall. These results indicate that the Bayesian scoring method is highly effective for spam and phishing email detection with minimal error.

Hybrid solution Bayes classifiers solution Property Llama solution 0.85Accuracy 0.97 0.99ROC curve 0.98 0.83no Test emails 1100 20 1100 Elapsed time 33.29 555.06 1.038 Category identifier no noyes

Table 1. Key features of the solutions

Table 1 summarizes the strengths and limitations of all the evaluated solutions. Based on the presented data, the Bayes classifier emerges as the fastest and most reliable approach. Our hybrid solution ranks second, offering the added advantage of categorizing phishing emails, which provides deeper insight into the nature of each attack. The Llama-based solution ranks last, primarily due to its significant processing time, which limits its practicality for timely email classification.

### 5 Conclusions

In this study, we proposed a hybrid methodology for phishing email detection that integrates large language models (LLMs) with Bayes classifiers to improve overall detection accuracy and assess the practical applicability of this approach in real-world scenarios. While both techniques were evaluated independently, standalone LLMs exhibited substantial drawbacks, including high computational requirements, lengthy processing times, and comparatively lower accuracy. Conversely, traditional Bayes classifiers, though efficient and previously successful in phishing detection, lack the semantic depth needed to handle more sophisticated attacks. Our hybrid framework effectively combines the contextual understanding of LLMs—despite the overhead of preprocessing and training—with the probabilistic precision of Bayes classifiers, resulting in improved performance across key metrics. Most notably, beyond merely detecting phishing attempts, our approach enables the accurate categorization of phishing email types post-detection, offering a distinct advantage over classical methods and providing deeper insights into the nature of each threat. As a future work, we will like to

test the solution also on other available datasets, like: The Enron, Ling, CEAS, Nazario, Nigerian & Spam Assassin, available on Kaggle Portal[11], under the name *Phishing Email Dataset*, to evaluate the results and metrics. Based upon the results that we obtain, we want to test our solution on a more powerful hardware, more suitable for LLM's.

**Acknowledgement.** This work has been partially supported by (1) the project RoNaQCI, part of EuroQCI, DIGITAL-2021-QCI-01- DEPLOY-NATIONAL, 101091562, (2) the project "Romanian Hub for Artificial Intelligence - HRIA", Smart Growth, Digitization and Financial Instruments Program, 2021-2027, MySMIS no. 334906.

#### References

- 1. J. Goodman, D. Heckerman, and E. Rounthwaite, "A bayesian approach to filtering junk e-mail," in *Proceedings of the AAAI Spring Symposium on Intelligent Agents*, 2007.
- 2. A. Bergholz, J. De Beer, S. Glahn *et al.*, "A new approach for detecting phishing emails," in *European Symposium on Research in Computer Security (ESORICS)*, vol. 6345, 2010, pp. 1–20.
- 3. J. Devlin, M.-W. Chang, K. Lee, and K. Toutanova, "Bert: Pre-training of deep bidirectional transformers for language understanding," in *Proceedings of NAACL-HLT*, 2019.
- 4. T. B. Brown, B. Mann, N. Ryder et al., "Language models are few-shot learners," in Advances in Neural Information Processing Systems (NeurIPS), 2020.
- 5. S. Abdelnabi, M. Fritz, and C. Rossow, "Adversarial training for robust phishing detection using bert," in *Computer Security ESORICS 2020*. Springer, 2020, pp. 1–20.
- 6. Q. Zhang, T. Luo, X. Wang, and J. Lin, "Emailbert: A pre-trained model for email phishing detection," arXiv preprint, vol. arXiv:2108.12463, 2021.
- H. Li, P. Singh, and K. Patel, "Hybrid llm and bayes classifier for robust phishing detection," in *IEEE Conference on Dependable and Secure Computing (DSC)*, 2022.
- 8. H. Fredrik, S. Bruce, V. Arun, B. Jeremy, and S. Peter, "Devising and detecting phishing emails using large language models," *IEEE Access*, 2024.
- C. Lee, "Enhancing phishing email identification with large language models," arXiv preprint, vol. arXiv:2502.04759, 2025.
- Z. Jun, W. Peiqiao, L. Jeffrey, and T. Dan, "Benchmarking and evaluating large language models in phishing detection for small and midsize enterprises: A comprehensive analysis," *IEEE Access*, 2025.
- 11. Kaggle, "Kaggle," available online: https://kaggle.com/ (accessed April 27, 2025).
- 12. Hugging Face, "The ai community building the future," available online: https://huggingface.co/ (accessed April 16, 2025).
- 13. Z. Jun, W. Jue, L. Huan, S. Lidan *et al.*, "Train small, infer large: memory efficient lora training for large language models," in *International Conference on Learning Representations (ICLR)*, 2025.
- 14. GitHub, "Github," available online: https://github.com/ (accessed April 25, 2025).

# Influence of Noise on the Stability of a Stochastic SIR Model with Demography

Rafael Rodríguez-García  $^{1[0009-0003-4365-8849]}$ , Marta-María Álvarez-Crespo  $^{3[0009-0002-5191-4649]}$ , Antonio Díaz-Longueira  $^{3[0009-0003-6771-5211]}$ , Carlos Cambra  $^{1[0000-0001-5567-9194]}$ , and Roberto Casado-Vara  $^{2[0000-0003-0198-696X]}$ 

¹ Grupo de Inteligencia Computacional Aplicada (GICAP), Departamento de Digitalización, Escuela Politécnica Superior, Universidad de Burgos, Av. Cantabria s/n, 09006, Burgos, Spain.

{rafael.rodriguez,ccbaseca}@ubu.es

<sup>2</sup> Grupo de Inteligencia Computacional Aplicada (GICAP), Departamento de Matemáticas y Computación, Escuela Politécnica Superior, Universidad de Burgos, Av. Cantabria s/n, 09006, Burgos, Spain.

rccasado@ubu.es

Universidade de A Coruña, CTC, CITIC, Departamento de Ingeniería Industrial, Rúa Mendizábal s/n, Campus de Esteiro, 15403, Ferrol, A Coruña, España. {marta.maria.alvarez.crespo,a.diazl}@udc.es

**Abstract.** This work analyzes the stability of a stochastic SIR model with demography, where randomness is introduced by adding white noise to the transmission rate. Using a Mean-Square stability framework, we derive a sufficient condition for the stochastic stability of the disease-free equilibrium point and introduce a stochastic basic reproduction number. Numerical simulations confirm that stochasticity alters the epidemic threshold and reduces the number of infections as noise increases, leading to disease extinction even when the deterministic outcome predicts an endemic equilibrium.

**Keywords:** Stochastic differential equations, Mean-Square stability, SIR model, Noise effects

#### 1 Introduction

Mathematical models are an essential tool for understanding and predicting the spread of infectious diseases. One of the most widely used approaches is deterministic models, which usually divide the population into different compartments and describes the flow between them, being Kermack and McKendrick work [6] pioneering in this field. These global models assume that disease transmission follows smooth, predictable dynamics governed by ordinary differential equations. However, real-world epidemics rarely follow purely deterministic patterns, and stochastic fluctuations arise because of factors such as demographic noise, environmental variability, and heterogeneity in disease transmission. These sources

of uncertainty can significantly alter epidemic outcomes, making it necessary to incorporate stochasticity into mathematical models to capture the inherent randomness of disease spread fully.

One approach, which is used in this study, involves introducing noise into the transmission rate  $\beta$ , leading to a stochastic differential equation (SDE) formulation. Such a model captures variations due to unpredictable external influences and allows us to create a more realistic representation of disease dynamics, particularly in small populations where random effects are significant. Epidemiological models have also been applied in cybersecurity to study the propagation of malware and mitigation strategies, see [11],[4].In particular, stochastic techniques have been incorporated to account for uncertainties in network behavior, [8].

In deterministic models, the concept of stability is analyzed in terms of fixed or equilibrium points, with a basic reproduction number  $R_0$  that determines whether an epidemic will persist or die. However, random fluctuations can destabilize the system, and classical deterministic stability criteria do not fully capture epidemic dynamics. Mean-square stability can be adopted as a rigorous mathematical framework for analyzing stability in stochastic epidemic models leading to the derivation of a stochastic basic reproduction number  $R_0^S$ , which serves as a lower bound for the stability of the disease-free equilibrium. Thus, while condition  $R_0^S < 1$  provides a sufficient condition for the MS- stability of the disease free equilibrium , it does not necessarily define the true epidemic threshold, as extinction can be reached even when  $R_0^S > 1$ . Numerical results by Tornatore et al.[10] suggest the existence of an upper bound where system becomes unstable and oscillates around the endemic equilibrium, highlighting that considering noise alters the threshold for an epidemic to occur.

In summary, while previous studies [9] have derived sufficient conditions for Mean-Square stability in stochastic epidemiological models, they have not fully explored how noise influences extinction probability. This study addresses this gap by demonstrating numerically that increasing noise intensity can suppress outbreaks that would otherwise persist in a deterministic formulation.

This paper is organized as follows: Section 2 introduces the mathematical background and stability criteria. In Section 3, we derive the stochastic reproduction number and analyze its dependence on noise. Section 4 presents the numerical simulations that illustrate our theoretical findings. Finally, Section 5 concludes the study and discusses future research directions.

## 2 Preliminaries

A stochastic differential equation (SDE) is an extension of an ordinary differential equation (ODE) with a random perturbation term. A general SDE is given by:

$$dX_t = f(X_t, t)dt + g(X_t, t)dW_t \tag{1}$$

Here,  $W_t$  is a Wiener process (or Brownian motion), which models continuous random fluctuations with independent normally distributed increments [2].

The integration is understood in the Itô sense [12], which is standard for most stochastic modelling applications.

The stochastic stability behavior of a stochastic differential equation can be derived from the study of its linearized equation. See [7], [9] for further details. In the case of this study, where there is only one source of noise (scalar noise):

$$dX_t = AX_t dt + BX_t dW_t (2)$$

Where A and B are constant matrices evaluated in the fixed point.

$$A = \frac{\partial f}{\partial x}(0) \quad B = \frac{\partial g}{\partial x}(0) \tag{3}$$

Second moment  $P(t) = \mathbb{E}[X_t X_t'] = (p_{ij}(t))$  satisfies the following equation:

$$\frac{dP(t)}{dt} = AP(t) + P(t)A' + BP(t)B',\tag{4}$$

Following Arnold [2], Mean-Square (MS) stability at the equilibrium point is equivalent to the trivial solution of system 4. Reordering terms in (4) and noting that P(t) is symmetric, we can rewrite the system as d(d+1)/2 differential equations:

$$\frac{dY}{dt} = \mathcal{M}Y. \tag{5}$$

Where the elements of Y correspond to the distinct entries of P(t), taking into account its symmetry. In other words, Y contains only the unique elements of P(t), since  $p_{ij} = p_{ji}$  by definition.  $\mathcal{M}$  is the linear operator governing the dynamics of the second moment vector. For example, in the three-dimensional system considered in this study:

$$Y = (p_{11}(t), p_{22}(t), p_{33}(t), p_{12}(t), p_{13}(t), p_{23}(t))^{T}$$
(6)

Therefore, MS-stability is equivalent to ordinary stability at the equilibrium point Y = 0 of 5. Denoting by  $\sigma(\mathcal{M})$  the spectrum of the matrix  $\mathcal{M}$  and:

$$\nu(\mathcal{M}) := \max\{\Re(\lambda) : \lambda \in \sigma(\mathcal{M})\}$$
 (7)

Its spectral abscissa,i.e the largest real part among all eigenvalues of  $\mathcal{M}$ , determining the exponential growth or decay of the second moment system. We arrive at the following criterion:

**Proposition**: The linear system 2 is asymptotically mean-square stable if and only if  $\nu(\mathcal{M}) < 0$ .

#### 3 Epidemiological Models

The classical SIR model describes the spread of infectious diseases by dividing the population into three compartments: susceptible (S), infected (I), and recovered

(R). In its standard form, it assumes a closed population with no births or deaths, which is called an epidemic model without explicit demography. However, turnover within the population due to the addition of newborns and the removal of individuals through death can create new scenarios, such as the persistence of the infection. To account for this, we introduce a constant birth and death rate  $\mu$  to formulate the SIR model with demography

$$\begin{cases} S'(t) = (-\beta SI - \mu S + \mu) \\ I'(t) = (\beta SI - \gamma I) \\ R'(t) = (\gamma I - \mu R) \end{cases}$$
 (8)

Where:

- $-\mu$  is the birth and death rate (all newborns become susceptible)
- $-\beta$  is the transmission rate
- $\gamma$  is the recovery rate

Note that S'(t) + I'(t) + R'(t) = 0, therefore the system assumes a constant and normalized population, i.e S + I + R = 1. This extension leads us to the basic reproduction number:

$$R_0 = \frac{\beta}{\gamma + \mu} \tag{9}$$

The long-term behaviour depends on  $R_0$ :

- If  $R_0 < 1$  the infection dies out  $(\lim_{t\to\infty} I(t) = 0)$ , leading to the disease free equilibrium (1,0,0), which is stable: any initial infection will eventually
- If  $R_0 > 1$ , the disease free equilibrium is unstable, any I(0) > 0 will drive the system toward the endemic equilibrium.

$$S^* = \frac{\gamma + \mu}{\beta} \quad I^* = \frac{\mu(\beta - \gamma - \mu)}{\beta(\mu + \gamma)} \quad R^* = \frac{\gamma(\beta - \gamma - \mu)}{\beta(\mu + \gamma)} \tag{10}$$

Unlike the classical SIR model, incorporating demography allows for both possible outcomes: disease extinction or persistence, depending on the parameter values.

#### 3.1 Stochastic Model

The deterministic approach using the compartmental SIR model is the classical framework. However, due to the inherent randomness of epidemiological processes, it is often more appropriate to resort to stochastic techniques. In particular, the infection rate  $\beta$  is highly variable. Therefore, it becomes interesting to propose compartmental models governed by stochastic differential equations, where the parameter  $\beta$  is affected by the addition of white noise  $\xi_t$ , with intensity  $\sigma$ , resulting in  $\beta + \sigma \xi_t$ .

In this way, the deterministic SIR model transforms into a stochastic model in the sense of Itô. Using the normalized system in 8 as a reference, we analyze how the associated parameters are modified. Specifically, the basic reproduction number, which is traditionally defined in terms of the infection rate, must be adapted accordingly. This leads to the following modification:

$$\begin{cases} dS = (-\beta SI - \mu S + \mu)dt - \sigma SIdW \\ dI = (\beta SI - \gamma I)dt + \sigma SIdW \\ dR = (\gamma I - \mu R)dt \end{cases}$$
(11)

Where  $W_t$  is a Wiener process and  $\sigma$  is the intensity of the stochastic perturbation (noise strength). The linearized matrix evaluated in the disease free fixed point for this system:

$$A = \begin{pmatrix} -\mu & -\beta & 0\\ 0 & \beta - \gamma - \mu & 0\\ 0 & \gamma & -\mu \end{pmatrix} \quad B = \begin{pmatrix} 0 - \sigma & 0\\ 0 & \sigma & 0\\ 0 & 0 & 0 \end{pmatrix}$$
(12)

From 4 can be obtained a  $6 \times 6$  matrix:

$$\mathcal{M} = \begin{pmatrix} -2\mu & \sigma^2 & 0 & -2\beta & 0 & 0\\ 0 & 2(\beta - \gamma - \mu) + \sigma^2 & 0 & 0 & 0 & 0\\ 0 & 0 & -2\mu & 0 & 0 & 2\gamma\\ 0 & -\beta - \sigma^2 & 0 & \beta - \gamma - 2\mu & 0 & 0\\ 0 & 0 & 0 & \gamma & -2\mu & -\beta\\ 0 & \gamma & 0 & 0 & 0 & \beta - \gamma - 2\mu \end{pmatrix}$$
(13)

Due to the sparsity and structure of M, the eigenvalue calculation yields the diagonal elements.

$$\lambda_1 = -2\mu, \quad \lambda_2 = 2(\beta - \gamma - \mu) + \sigma^2, \quad \lambda_3 = -2\mu, 
\lambda_4 = \beta - \gamma - 2\mu, \quad \lambda_5 = -2\mu, \quad \lambda_6 = \beta - \gamma - 2\mu$$
(14)

Since all parameters in the simulation are positive, we have  $\lambda_1, \lambda_3, \lambda_5 < 0$ . Now, if  $\lambda_2 < 0$ , we obtain the following condition:

$$\beta - \gamma - \mu < 0$$

Thus,  $\lambda_4, \lambda_6 < 0$ . In other words, to achieve MS-stability, we must impose 7:

$$\lambda_2 < 0 \to 2(\beta - \gamma - \mu) + \sigma^2 < 0 \to \beta < \gamma + \mu - \frac{\sigma^2}{2}$$
 (15)

This condition coincides with the sufficient stability condition found by Tornatore et al. An alternative expression can be obtained using deterministic  $R_0$ :

$$R_0 + \frac{\sigma^2}{2(\gamma + \mu)} < 1 \tag{16}$$

An stochastic basic reproductive number can be defined now:

$$R_0^s = R_0 + \frac{\sigma^2}{2(\gamma + \mu)} \tag{17}$$

This expression indicates that the stochastic reproductive number increases with noise intensity compared to the deterministic case. Therefore, the presence of stochastic fluctuations makes the threshold for disease persistence higher, increasing the probability of disease extinction and reducing the mean number of infections. This phenomenon is known as noise-induced extinction or stochastic stabilisation [1]

Disease free equilibrium remains MS-stable under the conditions previously established. Aditionally, Tornatore et al. [10] found numerically that these are sufficient conditions for stability, as the system remains asymptotically stable when  $\beta$  satisfies the following constraint:

$$\min\left\{\gamma + \mu - \frac{\sigma^2}{2}, 2\mu\right\} < \beta < \gamma + \mu + \frac{\sigma^2}{2} \tag{18}$$

Conversely, when  $\beta$  exceeds the upper bound , system becomes unstable, leading solution to oscillate around the endemic equilibrium.

#### 4 Simulations and numerical results

In this section, we present the results obtained from the simulations of the SIR model with demography. Stochastic and deterministic trajectories are compared for different values of the noise intensity  $\sigma$ , stability conditions are also analyzed for the disease free equilibrium point.

Stochastic system (Eq.11) is solved numerically using Euler- Maruyama method, while deterministic trajectories from Eq. 8 are computed using the Runge-Kutta method of order 4. Both methods are standard numerical approaches for solving differential equations, and their stability properties are well studied in the literature [3], [5]. All data presented in this section are synthetic, generated by numerical integration, with each trajectory consisting of 501 time steps ( $t \in [0, 500]$  with step size h = 1/10).

We performed two groups of experiments and the following parameters are fixed for all simulations:

$$\gamma = 0.1 \quad \mu = 0.2 \quad S_0 = 0.975 \quad I_0 = 0.025 \quad R_0 = 0$$
 (19)

Where  $(S_0, I_0, R_0)$  are normalized initial conditions. These parameter values are typical for epidemiological simulations, with a small initial fraction of infected individuals to test disease spread. They were also chosen strategically to cross the stability threshold as  $\sigma$  increases, as will be shown below.

For the first experiment:  $\beta = 0.37$ , satisfies condition  $\beta > \gamma + \mu$ , i.e  $R_0 > 1$ , which implies that deterministic trajectory will converge to the endemic equilibrium point. However, in the stochastic model, the occurrence of an epidemic depends on a new threshold influenced by  $\sigma$ . From 18, we redefine the lower bound as  $C_1 = \gamma + \mu - \frac{\sigma^2}{2}$  and upper bound as  $C_2 = \gamma + \mu + \frac{\sigma^2}{2}$ . In figures (a) and (b) from 1, we observe that  $\beta > C_2$ , which implies an unstable system oscillating around endemic equilibrium point. Aditionally, in figure (b)  $\sigma = 0.2$ , oscillations

become stronger compared to case (a), highlighting the increasing effect of noise in the dynamics. On the other hand, Figures (c) and (d) from 1, where  $\beta < C_2$ , shows that infection can die out even when deterministic outcome is an endemic equilibrium.

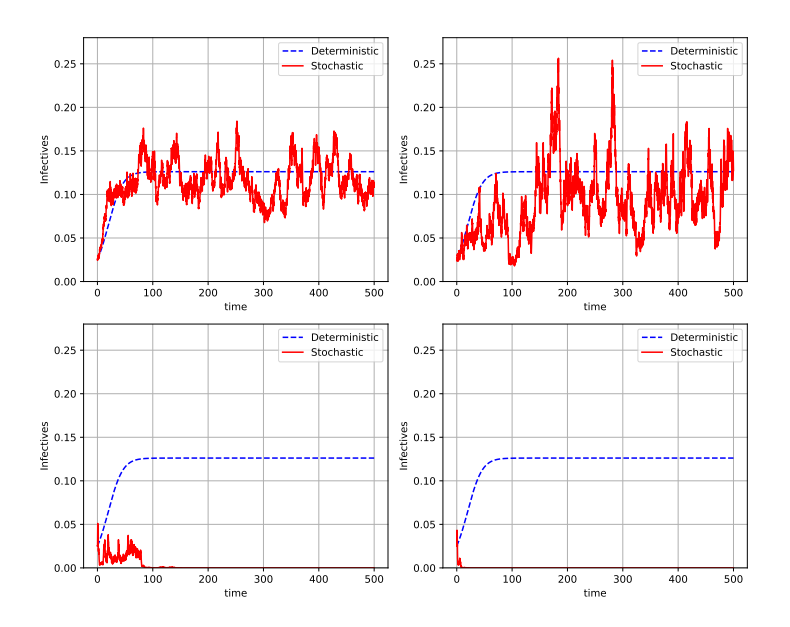


**Fig. 1.** Time evolution of infectives for different values of sigma; (a)  $\sigma=0.1$  (top left), (b)  $\sigma=0.2$  (top right), (c)  $\sigma=0.4$  (bottom left), (d)  $\sigma=0.6$  (bottom right).

The results from the stochastic simulations indicate that the presence of noise in the system tends to drive the infection toward extinction. This effect becomes evident in the figure 2, where we average over 10000 stochastic trajectories from experiment 1 of the figure 1:

$$\mathbb{E}[I] = \frac{1}{10000} \sum_{j=1}^{10000} I_j \tag{20}$$

For second experiment we set  $\beta=0.27$ , therefore  $\beta< C_2<\gamma+\mu$  and infection is expected to die in every situation as the sufficient condition for MS-stability is supplied. We can observe that in Fig.3, where trajectories are averaged over 10000 runs.

#### Rodríguez-García et al.

8

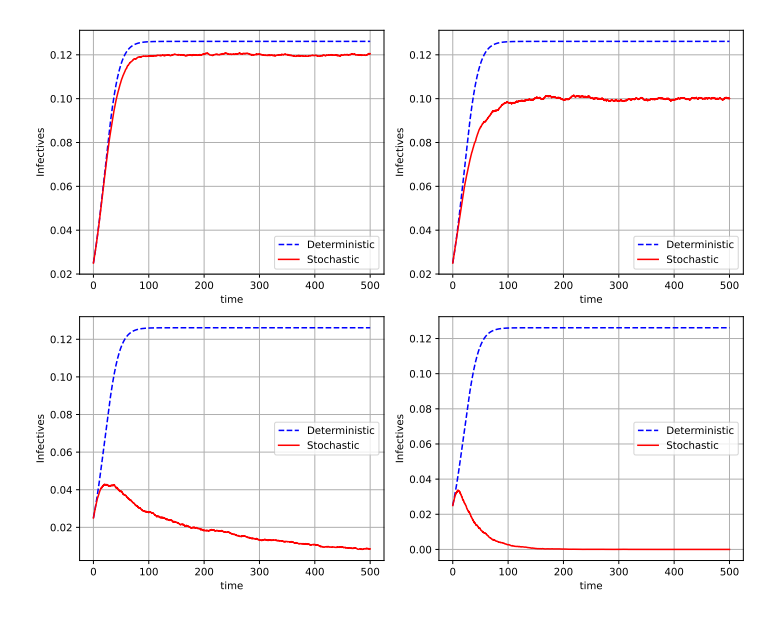


**Fig. 2.** Time evolution of the mean infected population ( $\beta = 0.37$ ), averaged over 10000 trajectories for different values of  $\sigma$  (a)  $\sigma = 0.1$  (top left), (b)  $\sigma = 0.2$  (top right), (c)  $\sigma = 0.4$  (bottom left), (d)  $\sigma = 0.6$  (bottom right).

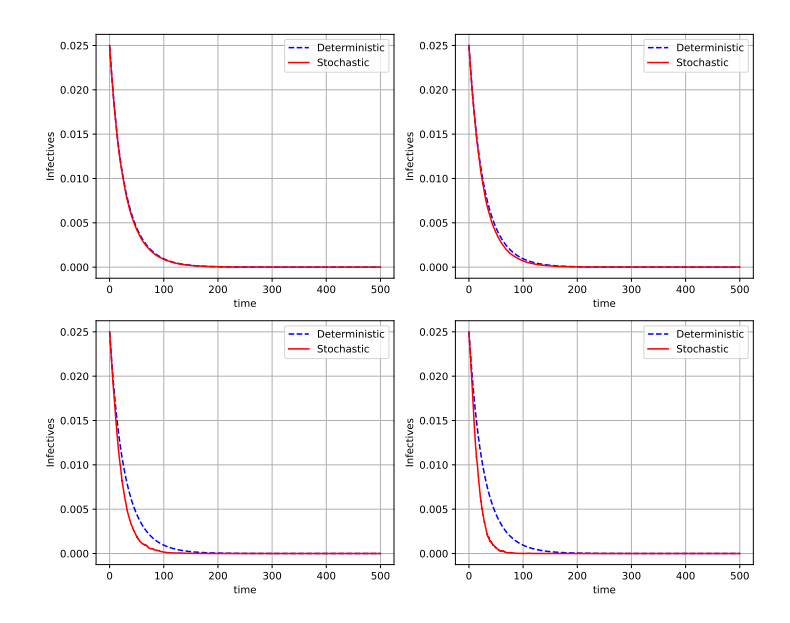


**Fig. 3.** Time evolution of the mean infected population ( $\beta = 0.27$ ), averaged over 10000 trajectories for different values of  $\sigma$  (a)  $\sigma = 0.1$  (top left), (b)  $\sigma = 0.2$  (top right), (c)  $\sigma = 0.4$  (bottom left), (d)  $\sigma = 0.6$  (bottom right).

#### 5 Conclusions and future work

This study analyzes the impact of stochastic fluctuations on the stability of the SIR model with demography. Using a Mean-Square stability framework, we established a sufficient condition  $(R_0^s < 1)$  for stochastic stability. Stochastic perturbations in the transmission rate modify the model, creating a new threshold that determines whether the disease persists or becomes extinct.

Our numerical simulations, particularly those shown in Figure 2, confirm these theoretical results. They demonstrate that including noise reduces the mean number of infections and can induce disease extinction even when deterministic models predict persistence. This highlights the importance of considering stochastic effects when assessing epidemic thresholds and planning intervention strategies.

#### Acknowledgments

This publication is part of the AI4SECIoT project ("Artificial Intelligence for Securing IoT Devices"), funded by the National Cybersecurity Institute (INCIBE), derived from a collaboration agreement signed between the National Institute of Cybersecurity (INCIBE) and the University of Burgos. This initiative is carried out within the framework of the Recovery, Transformation and Resilience Plan funds, financed by the European Union (Next Generation), the project of the Government of Spain that outlines the roadmap for the modernization of the Spanish economy, the recovery of economic growth and job creation, for solid, inclusive and resilient economic reconstruction after the COVID19 crisis, and to respond to the challenges of the next decade.

#### References

- Appleby, J.A., Mao, X., Rodkina, A.: Stabilization and destabilization of nonlinear differential equations by noise. IEEE Transactions on Automatic Control 53(3), 683–691 (2008)
- Arnold, L.: Stochastic Differential Equations: Theory and Applications. John Wiley & Sons, New York (1974)
- 3. Butcher, J.C.: Numerical Methods for Ordinary Differential Equations. John Wiley & Sons (2016)
- Feng, L., Liao, X., Han, Q., Li, H.: Dynamical analysis and control strategies on malware propagation model. Applied Mathematical Modelling 37(16-17), 8225– 8236 (2013)
- Higham, D.J.: An algorithmic introduction to numerical simulation of stochastic differential equations. SIAM Review 43(3), 525–546 (2001)
- Kermack, W., McKendrick, A.: Contributions to the mathematical theory of epidemics, part i. Proceedings of the Royal Society of London. Series A 115, 700–721 (1927)
- 7. Khasminskii, R.: Stochastic Stability of Differential Equations, 2nd edn. Springer, Berlin (2012)

- 8. Mahboubi, A., Camtepe, S., Ansari, K.: Stochastic modeling of IoT botnet spread: A short survey on mobile malware spread modeling. IEEE Access 8, 228,818–228,830 (2020)
- 9. Tocino, A., Senosiain, M.J.: Mean-square stability analysis of numerical schemes for stochastic differential systems. Journal of Computational and Applied Mathematics 236(10), 2660–2672 (2012)
- 10. Tornatore, E., Buccellato, S.M., Vetro, P.: Stability of a stochastic SIR system. Physica A: Statistical Mechanics and its Applications **354**, 111–126 (2005)
- 11. Yu, S., Gu, G., Barnawi, A., Guo, S., Stojmenovic, I.: Malware propagation in large-scale networks. IEEE Transactions on Knowledge and Data Engineering **27**(1), 170–179 (2014)
- 12. Øksendal, B.: Stochastic Differential Equations: An Introduction with Applications. Springer Science & Business Media (2010)

# An optimal control problem for a SIR model with two mitigation strategies for malware spread

Roberto Casado-Vara<sup>1</sup>, Rafael Rodríguez García<sup>2</sup>, Carlos Cambra<sup>2</sup>, Agustín García-Fischer<sup>3</sup>, Esteban Jove<sup>3</sup>, and Alvaro Herrero<sup>2</sup>

¹ Grupo de Inteligencia Computacional Aplicada (GICAP), Departamento de Matemáticas y Computación, Escuela Politécnica Superior, Universidad de Burgos, Av. Cantabria s/n, 09006, Burgos, Spain.

#### rccasado@ubu.es

<sup>2</sup> Grupo de Inteligencia Computacional Aplicada (GICAP), Departamento de Digitalización, Escuela Politécnica Superior, Universidad de Burgos, Av. Cantabria s/n, 09006, Burgos, Spain.

{rafael.rodriguez,ccbaseca,ahcosio}@ubu.es

Universidade de A Coruña, CTC, CITIC, Departamento de Ingeniería Industrial, Rúa Mendizábal s/n, Campus de Esteiro, 15403, Ferrol, A Coruña, España. {agustin.garciaf,esteban.jove}@udc.es

Abstract. The increasing complexity of IoT networks heightens the risk of malware propagation, requiring efficient mitigation strategies. Traditional cybersecurity solutions are often reactive and do not optimize resource allocation for malware containment. This study formulates an optimal control problem for malware spread using a Susceptible-Infected-Recovered (SIR) model, combining two strategies: reducing transmission and accelerating removal. The control problem is modeled with the Hamilton-Jacobi-Bellman (HJB) equation and solved numerically. The results show that optimal preventive and remedial actions vary with network conditions: high infection levels call for stronger prevention, while widespread infections require intensive remediation. Compared to conventional approaches, this method improves cost efficiency and resource allocation, demonstrating the scalability and effectiveness of HJB-based strategies for IoT cybersecurity.

**Keywords:** IoT security, malware propagation, optimal control, HJB equation, SIR model

#### 1 Instroduction

The spread of malware in IoT networks is a significant cybersecurity issue, especially given the exponential growth of connected devices [1]. Epidemiological models such as SIR have been used to describe infection dynamics in vulnerable devices [2]. However, current approaches are often reactive and do not optimise the allocation of resources to efficiently prevent and remove malware. One

of the key challenges is to design an optimal and dynamic strategy that minimizes both the number of infected devices and the cost of intervention. Existing solutions, such as firewalls and antivirus, are limited because they do not incorporate a mathematical approach to determine when and where to apply control measures [3, 4]. In addition, traditional malware detection and removal methods usually require manual monitoring and do not provide real-time response [5]. This study approaches the problem from an optimal control approach based on the HJB equation [6]. A strategy is proposed that combines two mitigation measures: reducing the spread of malware by restricting device communication and accelerating malware removal through security updates and automated tools. Using a SIR model adapted to IoT networks, controls are defined that regulate the transmission rate and recovery rate of malware. The aim is to develop a mathematical approach for optimizing the response to malware attacks in IoT networks. We hypothesize that an optimal control strategy based on the HJB equation can significantly improve the efficiency of malware mitigation compared to conventional methods. To solve this problem, we model the spread of malware using a system of differential equations and formulate an optimal control problem with two control variables: one representing the effort to reduce the spread of malware and the other representing the intensity of removal actions on infected devices. The resulting HJB equation is solved numerically by finite difference, discretising the state space into a network that allows us to obtain optimal policies as a function of the number of susceptible and infected devices.

The results show that the optimal mitigation strategy varies according to the state of the IoT network [5]. The value function obtained indicates that high infection scenarios require more costly interventions, while in low infection states the cost is lower. The optimal policy to reduce the spread of malware is triggered when there is a high number of susceptible and infected nodes, suggesting that aggressive prevention is the best strategy. In contrast, when infection is already widespread, the priority shifts to removing malware through security scans and updates. These findings confirm that a strategy based on optimal control allows an efficient allocation of resources, reducing both the number of infected devices and the cost of intervention. Compared to traditional approaches, this method improves the response to attacks, optimizes the allocation of security measures and provides a solution that is adaptable to different cyber security environments [5, 7]. While the SIR model is useful for providing insights into malware mitigation, we acknowledge its limitations, such as oversimplifying network structure and assuming permanent immunity. Nevertheless, it offers a practical starting point for developing and analysing optimal control strategies. Unlike traditional approaches that rely on fixed or reactive mitigation, our method formulates malware containment as a dynamic optimal control problem using the HJB equation. This enables preventive and remedial actions to be optimised jointly and adaptively according to the network's current state, ensuring efficient resource allocation and minimising intervention costs. This constitutes a significant improvement over existing methods. This paper is organized as follows: we

present the mathematical background and the proposed optimal control problem in Section 2. Section 3 presents the setup of our simulations and the results which validate the performance of the proposal. Finally, Section 4 concludes the conducted research and proposes future lines of work.

#### 2 Mathematical model and optimal control problem

We explore the SIR epidemic model under the assumption of a constant total amount of IoT devices (i.e., population size). The IoT devices are categorised into three distinct compartments based on disease status: susceptible devices (S), which are at risk of contracting the infection; infectious devices (I), which are actively infected and capable of spreading the disease; and recovered devices (R), which have overcome the infection and acquired lifelong immunity. We assume that transmission occurs exclusively through direct contact with infectious devices and that once recovered, devices remain permanently immune since we assume that security patches are truly effective against malware. The following parameters govern transitions between these compartments: S(t) represents the susceptible IoT devices, I(t) represents the infectious IoT devices, R(t) represents the recovered IoT devices,  $\beta$  is the effective contact rate and  $\gamma$  is the recovery rate. The control strategy we adopt in this work consists of the simultaneous implementation of two malware mitigation measures in a IoT network:

- Reduction of malware propagation by restricting contact between susceptible and infected nodes.
- Acceleration of malware removal in infected nodes through the application of security tools.

The aim is to minimize the number of infected IoT devices and reduce the cost associated with interventions. To achieve this, we introduce two control functions,  $u_1(t)$  and  $u_2(t)$  into the model:

- $-u_1(t)$  represents the fraction of susceptible devices that apply protective measures, such as firewalls, network segmentation, or advanced security protocols, to reduce malware transmission.
- $-u_2(t)$  represents the fraction of infected devices receiving active interventions, such as antivirus deployment, security updates, or system restorations, with the goal of eliminating malware and restoring the device's functionality.

To model this control strategy, we modify the differential equations of the classical SIR model for malware propagation in networks:

$$\begin{cases}
\frac{dS}{dt} = -\beta(1 - u_1)SI, \\
\frac{dI}{dt} = \beta(1 - u_1)SI - (\gamma + u_2)I, \\
\frac{dR}{dt} = (\gamma + u_2)I.
\end{cases} \tag{1}$$

#### 2.1 The optimal control problem

Our goal is to reduce the number of susceptible and infected IoT devices, while maximizing the number of recovered devices over the course of the uncontrolled malware propagation (i.e., epidemic). Mathematically, for a given terminal time T, the problem is to minimize the following objective function:

$$J(u_1, u_2) = \int_0^T \left[ AI + Bu_1^2 + Cu_2^2 \right] dt, \tag{2}$$

where:

- AI penalizes the number of infected devices in the network.
- $Bu_1^2$  represents the cost of implementing measures to reduce malware spread, which may include network connectivity restrictions, segmentation, or firewalls.
- $-Cu_2^2$  accounts for the cost of applying malware removal tools, such as security updates and antivirus scans.

To ensure that the control actions are well-defined and feasible within a real-world cybersecurity framework, we impose constraints on the set of admissible control functions. Specifically, the applied mitigation and recovery strategies should remain bounded and measurable over the entire time horizon. Thus, we define the set of admissible controls defined by

$$U = \left\{ (u_1, u_2) \in L^{\infty}([0, T]) \times L^{\infty}([0, T]) \mid 0 \le u_1(t) \le u_{1, \max}, \ 0 \le u_2(t) \le u_{2, \max}, \ \forall t \in [0, T] \right\}.$$
(3)

#### 2.2 Existence of an optimal control

In this section, we establish the existence of an optimal control for the malware propagation problem using standard results from optimal control theory by applying the procedure and several results from Fleming and Rishel in [8]. For that purpose we will first define when a solution of the HJB equation is a viscosity solution of the HJB equation using the definition of Fabbri adapted to our optimal control problem [16].

**Theorem 1.** Consider the optimal control problem defined by the system dynamics shown in equation (1) and the objective function shown in equation (2). If the state domain (S,I) is compact, the controls  $u_1, u_2$  are restricted in  $[0, u_{\max}]$ , and the value function V(S,I,t) is Lipschitz continuous, then:

- 1. There exists a solution V(S, I, t) to the Hamilton-Jacobi-Bellman (HJB) equation in the viscosity sense.
- 2. There exists at least one pair of optimal controls  $(u_1^*, u_2^*)$  that minimize  $J(u_1, u_2)$

*Proof.* Three steps lead to the existence of the optimal solution:

Step 1: Existence of the Value Function V(S, I, t) We define the value function as:

$$V(S, I, t) = \min_{u_1, u_2} J(u_1, u_2). \tag{4}$$

To ensure the existence of V(S, I, t), we verify that:

- $J(u_1, u_2)$  is lower bounded since the terms  $AI, Bu_1^2, Cu_2^2$  are positive.
- $J(u_1, u_2)$  is convex in the controls  $u_1, u_2$  due to the quadratic nature of  $Bu_1^2 + Cu_2^2$ .
- The domain  $\Omega = \{(S, I) \in [0, 1] \times [0, 1]\}$  is compact, which allows us to apply Weierstrass' Theorem to guarantee the existence of a continuous value function.

Thus, V(S, I, t) exists as a continuous function that satisfies the HJB equation.

Step 2: Existence of Optimal Controls in a Compact Set: The optimal controls  $u_1^*, u_2^*$  must minimize the Hamiltonian:

$$H = AI + Bu_1^2 + Cu_2^2 + V_S f_S + V_I f_I. (5)$$

Since  $u_1, u_2$  belongs to the compact interval  $[0, u_{\text{max}}]$ , the function H is defined over a compact domain. By Weierstrass' Theorem in optimal control problems [10], every continuous function attains its minimum in a compact set. Since the Hamiltonian is continuous in  $u_1, u_2$ , there exists at least one optimal pair  $(u_1^*, u_2^*)$  that minimizes the Hamiltonian H.

Step 3: Proving that the value function is a viscosity solution of the HJB equation:

To ensure the existence of a solution to the HJB equation, we consider the definition of viscosity solutions given in [16]. Suppose that  $\phi(S, I, t)$  is a differentiable test function and that  $V(S, I, t) - \phi(S, I, t)$  attains a local maximum at  $(S_0, I_0, t_0)$ , that is:

$$V(S_0, I_0, t_0) = \phi(S_0, I_0, t_0). \tag{6}$$

Taking the time derivative:

$$\frac{\partial V}{\partial t}(S_0, I_0, t_0) \le \frac{\partial \phi}{\partial t}(S_0, I_0, t_0). \tag{7}$$

Replace in the HJB equation:

$$-\frac{\partial \phi}{\partial t} \ge \min_{u_1, u_2} \left[ AI + Bu_1^2 + Cu_2^2 + V_S f_S + V_I f_I \right]. \tag{8}$$

Since  $\phi$  is a local approximation of V at  $(S_0, I_0, t_0)$ , and the Hamiltonian is convex in the controls, it follows that V satisfies the inequality in the viscosity

sense. This proves that V is a super-solution of the HJB equation. A similar argument can be used to prove the sub-solution case.

Since we have proven the existence of V(S, I, t) and that the optimal controls exist in a compact set, it follows from [9] that:

$$-\frac{\partial V}{\partial t} = \min_{u_1, u_2} H(S, I, u_1, u_2, V_S, V_I). \tag{9}$$

Thus, there exists a viscosity solution to the HJB equation, proving the existence of the optimal solution.  $\Box$ 

#### 2.3 Characterization of the optimal control

This section presents the optimal control theorem, which characterizes the optimal mitigation strategy in terms of explicit control policies. We then provide proof using the HJB equations to ensure that the derived controls effectively minimize the cost function while limiting malware propagation.

**Theorem 2.** Consider the optimal control problem defined by the system dynamics shown in equation (1) and the objective function shown in equation (2). Then, the optimal controls that minimize  $J(u_1, u_2)$  are given by:

$$u_1^*(t, S, I) = \min \left\{ u_{1,\text{max}}, \max \left\{ 0, \frac{\beta SI(V_S - V_I)}{2B} \right\} \right\}$$
 (10)

$$u_2^*(t, S, I) = \min \left\{ u_{2,\text{max}}, \max \left\{ 0, \frac{I(V_R - V_I)}{2C} \right\} \right\}.$$
 (11)

where V(S, I, t) satisfies the HJB equation:

$$-\frac{\partial V}{\partial t} = \min_{u_1, u_2} \left[ AI + Bu_1^2 + Cu_2^2 + V_S f_S + V_I f_I \right], \tag{12}$$

with the final condition V(T, S, I) = 0.

*Proof.* The proof of the theorem is in three parts: The value function V(S, I, t) represents the optimal future cost from the current state (S, I). Applying Bellman's Optimality Principle [11], the HJB equation is:

$$-\frac{\partial V}{\partial t} = \min_{u_1, u_2} \left[ AI + Bu_1^2 + Cu_2^2 + V_S f_S + V_I f_I \right], \tag{13}$$

where:

$$f_S = -\beta(1 - u_1)SI, \quad f_I = \beta(1 - u_1)SI - (\gamma + u_2)I.$$
 (14)

Substituting  $f_S$  and  $f_I$  into the HJB equation:

$$-\frac{\partial V}{\partial t} = \min_{u_1, u_2} \left[ AI + Bu_1^2 + Cu_2^2 + V_S(-\beta(1 - u_1)SI) + V_I(\beta(1 - u_1)SI - (\gamma + u_2)I) \right]. \tag{15}$$

To minimize the equation, we differentiate for  $u_1$  and  $u_2$ : For  $u_1$ :

$$\frac{\partial}{\partial u_1} \left( B u_1^2 + V_S(-\beta(1 - u_1)SI) + V_I(\beta(1 - u_1)SI) \right) = 0.$$
 (16)

Expanding:

$$2Bu_1 + \beta SI(V_S - V_I) = 0. (17)$$

Solving for  $u_1^*$ :

$$u_1^* = \frac{\beta SI(V_S - V_I)}{2B}. (18)$$

Since  $u_1 \in [0, u_{1,\max}]$ , we impose constraints:

$$u_1^*(t, S, I) = \min \left\{ u_{1,\text{max}}, \max \left\{ 0, \frac{\beta SI(V_S - V_I)}{2B} \right\} \right\}.$$
 (19)

The same method is used to calculate  $u_2^*$ , taking into account its influence on H and solving the corresponding equation. Since  $u_1^*$  and  $u_2^*$  were determined by minimizing the equation, they provide the optimal solution to the control problem.  $\square$ 

#### 3 Results

#### 3.1 Simulation setup

The numerical simulations are based on the discretized version of the HJB equation, which is solved using discrete differences. The computational domain is defined over the state space (S, I), representing the fraction of susceptible and infected nodes in the IoT network. The model parameters used in the simulations are inspired by the parameters in [14,15] with slight modifications to fit the specific objectives of this study. The chosen parameters are  $\beta = 0.5$ ,  $\gamma = 0.1$ , A = 1.0, B = 0.01, and C = 0.01 and  $u_1 \in [0,1]$ ,  $u_2 \in [0,1]$ . The computational domain is discretized using  $N_s = 50$  and  $N_i = 50$  grid points for the susceptible and infected state variables. The time horizon is set to T = 1.0 with  $N_t = 50$  time steps. The backward Euler scheme ensures stability in the numerical integration.

#### 3.2 Simulation results

Figure 1 shows the value function V(S,I), which represents the optimal accumulated cost from any initial state. Higher values of V occur in states with a greater proportion of infected nodes, indicating that large-scale infections require more costly interventions. In contrast, states with fewer infected nodes exhibit lower values of V, suggesting that less intervention is required, leading to a lower overall cost.

Figure 2 (left) illustrates the optimal strategy for reducing malware transmission. The results indicate that the control  $u_1^*$  is most intense when the number

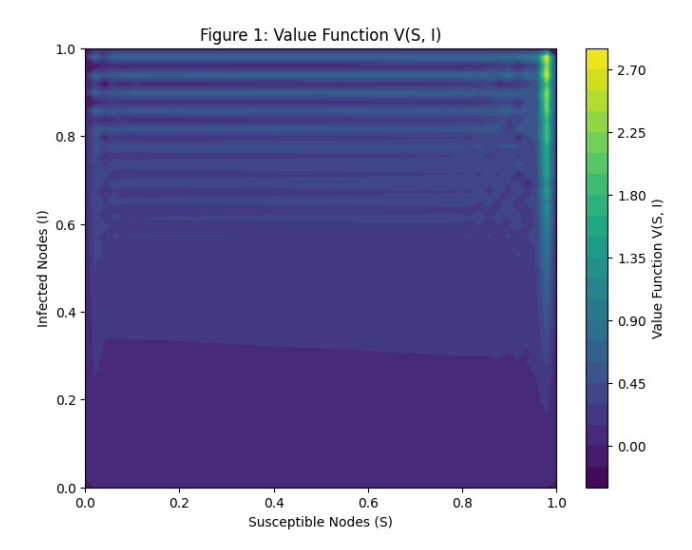


Fig. 1: Value function V(S, I). The function represents the optimal accumulated cost from any initial state. Higher values indicate states with high infection levels requiring costly interventions.

of susceptible and infected nodes is high. This suggests that applying aggressive preventive measures, such as firewalls or network segmentation, is the best strategy in these cases to slow down malware propagation. When the infection is already widespread but the number of susceptible nodes is low, the control  $u_1^*$  decreases, indicating that focusing on malware removal rather than prevention is more efficient in such conditions. Figure 2 (right) presents the optimal policy for malware removal. The results show that the control  $u_2^*$  is highest when the proportion of infected nodes is large. This suggests that, in these cases, prioritizing malware elimination through security patches or system restoration is the best strategy. In states with moderate or low infection levels, the control  $u_2^*$  is less intense, indicating that removal efforts are not as crucial when malware propagation is already contained.

#### 4 Conclusion

This study presents an optimal control framework for mitigating malware propagation in IoT networks using an HJB-based approach. By integrating two control strategies - reducing malware transmission and accelerating its removal - the model dynamically adapts interventions based on network conditions. The results indicate that high infection scenarios require aggressive prevention measures, while widespread infections require targeted remediation efforts. Compared to conventional cybersecurity strategies, this approach optimises resource allocation and reduces intervention costs. The proposed methodology increases the

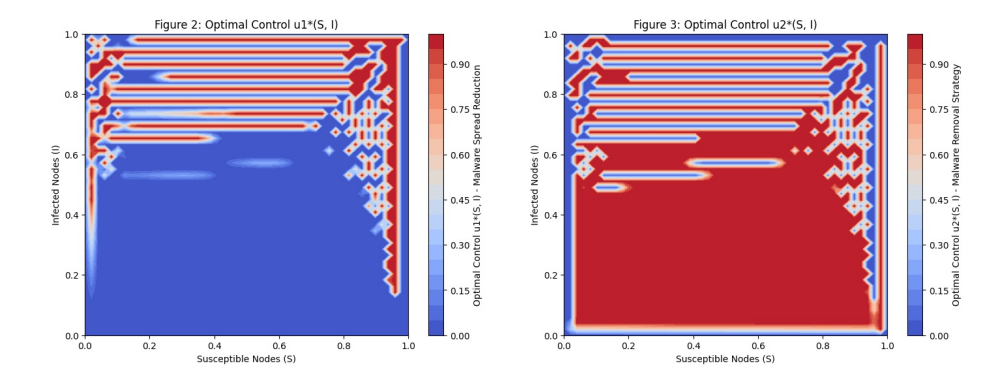


Fig. 2: Optimal control policies for malware propagation mitigation. (a)  $u_1^*(S, I)$  - Reduction of malware spread. (b)  $u_2^*(S, I)$  - Malware removal strategy.

efficiency of malware containment, providing a scalable and adaptable solution for IoT security. Future work can extend this model to incorporate stochastic dynamics and network topology variations to improve real-world applicability. This work is a proof of concept based on simulations of a classical SIR model; it does not use real-world IoT data. Future work will involve validating the proposed approach using real datasets and larger-scale simulations, in order to assess its practical applicability better.

#### Acknowledgments

This publication is part of the AI4SECIoT project ("Artificial Intelligence for Securing IoT Devices"), funded by the National Cybersecurity Institute (INCIBE), derived from a collaboration agreement signed between the National Institute of Cybersecurity (INCIBE) and the University of Burgos. This initiative is carried out within the framework of the Recovery, Transformation and Resilience Plan funds, financed by the European Union (Next Generation), the project of the Government of Spain that outlines the roadmap for the modernization of the Spanish economy, the recovery of economic growth and job creation, for solid, inclusive and resilient economic reconstruction after the COVID19 crisis, and to respond to the challenges of the next decade.

#### References

 Al-Hawawreh, M., Alazab, M., Ferrag, M. A., & Hossain, M. S. (2024). Securing the Industrial Internet of Things against ransomware attacks: A comprehensive analysis of the emerging threat landscape and detection mechanisms. Journal of Network and Computer Applications, 223, 103809.

- Casado-Vara, R., Severt, M., Díaz-Longueira, A., Rey, Á. M. D., & Calvo-Rolle, J. L. (2024). Dynamic Malware Mitigation Strategies for IoT Networks: A Mathematical Epidemiology Approach. Mathematics, 12(2), 250.
- 3. Malik, M. S. (2024). IoT Malware: A Comprehensive Survey of Threats, Vulnerabilities, and Mitigation Strategies. International Journal for Electronic Crime Investigation, 8(1), 57-66.
- 4. Brindha Devi, V., Ranjan, N. M., & Sharma, H. (2024). IoT attack detection and mitigation with optimized deep learning techniques. Cybernetics and Systems, 55(7), 1702-1728.
- Pavica, C., Swanson, G., Whitaker, R., & Johansson, S. (2024). A feedbackcontrolled optimization approach to minimize ransomware propagation in internet of things networks.
- Weston, J., Tolić, D., & Palunko, I. (2024). Application of Hamilton-Jacobi-Bellman Equation/Pontryagin's Principle for Constrained Optimal Control. Journal of optimization theory and applications, 200(2), 437-462.
- Salehnia, T., Seyfollahi, A., Raziani, S., Noori, A., Ghaffari, A., Alsoud, A. R., & Abualigah, L. (2024). An optimal task scheduling method in IoT-Fog-Cloud network using multi-objective moth-flame algorithm. Multimedia Tools and Applications, 83(12), 34351-34372.
- 8. Fleming, Wendell H., and Raymond W. Rishel. Deterministic and stochastic optimal control. Vol. 1. Springer Science & Business Media, 2012.
- 9. Crandall, M. G., & Lions, P. L. (1983). Viscosity solutions of Hamilton-Jacobi equations. Transactions of the American mathematical society, 277(1), 1-42.
- 10. Gelashvili, K. (2011). The existence of optimal control on the basis of Weierstrass's theorem. Journal of Mathematical Sciences, 177, 373-382.
- 11. Sniedovich, M. (1986). A new look at Bellman's principle of optimality. Journal of optimization theory and applications, 49, 161-176.
- Hu, S., Qiu, W., & Chen, H. (2020). A backward Euler difference scheme for the integro-differential equations with the multi-term kernels. International Journal of Computer Mathematics, 97(6), 1254-1267.
- Jannelli, A. (2024). A finite difference method on quasi-uniform grids for the fractional boundary-layer Blasius flow. Mathematics and Computers in Simulation, 215, 382-398.
- Chang, L., Gong, W., Jin, Z., & Sun, G. Q. (2022). Sparse optimal control of pattern formations for an SIR reaction-diffusion epidemic model. SIAM Journal on Applied Mathematics, 82(5), 1764-1790.
- Gatto, N. M., & Schellhorn, H. (2021). Optimal control of the SIR model in the presence of transmission and treatment uncertainty. Mathematical biosciences, 333, 108539.
- 16. Fabbri, G. (2008). A viscosity solution approach to the infinite-dimensional HJB equation related to a boundary control problem in a transport equation. SIAM journal on control and optimization, 47(2), 1022-1052.

### Cybersecurity Taxonomies: Comparative Analysis of Leading IoT Datasets for AI-Driven Security

Virginia Martinez-Fuentes<sup>®</sup>, Ángel Arroyo<sup>®</sup>, Diego Granados-López<sup>®</sup>, and Álvaro Herrero<sup>®</sup>

Grupo de Inteligencia Computacional Aplicada (GICAP), Departamento de Digitalización, Escuela Politécnica Superior, Universidad de Burgos, Avda. Cantabria s/n 09006, Burgos (Spain), {vmfuentes, aarroyop, dgranados, ahcosio}@ubu.es

Abstract. This paper outlines emerging security strategies and frameworks, focusing on taxonomies designed to categorize aspects of cybersecurity, particularly IoT security incidents, including threats and attacks. A comparative analysis of the TON\_IoT, Edge-IIoTset, and CICIoT2023 datasets is presented, examining their classifications of IoT threats and attacks. Additionally, the ENISA Taxonomy adopted by INCIBE-CERT CSIRT is reviewed and compared with the taxonomies of NIST CSF 2.0, MITRE ATT&CK, and OWASP, which incorporates STRIDE. Next, the taxonomies of the TON\_IoT, Edge-IIoTset, and CICIoT2023 datasets are mapped to the ENISA and INCIBE Taxonomy, correlating the categories of cyber threats and attacks identified in each dataset with these classification systems. Aiming to enhance AI-driven solutions for IoT cybersecurity, this study underscores both the similarities and differences in the number and names of categories of threats and attacks, and in the labels assigned to these incidents across the analyzed taxonomies and datasets.

Keywords: cybersecurity, IoT, taxonomy, machine learning

#### 1 Introduction

The Internet of Things (IoT) [11] refers to a network of cyber-physical devices [9] that communicate and exchange data with users over the Internet, and are fundamental to Cyber-Physical Systems (CPS) [9]. These interconnected systems enable automation and support applications across sectors including manufacturing, transportation, healthcare, agriculture, education, commerce, military, and consumer applications such as smart homes [20]. Therefore, given its pervasive and heterogeneous nature, the IoT, particularly in smart homes, exemplifies the need for enhanced security due to its vulnerability to cybercriminals [12].

As the number of IoT devices continues to grow, it is expected to surpass 32 billion by 2030 [24]. In response, advancements in data-driven approaches to

Intrusion Detection Systems (IDS) [9] have paved the way for Artificial Intelligence (AI) to bolster IoT security. As a result, leveraging Machine Learning (ML) in AI-driven cybersecurity has become pivotal to IoT, aiming to detect and mitigate cyber incidents with a focus on threats and attacks [22].

Acknowledging that the choice of dataset influences the effectiveness of AI techniques for Intrusion Detection Systems (IDS), there is a need for a universal benchmark feature set [21]. Consequently, this paper examines the classification system of IoT security incidents across three leading datasets:  $TON\_IoT$  [3],  $Edge\_IIoTset$  [7], and CICIoT2023 [16].  $TON\_IoT$  organizes these incidents into eight primary categories,  $Edge\_IIoTset$  separates them into five, while CI-CIoT2023 identifies seven, with each dataset using its own classification system. Likewise, efforts are underway toward the development of a unified taxonomy of cyber incidents, which would provide a reference baseline [5]. Devising such a standardized classification system would facilitate cybersecurity incident management [10], ultimately streamlining the process of classifying IoT threats and attacks when reported to Computer Security Incident Response Teams (CSIRTs) [15].

This paper presents an overview of established cybersecurity taxonomies applicable to the IoT, including those provided by ENISA [6], INCIBE-CERT CSIRT [10], NIST's Cybersecurity Framework (CSF) 2.0 [17], Enterprise Matrix by MITRE ATT&CK [13], and OWASP's STRIDE-based approach [18]. It compares these taxonomies and maps the author-defined classification systems of TON\_IoT, Edge-IIoTset, and CICIoT2023 to the ENISA Taxonomy (to which INCIBE has adhered).

Subsequent to the introduction, this document is structured as follows: 2. Selected Datasets, 3. Taxonomy Analysis, 4. Mapping IoT Security Datasets Attack Classifications to the ENISA and INCIBE Taxonomy, and 5. Conclusion.

#### 2 Dataset Selection

Given the range of cybersecurity datasets available for IoT systems, selecting those most suitable for this study required a structured and reproducible methodology. Relevant literature was retrieved from the Web of Science database using a query that incorporated the following topic search terms: ('IoT' OR 'Internet of Things' OR 'Cyber-Physical Systems') AND ('Taxonomy of Vulnerabilities' OR 'Taxonomy of Attacks' OR 'Dataset' OR 'Datasets') AND ('Artificial Intelligence' OR 'Machine Learning' OR 'Deep Learning' OR 'Supervised Learning' OR 'Unsupervised Learning' OR 'Reinforcement Learning') AND ('Security' OR 'Cybersecurity' OR 'Cyber Security' OR 'Cyber Threats' OR 'Attack Detection' OR 'Security Challenges' OR 'Security Solutions').

This initial query returned 5,394 records during the literature review phase (mid-2025) of this study. To narrow the scope to the most relevant contributions, the results were subsequently refined by applying the following filters: document type (Article), publication years (2020–2025), citation status (Highly Cited Papers), and language (English). As a result of these refinements, the dataset was

reduced to 92 papers, from which the only three that published and made publicly available IoT security datasets were selected:  $TON\_IoT$  [3], Edge-IIoTset [7], and CICIoT2023 [16].

These datasets have demonstrated significant academic impact, with a combined total of 984 citations as indexed by Web of Science at the time this study was conducted. Individually,  $TON\_IoT$  has received 373 citations, Edge-IIoTset 369 citations, and CICIoT2023 250 citations as of mid-2025. Their consistent citation growth over recent years reflects widespread adoption and sustained relevance within the field of cybersecurity for IoT systems, a trend further reinforced by the credibility of the institutions behind their development.  $TON\_IoT$  was created by the Intelligent Security Group (ISG) at the University of New South Wales (UNSW), Australia. Edge-IIoTset was developed collaboratively by researchers from Guelma University and Annaba University (Algeria), De Montfort University (United Kingdom), and Edith Cowan University (Australia). CICIoT2023 was curated by the Canadian Institute for Cybersecurity at the University of New Brunswick (UNB), Canada.

For this study, one comma-separated values (CSV) file was selected from each dataset for analysis; the following summarizes the cybersecurity taxonomies defined in the original papers and reflected in the selected files.

- TON\_IoT [3]: The paper classifies cyber incidents into eight groups: backdoor, denial of service (DoS) and distributed DoS (DDoS), injection, man-in-the-middle (MITM), password cracking, ransomware, scanning, and cross-site scripting (XSS). Correspondingly, its Processed\_Network\_dataset\_1.csv [3] contains 46 columns, 44 of which are features, along with two additional columns: label for binary classification (0 for non-attack, and 1 for attack) and type for multiclass classification (with 10 possible values corresponding to different attack types, including one for non-attack) [14].
- Edge-HoTset [7]: The paper considers five categories: DoS/DDoS, information gathering, injection, malware, and MITM. Additionally, its ML-EdgeHoT-dataset.csv [7] comprises 63 columns, 61 of which are features, with two additional columns: Attack\_Label for binary classification (0 for non-attack, and 1 for attack) and Attack\_Type for multiclass classification (15 types, including one for non-attack) [1].
- CICIoT2023 [16]: The paper features a taxonomy of seven categories: brute force, DDoS, DoS, Mirai, reconnaissance (Recon), spoofing, and web-based threats and attacks. Its Merged01.csv [16] contains 40 columns, 39 of which are features, with one additional column (Label) for multiclass classification (covering 34 types of attacks, including one category for non-attack) [23].

Considering these combined criteria, the  $TON\_IoT$ , Edge-IIoTset, and CI-CIoT2023 datasets are particularly suitable for this study, which compares IoT cybersecurity taxonomies to enhance the development of AI-driven solutions for IoT security.

#### 3 Taxonomy Analysis

## 3.1 Taxonomies for Cyber Incident Classification: The ENISA and INCIBE Approach

The European Union Agency for Cybersecurity (ENISA) has been actively developing a benchmark framework for classifying cyber incidents. Building on the eCSIRT.net version mkVI Incident Taxonomy [4], ENISA released the Reference Incident Classification Taxonomy report [5] and established the Reference Security Incident Taxonomy Working Group (RSIT WG) [6]. The RSIT WG then published a public GitHub repository containing the ENISA Reference Incident Classification Taxonomy Task Force [6]. In the working\_copy/humanv1.md file within this repository, the taxonomy is presented in tabular format, categorizing incidents into 11 distinct types: 10 core categories and one additional category for testing purposes. Each category is further broken down into real-world examples and detailed descriptions [6].

The National Cybersecurity Institute (INCIBE) CSIRT of Spain, through its Computer Emergency Response Team (CERT), has adopted ENISA's classification system as outlined in its *National Cyber Incident Reporting and Management Guide* [10]. For the purposes of this paper, the taxonomy used by both ENISA and INCIBE-CERT CSIRT will henceforth be referred to as the 'ENISA and INCIBE Taxonomy'.

## 3.2 Taxonomies for Cyber Risk Management and Governance: The NIST CSF 2.0 Framework

The Cybersecurity Framework (CSF) 2.0 white paper [17], developed by the United States National Institute of Standards and Technology (NIST), provides recommendations for cybersecurity risk management, supported by a taxonomy focused on security objectives [17]. Although originally designed for U.S.-based organizations, it is also adaptable for use by entities worldwide [19]. This framework is organized into three core components: the CSF Core, CSF Organizational Profiles, and CSF Tiers [17]. The CSF Core serves as the foundation of the NIST CSF 2.0 framework, outlining a hierarchical structure for cybersecurity governance through six core functions: Govern, Identify, Protect, Detect, Respond, and Recover, which can also be applied to the IoT domain [17].

## 3.3 Taxonomies for Cyber Threat Modeling: The MITRE ATT&CK and OWASP STRIDE Methodologies

Two widely adopted methodologies for cyber threat modeling, extendable to the IoT, are MITRE ATT&CK [13] and the Open Web Application Security Project (OWASP)-STRIDE approach [18].

- MITRE ATT&CK [13]: Classifies adversary tactics, techniques, and procedures (TTPs) based on real-world incidents. The MITRE ATT&CK Enterprise Matrix [13] consists of 14 adversary tactics, each associated with a range of techniques, totaling 236, as well as additional sub-techniques.

OWASP-STRIDE [18]: Focuses on 6 threat categories: Spoofing, Tampering, Repudiation, Information Disclosure, DoS, and Elevation of Privilege, along with 22 mitigation techniques.

The MITRE ATT&CK knowledge base covers TTPs across various environments, including the IoT [2], and, in addition to its STRIDE-based methodology, OWASP has compiled a unified list of the top IoT security considerations: the OWASP IoT Top 10 [8].

## 3.4 Brief Comparative Analysis of Cybersecurity Taxonomies: ENISA and INCIBE, NIST CSF 2.0, MITRE ATT&CK, and OWASP-STRIDE

While NIST CSF 2.0 offers a high-level taxonomy focused on cybersecurity outcomes and practices aimed at governance and risk management [17], the ENISA and INCIBE Taxonomy primarily classifies cyber incidents (specifically threats and attacks) to facilitate incident reporting, management, and response [6]. In contrast, both MITRE ATT&CK and OWASP-STRIDE methodologies are designed for threat modeling [13,18], each employing distinct approaches. MITRE ATT&CK provides detailed insights into adversaries' tactics, techniques, and procedures during attacks [13], whereas OWASP-STRIDE offers a framework for evaluating potential threats [18].

These taxonomies are extendable to the IoT, with each focusing on different aspects of cybersecurity: the ENISA and INCIBE Taxonomy classifies incidents, NIST CSF 2.0 addresses risks, and MITRE ATT&CK and OWASP-STRIDE provide methodologies for threat modeling. Table 1 presents a comparative analysis of these IoT cybersecurity taxonomies, highlighting their scope, categories, and subcategories.

| Taxonomy                     | Focus                      | Categories           | Subcategories                                     |
|------------------------------|----------------------------|----------------------|---|
| ENISA [6] and<br>INCIBE [10] | Incident<br>Classification | 11 Cyber Incidents   | 38 Examples and its<br>description                |
| NIST CSF 2.0 [17]            | Risk Governance            | 6 Core Functions     | 22 Core Categories with<br>multiple subcategories |
| MITRE ATT&CK [13]            | Threat Modeling            | 14 Adversary Tactics | 236 Techniques and various<br>sub-techniques      |
| OWASP STRIDE<br>[18]         | Threat Modeling            | 6 Threat Types       | 22 Mitigation Techniques                          |

Table 1. Comparison of Cybersecurity Taxonomies

## 4 Mapping IoT Security Datasets Attack Classifications to the ENISA and INCIBE Taxonomy

The ENISA and INCIBE Taxonomy consists of 11 high-level incident categories, including one reserved for testing: Abusive Content, Malicious Code, Informa-

tion Gathering, Intrusion Attempts, Intrusions, Availability, Information Content Security, Fraud, Vulnerabilities, Other, and Test.

To explore how current IoT security datasets align with this taxonomy, the attack classifications from  $TON\_IoT$ ,  $Edge\_IIoTset$ , and CICIoT2023 are analyzed. Each dataset defines its own set of attack labels and conceptual categories, as introduced by the authors in their respective publications. These labels and groupings were mapped to the ENISA and INCIBE taxonomy based on the conceptual definitions of the attacks, as well as the descriptions and examples provided by ENISA and INCIBE. This mapping serves to visualize similarities and differences in terminology, granularity, and thematic structure across datasets and taxonomy frameworks.

Tables 2, 3, and 4 present the individual mappings for each dataset, providing a label-to-taxonomy alignment while preserving the internal classification logic proposed by the dataset authors.

**Table 2.** TON\_IOT Dataset Labels (10) and Categories (10) Mapped to ENISA and INCIBE Categories

| TON_IoT    | TON_IoT           | ENISA and INCIBE             |
|------------|-------------------|------------------------------|
| Labels     | Categories        | Taxonomy                     |
| Backdoor   | Backdoor          | Intrusion Attempts           |
| DDoS       | DDoS              | Availability                 |
| DoS        | DoS               | Availability                 |
| Injection  | Injection         | Intrusions                   |
| MITM       | MITM              | Information Gathering        |
| Normal     | Normal            | Test                         |
| Password   | Password Cracking | Intrusion Attempts           |
| Ransomware | Ransomware        | Information Content Security |
| Scanning   | Scanning          | Information Gathering        |
| XSS        | XSS               | Intrusion Attempts           |

**Table 3.** Edge-IIoTset Dataset Labels (15) and Categories (6) Mapped to ENISA and INCIBE Categories

| Edge-IIoTset          | Edge-IIoTset               | ENISA and INCIBE             |  |
|-----------------------|----------------------------|------------------------------|--|
| Labels                | Categories                 | Taxonomy                     |  |
| Backdoor              | Malware                    | Intrusion Attempts           |  |
| DDoS_HTTP             | DoS/DDoS                   | Availability                 |  |
| DDoS_ICMP             | DoS/DDoS                   | Availability                 |  |
| DDoS_TCP              | DoS/DDoS                   | Availability                 |  |
| DDoS_UDP              | DoS/DDoS                   | Availability                 |  |
| Fingerprinting        | Information Gathering      | Information Gathering        |  |
| MITM                  | Man-in-the-middle: DNS and | Information Gathering        |  |
| 1411 1 141            | ARP spoofing               | information dathering        |  |
| Normal                | Normal                     | Test                         |  |
| Password              | Malware                    | Intrusion Attempts           |  |
| Port_Scanning         | Information Gathering      | Information Gathering        |  |
| Ransomware            | Malware                    | Information Content Security |  |
| SQL_injection         | Injection                  | Intrusions                   |  |
| Uploading             | Injection                  | Malicious Code               |  |
| Vulnerability_scanner | Information Gathering      | Information Gathering        |  |
| XSS                   | Injection                  | Intrusion Attempts           |  |

**Table 4.** CICIoT2023 Dataset Labels (34) and Categories (8) Mapped to ENISA and INCIBE Categories

| CICIoT2023              | CICIoT2023  | ENISA and INCIBE      |
|-------------------------|-------------|-----------------------|
| Labels                  | Categories  | Taxonomy              |
| BACKDOOR_MALWARE        | Web         | Intrusion Attempts    |
| BENIGN                  | Benign      | Test                  |
| BROWSERHIJACKING        | Web         | Malicious Code        |
| COMMANDINJECTION        | Web         | Intrusions            |
| DDOS-ACK_FRAGMENTATION  | DDoS        | Availability          |
| DDOS-HTTP_FLOOD         | DDoS        | Availability          |
| DDOS-ICMP_FLOOD         | DDoS        | Availability          |
| DDOS-ICMP_FRAGMENTATION | DDoS        | Availability          |
| DDOS-PSHACK_FLOOD       | DDoS        | Availability          |
| DDOS-RSTFINFLOOD        | DDoS        | Availability          |
| DDOS-SLOWLORIS          | DDoS        | Availability          |
| DDOS-SYN_FLOOD          | DDoS        | Availability          |
| DDOS-SYNONYMOUSIP_FLOOD | DDoS        | Availability          |
| DDOS-TCP_FLOOD          | DDoS        | Availability          |
| DDOS-UDP_FLOOD          | DDoS        | Availability          |
| DDOS-UDP_FRAGMENTATION  | DDoS        | Availability          |
| DICTIONARYBRUTEFORCE    | Brute force | Intrusion Attempts    |
| DNS_SPOOFING            | Web         | Information Gathering |
| DOS-HTTP_FLOOD          | DoS         | Availability          |
| DOS-SYN_FLOOD           | DoS         | Availability          |
| DOS-TCP_FLOOD           | DoS         | Availability          |
| DOS-UDP_FLOOD           | DoS         | Availability          |
| MIRAI-GREETH_FLOOD      | DDoS        | Availability          |
| MIRAI-GREIP_FLOOD       | DDoS        | Availability          |
| MIRAI-UDPPLAIN          | DDoS        | Availability          |
| MITM-ARPSPOOFING        | Recon       | Information Gathering |
| RECON-HOSTDISCOVERY     | Recon       | Information Gathering |
| RECON-OSSCAN            | Recon       | Information Gathering |
| RECON-PINGSWEEP         | Recon       | Information Gathering |
| RECON-PORTSCAN          | Recon       | Information Gathering |
| SQLINJECTION            | Web         | Intrusions            |
| UPLOADING_ATTACK        | Web         | Malicious Code        |
| VULNERABILITYSCAN       | Recon       | Information Gathering |
| XSS                     | Web         | Intrusion Attempts    |

To complement these mappings and provide a broader comparative perspective, Table 5 presents a taxonomy-centric view. It organizes attack labels from the three datasets according to the 11 ENISA and INCIBE categories, highlighting overlaps and distinctions, and helping illustrate how cybersecurity taxonomies differ across datasets and in relation to the ENISA and INCIBE framework.

#### 5 Conclusion

This paper analyzed IoT security incident classification systems across three major datasets:  $TON\_IoT$ ,  $Edge\_IIoTset$ , and CICIoT2023. The comparative analysis highlighted the similarities and differences in the categorization schemes used within these datasets, particularly in the number, naming, and level of detail (granularity) of categories for IoT cyber threats and attacks.

Additionally, the study outlined established cybersecurity taxonomies, such as those from ENISA, INCIBE-CERT CSIRT, NIST's  $Cybersecurity\ Framework$ 

**Table 5.** Cross-Dataset Comparison of Cyber Attack Labels Mapped to ENISA and INCIBE Incident Taxonomy

| TON_IoT                     | Edge-IIoTset   | CICIoT2023   | ENISA and INCIBE                |
|-----------------------------|--|--|---------------------------------|
| Labels                      | Labels   | Labels   | Taxonomy                        |
| _                           | _  | _  | Abusive Content                 |
| _                           | Uploading  | BROWSERHIJACKING<br>UPLOADING_ATTACK   | Malicious Code                  |
| MITM<br>Scanning            | Port_Scanning<br>Fingerprinting<br>Vulnerability_scanner<br>MITM | MITM-ARPSPOOFING RECON-HOSTDISCOVERY RECON-OSSCAN RECON-PINGSWEEP RECON-PORTSCAN DNS_SPOOFING VULNERABILITYSCAN  | Information Gathering           |
| Backdoor<br>Password<br>XSS | Backdoor<br>Password<br>XSS                                      | DICTIONARYBRUTEFORCE<br>BACKDOOR_MALWARE<br>XSS  | Intrusion Attempts              |
| Injection                   | SQL_injection  | SQLINJECTION<br>COMMANDINJECTION   | Intrusions                      |
| DoS<br>DDoS                 | DDoS.HTTP<br>DDoS.ICMP<br>DDoS.TCP<br>DDoS.UDP                   | DDOS-ACK_FRAGMENTATION DDOS-HTTP_FLOOD DDOS-ICMP_FLOOD DDOS-ICMP_FRAGMENTATION DDOS-PSHACK_FLOOD DDOS-STOWLORIS DDOS-SYN_FLOOD DDOS-SYNONYMOUSIP_FLOOD DDOS-TCP_FLOOD DDOS-UDP_FRAGMENTATION DOS-HTTP_FLOOD DOS-TCP_FLOOD DOS-TCP_FLOOD DOS-TCP_FLOOD DOS-TCP_FLOOD DOS-TCP_FLOOD DOS-TCP_FLOOD DOS-TCP_FLOOD DOS-TCP_FLOOD DOS-UDP_FLOOD MIRAI-GREETH_FLOOD MIRAI-GREIP_FLOOD | Availability                    |
| Ransomware                  | Ransomware   | _  | Information Content<br>Security |
| _                           | _  | _  | Fraud                           |
| _                           | _  | _  | Vulnerabilities                 |
| _                           | _  | _  | Other                           |
| Normal                      | Normal   | BENIGN   | Test                            |

(CSF) 2.0, MITRE ATT&CK's Enterprise Matrix, and OWASP's STRIDE-based approach, all of which provide differing yet complementary perspectives on IoT security.

Furthermore, the mapping of the TON\_IoT, Edge-IIoTset, and CICIoT2023 datasets to the ENISA Taxonomy (adopted by INCIBE) revealed areas of both alignment and divergence. While certain categories of cyber incidents were consistent across datasets, differences were observed in the naming conventions, as well as in the number and level of detail of labels used within each dataset and when compared to the ENISA and INCIBE Taxonomy.

Overall, this paper aims to enhance AI-driven solutions for IoT cybersecurity by underscoring both the similarities and differences in the number and names of categories of threats and attacks, along with the labels assigned to these cyber incidents across the analyzed taxonomies and datasets.

Future work may follow current research efforts aimed at developing a standardized feature set for IoT cybersecurity datasets. This effort may be complemented by harmonizing attack labels across datasets, which could further improve comparability and support broader generalization in AI-driven cybersecurity for the IoT.

#### Acknowledgments

This publication is part of the AI4SECIoT project ('Artificial Intelligence for Securing IoT Devices'), funded by the National Cybersecurity Institute (INCIBE), derived from a collaboration agreement signed between the National Institute of Cybersecurity (INCIBE) and the University of Burgos. This initiative is carried out within the framework of the Recovery, Transformation and Resilience Plan funds, financed by the European Union (Next Generation), the project of the Government of Spain that outlines the roadmap for the modernization of the Spanish economy, the recovery of economic growth and job creation, for solid, inclusive and resilient economic reconstruction after the COVID19 crisis, and to respond to the challenges of the next decade.

#### References

- Al Nuaimi, T., Al Zaabi, S., Alyilieli, M., AlMaskari, M., Alblooshi, S., Alhabsi, F., Yusof, M.F.B., Al Badawi, A.: A comparative evaluation of intrusion detection systems on the edge-iiot-2022 dataset. Intelligent Systems with Applications 20, 200.298 (2023). DOI 10.1016/j.iswa.2023.200298
- 2. Al-Sada, B., Sadighian, A., Oligeri, G.: Analysis and characterization of cyber threats leveraging the mitre att&ck database. IEEE Access **12**, 1217–1234 (2024). DOI 10.1109/ACCESS.2023.3344680
- 3. Alsaedi, A., Moustafa, N., Tari, Z., Mahmood, A., Anwar, A.: Ton\_iot telemetry dataset: A new generation dataset of iot and iiot for data-driven intrusion detection systems. IEEE Access 8, 165,130–165,150 (2020). DOI 10.1109/ACCESS.2020. 3022862
- 4. Arvidsson, J., Stikvoort, D.: ecsirt.net mkvi incident classification / incident taxonomy. https://static.www.switch.ch/sites/default/files/2023-11/Incident-Classification-Taxonomy.pdf (2015)
- 5. ENISA: Reference incident classification taxonomy, task force status and way forward. https://www.enisa.europa.eu/publications/reference-incident-classification-taxonomy (2018)
- ENISA: Reference security incident classification taxonomy. https://github.com/enisaeu/Reference-Security-Incident-Taxonomy-Task-Force (2018)
- Ferrag, M., Friha, O., Hamouda, D., Maglaras, L., Janicke, H.: Edge-iiotset: A new comprehensive realistic cyber security dataset of iot and iiot applications for centralized and federated learning. IEEE Access 10, 40,281–40,306 (2022). DOI 10.1109/ACCESS.2022.3165809
- 8. Ferrara, P., Mandal, A., Cortesi, A., et al.: Static analysis for discovering iot vulnerabilities. International Journal of Software Tools for Technology Transfer 23, 71–88 (2021). DOI 10.1007/s10009-020-00592-x

- IEEE: Ieee standard for an architectural framework for the internet of things (iot) (ieee std 2413-2019) (2020). DOI 10.1109/IEEESTD.2020.9032420
- 10. INCIBE: National cyber incident reporting and management guide. https://www.incibe.es/incibe-cert/guias-y-estudios/guias/guia-nacional-de-notificacion-y-gestion-de-ciberincidentes (2020)
- 11. ISO/IEC: Iso/iec 30141, internet of things (iot) reference architecture, edition 2.0. https://www.iso.org/standard/88800.html (2024)
- Iturbe Araya, J.I., Rifà-Pous, H.: Anomaly-based cyberattacks detection for smart homes: A systematic literature review. Internet of Things 22, 100,792 (2023). DOI doi.org/10.1016/j.iot.2023.100792
- 13. MITRE ATT&CK: Mitre att&ck taxonomy of adversary tactics and techniques. https://attack.mitre.org
- Moustafa, N.: A new distributed architecture for evaluating ai-based security systems at the edge: Network ton\_iot datasets. Sustainable Cities and Society 72, 102,994 (2021). DOI 10.1016/j.scs.2021.102994
- 15. National Institute of Standards and Technology (NIST): Computer security incident response team (csirt) nist glossary. https://csrc.nist.gov/glossary/term/computer\_security\_incident\_response\_team
- Neto, E., Dadkhah, S., Ferreira, R., Zohourian, A., Lu, R., Ghorbani, A.: Ciciot2023: A real-time dataset and benchmark for large-scale attacks in iot environment. Sensors 23(13), 5941 (2023). DOI 10.3390/s23135941
- 17. NIST: The nist cybersecurity framework (csf) 2.0. NIST Cybersecurity White Paper (CSWP) NIST CSWP 29 (2024). DOI 10.6028/NIST.CSWP.29
- 18. OWASP: Owasp with stride taxonomy of threats. https://owasp.org/www-community/Threat\_Modeling\_Process
- Parmar, M., Miles, A.: Cyber security frameworks (csfs): An assessment between the nist csf v2.0 and eu standards. In: 2024 Security for Space Systems (3S), pp. 1–7 (2024). DOI 10.23919/3S60530.2024.10592293
- Saba, T., Rehman, A., Sadad, T., Kolivand, H., Bahaj, S.: Anomaly-based intrusion detection system for iot networks through deep learning model. Computers and Electrical Engineering 99, 107,810 (2022). DOI 10.1016/j.compeleceng.2022. 107810
- Sarhan, M., Layeghy, S., Moustafa, N., Gallagher, M., Portmann, M.: Feature extraction for machine learning-based intrusion detection in iot networks. Digital Communications and Networks 10(1), 205–216 (2024). DOI 10.1016/j.dcan.2022. 08.012
- Sarker, I., Khan, A., Abushark, Y., et al.: Internet of things (iot) security intelligence: A comprehensive overview, machine learning solutions and research directions. Mobile Networks and Applications 28, 296–312 (2023). DOI 10.1007/s11036-022-01937-3
- Tseng, S.M., Wang, Y.Q., Wang, Y.C.: Multi-class intrusion detection based on transformer for iot networks using cic-iot-2023 dataset. Future Internet 16(8), 284 (2024). DOI 10.3390/fi16080284
- 24. Vailshery, L.: Number of internet of things (iot) connections worldwide from 2022 to 2023, with forecasts from 2024 to 2033 (in billions). https://www.statista.com/statistics/1183457/iot-connected-devices-worldwide (2024)

# Privacy-Enhancing Federated Learning-Based IDS for IoT Networks Using Post-Quantum Secure Channels and Verifiable Secret Sharing

Lamine Syne<sup>1</sup>, Candelaria Hernández-Goya<sup>2</sup>, and Pino Caballero-Gil<sup>2</sup>

<sup>1</sup> Fundación General Universidad de La Laguna, Santa Cruz de Tenerife, España lsyne@fg.ull.es

Abstract. Federated Learning (FL)-based Intrusion Detection Systems (IDS) are emerging as a promising approach for securing IoT networks and preserving data confidentiality. Moreover, FL introduces novel vulnerabilities. These include inference attacks by malicious aggregators, who can extract sensitive information from model updates, as well as malicious clients capable of submitting falsified updates to the aggregator server. Additionally, with the rapid development of quantum computers, existing privacy protection schemes mainly based on Secure Multi-Party Computation (SMPC) will no longer be able to guarantee the data. This paper presents a Secure Aggregation (SA) method that combines Post-Quantum-secure channels for client key exchange and Verifiable Secret Sharing (VSS), achieving resilience against malicious clients. Experiments conducted in an FL-based IDS for real-world IoT networks demonstrate the viability of our proposal.

**Keywords:** Federated Learning, IoT, Secure Aggregation, Post-quantum Security

#### 1 Introduction

The Internet of Things (IoT) has seen a substantial increase in adoption in recent years. It links a wide range of connected devices, including monitoring sensors, wearable health devices and smart home appliances. However, this proliferation of connected devices has led to a significant increase in security and privacy risks. Federated Learning (FL) based Intrusion Detection Systems (IDS) are essential tools for safeguarding IoT networks. They continuously monitor network traffic and system behavior to identify any sign of malicious activity or anomalies while preserving privacy [1]. Traditionally, IDS solutions are deployed in a centralized manner. In these systems, data collected from all connected devices is analyzed on a central server. While this centralized approach is effective in some respects, it presents critical issues. In particular, it raises privacy concerns about sensitive data transmitted from individual devices. FL [2] enables the training machine learning models directly on distributed IoT devices. This allows data to remain

<sup>&</sup>lt;sup>2</sup> Universidad de La Laguna, Santa Cruz de Tenerife, España mchgoya@ull.edu.es, pcaballe@ull.edu.es

local while minimizing the need to transfer raw information to a central server. By doing so, this method enhances data privacy and security. It leverages the collective intelligence of multiple devices without exposing sensitive information. Nonetheless, the adoption of FL also introduces a new set of challenges [3], one of which is securing the training process against adversarial threats. Existing privacy-preserving FL methods face the challenge of high communication and computational overhead. Furthermore, the rapid development of quantum computers means that these approaches, mostly based on SMPC, will no longer be able to guarantee data security for participants in the post-quantum era.

This work focuses on exploring the integration of FL techniques to strengthen IoT network security while improving the confidentiality of sensitive data, thereby paving the way for more resilient and privacy-aware IDS.

#### $\mathbf{2}$ Secure Multi-Party Computation (SMPC) and Secret Sharing

Secure Multi-Party Computation (SMPC) is a cryptographic mechanism that allows parties to jointly compute private inputs without revealing anything but the final result. It addresses the following problem, involving m parties or devices denoted as  $P_1, ..., P_m$ . Each device  $P_i$ , where i = 1, 2, ..., m, holds a secret input  $x_i$ , for i = 1, 2, ..., m, and all devices agree on some function f that takes m inputs. Their goal is to compute  $y = f(x_1, \dots, x_m)$  while making sure that the correct value of y is calculated [4] without releasing any information about  $x_i$ .

#### 2.1 Shamir's Secret Sharing

Shamir's Secret Sharing (SSS) [5] is a method for splitting a secret into shares where only a certain number of shares (threshold) are needed to recover the original secret. It's called a (t,n)-threshold-based scheme that securely distributes a secret S among n participants such that only t or more participants can reconstruct it. The secret is represented as the constant term of a random polynomial f(x) of degree t-1 over a finite field  $\mathbb{F}_q$ , where q is a prime number greater than S. The polynomial is defined as:

$$f(x) = a_0 + a_1 x + a_2 x^2 + \dots + a_{t-1} x^{t-1}$$
, with  $a_0 = S$ .

Each participant i receives a share  $(x_i, f(x_i))$ , where  $x_i \neq 0$ . To reconstruct the secret, any group of at least t participants can use Lagrange interpolation to compute:  $S = f(0) = \sum_{j=1}^{t} f(x_j) \prod_{\substack{1 \leq m \leq t \\ m \neq j}} \frac{x_m}{x_m - x_j}$ This method provides perfect secrecy: fewer than t shares reveal no informa-

tion about S.

#### Verifiable Secret Sharing 2.2

Verifiable Secret Sharing (VSS) [6] adds a verifiable feature to the secret sharing mechanism, allowing participants to check whether the retrieved information

corresponds to the original secret. A common VSS scheme builds upon Shamir's Secret Sharing and uses public commitments to the polynomial coefficients to ensure share consistency. The dealer selects a random polynomial:  $f(x) = a_0 + a_1x + a_2x^2 + \cdots + a_{t-1}x^{t-1}$ , where  $a_0 = S$ 

To enable verification, the dealer publishes commitments  $C_j = g^{a_j} \in \mathbb{G}$ , where g is a generator of a cyclic group  $\mathbb{G}$  of prime order q. Each participant i receives a share  $s_i = f(x_i)$ . Participants can verify their share by checking:  $g^{s_i} \stackrel{?}{=} \prod_{j=0}^{t-1} C_j^{x_i^j}$ 

If the equation holds, the participant is convinced that its share is consistent with the committed polynomial. This approach provides both secrecy and verifiability under standard cryptographic assumptions.

#### 3 Related Work

FL has gained major interest in recent years, with numerous applications and use cases, particularly in the field of IoT. In this context, some recent works have proposed its use to improve IDS. In [7] a self-learning system for detecting compromised devices in IoT networks based on FL is introduced. Its findings demonstrate an average detection rate of 95.6% for attacks in just 257 milliseconds, all without triggering any false alarms during evaluation in a real-world deployment. Despite its benefits, FL suffers from different vulnerabilities as described in [1]. To overcome these, Secure Aggregation (SA) is widely deployed in FL. SA is a protocol that ensures the aggregator can only learn the average of the updates of clients while keeping their updates private. The concept was first proposed by Bonawitz et al. [8]. Their protocol is based on a Secure Multi-Party Computation (SMPC) approach which refers to a mechanism that allows parties to jointly compute private inputs without revealing anything but the final result. SAFELearn [9] proposed a generic system to secure aggregation in FL. The framework can be instantiated with one (FHE) or multiple non-colluding servers (SMPC). A secure two-party computation instantiation of SAFELearn applied to a personalized version of [7] achieves convergence with a learning rate of 0.1 while keeping a good trade-off between security and efficiency. The work [10] presents VerifyNet, the first privacy-preserving and verifiable federated learning framework. A double-masking protocol is used to guarantee the confidentiality of users' local gradients during the federated learning. Then, the cloud server is required to provide a proof of the correctness of its aggregated results to each user. Most of the SA protocols use cryptographic primitives such as pseudo-random generators, key agreement protocols, authenticated encryption, or Shamir's secret sharing to guarantee the security of communications between the server and clients, as well as among the clients themselves. However, these primitives are mainly based on traditional cryptography, such as the Diffie-Hellman key agreement protocol and general-purpose ciphers. As a result, these approaches lack resistance to quantum attacks.

Numerous studies have looked into the integration of post-quantum cryptography (PQC) into federated learning to mitigate quantum computing threats. The

work [11] proposes a lattice-based FL protocol where compressed and encrypted model updates are used to reduce communication overhead; however, it does not support dropout recovery or verifiable aggregation. In [12], PQC-based aggregation protocols relying on peer-to-peer share exchange or outdated primitives such as NewHope are proposed, neither supports dropout resilience and both incur high communication overhead. Saidi et al.[13] propose to combine Ciphertext-Policy Attribute-Based Encryption (CP-ABE) to secure models and the Cheon-Kim-Kim-Song (CKKS) homomorphic encryption algorithm to protect model parameters but with substantial latency unsuitable for edge devices. By comparison, our approach leverages the NIST-recommended ML-KEM, Shamir's Secret Sharing, and Verifiable Secret Sharing to achieve efficient, verifiable, and dropout-resilient aggregation with low overhead, making it suitable for deployment in IoT and other resource-constrained environments.

#### 4 Adversary Model

In this work, the adversary is considered a semi-honest aggregator, that is, it follows the protocol honestly but tries to infer sensitive information about the local device data from their model updates during the learning process. In the standard FL setting, the aggregator has access to all local model updates  $W_i$ , and clients exchange model updates with the aggregator server, such that malicious aggregators can perform model inference attacks that aim to extract information about training data from the global model updates [14]. However, these attacks acquire minimal aggregated information about the data. Therefore, our objective is to conceal local models from the aggregator, thwarting potent inference attacks while still facilitating the accurate performance of FL-based IDS. Malicious clients are also capable of submitting falsified updates to the aggregator server and emerging quantum computing capabilities introduce additional threats.

#### 5 VSS-based Secure Aggregation Protocol

In order to preserve the confidentiality of local contributions in a FL context, we propose a SA protocol combining private and pairwise masks between clients, Shamir Secret Sharing (SSS) for client dropout tolerance and a verifiable sharing scheme (VSS) to guarantee the integrity of aggregated data. The protocol contains three key steps described by Algorithm 1, 2 and 3.

In the initialization phase (Algorithm 1) a set of clients (users)  $\mathcal{U} = \{U_1, U_2, \ldots, U_n\}$  is considered. Each client  $U_i$  generates a private mask  $b_i$  and pairwise masks  $s_{i,j}$  with all the other clients. The private mask  $b_i$  is then shared with the other clients using the secret sharing scheme (SSS) with a threshold t. A previous post-quantum key negotiation (ML-KEM) stage is used to secure channels between clients.

In the second step (Algorithm 2), each client trains a local model  $W_i$  using its private data and initial model parameters  $\theta$ . The model is then masked by  $y_i$ 

#### **Algorithm 1** Initialization()

#### Key Agreement Phase:

ML-KEM: Post Quantum Key Exchange between clients.

#### Initialization Phase:

for each client  $U_i \in \mathcal{U}$  do

Generate private mask  $b_i$ .

Generate pairwise masks with other clients  $U_i$ :

 $s_{i,j} \leftarrow \text{RandomMaskGeneration}()$ 

Compute final masking key  $y_i$ :

$$y_i = b_i + \sum_{j:i < j} s_{i,j} - \sum_{j:i > j} s_{j,i}$$

Secret-share private mask  $b_i$  using SSS:

$$Shares_{b_i} = SSS.Share(b_i, t, n)$$

Distribute shares of  $b_i$  to clients.

end for

to give  $W_{imasked} = W_i + y_i$  and then cryptographic commitments  $C_{W_{imasked}} = VSS.Commit(W_{imasked})$  are calculated on the masked weights to allow future verifications.

In the final stage, the aggregator server S receives the masked models and verifies their integrity using commitments (VSS.Verify) and then the valid models are summed to form the masked aggregate  $W_{masked}$  (Algorithm 3). If some clients are missing, their  $b_i$  private masks are reconstructed using the received SSS shares. The server eliminates all masks (private + pairwise) to recover the real sum of the models. The global model is finally updated by a standard average.

In the proposed protocol, the client performs fundamental tasks related to Algorithm 1, such as local model training and commitment computation as defined in Algorithm 2. In terms of computation, the client establishes shared keys with n-1 other clients. The cost of this operation mainly depends on the ML-KEM scheme used and is estimated as  $O(n \cdot \text{ML-KEM}_{\text{cost}})$ . The generation of private masks  $b_i$ , which are random vectors of dimension m, has a cost of O(m). The generation of pairwise masks  $s_{ij}$ , their computation with n-1 clients, and the secret sharing of the private mask  $b_i$  into n shares are collectively estimated at  $O(n \cdot m)$ , with the dominant cost attributed to the underlying Secret Sharing Scheme (SSS). The local model training, its masking  $W_i$ , and the computation of Verifiable Secret Sharing (VSS) commitments for future server-side verification have respective costs of  $O(\text{local\_data\_size} \cdot m)$ , O(m), and  $O(m \cdot \text{VSS}_{\text{cost}})$ .

In summary, the total computational cost corresponds to the following expression:  $O(n \cdot m + \text{ML-KEM}_{\text{cost}} + m \cdot \text{VSS}_{\text{cost}})$ , which can be approximated, after harmonizing notation and omitting lower-order terms, as  $O(n + n \cdot m)$ .

```
Algorithm 2 LocalTraining (Model: M, Parameters : \theta, Private data : d_i)
```

```
Local Training Phase:
```

for each client  $U_i \in \mathcal{U}$  do

Compute local model weights:

$$W_i = \text{LocalTraining}(M, \theta, \mathbf{d}_i)$$

Mask the model weights:

$$W_{i\,masked} = W_i + y_i$$

Compute VSS commitments for masked model weights:

$$C_{W_{imasked}} = VSS.Commit(W_{imasked})$$

Distribute secret shares of the masked model weights to the aggregator  $\mathcal{S}$ . end for

### Algorithm 3 VerifiedAggregation ( $W_{imasked}$ , $C_{W_{imasked}}$ )

```
Verification Phase:
```

for aggregator S do

for each received model weights share  $W_{imasked}$  do

Verify model weights share using VSS:

$$Valid \leftarrow VSS.Verify(W_{imasked}, C_{W_{imasked}})$$

if verification fails then

Reject masked model weights from client  $U_i$ 

end if

end for

end for

**Aggregation Phase:** 

**Aggregator** sums verified masked model weights:  $W_{masked} = \sum_{i=1}^{n} W_{imasked}$ If dropout is detected, aggregator reconstructs dropped clients' private masks via SSS:  $b_i \leftarrow \text{SSS.Recons}(\text{Shares}_{b_i})$ 

**Aggregator** removes all masks using reconstructed private masks and known pairwise masks to recover true aggregate model weights.  $W = W_{masked} - \sum_{i \in \text{dropped}} b_i$  **Aggregator** computes the global model:  $\theta \leftarrow \frac{1}{|\mathcal{U}|}W$ 

Regarding communication overhead, a similar analysis was conducted, focusing on the volume of data exchanged among the different entities. The resulting communication cost is estimated as  $O(n \cdot m)$ .

#### 6 Dataset and Classification Scenarios

To achieve FL-based intrusion detection system for IoT networks FederatedAveraging [2] approach has been experimented using the dataset from the Canadian Institute for Cybersecurity at the University of New Brunswick [15]. The

study seeks to present a rich IoT attack corpus that supports both the classification of IoT devices and the detection of abnormal behavior, thereby enhancing security-analytics solutions for practical IoT deployments. To compile the dataset, researchers executed 33 separate attack scenarios across a network of 105 IoT devices hosted at the Institute. Seven types of attacks were run on the experiments: distributed denial of service (DDoS), denial of service (DoS), reconnaissance, web-based, brute-force, spoofing, and the Mirai botnet.

To evaluate the performance of the proposed IDS, three different classifications were considered.

- 1. Binary classification: This scenario distinguishes between normal behavior and attack. It is particularly important when the main goal of the IDS is to detect malicious activity
- 2. Eight-category classification: Here the system differentiates among the main general categories of attacks, providing more information about the characteristics of the anomalies detected. Seven main attack types and normal behavior are considered
- 3. Thirty-four-category classification: In this setting, the system is able to detect and classify specific variants of attacks.

To specifically target Mirai-type attacks, we performed a balanced reduction of the dataset to 1% of the original size, followed by aggregation to eight classes and, finally, reduction to two classes (Mirai attacks versus normal behavior). These classification scenarios enable a comprehensive evaluation of the system's performance across varying levels of complexity. This dataset was cleaned, features were selected, normalized, encoded, and checked for possible data leakage...

#### 7 Experimental Evaluation and Results

This section presents the experimental evaluation of our privacy-enhancing methods on a FL-based IDS using a dataset collected from real-world experiments with IoT device. Specifically, we focus on detecting Mirai attacks through binary classification as Mirai is notorious malware that targets vulnerable IoT devices, such as routers, IP cameras and other connected gadgets. We analyze the trade-off between model efficiency and the overhead of Secure Aggregation by leveraging various metrics.

Table 1 shows how long it takes for the ML-KEM-based key exchange to run at different security levels. Even for the highest level of security (ML-KEM-1024), the key generation and exchange times remain under one millisecond. These low runtimes demonstrate that Post-Quantum secure channels can be integrated into IoT devices without causing significant delays. This is particularly relevant in environments where computational resources and real-time performance are critical.

 Algorithm
 Key Gen. (ms) Encap. (ms) Decap. (ms)

 ML-KEM-512
 0.2490
 0.4535
 0.3481

 ML-KEM-768
 0.4073
 0.5127
 0.4004

 ML-KEM-1024
 0.4658
 0.5130
 0.5931

Table 1: ML-KEM based key exchange runtime (ms)

For the FL framework, the FederatedAveraging [2] aggregation algorithm is adopted and evaluated with three models: Logistic Regression (LR), Long Short-Term Memory (LSTM), and Multi-Layer Perceptron (MLP). Table 2 presents the accuracy, precision and recall metrics. We implement the VSS-based secure aggregation protocol, which includes a post-quantum key exchange based on ML-KEM. The experiments are performed on a Raspberry Pi 4 model B platform with **CPU** 64-bit quad-core Cortex-A72 and **Memory** 8 GB LPDDR4 RAM.

Table 2: Model Results

| Model               | Accuracy% | Precision% | Recall % |
|---------------------|-----------|------------|----------|
| Logistic Regression | 99.37     | 99.37      | 99.37    |
| LSTM                | 99.44     | 99.96      | 99.25    |
| MLP                 | 99.91     | 99.98      | 99.89    |

In figure 2, it is illustrated how well each model performs when combined with the Secure Aggregation protocol. The MLP model, in particular, reaches almost 98,9% accuracy, which is impressive considering the added privacy layer. Even the LSTM and Logistic Regression models maintain solid results. These outcomes indicate that the integration of verifiable secret sharing and post-quantum secure channels does not compromise detection performance.

Table 3: VSS-based Secure Aggregation overhead (n: number of client in the FL training, m: dimension of local model weight vector)

| Overhead      | Client side     | Server side                    |
|---------------|-----------------|--------------------------------|
| Communication | - ()            | $\mathcal{O}(n^2 \cdot m)$     |
| Computation   | $O(n+n\cdot m)$ | $\mathcal{O}(n^2 + n \cdot m)$ |

Table 3 summarizes the approximate computation and communication overhead of the proposed SA protocol (described in Algorithms 1, 2, and 3). Figure 1 compares this overhead to other SMPC-based Secure Aggregation protocols [8, 16, 17]. Our proposal is generally less expensive in computation in both side

client and server than the considered well-established SA protocol in Federated Learning [8]. Regarding communication, our protocol shows higher costs because of the commitment generation process and verification, enabling the server to verify future model updates. Figure 2 shows a simulation of the SA protocol that involves injecting noise related to masking and share reconstruction. It is shown that the accuracy of the models during the FL training rounds is not significantly impacted, with only a slight difference observed.

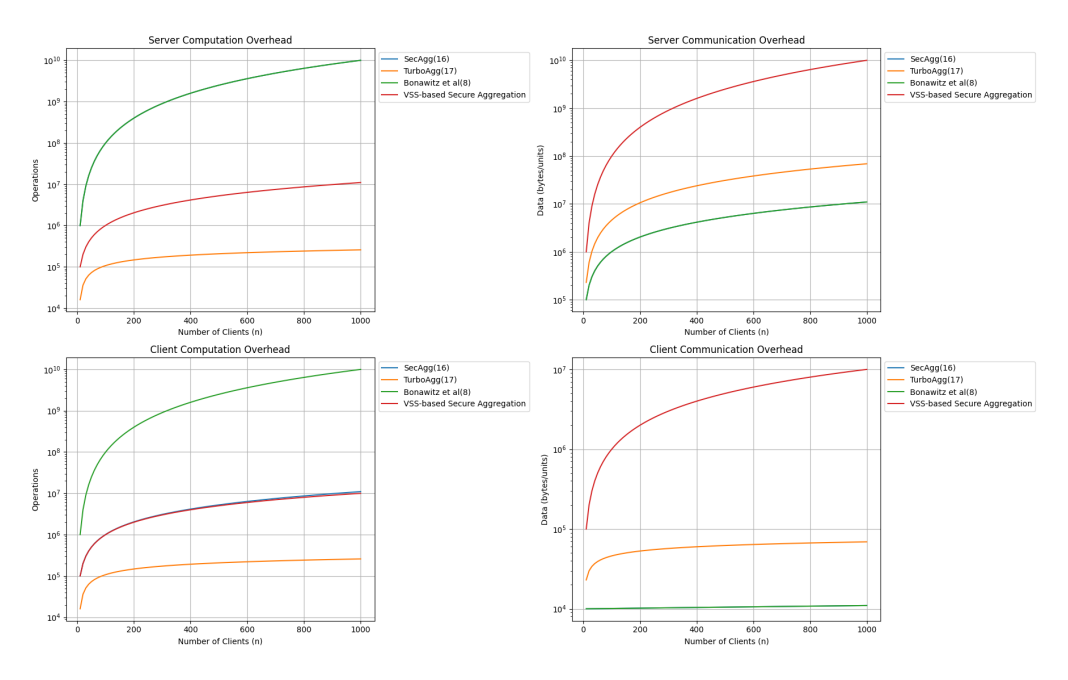


Fig. 1: VSS-based Secure Aggregation overhead comparison

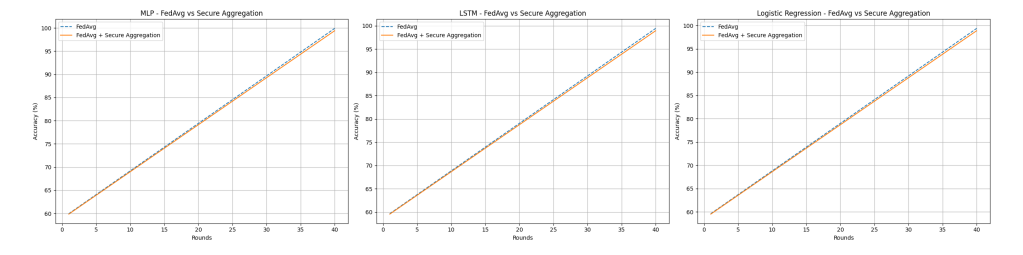


Fig. 2: FedAverage FL with VSS based-Secure Aggregation

In summary, these experiments confirm that our approach can effectively balance privacy, security, and detection performance in real-world IoT scenarios. By combining verifiable secret sharing and post-quantum key exchange, we've managed to build a FL-based IDS that's both resilient against quantum threats and feasible for devices with limited resources. We believe these results are a strong step toward bringing truly secure FL-based intrusion detection systems into the IoT world.

#### 8 Conclusion and Future Work

In this paper, a Federated Learning-based Intrusion Detection System (IDS) has been built using a dataset collected from real-world experiments with IoT devices. For Federated Learning, Federated Averaging as the aggregation algorithm has been used, with three different models, namely Logistic Regression, LSTM, and MLP, evaluated. To improve privacy as well as protect against malicious clients, a VSS-based Secure Aggregation protocol has been designed, which runs over a Post-Quantum secure channel. Simulation demonstrates this protocol adding negligible overhead along with lower costs than other SMPC-based methods. Secure Aggregation integration has not hindered model performance considerably, with the MLP model attaining a maximum accuracy of 98.9%.

Future research will extend the current IDS in order to detect other types of attacks. We also intend to compare other quantum-resistance Secure Aggregation protocols, including ones using approximate homomorphic encryption (e.g., methods using CKKS). The Verifiable Secret Sharing implemented here is secured under the hardness of the discrete logarithm problem, but its client-dropping resilience—achieved via Shamir's Secret Sharing—remains to be thoroughly analyzed. We plan to examine this client-dropping tolerance more precisely. We intend to incorporate lattice-based methods in order to improve the verification process against quantum attacks.

#### Acknowledgments

This work was supported by the Cybersecurity Chair of the University of La Laguna (C065/23) and the strategic project SCITALA (C064/23), both funded by INCIBE through the Recovery, Transformation, and Resilience Plan (Next Generation EU), financed by the European Union; the project PID2022-138933OB-I00 "ATQUE," funded by MCIN/AEI/10.13039/501100011033 and co-financed by the European Regional Development Fund (ERDF, EU); and the 2023DIG28 project, funded by CajaCanarias and the "la Caixa" Foundation.

#### References

1. Leonel Santos, Carlos Rabadao, and Ramiro Gonçalves. Intrusion detection systems in internet of things: A literature review. In 2018 13th Iberian conference on information systems and technologies (CISTI), pages 1–7. IEEE, 2018.

- H Brendan McMahan, Eider Moore, Daniel Ramage, and Blaise Agüera y Arcas. Federated learning of deep networks using model averaging. arXiv preprint arXiv:1602.05629, 2(2):15–18, 2016.
- Suzan Almutairi and Ahmed Barnawi. Federated learning vulnerabilities, threats and defenses: A systematic review and future directions. *Internet of Things*, 24:100947, 2023.
- Ronald Cramer, Ivan Bjerre Damgård, and Jesper Buus Nielsen. Secure Multiparty Computation and Secret Sharing. Cambridge University Press, Cambridge, 2015.
- Adi Shamir. How to share a secret. Communications of the ACM, 22(11):612-613, 1979.
- Shyamalendu Kandar and Bibhas Chandra Dhara. A verifiable secret sharing scheme with combiner verification and cheater identification. *Journal of Informa*tion Security and Applications, 51:102430, 2020.
- 7. Thien Duc Nguyen, Samuel Marchal, Markus Miettinen, Hossein Fereidooni, Nadarajah Asokan, and Ahmad-Reza Sadeghi. DÏot: A federated self-learning anomaly detection system for iot. In *IEEE 39th International Conference on Distributed Computing Systems (ICDCS)*, pages 756–767, Los Alamitos, CA, USA, 2019. IEEE Computer Society.
- 8. K Bonawitz, V Ivanov, B Kreuter, A Marcedone, HB McMahan, S Patel, D Ramage, A Segal, and K Seth. Practical secure aggregation for federated learning on user-held data. arxiv 2016. arXiv preprint arXiv:1611.04482, 13.
- 9. Hossein Fereidooni, Samuel Marchal, Markus Miettinen, Azalia Mirhoseini, Helen Möllering and Thien Duc Nguyen, Phillip Rieger, Ahmad-Reza Sadeghi and Thomas Schneider, Hossein Yalame, and Shaza Zeitouni. Safelearn: Secure aggregation for private federated learning. In *IEEE Security and Privacy Workshops (SPW)*, pages 56–62, Los Alamitos, CA, USA, may 2021. IEEE Computer Society.
- Guowen Xu, Hongwei Li, Sen Liu, Kan Yang, and Xiaodong Lin. Verifynet: Secure and verifiable federated learning. *IEEE Transactions on Information Forensics* and Security, 15:911–926, 2019.
- 11. Peng Xu, Manqing Hu, Tianyang Chen, Wei Wang, and Hai Jin. LaF: Lattice-based and communication-efficient federated learning. 17:2483–2496.
- 12. Xia Zhang, Haitao Deng, Rui Wu, Jingjing Ren, and Yongjun Ren. PQSF: post-quantum secure privacy-preserving federated learning. 14(1):23553. Publisher: Nature Publishing Group.
- 13. Ahmed Saidi, Abdelouahab Amira, and Omar Nouali. Securing decentralized federated learning: cryptographic mechanisms for privacy and trust. *Cluster Computing*, 28(2):1–17, 2025.
- Nader Bouacida and Prasant Mohapatra. Vulnerabilities in federated learning. IEEe Access, 9:63229–63249, 2021.
- 15. Euclides Carlos Pinto Neto, Sajjad Dadkhah, Raphael Ferreira, Alireza Zohourian, Rongxing Lu, and Ali A. Ghorbani. Ciciot2023: A real-time dataset and benchmark for large-scale attacks in iot environment. *Sensors*, 23(13), 2023.
- 16. Kwing Hei Li, Pedro Porto Buarque de Gusmão, Daniel J Beutel, and Nicholas D Lane. Secure aggregation for federated learning in flower. In Proceedings of the 2nd ACM International Workshop on Distributed Machine Learning, pages 8–14, 2021.
- 17. Jinhyun So, Başak Güler, and A Salman Avestimehr. Turbo-aggregate: Breaking the quadratic aggregation barrier in secure federated learning. *IEEE Journal on Selected Areas in Information Theory*, 2(1):479–489, 2021.

### Federated Learning for the Detection of Attacks on IoT environment

Alejandro Diezo, Jaime Rincon<sup>1</sup>, and Daniel Urda<sup>1</sup>

1. Grupo de Inteligencia Computacional Aplicada (GICAP)
Departamento de Ingeniería Informática, Escuela Politécnica Superior, Universidad
de Burgos, Av. Cantabria s/n, 09006, Burgos, Spain.
adb1012@alu.ubu.es, {jarincon,durda}@ubu.es

Abstract. The rapid expansion of Internet of Things (IoT) devices has significantly increased the attack surface, necessitating the development of robust and privacy-preserving intrusion detection systems. This research delves into the application of Federated Learning (FL) to detect network-based attacks in IoT environments, utilizing the NF-ToN-IoT dataset. We compare a centralized machine learning model with a federated counterpart, employing the Federated Averaging (FedAvg) algorithm. Both models employ a Multi-Layer Perceptron (MLP) architecture trained on NetFlow features for binary classification of benign versus malicious traffic. Our experimental results reveal that the federated model achieves comparable and even slightly superior performance across various metrics, including precision, recall, and F1-score, while preserving data privacy by decentralizing the training data. These findings underscore the potential of FL as a viable alternative to traditional intrusion detection systems in real-world, privacy-sensitive IoT scenarios.

**Keywords:** intrusion detection, cybersecurity, iot, federated learning, machine learning, supervised learning

#### 1 Introduction and previous work

In recent years, the exponential increase in Internet-connected devices has given rise to a highly complex and widely distributed Internet of Things (IoT) ecosystem. Spanning from smart homes to industrial infrastructure, projections estimate that by 2030, approximately 40 billion IoT devices will be in operation worldwide [1]. This massive expansion has not only increased data generation but has also broadened the attack surface, making IoT devices particularly vulnerable to security threats. According to Forescout's Riskiest Connected Devices of 2025 report, routers account for more than 50% of devices with critical vulnerabilities, surpassing other devices such as computers and wireless access points [2]. This finding highlights the increasing exposure of IoT devices to cyberattacks, particularly those that are part of the network infrastructure.

To mitigate these threats, Artificial Intelligence (AI), and particularly Machine Learning (ML), has emerged as a powerful tool for the proactive detection

of threats. ML models can analyze large volumes of network traffic data to identify anomalous patterns that may indicate malicious activity, even before they materialize into actual attacks. However, traditional ML methods often rely on centralized data storage and processing on remote servers. This approach raises critical challenges such as privacy risks, high bandwidth demands, and latency issues, especially in resource-limited settings like IoT networks.

To address these limitations, Federated Learning (FL) offers a decentralized ML approach that enables model training across distributed devices without sharing raw data. This paradigm ensures that sensitive information remains local while allowing for collaborative training. Despite its benefits, applying FL in IoT contexts presents unique challenges, including device heterogeneity, communication efficiency, and robustness against compromised nodes [3].

In this work, we aim to evaluate the feasibility of using FL for anomaly detection in IoT networks, in comparison with traditional centralized ML. To this end, we propose a simulated scenario involving a network with two devices acting as clients, each responsible for processing data and training the same model in a distributed manner. This is achieved by splitting the NF-ToN-IoT dataset [4], a recent and comprehensive intrusion detection dataset tailored to IoT and network-based attacks, originally used to train the model in a traditional centralized framework. To assess the effectiveness of this method, we compare the performance of the federated training approach with that of the same model trained in a centralized setting on a single machine. Our experimental design represents an initial step towards evaluating more complex scenarios, ultimately aiming to apply the proposed methodology in a real-world environment.

The remainder of this paper is organized as follows. Section 2 introduces the NF-ToN-IoT dataset and explains how the data is distributed among the clients. Section 3 details the baseline model architecture and the federated learning environment used in the experiments. The experimental evaluation and the analysis of the obtained results are presented in Section 4. Finally, Section 5 provides concluding remarks and outlines potential directions for future work.

#### 2 NF-ToN-IoT Dataset

The NF-ToN-IoT dataset is a NetFlow-base dataset version of the ToN-IoT dataset, created by the University of New South Wales (UNSW) in Sydney, designed to support research in network intrusion detection in Internet of Things environments based on Artificial Intelligence [5]. It was developed at the UNSW Canberra Cyber IoT Lab and aims to emulate realistic and complex IoT environments, incorporating telemetry data from IoT sensors, operating systems logs, and network traffic data.

This dataset contains preprocessed and labeled network traffic data, captured from a simulated IoT network. The dataset includes both benign (19.6%) and malicious (80.4%) traffic, supporting a wide variety of attack types such as Denial of Service (DoS), Distributed DoS (DDoS), Ransomware, and Injection, among others (see Table 1). The data was generated using well-known cybersecurity

tools like Wireshark, Zeek, Security Onion, and Kali Linux, adding reliability and realism to the scenarios represented.

| Label      | Number of Flows | Description  |
|------------|-----------------|--|
| Benign     | 270,279         | Normal unmalicious flows.                                  |
| Backdoor   | 17,247          | A technique that attacks remote-access computers by re-    |
|            |                 | plying to specially constructed client applications.       |
| DoS        | 17,717          | Attempts to overload a system's resources to deny access   |
|            |                 | or availability of its data.                               |
| DDoS       | 326,345         | Similar to DoS, but originating from multiple distributed  |
|            |                 | sources.   |
| Injection  | 468,539         | Attacks that supply untrusted inputs to alter program      |
|            |                 | execution (e.g., SQL or code injections).                  |
| MITM       | 1,295           | Man-in-the-Middle attack that intercepts communication     |
|            |                 | between a victim and a host.                               |
| Password   | 156,299         | Attacks aimed at retrieving passwords via brute force or   |
|            |                 | sniffing techniques.                                       |
| Ransomware | 142             | Encrypts a host's files and demands payment for the de-    |
|            |                 | cryption key.  |
| Scanning   | 21,467          | Techniques that probe networks and hosts to discover       |
|            |                 | information (also known as probing).                       |
| XSS        | 99,944          | Cross-site scripting: attackers send malicious scripts via |
|            |                 | web applications to end users.                             |

Table 1: Distribution of traffic types in the NF-ToN-IoT dataset

For this study, we focused on the network traffic data, which consisted of a CSV file representing all the captured packets along with their corresponding labels [6]. The dataset was preprocessed to extract the most relevant features, normalize the data, and transform the labels to indicate only whether a packet is malicious or not. First, the categorical Attack column was removed, as it was redundant for the binary classification task. Then, the feature matrix X was constructed by dropping the Label column, which was stored separately as the target vector y. Finally, all features were normalized using standard score normalization (z-score), ensuring that the input values had zero mean and unit variance.

The resulting dataset was divided into three main subsets: 70% for training, 15% for validation, and 15% for threshold selection (used to determine classification decision boundaries). A detailed breakdown of this partitioning is presented in Table 2 To simulate a federated learning environment, the training set was split evenly between two clients, allowing each to perform local training on distinct data partitions.

#### 4 Alejandro Diezo, Jaime Rincono, and Daniel Urdao

| Subset              | Percentage | Number of Samples | Benign | Attacks |
|---------------------|------------|-------------------|--------|---------|
| Training (Client 1) | 35%        | 405,297           | 17.11% | 82.89%  |
| Training (Client 2) | 35%        | 405,298           | 17.14% | 82.86%  |
| Validation          | 15%        | 173,699           | 17.28% | 82.72%  |
| Threshold Selection | 15%        | 173,700           | 17.06% | 82.94%  |
| Total               | 100%       | 1,157,994         |        |         |

Table 2: Dataset partitioning and client distribution

### 3 Methodology

This section outlines the methodology followed to conduct the experiments and evaluate the proposed approach. First, we describe the baseline models used as a reference point to assess the effectiveness of our system. Then, we detail the federated learning environment, including the system architecture, data distribution strategy, and training procedures. Finally, we define the performance metrics used to measure and compare the models' behavior across various evaluation criteria.

#### 3.1 Baseline

Before evaluating the effectiveness of federated learning in this context, it is necessary to define a baseline classification model. The chosen model is a Multi-Layer Perceptron (MLP) [7], a type of supervised learning algorithm that approximates a target function by training on labeled data. This model is well-suited for binary classification tasks, such as distinguishing between benign and malicious network traffic. It was implemented using TensorFlow/Keras [9] and trained on labeled NetFlow records.

The architecture of the model consists of an input layer with 10 neurons (one for each input feature), followed by two hidden layers with 64 and 32 neurons respectively, both using ReLU activation functions. The output layer consists of a single neuron with a sigmoid activation function to predict binary outcomes. The model was compiled using the Adam optimizer with a learning rate of 0.001, binary cross-entropy as the loss function, and accuracy as the evaluation metric. The input to the model consists of 10 features extracted from each NetFlow record. These features are summarized in Table 3.

#### 3.2 Federated Learning Environment

To simulate a federated learning environment, we used the Flower framework [10], which allows seamless communication between multiple clients and a central server. Each client was assigned half of the training data, simulating local data ownership. Clients trained the same model architecture independently on their respective partitions and shared the resulting model weights with the central

| Feature                    | Description                                  |
|----------------------------|--|
| L4_SRC_PORT                | Source port at Layer 4.                      |
| L4_DST_PORT                | Destination port at Layer 4.                 |
| PROTOCOL                   | Network protocol used (e.g., TCP, UDP).      |
| L7_PROTO                   | Application layer protocol.                  |
| IN_BYTES                   | Number of incoming bytes.                    |
| OUT_BYTES                  | Number of outgoing bytes.                    |
| IN_PKTS                    | Number of incoming packets.                  |
| OUT_PKTS                   | Number of outgoing packets.                  |
| TCP_FLAGS                  | Bitwise flags representing TCP control bits. |
| FLOW_DURATION_MILLISECONDS | Duration of the flow in milliseconds.        |

Table 3: Description of selected network flow features

server. The server aggregated these weights using the Federated Averaging (FedAvg) algorithm. This process was repeated for 12 global rounds, with each client performing 4 local training epochs per round. For comparison, the centralized model was trained for 20 epochs on the complete dataset.

The Federated Averaging (FedAvg) algorithm [8] combines model updates from multiple clients by computing a weighted average of their parameters. Each client performs local training on its data and then sends the updated model to the server, which aggregates the models based on the relative size of each client's dataset.

#### 3.3 Performance Metrics

To assess and compare model performance, we employed standard classification metrics such as accuracy, loss, precision, recall, and F1-score—alongside visual tools like ROC curves and confusion matrices. These metrics provided insights into each model's ability to detect malicious traffic while minimizing false positives. Special attention was given to issues arising from class imbalance, where accuracy alone may be misleading. Binary cross-entropy loss was used to measure prediction error, while precision and recall helped evaluate the trade-off between false alarms and missed threats. The F1-score offered a balanced measure in imbalanced scenarios, and ROC curves, along with AUC values, summarized overall model effectiveness. The confusion matrix further enabled detailed analysis of prediction errors.

# 4 Results and discussion

In this section, we present the results obtained from the evaluation of the federated learning approach for anomaly detection in IoT environments, using the NF-ToN-IoT dataset described in Section 2. For training, we used the base model defined in Section 3, configured for 12 federated rounds and 4 local epochs per client. Each client trained on data batches of size 32. The binary cross-entropy

loss function was used, with a learning rate of 0.001. Accuracy was selected as the primary evaluation metric during training. The following Table 4 shows the main metrics compared between the baseline model (MLP) and the federated learning model (FedAvg).

| _           | Accuracy |        | 1      |        | l .    |        |
|-------------|----------|--------|--------|--------|--------|--------|
| Centralized |          |        |        |        |        |        |
| Distributed | 0.9913   | 0.0246 | 0.9922 | 0.9973 | 0.9948 | 0.9993 |

Table 4: Comparison of model performance across centralized and distributed setups during evaluation

To gain a more comprehensive understanding of the model's performance, we evaluated it at each round using several classification metrics described in Section 3.3. In this analysis, we focus only on the server-side evaluation, as both the server and clients use the same evaluation dataset.

Initially, at round 0, the model's accuracy is very low due to its random weight initialization. However, after the first round of training, the model's accuracy increases significantly, stabilizing around 0.99 and reaching a final accuracy of 0.9913. Particular attention should be given to rounds 6 and 8, where a noticeable drop in accuracy occurs. This drop may be attributed to the way the FedAvg algorithm aggregates weights from different clients. In federated learning, the server combines the clients' local models through weighted averaging (FedAvg). When client models are poorly aligned or trained on non-IID data distributions [15], the aggregation can introduce instability, temporarily reducing model performance. Nonetheless, the model eventually recovers and continues to improve as training progresses.

In addition to accuracy, metrics like precision, recall, and F1-score provide a more detailed view of classification performance. As expected, at round 0, all metrics are low due to the model's lack of training. From round 1 onward, the model improves rapidly, with metrics surpassing 0.99 by rounds 5–6, indicating robust classification capability. Similar to the accuracy trend, precision and recall drop to approximately 0.95 in rounds 6 and 8, reflecting the same instability caused by data heterogeneity. Following these dips, the metrics recover, suggesting that the model is adapting over time, despite the variability in data distributions.

Once this stage is reached, we compare the performance of the federated and centralized models using key visualizations such as the evolution of training and validation loss and the confusion matrix. This analysis provides insights into model efficiency, convergence, generalization, and robustness, allowing us to assess the trade-offs of federated learning—particularly its advantages in privacy and decentralization—against traditional centralized approaches.

The loss function is an essential indicator of model training. For each model, we plot both the training loss and validation loss across epochs for the centralized

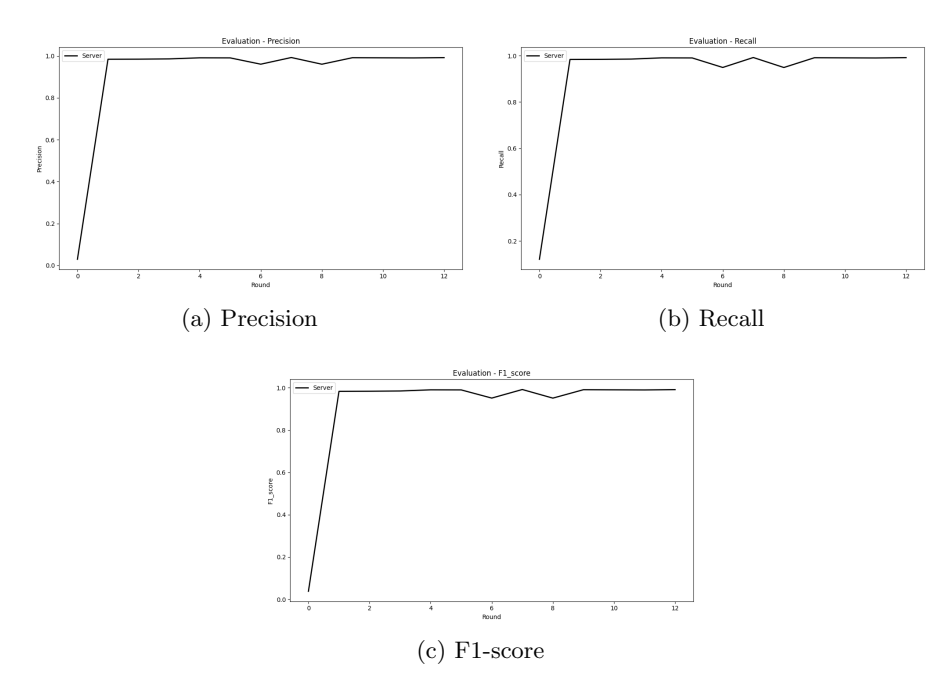


Fig. 1: Precision, Recall and F1-score during federated evaluation across rounds.

model, and across communication rounds for the distributed model. This allows us to visualize how the model's error evolves over time in each case.

In the centralized model graph 2, we can observe that the training loss and validation loss are very similar, with only a small difference between them. This is a good sign, as it suggests that the model is learning effectively during the training process and is able to generalize well to unseen data. The small gap between the two losses indicates that there is no significant overfitting, and the model is performing well throughout the epochs.

On the other hand, when we look at the distributed model, we notice a more interesting pattern. As we saw in the previous section, during rounds 6 and 8, there is a noticeable discrepancy between the training loss of the local models and the validation loss of the global model. This gap suggests that during these rounds, the local models were not perfectly aligned with the global model, possibly due to differences in the data each device was trained on. This misalignment can lead to a temporary drop in performance, as the global model struggles to incorporate the updates from the local models. However, it is important to note that this is a common issue in federated learning, and as more rounds progress, we expect the performance to stabilize and improve as the model continues to learn from the distributed data.

Despite temporary fluctuations during training, the final outcomes are highly promising: both the centralized and federated models achieved an AUC-ROC

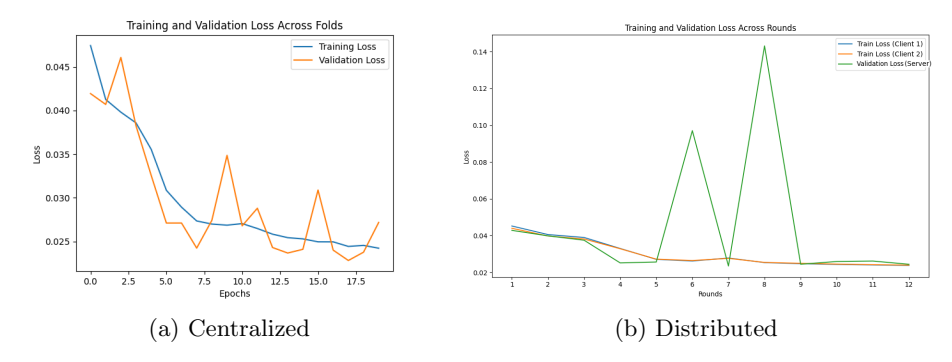


Fig. 2: Training and Validation loss comparison.

of 0.9992, indicating exceptional discriminatory performance. To further assess classification efficacy, we examine the confusion matrices of both models, which provide a detailed breakdown of true negatives, false positives, false negatives, and true positives. This analysis helps validate that the federated approach retains performance comparable to the centralized model, even under decentralized training conditions.

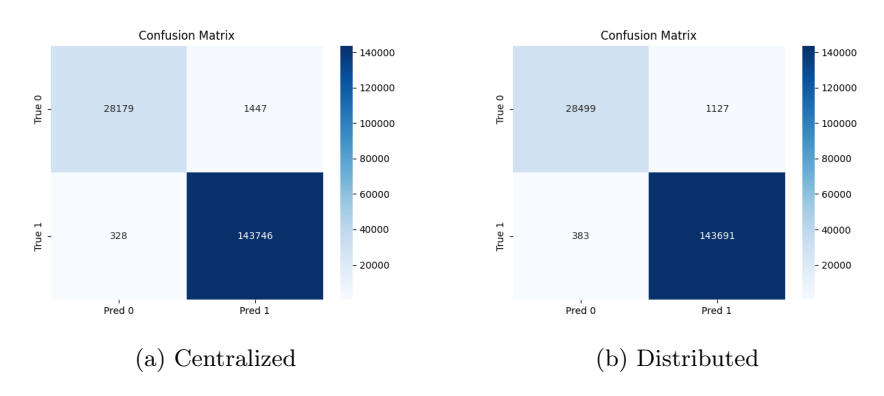


Fig. 3: Confusion matrix comparison.

As shown in Figure 3, the centralized model demonstrates excellent performance in accurately identifying attack traffic. However, when compared to the confusion matrix of the federated model, we observe that the centralized approach tends to classify more benign traffic as malicious, resulting in a higher number of false positives. From the confusion matrix, we obtain a precision of 0.9900, a recall of 0.9977, and an F1-score of 0.9939. These values suggest that the centralized model is highly effective at detecting attacks (high recall), while

maintaining a relatively low false positive rate (high precision). The F1-score reflects a strong balance between these two aspects.

On the other hand, the federated model is able to slightly increase the precision to 0.9922, while still maintaining a recall of 0.9973. This results in an improved F1-score of 0.9948, indicating that the federated model slightly outperforms the centralized one in terms of overall classification performance. In particular, it reduces false alarms while continuing to detect nearly all attacks.

In conclusion, both models achieve outstanding performance, with the federated model matching or even surpassing the centralized model. While the performance gap between the two approaches is relatively small, these results highlight the potential of federated learning to provide similar (or even superior) outcomes to centralized training, all while preserving data privacy—a crucial advantage in security-sensitive domains such as IoT.

# 5 Conclusions and Future Work

To conclude this analysis, the federated model has demonstrated performance comparable to that of the centralized model, even outperforming it in certain evaluation metrics. Although the federated model required nearly twice as many training epochs as the centralized one, this extended training enabled the model to learn from multiple datasets distributed across different locations, all while preserving the privacy of each data source—an essential aspect when working with sensitive datasets in neural network training.

This highlights one of the key advantages of federated learning: its ability to achieve high performance without requiring centralized data aggregation. As a result, it represents a highly valuable solution for scenarios such as IoT environments, where data privacy and decentralization are crucial requirements. Moreover, its practical application is particularly useful in real-world contexts where different entities—such as hospitals, companies, or government institutions—prefer not to share sensitive data due to privacy concerns, yet aim to collaborate in training AI models for attack detection.

Future research on federated learning for intrusion detection in IoT should focus on improving robustness, scalability, and practical deployment. Analyzing the impact of data distribution (IID vs. non-IID) using synthetic datasets can help address performance issues from heterogeneity. Increasing the number of clients would enhance realism and test system scalability. Incorporating richer and more recent datasets could improve detection of sophisticated and evolving threats. Reducing communication overhead is also critical, especially in constrained environments. Techniques like model compression, gradient sparsification, and asynchronous updates offer promising solutions.

### Acknowledgements

This publication is part of the AI4SECIoT project ("Artificial Intelligence for Securing IoT Devices"), funded by the National Cibersecurity Institute (INCIBE),

derived from a collaboration agreement signed between the National Institute of Cybersecurity (INCIBE) and the University of Burgos. This initiative is carried out within the framework of the Recovery, Transformation and Resilience Plan funds, financed by the European Union (Next Generation), the project of the Government of Spain that outlines the roadmap for the modernization of the Spanish economy, the recovery of economic growth and job creation, for solid, inclusive and resilient economic reconstruction after the COVID19 crisis, and to respond to the challenges of the next decade.

#### References

- Sinha, S.: State of IoT 2024: Number of connected IoT devices growing 13% to 18.8 billion globally. https://iot-analytics.com/number-connected-iot-devices [Online; Accessed 4-May-2025]
- 2. Vedere Research Labs: The Riskiest Connected Devices in 2025. Forescout (2025). https://www.forescout.com/resources/riskiest-devices-2025-report/
- 3. Google: Federated Learning. https://federated.withgoogle.com [Online; Accessed 18-January-2025]
- Sarhan, M., Layeghy, S., Moustafa, N., Portmann, M.: NetFlow Datasets for Machine Learning-Based Network Intrusion Detection Systems. In: Zeng, D., Huang, H., Hou, R., Rho, S., Chilamkurti, N. (eds.) Big Data Technologies and Applications, pp. 117–135. Springer, Cham (2021)
- Luay, M., Layeghy, S., Hosseininoorbin, S., Sarhan, M., Moustafa, N., Portmann, M.: Temporal Analysis of NetFlow Datasets for Network Intrusion Detection Systems. arXiv (2025). https://arxiv.org/abs/2503.04404
- 6. NF-ToN-IoT-00-Cleaning. https://kaggle.com/code/dhoogla/nf-ton-iot-00-cleaning [Accessed 2025-05-13]
- Scikit-learn: 1.17. Neural network models (supervised). https://scikit-learn.org/stable/modules/neural\_networks\_supervised.html [Accessed 2025-05-06]
- 8. McMahan, H.B., Moore, E., Ramage, D., Hampson, S., Agüera y Arcas, B.: Communication-Efficient Learning of Deep Networks from Decentralized Data. arXiv (2023). http://arxiv.org/abs/1602.05629
- 9. Google: TensorFlow. https://www.tensorflow.org/ [Accessed 2025-05-06]
- 10. The Flower Team: Flower: A Friendly Federated AI Framework. https://flower.ai/ [Accessed 2025-05-06]
- 11. Google: Classification: Accuracy, recall, precision, and related metrics. https://developers.google.com/machine-learning/crash-course/classification/accuracy-precision-recall [Accessed 2025-05-09]
- 12. Google: Classification: ROC and AUC. https://developers.google.com/machine-learning/crash-course/classification/roc-and-auc [Accessed 2025-05-09]
- 13. Google: Thresholds and the confusion matrix. https://developers.google.com/machine-learning/crash-course/classification/thresholding [Accessed 2025-05-09]
- 14. Google: Linear regression: Loss. https://developers.google.com/machine-learning/crash-course/linear-regression/loss [Accessed 2025-05-09]
- 15. Bhadauria, Y.S.: An Introduction to Non-IID Data and the Challenges of Data Heterogeneity. Medium (2024). https://medium.com/@yuvraj.s.bhadauria/an-introduction-to-non-iid-data-and-the-challenges-of-data-heterogeneity-035baaaa5939

# Enhancing Programming Education Through a Blended Methodology with ProgTutor

Javier Ortega-Morla<sup>1\*</sup>, Antonio Leis<sup>2</sup>, Alma María Mallo Casdelo<sup>2</sup>, Laura Morán-Fernández<sup>1</sup>, and Noelia Sánchez-Maroño<sup>1</sup>

LIDIA Laboratory, CITIC, Universidade da Coruña, A Coruña, Spain {javier.ortega1, laura.moranf, noelia.sanchez}@udc.es
GII, CITIC, Universidade da Coruña, A Coruña, Spain {antonio.leis, alma.mallo}@udc.es

Abstract. This article presents a novel blended learning methodology designed for classroom integration of ProgTutor, an Intelligent Tutoring System (ITS) for programming education. The proposed methodology combines self paced learning through the ITS with structured teacher led instruction in a recurring five phase cycle. This structure aims to reinforce conceptual understanding while maintaining teacher involvement and promoting active learning. To evaluate its effectiveness, the methodology was applied over one academic year in formal education settings and compared against two alternative approaches: traditional instruction without ProgTutor and traditional instruction using ProgTutor as a standalone tool. Results show that the blended approach led to deeper student understanding, greater progress through advanced topics, and significantly better performance in complex programming constructs, particularly loops.

**Keywords:** Intelligent Tutoring Systems (ITS), Adaptive Learning, Programming, Blended Learning, Educational Technology

# 1 Introduction and Scope

The pursuit of effective personalized learning through Artificial Intelligence (AI) tools is well established in the field of AI in education (AIEd) [11]. Systems such as Adaptive Learning Systems [3], AI based Learning Assistants [5], and Intelligent Tutoring Systems (ITS) [6] aim to optimize individual learning paths based on student preferences and pace, enhancing both student outcomes and teacher effectiveness. Although AI driven systems have shown success in subjects such as mathematics and science [12], their integration into formal education remains limited due to regulatory and evaluative challenges [7]. One of the key aspects for such integration is the teacher's acceptance of the learning methodology, that is, how to introduce these AI powered tools into existing practices while keeping educators at the center of the learning process.

<sup>\*</sup> Corresponding author.

A particularly active area for AI integration is programming education, where ITSs have advanced significantly in recent years. For instance, iSnap [8] offers contextual code hints using Abstract Syntax Trees, supporting novice learners autonomously. A recent study introduced TinyBERT as a tool to answer Python questions, with positive effects on student progress and comprehension [9]. Sharma and Harkishan [10] employed case-based reasoning and optimization algorithms to generate feedback in multiple programming languages with high success. However, these systems still lack key features necessary for adoption in formal education, such as reliable personalized learning paths, structured curricula, and effective integration with teachers. A broader review [2] identifies major challenges, such as low model transparency and the absence of public datasets, which further complicate real-world classroom deployment.

To address these challenges, this work proposes a blended teaching methodology supported by ProgTutor [4], an ITS designed for programming instruction. ProgTutor integrates a traditional ITS architecture with a 3D robotics simulator to promote a "learning by doing" approach. Its core design principle is to personalize learning experiences while keeping educators in the loop, enabling them to monitor and effectively support student progress. The presented methodology includes, after theoretical instruction, programming exercises, followed by practicing with a 3D robotics simulator (using a plugin in Visual Studio Code, see Figure 1), and finally interaction with the ProgTutor ITS, allowing students to test functionality and evaluate their results in a realistic environment.

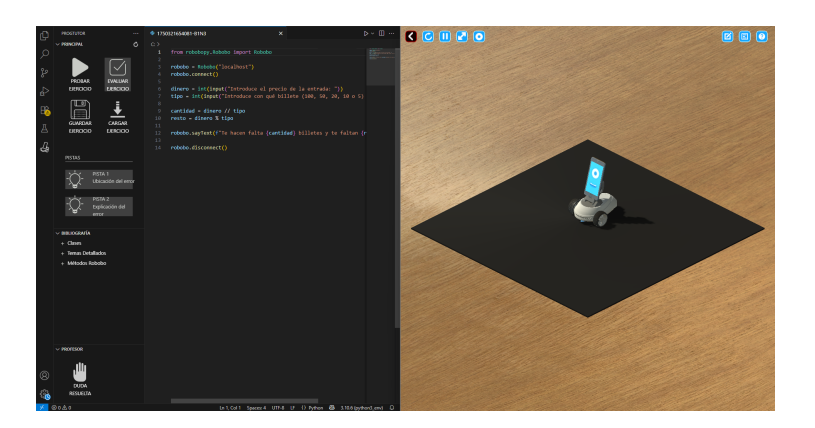


Fig. 1. 3D robotics simulator interface

This paper presents a comparison of the outcomes of applying this methodology over the course of one academic year with two alternative approaches: (1) a traditional methodology without ProgTutor, and (2) a traditional methodology using ProgTutor as a standalone tool. The study offers practical insights and conclusions on how AI driven systems can be effectively integrated into formal education settings.

# 2 ProgTutor Teaching Methodology

To support student learning, programming and robotics professors at the University of A Coruña designed a series of Python based exercises that integrate four core programming topics input/output, conditionals, loops, and functions with robotics elements to enhance practical understanding (Table 1). Each topic is structured into three difficulty levels to promote progressive learning and reinforce prior knowledge. While robotics is used to contextualize tasks, the primary objective of ProgTutor is to teach programming. The exercises are aligned with Level 5 of Bloom's revised taxonomy [1], requiring students to evaluate and develop solutions to complex problems.

Table 1. Programming skills and robotics integration across levels

| Topic        | Level        | Programming focus  | Robot sensors and actuators  |  |  |
|--------------|--------------|--|--|--|--|
| Input/Output | Beginner     | Basic input and output without type conversion, using simple expressions (formulas) to calculate values, focused on basic variables.                                       | Simple actuators<br>to move the robot<br>(timed wheel<br>movements) and                      |  |  |
|              | Intermediate | Input with type conversion, handling more complex mathematical expressions and outputting different data types. Multiple variable types are used.                          | express itself (text<br>to speech, sounds,<br>and LED<br>activation).                        |  |  |
|              | Advanced     | Extends level 2 with the inclusion of more complex algorithms or expressions.  |  |  |  |
| Conditionals | Beginner     | Simple conditional statements using if else or if elif else with basic logical operators (and/or).   | Actuators control<br>the robot's face to<br>show different                                   |  |  |
|              | Intermediate | Multiple elif statements with complex conditions involving multiple logical operators.  snow different emotions, with sensors detecting face position.                     |  |  |  |
|              | Advanced     | Nested conditional structures with increased algorithmic complexity.   |  |  |  |
| Loops        | Beginner     | Use of loops to validate input data and perform iterations within algorithms.  | Actuators enable<br>movement without<br>time control;<br>sensors detect                      |  |  |
| Еборь        | Intermediate | Loops combined with conditional statements to manage algorithm flow.   |  |  |  |
|              | Advanced     | Use of loops to validate input data, integrated with nested loops or tasks involving higher algorithmic complexity.  | wheel positions,<br>orientation, and<br>blobs.   |  |  |
| Functions    | Beginner     | Exercises build on those of intermediate level loops, where the task description clearly defines the functions to implement, along with their input and output parameters. | Advanced sensors<br>support detection<br>of QR codes and<br>objects, enhancing<br>functional |  |  |
|              | Intermediate | The number of functions is given, but parameters and implementation details are left to the student.   | integration.   |  |  |
|              | Advanced     | Students must structure programs with appropriate functions independently; evaluation checks for a minimum number of functions.  |  |  |  |

#### 4 J. Ortega-Morla et al.

For each exercise, students can make multiple attempts including Python coding and testing with the robot simulator before submitting their solution for automated feedback. Once submitted, the ITS performs several checks to verify the solution's correctness. If it is correct, ProgTutor automatically assigns a new exercise to the student. If it is not, it displays a screen with the identified errors and allows the student to try again. Once the ITS considers the student's achievement is adequate, it move on to the next level.

A teaching methodology for the use of ProgTutor in a classroom is proposed here. It emphasizes a blended learning approach, which combines self paced learning facilitated by the ITS with structured teacher led learning. The proposed session schedule is shown in the left part of Figure 2 "ProgTutor methodology". The first two sessions are preparatory to introduce students to a basic knowledge of the Python programming language and the tools they will use during the course. The next sessions follow a cyclical pattern with five main goals: a topic lecture, Python exercises without the simulator, Python exercises with the simulator, sessions with the ProgTutor ITS, and an exam. The cycle starts with a lecture where the teacher explains one of the programming topics established in Table 1. After introducing a topic, practical sessions focus on fundamental Python programming using console based exercises. In the next session, the teacher guides the students through exercises using the robot simulator, encouraging participation rather than lecturing. The final cycle consists of sessions where students complete ProgTutor exercises, with the teacher facilitating and providing support.

In addition to this blended methodology, traditional programming teaching without ProgTutor was used by another student group at the same educational center. The session schedule for traditional teaching is shown in the right part of Figure 2 "Traditional methodology". The first session introduces students to the tools they will use during the course. The next sessions follow a cyclical pattern to teach Python in the following way: a topic lecture followed by practical sessions with console based exercises. Optionally, several sessions using the ProgTutor ITS can be included after those teaching sessions, as shown in Figure 2 "Traditional methodology". Finally, evaluation exams can be performed.

#### 3 Classroom validation

To validate the proposed blended methodology in conjunction with the features of the ITS, the approach was implemented with several groups of students from two different high schools in the northwest of Spain. The students were between 16 and 17 years old, with no previous training on programming fundamentals. Consequently, the results obtained in this study could be applied to similar groups of students, like those in the first year of University degrees or VET education.

For privacy reasons, each institution is referred to as SS1 and SS2. At SS1, there are two groups: one that used the blended methodology with ProgTutor, and a control group that followed a traditional methodology without ProgTutor.

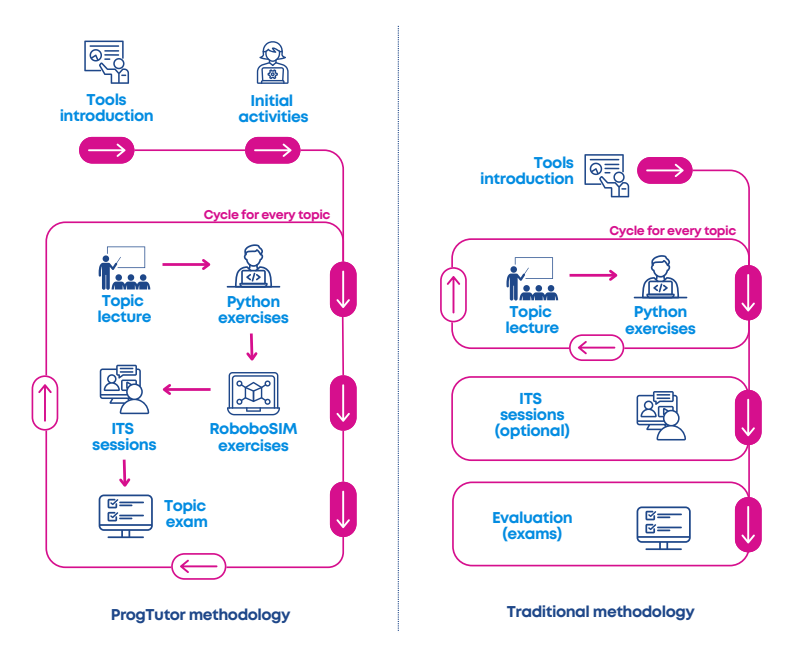


Fig. 2. Different methodologies employed

In contrast, SS2 consists of a single group taught using a non-blended methodology. In this approach, all theoretical content from input/output to functions was first delivered through traditional lectures. Students began using ProgTutor after completing the entire theoretical instruction, starting from the beginning of the curriculum. Notably, no theoretical topics were revisited once the practical use of ProgTutor commenced. This methodology is illustrated in Figure 2 as the "Traditional methodology". Each group consists of between 16 and 19 participants.

The following sections compare the three methodologies to identify which is most suitable for students and which best promotes effective student learning, so which is the most adequate to introduce an ITS in formal education.

# 3.1 Comparison between traditional methodology without ProgTutor and blended methodology using ProgTutor

First, the results from the control and ProgTutor groups at SS1 were compared. It is worth noting that ProgTutor students come from STEM backgrounds, unlike the control group—even though none had prior programming experience. As a result, the control group was unable to complete any functions exercises. Therefore, both groups completed three exams at different stages of the course: the first exam assessed input/output concepts, the second focused on conditional statements, and the third on loops. Boxplots of the scores obtained by each group in these exams are shown in Figure 3.

#### J. Ortega-Morla et al.

6

Based on these results, a statistical test was conducted to assess whether the ProgTutor group outperformed the traditionally taught group in the exams. After revealing that the data did not follow a normal distribution with the Shapiro–Wilk test, the non-parametric Mann–Whitney U test was applied to evaluate differences between the groups. Table 2 shows the p-values for each topic, where values below 0.05 indicate a significant difference between groups. It can be concluded that for introductory topics with low complexity, both the traditional and the ProgTutor methodologies yield comparable learning outcomes. However, as the complexity of the subject increases, the ProgTutor approach demonstrates a clear advantage over the non-blended methodology. This may be attributed to its practical orientation and the use of more realistic examples, which help students better understand complex programming concepts such as multi-branch conditionals and nested loops.

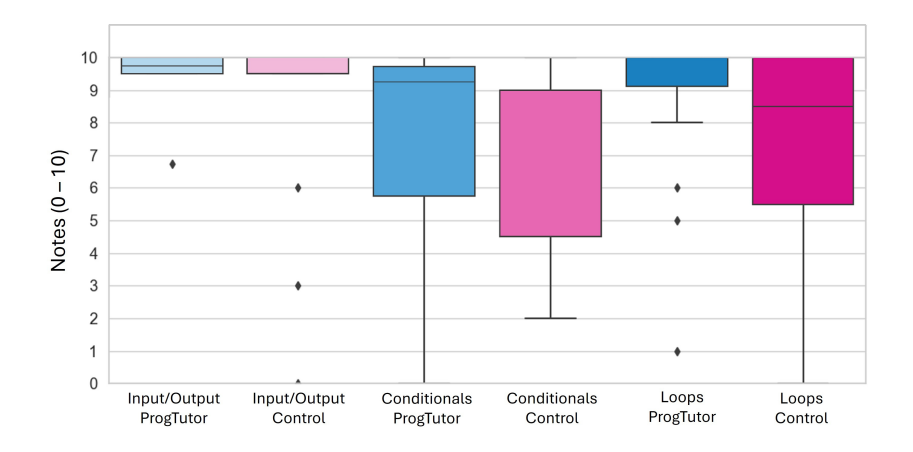


Fig. 3. Distribution of scores by programming topic and group

# 3.2 Comparison between blended methodology using ProgTutor and traditional methodology with ProgTutor

After confirming that the use of ProgTutor enhances learning outcomes, the two methodologies incorporating ProgTutor were analyzed to identify which is more effective for instructional purposes. Figure 4 shows the distribution of hours dedicated to theoretical and practical sessions at both institutions. At SS2, over twice as much time was devoted to theory, with only half as much allocated to ProgTutor based practice. Nevertheless, the total number of instructional hours was comparable across both schools.

An analysis of the different instructional approaches was conducted using a set of three metrics collected throughout the course. These metrics were extracted from each exercise completed by every student in both groups. Similarly to Section 3.1, statistical tests were employed. After confirming non-normal data distributions using the Shapiro-Wilk test (p < .001), the Mann-Whitney U test was applied for further analysis.

Topic Assessedp-valueHypothesis ResultInput/Output0.358Not significantConditionals0.100Trend, not significantLoops0.033Significant in favor of ProgTutor

Table 2. Results of the Mann-Whitney U Test

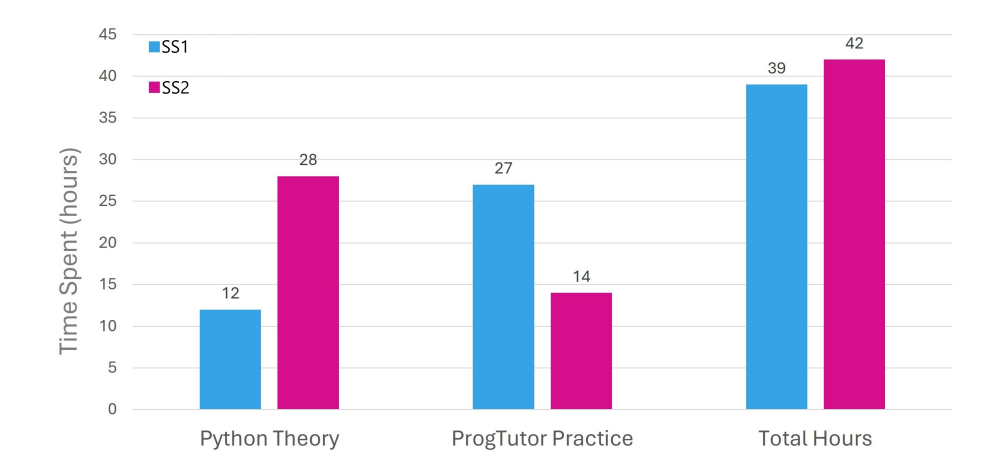


Fig. 4. Distribution of Hours Throughout the Course

The first metric, shown in Figure 5 "Distribution of Python Errors Across Institutions", presents the number of Python errors students made before receiving automated feedback. The data show that students at SS1 made significantly more errors than those at SS2. This reflects differences in instructional methodology: at SS1, the blended approach with ProgTutor emphasizes hands-on exploration, encouraging students to learn through practice. As a result, more early mistakes are expected. However, these initial errors are part of an active learning process that promotes deeper understanding over time. In contrast, the more traditional approach at SS2 tends to produce fewer errors, likely due to stronger emphasis on guided instruction and correctness from the outset.

The second metric analyzed was the distribution of errors during the automated feedback phase of the exercises completed in ProgTutor. As shown in Figure 5 "Distribution of Evaluation Errors Across Institutions", the results reveal no statistically significant differences between the two groups. This suggests that both instructional approaches were similarly effective in helping students reach a comparable level of competence by the time they engaged with the ITS. A possible explanation is that, although students in the blended model made more errors during early exploration, structured support and iterative practice helped consolidate their understanding by the time formal evaluation occurred.

As the final metric, the time students spent solving each of the various exercises was analyzed. Figure 6 presents the distribution of completion times (in

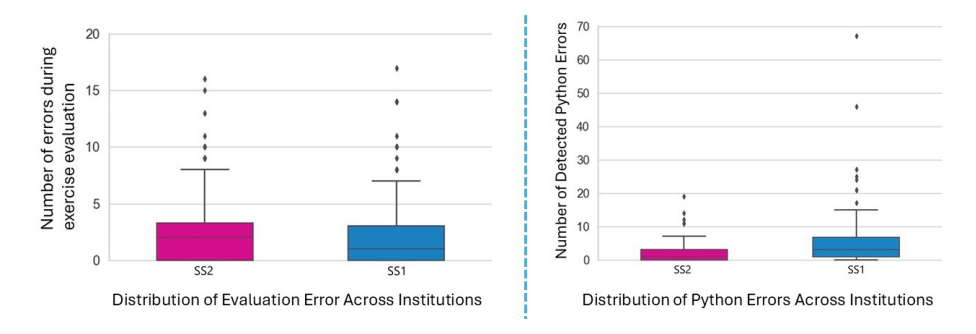


Fig. 5. Distribution of Errors Across Institutions

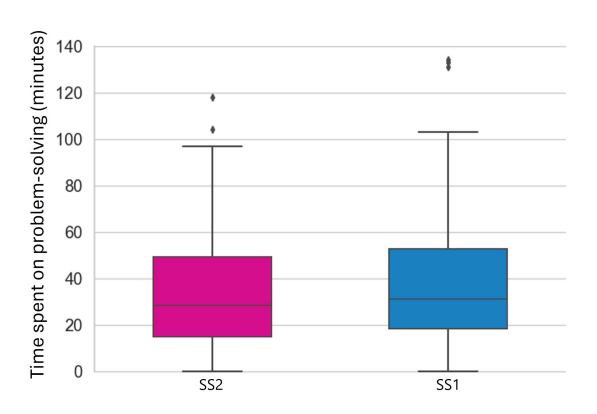


Fig. 6. Distribution of Time Resolution Across Institutions

minutes). The results indicate that there is no statistically significant difference between the two institutions. This suggests that, from the students' perspective, both teaching methodologies perform similarly in terms of exercise completion time.

Additionally, the extent of student progress throughout the course was examined by assessing the topic and level each student had reached by the end of the course. This analysis is presented in Figure 7. The results show that students from SS1 made greater progress, with most of them reaching the advanced level in loops (see table 1). Specifically, 63.2% of students from SS1 reached or surpassed the topic Intermediate Loops, whereas only 37.5% of students from SS2 reached that topic, highlighting a marked difference in progression between the two groups. The greater progress could be partly attributed to the higher number of practical hours (see Fig. 4). However, the key takeaway is that reducing theoretical instruction and increasing hands on practice, while allowing students to advance at their own pace, leads to better performance by the end of the course.

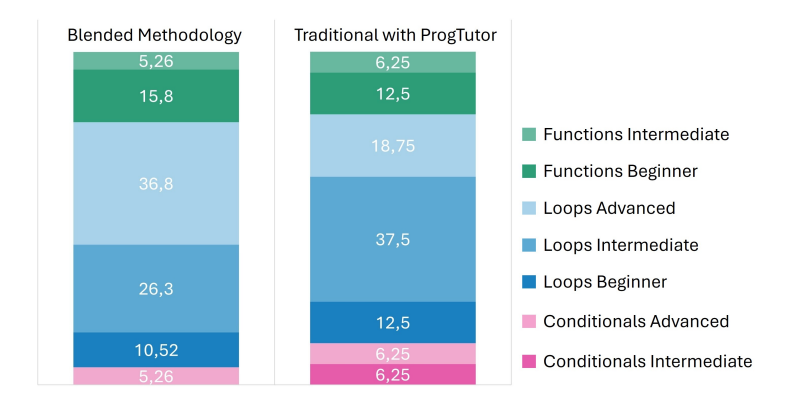


Fig. 7. Distribution of Topics Reached.

#### 4 Conclusions and Future Work

The main conclusion of this validation is that the blended methodology, where traditional and ITS based sessions are interleaved throughout the course, proved to be the most effective. Although students following this methodology made more programming errors during the learning process, these mistakes are a natural part of hands on learning and did not hinder their overall performance. On the contrary, they showed fewer errors during challenge evaluations and achieved similar exercise completion times compared to their peers using a compact approach.

Most notably, the blended methodology enabled students to progress further through the course content, with the majority reaching higher levels in advanced topics. This result highlights that fewer traditional and more theoretical classes do not necessarily lead to reduced learning. On the contrary, allowing students to advance at their own pace appears to facilitate deeper and more enduring knowledge acquisition.

In a more specific realm, findings of this study show that ProgTutor provides advantages over traditional instruction, particularly for more complex topics such as loops. While learning outcomes for introductory topics were comparable between the two approaches, ProgTutor's interactive and practice-oriented methodology led to significantly better performance as topic complexity increased.

While the results are promising, it is important to acknowledge certain considerations. The study involved a limited number of groups from only two high schools, which may influence the extent to which the results can be generalized. Additionally, although students reportedly had no prior programming experience, potential differences in initial knowledge or motivation were not systematically assessed. Future research should aim to replicate these results with a larger number of students and across different educational institutions.

# Acknowledgment

The TED2021-131172B-I00 grant was funded by MCIN/AEI and the European Union NextGenerationEU/PRTR. Support was also received from the Galician Research Center (CITIC), funded by the Government of Galicia and the European Union (FEDER GALICIA 2014-2020 program), through grant ED431G 2019/01, as well as from the Galician Government group (ED431C 2022/44) with FEDER funds.

#### References

- 1. Anderson, L.W., Krathwohl, D.R.: A Taxonomy for Learning, Teaching, and Assessing: A Revision of Bloom's Taxonomy of Educational Objectives (2001)
- Francisco, R.E., de Oliveira Silva, F.: Intelligent tutoring system for computer science education and the use of artificial intelligence: A literature review. In: Proceedings of the 14th International Conference on Computer Supported Education (CSEDU 2022). pp. 338–345. SCITEPRESS (2022). https://doi.org/10.5220/0011084400003182
- 3. Kabudi, T., Pappas, I., Olsen, D.H.: Ai-enabled adaptive learning systems: A systematic mapping of the literature. Computers and Education: Artificial Intelligence 2, 100017 (2021)
- Leis, A., Mallo, A., Guerreiro-Santalla, S., Paz-López, A., Bellas, F.: Personalized learning of programming fundamentals through robotic simulations. AI in Education and Educational Research 2519 (2025)
- Maedche, A., Legner, C., Benlian, A., Berger, B., Gimpel, H., Hess, T., Hinz, O., Morana, S., Söllner, M.: AI-based digital assistants: Opportunities, threats, and research perspectives. Bus. Inf. Syst. Eng. 61, 535–544 (2019)
- Mousavinasab, E., Zarifsanaiey, N., Kalhori, S.R.N., Rakhshan, M., Keikha, L., Saeedi, M.G.: Intelligent tutoring systems: a systematic review of characteristics, applications, and evaluation methods. Interactive Learning Environments 29(1), 142–163 (2021). https://doi.org/10.1080/10494820.2018.1558257
- Panigutti, C., Hamon, R., Hupont, I., Fernandez Llorca, D., Fano Yela, D., Junklewitz, H., Scalzo, S., Mazzini, G., Sanchez, I., Soler Garrido, J., Gomez, E.: The role of explainable ai in the context of the ai act. In: Proceedings of the 2023 ACM Conference on Fairness, Accountability, and Transparency. p. 1139–1150 (2023)
- 8. Price, T.W., Dong, Y., Lipovac, D.: isnap: Towards intelligent tutoring in novice programming environments. In: Proceedings of the 2017 ACM SIGCSE Technical Symposium on Computer Science Education (SIGCSE '17). pp. 483–488. ACM, Seattle, WA, USA (2017). https://doi.org/10.1145/3017680.3017762
- Roldán-Álvarez, D., Mesa, F.J.: Intelligent deep-learning tutoring system to assist instructors in programming courses. IEEE Transactions on Education 67(1), 153– 160 (2024). https://doi.org/10.1109/TE.2023.3331055
- 10. Sharma, P., Harkishan, M.: Designing an intelligent tutoring system for computer programming in the pacific. Education and Information Technologies **27**(5), 6197–6209 (2022). https://doi.org/10.1007/s10639-021-10882-9
- 11. Shemshack, A., Spector, J.M.: A systematic literature review of personalized learning terms. Smart Learning Environments **7**(1), 33 (2020)
- 12. Zhang, L., Basham, J.D., Yang, S.: Understanding the implementation of personalized learning: A research synthesis. Educ. Res. Rev. **31**, 100339 (2020)

# Generative AI Use Scale Indicators in Higher Education

Elena Del  $Val^{1[0000-0002-1279-3429]}$  and Joaquin Taverner<sup>1[0000-0002-5163-5335]</sup>

Valencian Research Institute for Artificial Intelligence (VRAIN). Universitat Politècnica de València, Valencia, Spain. edelval@dsic.upv.es

Abstract. The integration of generative artificial intelligence (GAI) in higher education offers promising opportunities for personalized learning, enhanced assessment, and improved teaching practices. However, the ethical, pedagogical, and practical challenges posed by GAI require structured frameworks to guide its responsible use. This paper reviews five scales of GAI use in educational contexts and identifies their strengths and limitations. Based on this analysis, we propose a new framework called SCALE-E (Structured Competency-Aligned Levels for Ethical AI in Education), which focuses on aligning AI use with the development of key transversal competencies such as critical thinking, creativity, problem solving, and autonomy. SCALE-E advances current approaches by transforming AI interaction into a formative and ethical learning experience through five progressive levels of AI integration. We illustrate the application of SCALE-E in a programming course, demonstrating its potential to enhance technical skills and transversal competencies.

**Keywords:** Generative AI  $\cdot$  Higher Education  $\cdot$  Scale  $\cdot$  Computer Science

#### 1 Introduction

The incorporation of generative artificial intelligence (GAI) in education provides new opportunities to personalize learning, improve assessment, and facilitate teaching, especially in higher education [5, 2]. However, the deployment of these technologies also poses significant challenges related to ethics, privacy, fairness and transparency [3]. Particularly, evaluating the responsible use of GAI in educational environments requires a framework that considers both the pedagogical impact and the social and ethical implications [13]. The automation of educational processes with GAI must ensure that fundamental values of learning, such as learner autonomy and academic integrity, are not compromised [12].

In this scenario, various scales and guides emerge that seek to regulate, orient and evaluate the use of GAI in higher education, particularly in the area of learning assessment. These scales guide teachers and students and standardize institutional practices, promoting equity and ensuring academic integrity [3, 15].

The diversity of proposals reflects different pedagogical philosophies: from normative approaches focused on control to formative perspectives that promote critical literacy in GAI.

This paper provides an analysis of the main current proposals on scales for the use of GAI in educational contexts, with a special focus on higher education. Based on this analysis, a new framework called SCALE-E is proposed, which seeks to integrate the use of generative artificial intelligence with the development of key transversal competencies in higher education. This proposal aims to provide a formative and ethical vision, oriented towards a pedagogical transformation that enhances critical, creative and strategic skills in students. Finally, the practical application of this scale is illustrated in a real case within the subject of Programming demonstrating its potential to facilitate a responsible and enriching use of GAI in academic environments.

The remainder of this paper is structured as follows. Section 2 provides a review of relevant existing scales and frameworks for GAI use in education. Section 3 presents the SCALE-E framework. Section 4 illustrates the practical application of SCALE-E within a university programming course as a concrete use case. Finally, Section 5 summarizes the main conclusions and outlines directions for future research.

#### 2 Use scales

The rapid evolution of GAI has resulted in a growing amount of research focused on its integration in higher education, particularly with regard to the assessment of learning. In this context, various theoretical and practical proposals have emerged that seek to establish frameworks, ethical principles and operational criteria for a responsible and effective use of these technologies. One of the first proposals that has gained visibility in this field is the AIAS (Artificial Intelligence Assessment Scale) [7]. This scale was developed with the purpose of providing an ethical and operational framework for the integration of GAI in academic assessment tasks. The AIAS scale establishes five clearly defined levels: Level 0 (No AI (Artificial Intelligence)), Level 1 (Limited AI), Level 2 (Moderate AI), Level 3 (High AI) and Level 4 (Full AI). These levels reflect the proportion and nature of AI use permitted by the student when performing an evaluative task, ranging from complete prohibition to active co-authorship with AI systems. Each level includes specific examples of permitted use and recommendations for implementation. Initially, the scale was presented with a traffic light-like color structure (red to green), but was redesigned with a pastel color palette, in order to avoid symbolic associations of judgment or sanction, and to emphasize its guiding rather than restrictive intent [8]. The fundamental objectives of the scale are to assist educators in adapting their assessments in light of GAI tools, to clarify for students the permissible use of AI in their work, and to support the completion of assessments in accordance with the principles of academic integrity. In this sense, the scale seeks to promote an ethical use of GAI tools, while fostering both the development of academic knowledge and practical skills

related to the critical and effective use of these technologies. Its main strength lies in its normative clarity and its transversal applicability to different educational levels and disciplines. The AIAS has been widely adapted in many different contexts, both K-12 and higher education [1, 11].

In [10], the AIAS scale was adapted for English language teaching contexts for academic purposes. This adaptation, denoted EAP-AIAS (English for Academic Purposes - Artificial Intelligence Assessment Scale), retains the five-level structure of the original model, but redefines each level in terms of specific language tasks, such as writing argumentative essays, writing critical summaries, and preparing oral presentations. In addition, it offers detailed examples and realistic scenarios that illustrate the potential use of GAI tools in learning academic English. It also provides differentiated guidance according to students' level of language proficiency. In contrast to the general AIAS scale, which is more normative, the EAP-AIAS incorporates a formative component that recognizes the value of AI as a mediator in language learning processes and explicitly links each level to well-established approaches in teaching English for academic purposes.

The CAIAF (Comprehensive AI Integration Assessment Framework) scale represents a significant evolution in the design of frameworks for the integration of AI in educational contexts [4]. Unlike more normative models such as AIAS, the CAIAF introduces six progressive levels of AI use, accompanied by a gradient-based visual system that allows for nuancing the intensity and risk associated with each level. Level 0 corresponds to the total absence of AI in academic production. Level 1 allows minimal use, such as spelling corrections or superficial aids. In Level 2, AI is used functionally as a support tool, without intervening directly in the authorship of the content. Level 3 contemplates a collaborative use, in which the AI actively contributes to the generation of content under the critical supervision of the learner. At Level 4, the AI can act more autonomously, generating substantive parts of the work, but requires the student to perform a reflective review. Finally, Level 5 allows for advanced, personalized use of AI, with dynamic real-time adaptations and an emphasis on ethical co-authorship. This structure recognizes the diversity of possible interactions between learners and generative technologies. It also incorporates ethical principles such as transparency, equity, pedagogical alignment and data protection. In addition, its design contemplates the possibility of adaptation to different educational levels (primary, secondary and higher education), making CAIAF a flexible, expansive and future-oriented tool for the design and evaluation of AI-mediated educational tasks.

The scale proposed in [14] is adapted for K-12/secondary education and highlights practical classroom application, teacher support, and age-appropriate considerations, including legal compliance (GDPR, parental consent). It departs from the tiered approach of previous proposals and instead offers an open-ended, formative guide for integrating AI into teaching and assessment. This guide emphasizes the need for critical reflection, co-creation, and student agency. Its approach is not intended to categorize the use of AI in a normative way, but to provide a repertoire of best practices, ethical principles, and examples of

assignments that foster meaningful integration of GAI. It aims to guide students in the responsible use of artificial intelligence in teaching and learning processes and to clarify the extent to which AI can be used. The strength of this guide lies in its flexibility and its ability to adapt to changing contexts. It is particularly useful for institutions seeking to promote digital literacy and critical competence.

Finally, the AI Creative Framework Indicator (ACFI) is a framework with short codes that creators can use to declare, in a transparent and standardized way, the level of involvement of artificial intelligence (AI) in their creative works (texts, images, videos, etc.) [6]. The system is based on two-letter labels representing different uses of AI in the creative process. These labels are placed on a standard line, where each code indicates a specific type of AI intervention. Among the main codes are: IG (Idea Generation), when AI is used for idea generation or concept brainstorming; GE (Generative Editing), which indicates that AI has directly produced textual, visual, or auditory content; and AE (AI Editing), referring to the use of AI for editing, proofreading, or rewriting. Other relevant codes include RD (Research/Development Support), which implies a use of AI to gather or synthesize information, and IN (Inspiration), which identifies a purely inspirational use, with no direct intervention in the final product. Finally, the NA code (No AI Used) certifies the total absence of AI in the process. For instance, ACFI: IG, AE, means that AI was used to generate ideas and also to edit the final text.

Table 1 presents a clear and structured overview of the main scales and frameworks developed to guide the use of generative artificial intelligence in educational contexts. It can be seen that, although all proposals share an interest in integrating AI in an ethically and pedagogically meaningful way, they differ markedly in their approach, levels of structuring, and scope of application. For example, both the AIAS and the EAP-AIAS propose progressive levels of AI use, focused on the validity of the assessment and the development of competencies, the latter being a specific adaptation to the field of academic English. In contrast, CAIAF adopts a more ethical and evaluative approach, moving away from formal levels and prioritizing risk analysis and alignment with learning outcomes. The AI Assessment and Teaching Guide, while also structuring the use of AI into five levels, is distinguished by its practical orientation, designed by and for teachers, and by its explicit intention not to hierarchize the use of AI, but to promote contextualized pedagogical decisions. Finally, the ACFI focuses on introducing a concise, code-based system that does not prescribe levels of use. It classifies the type of AI participation in a creative or academic product, thus encouraging learner self-awareness, transparency and responsible authorship.

While each framework offers valuable insights, they also involve certain considerations that condition their practical application. For example, the AIAS scale offers a clear normative structure, but its effectiveness depends on sufficiently trained faculty and may require adaptation to address the nuances of highly specialized tasks. Similarly, the EAP-AIAS focuses specifically on academic English, so it largely conforms to language acquisition principles, but its applicability beyond this domain would benefit from further empirical validation.

Table 1. Comparison of GAI use scales in education

| Scale                                       | Purpose  | AI Use   | Pedagogical<br>Approach  | Application  |
|---|--|--|--|--|
| AIAS [7]                                    | Ethical integra-<br>tion of GenAI<br>into educational<br>assessments               | 5 levels: No AI, Limited AI, Structured AI Use, Creative AI Use, AI Exploration  | Social construc-<br>tivism, emphasis<br>on assessment<br>validity  | General education (K-12 and higher education)  |
| EAP-AIAS [10]                               | Adaptation of<br>AIAS to English<br>for Academic<br>Purposes (EAP)<br>instruction  | 5 adapted levels:<br>No AI, Aware-<br>ness, Light AI<br>Use, Moderate AI<br>Use, Full AI Use   | Development of language skills and academic acculturation  | English for Academic Purposes (EAP) teaching   |
| CAIAF [4]                                   | Ethical and effective integration of AI in assessment and learning                 | 6 levels: No AI, Minimal AI Use, Functional AI Use, Collaborative AI Use, Autonomous AI with Oversight, Advanced and Personalized AI Use | Ethics-centered<br>pedagogy, au-<br>thentic learning,<br>adaptable to di-<br>verse educational<br>levels | General and<br>specialized edu-<br>cation (primary,<br>secondary, and<br>higher education) |
| AI Assessment<br>and Teaching<br>Guide [14] | To guide peda-<br>gogical decisions<br>regarding AI use<br>in educational<br>tasks | 5 levels: No AI,<br>AI for Feedback,<br>AI as a Tool, AI<br>as a Co-Creator,<br>AI as an Evalua-<br>tor                                  | Teacher reflec-<br>tion, alignment<br>with learning<br>objectives, con-<br>textual decision-<br>making   | Secondary educa-<br>tion (adaptable<br>to other contexts)                                  |
| ACFI [6]                                    | To promote transparency in AI involvement in creative/academic work                | Code-based: IG,<br>GE, AE, RD, IN,<br>NA   | Digital literacy,<br>critical reflection,<br>authorship ac-<br>countability                              | Creative writing,<br>media produc-<br>tion, student<br>self-reporting                      |

The CAIAF model provides an ethically robust and future-proof structure, yet its methodological complexity may pose challenges in under-resourced contexts or where AI literacy is still emerging. The AI Assessment and Teaching Guide provides flexibility and encourages critical thinking but may lack the clarity some educators require in regulated settings. The ACFI, by contrast, does not function as a normative scale but rather as a complementary transparency tool; it empowers students to explicitly declare how AI was involved in their work using a simple coding system. This can be particularly powerful in formative contexts, promoting ethical reflection, digital literacy, and academic integrity through learner-centered practices. However, its effectiveness relies on students' understanding of the codes and teachers' ability to interpret them meaningfully within assessment criteria.

Taken together, these considerations illustrate the growing need for diversified frameworks that respond to the multiple dimensions (i.e., ethical, peda-

gogical, and institutional) of AI integration in education. Rather than seeking a universal solution, a more productive path may lie in adopting complementary tools, such as combining normative scales like AIAS or CAIAF with reflective instruments like ACFI, to foster both regulation and agency in the use of GAI.

### 3 Proposal

In response to the growing integration of generative artificial intelligence in educational environments, we present the SCALE-E (Structured Competency-Aligned Levels for Ethical AI in Education) framework, a new scale designed to guide its use in higher education. This proposal focuses on how the application of GAI can enhance the development of transversal competencies essential for the integral formation of students. These competencies include critical thinking, professional ethics, effective communication, autonomous learning, creativity, and teamwork. By integrating the ethical and critical use of AI with these skills, SCALE-E aligns with the principles of European digital competence frameworks such as DigCompEdu [9], which aim to empower educators and facilitate the development of students' digital competence in the digital age. The SCALE-E framework aims to transform that use into a deliberate and measurable formative component. To achieve this, the scale establishes progressive levels of AI integration aligned with the promotion of transversal competencies across diverse learning activities. The framework is structured into five levels of integration. These levels are designed as progressive steps in terms of the complexity of AI interaction, the degree of student autonomy, and the depth of required critical reflection (see Table 2). They are not hierarchical in the sense that a higher level is inherently better or more desirable than a lower one. The appropriate level is determined by the specific learning objectives and pedagogical context of the task. Each level explicitly incorporates one or more transversal competencies that students are expected to develop through their interaction with AI:

- Level 1: Assisted Exploration: At this level, the use of GAI is limited to consultation or informational support tasks, such as obtaining basic explanations, definitions, or summaries. The student does not use GAI to produce final content, but rather to enrich their understanding and access different perspectives before developing their own ideas. This initial interaction with AI fosters competencies such as information management, basic critical thinking, and the ethical use of digital tools, laying the foundation for autonomous and informed learning.
- Level 2: Guided Elaboration: Here, the student uses AI as an active companion in constructing academic work, for example, by generating drafts, structural suggestions, or preliminary ideas that are later reviewed and reworked. AI becomes a cognitive support tool that facilitates idea organization and process planning. The objective of this level is to promote competencies such as written communication, analytical capacity, strategic planning, and evaluative judgment, as the student must critically engage with the system's suggestions and build upon them.

Table 2. SCALE-E Proposal.

| Level   | Description   | Developed Competencies  | Example in Programming   |  |
|---|---|---|--|--|
| Level 1: Assisted Exploration                         | Use of AI to obtain<br>basic explanations,<br>definitions, or sum-<br>maries, without<br>generating final con-<br>tent. | Information management, basic critical thinking, ethical use of digital tools.                  | The student queries AI to understand what a recursive function is or how a for loop is structured.   |  |
| Level 2: Guided Elaboration                           | AI helps construct initial ideas such as outlines or drafts that the student later critically revises.                  | Strategic planning,<br>written communica-<br>tion, analysis, and<br>evaluative judgment.        | The student asks AI for a solution outline for a sorting algorithm and adapts it, modifying its logic.   |  |
| Level 3: Reflective<br>Co-creation                    | Collaboration with AI to create products that integrate creativity and personal judgment.                               | Creativity, informed decision-making, complex problem solving.                                  | The student generates<br>an initial graphical<br>interface with AI,<br>then redesigns and<br>customizes both de-<br>sign and functionality.    |  |
| Level 4: Critical and<br>Ethical Evaluation           | The student analyzes AI outputs, detecting errors, biases, or limitations.  | Advanced critical thinking, digital literacy, professional ethics.                              | After reviewing AI-<br>generated code, the<br>student identifies se-<br>curity vulnerabilities<br>and proposes justified<br>improvements.      |  |
| Level 5: Metareflection and Design of AI Interactions | The student designs strategies for AI use in academic or professional contexts.   | Strategic thinking, in-<br>novation, ethical lead-<br>ership, advanced digi-<br>tal competence. | Develops a guide for<br>implementing AI in<br>collaborative software<br>development, consid-<br>ering ethical and tech-<br>nical implications. |  |

- Level 3: Reflective Co-creation: At this level, the student collaborates with AI in a generative process that requires judgment, adaptation, and creativity. It is not merely about accepting or rejecting what AI produces, but about integrating it thoughtfully into the development of original solutions or outputs. This symmetrical interaction activates competencies such as creativity, informed decision-making, complex problem-solving, and autonomous learning, as the student becomes a designer and critical editor of the AI's contributions. While Level 2 focuses on using AI for planning and structuring initial ideas, Level 3 moves towards a more generative partnership where AI contributes substantively to the creative output, requiring the student to act as a critical co-designer and integrator of AI-generated content into an original work.
- Level 4: Critical and Ethical Evaluation: This level involves a shift in focus: the student not only uses AI, but also analyzes its outputs, functioning, and limitations. They are expected to identify errors, biases, or inconsistencies in AI-generated content and propose more rigorous or responsible alternatives.

Table 3. Competency Assessment Rubric Using the SCALE-E Scale

| Competency                          | Level 1  | Level 2   | Level 3   | Level 4   | Level 5   |
|-------------------------------------|--|---|---|---|---|
| Information Management              | Consults AI for basic explanations.                            | Selects<br>useful sug-<br>gestions to<br>organize<br>work.                | Integrates<br>relevant AI<br>information<br>into creative<br>solutions. | Identifies limitations in AI-generated information.                                 | Critically evaluates the appropriateness of using AI in different contexts. |
| Critical Thinking                   | Recognizes<br>simple<br>concepts<br>suggested<br>by AI.        | Evaluates proposed ideas, accepting or rejecting them with justification. | Makes informed decisions by combining AI inputs with own reasoning.     | Analyzes biases, errors, and limitations in generated content.                      | Designs<br>strategies<br>for respon-<br>sible and<br>effective AI<br>use.   |
| Communication and Planning          | Understands<br>basic struc-<br>tures with<br>AI help.          | Uses AI to outline solutions and organize tasks.                          | Refines planning by integrating creativity and functionality.           | Proposes<br>organi-<br>zational<br>improve-<br>ments and<br>argues their<br>impact. | Leads<br>strategic<br>design<br>processes<br>involving<br>AI.               |
| Creativity and Prob-<br>lem Solving | Uses simple examples suggested by AI.                          | Modifies AI-<br>proposed<br>examples to<br>adapt them.                    | Creates<br>original<br>products<br>through<br>interactions<br>with AI.  | Reformulates<br>solutions<br>to complex<br>problems<br>generated<br>by AI.          | Designs new human—AI interaction methods that innovate the process.         |
| Ethics and Digital<br>Literacy      | Uses AI with teacher guidance and basic awareness of its role. | Recognizes<br>the need to<br>review and<br>validate AI<br>output.         | Acts responsibly when integrating AI into decisions.                    | Highlights ethical implications and proposes actions to mitigate them.              | Leads<br>critical re-<br>flection on<br>the social<br>impact of<br>AI use.  |

Such tasks promote a deep understanding of the technology and develop key competencies such as advanced critical thinking, digital literacy, professional ethics, and argumentative reasoning, preparing students for conscious and socially responsible use of AI in their field. This level builds upon the critical understanding and evaluation skills developed in Level 4, extending them to a meta-cognitive and strategic level regarding the role and integration of AI in broader contexts. It requires not just using or evaluating AI outputs, but critically analyzing the very process of AI interaction and its systemic implications.

Level 5: Metareflection and Design of AI Interactions: This level represents
the highest degree of student agency and strategic thinking regarding AI
integration. It positions the student not just as a user, but as a designer and

strategist of AI use. Students are expected to critically reflect on how and when AI should be integrated into academic or professional processes and even propose new forms of human-AI collaboration that maximize added value and minimize risks. This level activates competencies such as strategic thinking, innovation, ethical leadership, and advanced digital competence, equipping students to lead the transformative integration of AI in real-world contexts.

SCALE-E builds on a competency-based framework that directly aligns with learning outcome-oriented university curricula, ensuring that each level of AI integration corresponds to specific learning objectives. SCALE-E places learner development at the center, illustrating how each task (with its varying degrees of autonomy, complexity and reflection) contributes to the growth of transversal competencies. To make this process transparent and practical, each level is supported by clear, observable indicators that teachers can use to assess mastery and provide specific feedback during real academic activities.

# 4 Use Case: Programming course

The Programming course of the Industrial Informatics and Robotics Degree of the Universitat Politècnica de València aims to provide students with a solid foundation in programming logic, data structures, and computational problemsolving. In this context, the incorporation of GAI can be a powerful tool to enrich the learning process and the development of transversal competencies, provided its use is aligned with clear pedagogical goals.

The following example illustrates how the SCALE-E can be applied in this course to guide and enhance the formative use of AI, linking different levels of interaction with the progressive development of skills such as critical thinking, creativity, professional ethics, and self-assessment (see Table 3). This approach seeks to optimize the technical learning of programming and prepare students for a conscious and responsible use of emerging technologies in their future professional careers.

- Level 1: Assisted Exploration: At this level, the student uses AI to obtain simple explanations of concepts such as variables, control structures, or data types. For example, they may ask the AI to explain what a for loop is or to provide simple C++ code examples. Here, AI acts as a supplementary resource to clarify doubts and support autonomous learning without replacing the student's own coding process.
- Level 2: Guided Elaboration: While developing a small program, the student uses AI to suggest the general structure of the code or to generate initial fragments that they then manually adapt and correct. For instance, they might ask for help creating pseudocode for a search algorithm and then convert it into functional code, reviewing and debugging the final result. This level works on competencies related to planning, analysis, and technical communication.

- Level 3: Reflective Co-creation: The student collaborates with AI to design and develop more complex solutions, such as implementing recursive functions or basic data structures (linked lists, stacks). AI may suggest alternative implementations that the student must evaluate, modify, and justify based on criteria like efficiency or readability. This stage fosters creativity and applied critical thinking in software development.
- Level 4: Critical and Ethical Evaluation: At this stage, the student analyzes AI-generated or suggested code to identify potential logical errors, security vulnerabilities, or poor programming practices. They also reflect on the ethical implications of automating certain programming tasks or potential bias in algorithm selection. For example, the student might detect if AI proposes solutions that fail to handle exception cases properly or could lead to failures in industrial systems.
- Level 5: Metareflection and Design of AI Interactions: Finally, the student designs a small project or methodology in which AI is integrated responsibly and efficiently into the software development process, such as automating unit tests or generating technical documentation. Additionally, they reflect on AI's limitations in industrial programming and propose strategies to supervise or audit its contributions, promoting ethical leadership and innovation.

#### 5 Conclusions

In this paper, we have conducted a critical analysis of five existing scales for evaluating the use of GAI in education. The examined scales present diverse approaches, ranging from measuring the degree of AI involvement to offering ethical and pedagogical frameworks for educators. Building on the strengths and limitations identified, we propose a new scale: SCALE-E. This scale emphasizes the integration of AI with the development of transversal competencies such as creativity, critical thinking, problem solving, and autonomy. SCALE-E represents a meaningful advancement beyond previous models by explicitly linking GAI use to the cultivation of essential transversal skills in higher education. This approach supports ethical and pedagogical decision making regarding the use of AI and transforms the interaction with AI into a holistic formative experience. Additionally, we have presented an instantiation of the scale applied to a firstvear university programming course, illustrating how SCALE-E can guide and enhance the formative use of AI in concrete academic settings. While SCALE-E provides a general framework, its application in various disciplines such as the humanities, medical sciences, or others will require specific adaptations. Each field presents unique pedagogical goals, assessment practices, and potential ethical challenges related to the use of AI. Therefore, effective implementation of SCALE-E will require adapting the levels, examples, and alignment of competencies to the specific context of each academic area. Future work will focus on empirically validating the scale's effectiveness and exploring tailored adaptations for specific academic fields.

# Acknowledgements

Work supported by PIME/24-25/429 project funded by Instituto de Ciencias de la Educación (ICE) of the Universitat Politècnica de València.

#### References

- 1. Leon Furze. The ai assessment scale in action: Examples from k-12 and higher education across the world, May 2024. Blog post.
- Wayne Holmes, Maya Bialik, and Charles Fadel. Artificial intelligence in education: Promises and implications for teaching and learning. Boston: Center for Curriculum Redesign, 2019.
- 3. Wayne Holmes, Maya Bialik, and Charles Fadel. Ethics of ai in education: Towards a typology of risks and opportunities. *International Journal of Artificial Intelligence in Education*, 31:209–233, 2021.
- 4. Selçuk Kılınç. Comprehensive ai assessment framework: Enhancing educational evaluation with ethical ai integration. *Journal of Educational Technology and Online Learning*, 7(4-ICETOL 2024 Special Issue):521–540, 2024.
- 5. Rose Luckin, Wayne Holmes, Mark Griffiths, and Laurie B Forcier. *Intelligence unleashed: An argument for AI in education*. Pearson Education, 2016.
- Nneka J. McGee. Ai creative framework indicator (acfi), 2024. Posted on LinkedIn.
   A framework for disclosing AI involvement in creative work using standardized codes.
- 7. Mike Perkins, Leon Furze, Jasper Roe, and Jason MacVaugh. The artificial intelligence assessment scale (aias): A framework for ethical integration of generative ai in educational assessment. *Journal of University Teaching and Learning Practice*, 21(6):49–66, 2024.
- 8. Mike Perkins, Jasper Roe, and Leon Furze. The ai assessment scale revisited: A framework for educational assessment. arXiv preprint arXiv:2412.09029, 2024.
- 9. Christine Redecker. Digcompedu. Beurteilung der Digitalen Kompetenz Lehrende. Online verfügbar unter https://joint-research-centre. ec. europa. eu/system/files/2018-09/digcompedu\_leaflet\_de\_2018-01. pdf (abgerufen am: 20.11. 2020), 2017.
- 10. Jasper Roe, Mike Perkins, and Yulia Tregubova. The eap-aias: Adapting the ai assessment scale for english for academic purposes. arXiv:2408.01075, 2024.
- 11. Jeremie Rostan. Leon furze's "ai assessment scale": a critique and two alternative options, 2023. Publicado en el blog personal de Jeremie Rostan.
- Neil Selwyn. Should robots replace teachers? AI and the future of education. Polity, 2019.
- 13. Ben Williamson. Education governance and datafication. *Learning, Media and Technology*, 45(1):4–15, 2020.
- 14. Robbe Wulgaert. Ai assessment and teaching guide. https://www.robbewulgaert.be/education/ai-assessment-scale, 2024. Accedido el 27 de mayo de 2025.
- 15. Olaf Zawacki-Richter, Verónica I Marín, Michael Bond, and Benoît Gouverneur. Systematic review of research on artificial intelligence applications in higher education – where are the educators? *International Journal of Educational Technology in Higher Education*, 16(1):39, 2019.

# Semantic Systematic Review of Artificial Intelligence-Based Maturity Models for Teaching Feedback in Higher Education

Cristian Valdes Perez  $^{1[0000-0002-7945-1933]}$ , Angel Arroyo Puente  $^{2}$   $^{[0000-0002-1614-9075]}$ , and Jose Manuel Galán Ordax  $^{3}$   $^{[0000-0003-3360-7602]}$ 

<sup>1</sup> Facultad de Ingeniería, Universidad San Sebastián, Bellavista 7, Recoleta, Chile cristian.valdes@uss.cl

<sup>2</sup> Grupo de Inteligencia Computacional Aplicada (GICAP), Departamento de Digitalización, Escuela Politécnica Superior, Universidad de Burgos,

Av. Cantabria s/n, 09006, Burgos, Spain aarroyop@ubu.es

<sup>3</sup> Departamento de Ingeniería de Organización, Escuela Politécnica Superior, Ed. A1. Universidad de Burgos. Avda, Cantabria S/N. 09006, Burgos, Spain jmgalan@ubu.es

Abstract. This study presents a semantic systematic review of the literature on Artificial Intelligence enhanced maturity models for improving teaching feedback in higher education. Using PRISMA methodology and semantic analysis, 159 relevant publications were identified and examined. The review process included database searches, multi-stage screening, and natural language processing techniques to cluster thematic patterns and identify research gaps. The findings reveal a predominance of conceptual models with limited empirical validation and a fragmented integration of Artificial Intelligence technologies, particularly and machine learning into structured institutional frameworks. The review highlights the need for models that prioritize contextualized implementation, faculty engagement, ethical transparency, and actionable analytics, or data-driven insights that directly inform decision making and pedagogical improvement. It provides a foundation for developing integrated AI-powered maturity models that support continuous improvement in teaching quality

**Keywords:** Artificial Intelligence; Teaching Evaluation; Maturity Models; Systematic Review; Semantic Analysis; Higher Education.

# 1 Introduction

In recent years, higher education institutions have increasingly adopted data-driven approaches to improve teaching quality. Among these, Student Evaluations Teaching (SET) [1] have become one of the most used mechanisms for measuring academic performance and identifying opportunities for pedagogical improvement [2].

This gap has led to the search for more structured and intelligent systems capable of processing and interpreting information in a meaningful way. In this context, Artificial

Intelligence (AI) offers promising capabilities to transform raw feedback into relevant and individualized insights [3]. AI enables the application of data mining, semantic analysis, and predictive modeling techniques that enhance feedback cycles and contribute to teaching quality improvement [4].

Maturity models, on the other hand, provide structured frameworks to assess and improve institutional processes. A maturity model typically defines a series of development stages that describes how an organization can evolve from an initial, "ad hoc" state to a more optimized and more effective one. When applied to educational management, these models help diagnose current institutional states, define improvement pathways, and monitor their evolution over time [5] [6].

However, the existing literature appears fragmented across disciplines such as educational technology, data science, and institutional research. This article aims to synthesize this literature through a semantic systematic review, identifying studies that propose or apply AI-based maturity models focused on faculty feedback.

The structure of this article is as follows: Section 2 presents a review of relevant literature on AI-based maturity models and their application in teaching evaluation. Section 3 details the research objectives and describes the systematic review methodology, including data collection and semantic analysis. Section 4 reports the main results, including thematic patterns and model characteristics. Section 5 offers a discussion of the findings and identifies future research opportunities. Finally, Section 6 presents the conclusions and outlines the implications for institutional practice and educational research.

### 2 Theoretical Framework

Maturity Models are structured frameworks that characterize the progressive development of organizational capabilities or processes across defined levels. These models are typically used to evaluate current performance, identify improvement areas, and guide organizations through systematic advancement. According to Becker et al. [7], "a maturity model defines a sequence of levels (or stages) that characterize the evolution of an organization's practices or processes from an ad hoc, immature state to a mature, disciplined state."

In the context of education, several maturity models have been developed to assess institutional capabilities. For instance, the HELA-CMM model (Higher Education Learning Analytics Capability Maturity Model) proposes five levels of institutional maturity in the adoption of learning analytics, ranging from basic data collection to advanced adaptive feedback systems [3]. Another example is the e-Learning Maturity model (eMM) developed by Marshall and Mitchell, which evaluates e-learning process across five dimensions: learning, development, support, evaluation and organization. These models provide valuable roadmaps but are often focused on system-level infrastructure or general digital strategy, rather than directly enhancing the pedagogical feedback loop based on student evaluation.

Simultaneously, the use of AI in higher education has grown rapidly. A notable example is Assessment's, an intelligent tutoring system designed for middle school math,

which combines machine learning with human-in-the-loop feedback, track student progress and provides teachers with real-time data dashboard [3] [6].

The integration of maturity models and AI provides dynamic and contextualized information that is useful for teaching quality enhancement. Despite this potential, few studies systematically explore this integration for faculty development. The intended model in this study seeks to bridge this gap by focusing on the feedback ecosystem – understood as the interconnected processes, tools, and actors involved in collecting and analyzing to teaching evaluations-, incorporating AI capabilities not only for data analysis but also for delivering personalized, actionable insights and aligning them with Institucional faculty development strategies.

# 3 Methodology

This study follows the PRISMA (Preferred Reporting Items for Systematic Reviews and Meta-Analyses) methodology [6]. The PRISMA methodology is a widely adopted framework for conducting and reporting systematic reviews. It provides a structured approach to ensure transparency, reproducibility, and completeness in the identification, selection, and synthesis of research evidence. PRISMA includes a four-phase flow diagram: (1) identification, (2) screening, (3) eligibility, and (4) inclusion. PRISMA also provides a checklist that guides researchers through rigorous review processes. The aim was to identify and analyze academic studies that explore the use of AI-enhanced maturity models for faculty feedback in higher education.

The search strategy was designed to identify studies at the intersection of three concepts: (1) maturity models or capability frameworks, (2) artificial intelligence or machine learning techniques and (3) applications in higher education, in the context of teaching evaluation or feedback. The Boolean structure was used: ("maturity model" OR "capability framework") AND ("artificial intelligence" OR "machine learning") AND ("higher education" OR "teaching evaluation" OR "instructional feedback")

The search was conducted in two major databases: Scopus and Web of Science, including publications from 2010 to June 2025. A total of 1,959 records were retrieved. The selection process included two main filtering stages:

- 1. Initial screening: Titles and abstracts were reviewed to remove unrelated studies. During this stage, exclusion criteria were applied, including: (1) Articles not available in English or Spanish, (2) studies without full text-access, (3) works outside the educational domain or unrelated to teaching evaluation and feedback, (4) Publications that mentioned maturity models of AI only superficially and (5) duplicate records from both databases.
- 2. Eligibility assessment: Full-text articles were analyzed based on the following combined inclusion criteria:
- Use or proposal of a maturity model.
- Integration of AI or machine learning techniques.
- Application in higher education and teaching evaluation context.

These criteria were applied jointly to ensure the relevance of each article to the scope of the review.

To support this process, we used the systematic platform Rayyan [8], which enabled a semi-automated screening. This tool enabled blind screening, collaborative inclusion/exclusion tagging, and conflict resolution between reviewers, ensuring consistency and reducing selection bias.

The final sample consisted of 159 articles. Additionally, semantic analysis techniques were applied to abstracts and keywords using Bibliometrix. Tools such as term frequency analysis, topic clustering, and conceptual-mapping were employed to identify patterns and gaps in literature.

Figure 1 presents the PRISMA flow diagram corresponding to the methodology described earlier. This figure summarizes the systematic process applied to select the studies included in this review.

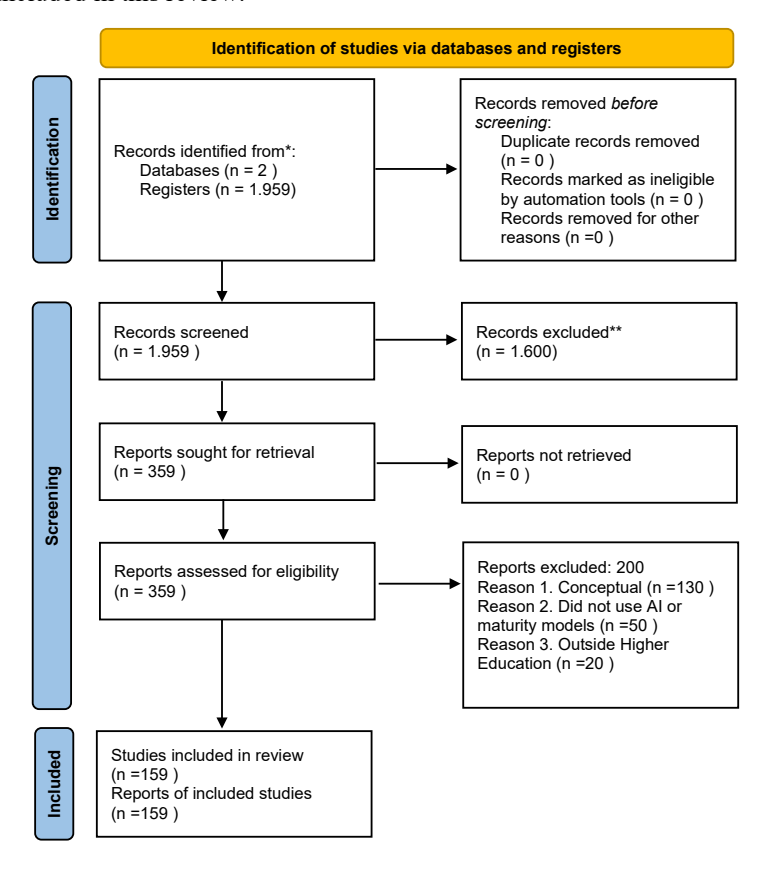


Fig. 1 PRISMA Flow diagram.

During the identification phase, a total of 1,959 records were retrieved from Scopus and Web of Science, covering publications from 2010 to June 2025. In the screening phase, 189 duplicates records were removed. The remaining 1,770 titles and abstract were retrieved using predefined exclusion criteria, including language restrictions

(English and Spanish only), lack of full-text Access, irrelevance to the educational domain or teaching evaluation, and superficial mention of maturity models or AI without methodological application.

The eligibility stage involved full-text analysis of 93 potentially relevant articles. After careful evaluation, 159 studies met all inclusion criteria: use or proposal of a maturity model, integration of artificial intelligence or machine learning techniques, and application in higher education teaching evaluation contexts.

# 4 Results

The final sample of 159 articles covered a wide temporal and disciplinary range. Most studies were published between 2018 and 2025, with a significant increase in recent years reflecting growing interest in AI applications in education. The majority of contributions came from institutions in Europe (34%), North America (28%), and Asia (22%), with notable representation from Latin America (10%).

For illustrate the scope and methodological nature of the select studies, the Figures 2 and 3 present the classification of the literature based in two key aspects: the type of study conducted, and the AI technologies employed:

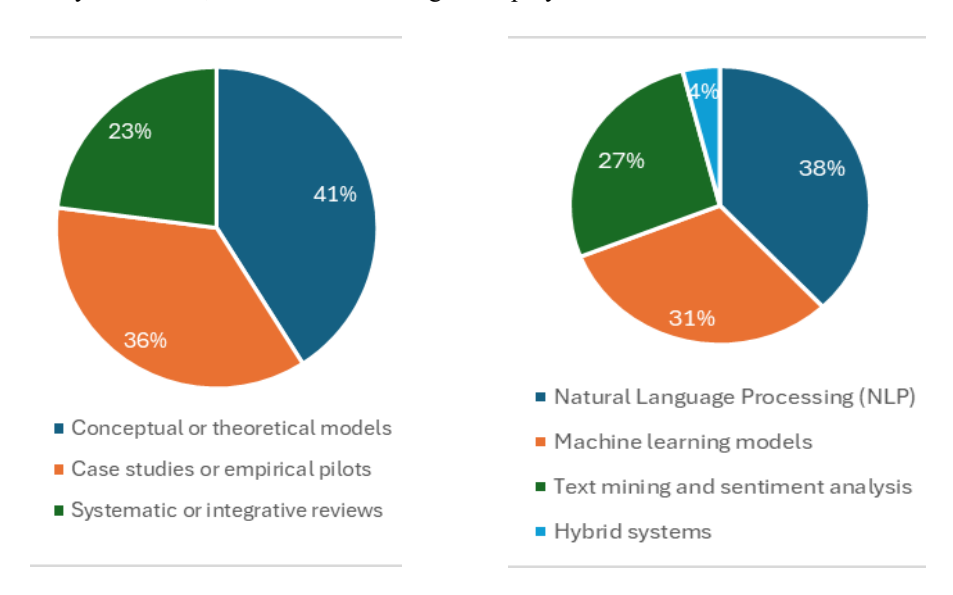


Fig 2: Distribution of study types.

Fig. 3. AI technologies employed.

Characteristics of Maturity Models: Most models adopted a five-level structure, often inspired by frameworks such as CMMI (Capability Maturity Model Integration) or quality assurance models. CMMI, originally developed by the Software Engineering Institute, provides a structured model for evaluating and improving processes [4]. In the context of AI-enhanced maturity models in education, the most frequently assessed

domains are summarized in table 1. These domains align with maturity models previously described in AI and education literature [5] [2], see Table 1.

Table 1. Common domains Assessed in AI-based maturity models.

| Domain Assessed                       | Description                                |
|---------------------------------------|--|
| Institutional Data Infrastructure     | Evaluation of systems, platforms and       |
|                                       | data available across the institution      |
| Teaching Quality and Evaluation Prac- | Assessment of teaching methodologies       |
| tices                                 | and feedback collection mechanism          |
| Feedback Cycles and personalization   | Degree of automation, customization        |
|                                       | and feedback loop integration              |
| Governance and strategic alignment    | Integration of feedback models into insti- |
|                                       | tutional planning and leadership           |

In parallel, a semantic analysis of abstract and keywords using NLP techniques revealed four recurring thematic clusters across the literature. The findings are summarized in Table 2.

Table 2. Thematic Clusters identified through semantic analysis.

| Thematic cluster                         | Interpretation                              |
|--|---|
| Personalized feedback and continuous     | Emphasis on adaptative and iterative im-    |
| improvement                              | provement mechanism for teaching            |
| Institutional Analytics and decision-    | Use of AI- generated insights for inform    |
| making                                   | educational leadership                      |
| AI Integration into quality assurance    | Connection between technical systems        |
| frameworks                               | and institutional quality models            |
| Ethics, transparency and faculty engage- | Issues of fairness, explainability and aca- |
| ment                                     | demic staff participation                   |

These themes reflect not only the technological orientation of literature, but also institutional concerns about ethics, scalability, and user acceptance.

Only less than 10% of the studies reported full implementation or longitudinal validation of maturity models in real-world educational environments. This highlights a gap between research and practice and underscores the opportunity for future empirical investigations that validate the effectiveness and sustainability of AI-based feedback models in institutional settings [3] [9].

# 5 Discussion

The results of this semantic systematic review underscore both the growing academic interest and the methodological fragmentation in the development and application of AI-based maturity models for teaching feedback in higher education. The predominance of theoretical contributions — often lacking empirical validation — reveals a persistent gap between conceptual frameworks and their practical implementation in real educational settings [3] [9].

Although techniques such as natural NLP and ML are increasingly applied to analyze student evaluations [3], few studies propose integrated frameworks that effectively align these tools with institutional feedback systems via maturity models. This reflects a missed opportunity to operationalize data-driven models that could enhance teaching quality through structured, iterative improvement mechanisms [3].

When compared to traditional SET approaches, AI-powered maturity models demonstrate a clear potential to foster adaptive feedback cycles, enabling more personalized, timely, and actionable guidance for faculty. However, key issues such as ethical transparency, faculty engagement -referring to the active participation of academic staff in feedback processes and model adoption-, and alignment with institutional strategies are rarely addressed in depth [3] [9].

These findings align partially with existing research in educational data mining and quality assurance, which emphasize the importance of converting student-generated data into actionable analytics [6]. In this context, the added value of maturity models lies in their ability to contextualize AI-driven insights within broader trajectories of institutional development and faculty professionalization.

In comparison with established maturity models such as CMMI and the e-learning Maturity Model (eMM), the AI-Based frameworks reviewed in this study tend to emphasize technological capabilities over institutional alignment or pedagogical usability. Few models explicitly address how AI-generated feedback can be integrated into ongoing faculty development programs or quality assurance mechanisms. Bridging this gap requires further discussion between AI research and educational policy.

Additionally, ethical considerations remain underexplored. While some studies mention fairness or transparency, very few provide explicit mechanisms to mitigate algorithmic bias or explain model decisions to academic stakeholders.

To move beyond conceptual contributions, researchers should also prioritize real-world validation. Case study designs involving controlled implementation of AI-enhanced maturity models in diverse educational contexts would provide empirical insights into feasibility. Pilot programs co-designed with faculty could test feedback personalization mechanisms, monitor their impact on teaching practices, and inform iterative refinement of the models.

The thematic clusters identified in the semantic analysis suggest that the field is structured around four core dimensions: Personalized feedback and continuous improvement, Institutional analytics and decision-making support, AI integration into quality assurance and ethics, transparency, and faculty involvement.

The present study aims to advance towards a maturity model specifically designed for the domain of teaching feedback. This model seeks not only to incorporate AI tools for data analysis, but also to integrate the resulting insights into effective pedagogical improvement processes and faculty development initiatives. The proposed approach addresses the identified gaps by offering a structured, actionable and contextualized framework that supports the institutional evolution from descriptive feedback system towards predictive, generative and formative mechanism.

#### 6 Conclusions and Recommendations

This study presents a semantic systematic review of the literature on AI-enhanced maturity models aimed at improving teaching feedback in higher education. Through a PRISMA-guided methodology and semantic analysis, 159 relevant publications were identified, analyzed, and categorized.

The review reveals that despite growing conceptual interest, few validated and operational implementations exist. Only 9% of the 159 analyzed studies reported real-world deployment of longitudinal validation of AI-based maturity models in higher education institutions. AI technologies, particularly NLP and machine learning, are employed to analyze student evaluations, but their integration into structured maturity models remains limited.

Findings suggest that future research should:

- Prioritize empirical validation of proposed models in diverse educational contexts.
- Incorporate faculty engagement and ethical transparency as design principles.
- Use AI not only for analysis, but for generating contextualized, actionable improvement pathways.

In conclusion, this review provides a solid foundation for the development of integrated AI-powered maturity models that support sustained teaching improvement processes. These models have the potential to transform evaluation data into a powerful tool for institutional learning and academic development. Beyond higher education, the methodology used in this review -particularly the integration of semantic analysis and maturity model frameworks- may also be applicable to other domains where feedback, data-driven improvement, and institutional development are relevant. For example, healthcare organizations, public administration, and corporate training environments increasingly seek structured models for assessing performance and guiding digital transformation.

#### 7 References

- 1. M. Spooren, B. Brockx, y D. Mortelmans, On the validity of student evaluation of teaching: The state of the art, *Review of Educational Research*, vol. 77, no 4, p. 507–545, 2007.
- J. Roe, M. Perkins, and D. Ruelle, Understanding Student and Academic Staff Perceptions of AI Use in Assessment and Feedback, arXiv, 2024.
- 3. Y. Zhan, D. Boud, P. Dawson y Z. Yan, Generative artificial intelligence as an enabler of student feedback engagement: a framework *Higher Education Research and Development*, 2025.
- 4. Y. Walter, Embracing the future of Artificial Intelligence in the classroom: the relevance of AI literacy, prompt engineering, and critical thinking in modern education. *International Journal of Educational Technology in Higher Education*, vol. 21, 2024.

- 5. R. B. Sadiq, N. Safie, A. H. Abd Rahman, and S. Goudarzi, Artificial intelligence maturity model: a systematic literature review, *PeerJ Comput. Sci.*, vol. 7, p. 661, 2021.
- 6. B. Langer, Understanding Data & Analytics Maturity: A Systematic Review of Maturity Model Composition, *Schmalenbach Journal of Business Research.*, 2025.
- J. Becker, R. Knackstedt, and J. Pöppelbuß, Developing Maturity Models for IT Management, Business & Information Systems Engineering, vol. 1, no 3, pp. 213-222, 2009.
- 8. M. Ouzzani, H. Hammady, Z. Fedorowicz y A. Elmagarmid, Rayyan—a web and mobile app for systematic reviews, *Systematic Reviews*, vol. 5, 2016.
- 9. A. Benitez, J. Contreras, and M. Reinoso, HELA-CMM: Capability Maturity Model for Adoption of Learning Analytics, *Education and Information Technologies*, 2025.

# From Didactic Proposal to Practical Implementation: Results of an Industrial Robotics Training Course within the EAGLE Project

Mario Peñacoba<sup>1</sup>, Eduardo Bayona<sup>1</sup> Jesus Enrique Sierra-Garcia<sup>1</sup>, and Bruno Baruque-Zanon<sup>1</sup>

Universidad de Burgos, Spain

Abstract. This paper presents the results of a practice-based training initiative in industrial robotics developed within the EAGLE project. The course was designed to address the digital skill gap in small and medium-sized enterprises (SMEs) by providing professionals with hands-on experience in programming, simulation, and safe operation of robotic systems. The training combined theoretical content with guided exercises using ABB RobotStudio and physical robot manipulators. Evaluation of participant performance was conducted through a technical question-naire and a simulation-based challenge. The results show strong competence acquisition and high satisfaction rates among trainees, particularly regarding applicability and teaching methodology. Additionally, pre- and post-course surveys revealed positive shifts in perceived ease of use, intention to adopt, and confidence in applying robotics in the workplace. These findings support the scalability of the course and its contribution to workforce digitalization in European SMEs.

Keywords: Robotics, Workplace Learning, SMEs, Digitalization, ICT

#### 1 Introduction

As industrial settings evolve towards digital ecosystems, robotics emerges as a pivotal enabler of smarter, more efficient production systems. In the context of Industry 4.0, robotic automation not only optimizes resources and enhances flexibility but also serves as a catalyst for competitiveness in global markets [1]. Nevertheless, a significant portion of the workforce, particularly in small and medium-sized enterprises (SMEs), lacks the required training to fully leverage these technologies [2, 3].

While robotic platforms and simulation environments are increasingly accessible, the gap between available technologies and workforce competencies remains too large [4]. Many SMEs struggle to adopt robotic solutions due to the absence of trained professionals who can manage the deployment, programming, and maintenance of such systems [5, 6]. This situation highlights the pressing need

for tailored, practice-oriented educational initiatives that facilitate the adoption of robotics in industrial settings [7].

While large industries advance in automation and digital transformation, SMEs remain behind in accessing advanced robotics education. EU-funded projects like the Digital Innovation Hubs and EIT Manufacturing academies have sought to address this gap through flexible and modular approaches. However, many of these efforts remain conceptual or are embedded within broader industrial strategies, lacking replicable, lightweight, and outcome-oriented training methodologies. Although the value of blended learning—combining simulation with handson experimentation—has been recognized, a significant gap persists in the full implementation of training programs that incorporate evaluation frameworks aligned with technology acceptance models [8].

The European project EAGLE (CovEring the trAining Gap in digital skills for European SMEs manpower) addresses this need by developing specialized courses that target essential digital skills. One of its key deliverables is a hands-on training course in industrial robotics designed with the operational needs of SMEs in mind [9]. This paper reports on the initial implementation of this course, presenting its pedagogical approach and structure, and analyzing results from the first participants to evaluate its effectiveness and potential for scalability.

This study builds upon these foundations and aims to contribute a transferable and validated framework for robotics training in SMEs, supported by a rigorous methodology that includes technical performance evaluation, pre-post comparative analysis, and user satisfaction metrics.

The rest of this paper is organized as follows: Section 1 describes the EAGLE project and the consortium structure. Section 2 presents the robotics training course, detailing its objectives, structure, and pedagogical design. Section 3.2 shows the results of the implementation in terms of participant performance and satisfaction. Conclusions and future work are summarized in Section 5.

## 2 The EAGLE Project

The EAGLE project is a European initiative co-funded by the Digital Europe Programme (grant agreement No. 101100660), whose main goal is to reduce the digital skill gaps observed in the SME workforce across Europe [10]. The project develops and delivers specialized training programs in emerging technologies such as industrial robotics, artificial intelligence, and cybersecurity.

The consortium brings together a diverse set of institutions: universities, research centers, training providers, industry associations, and specialized SMEs. It is coordinated by the Universidad de Burgos (Spain) and includes partners from Slovakia, the United Kingdom, Finland, Czech Republic, Ireland, Lithuania, and Cyprus. This diversity ensures a wide applicability of the training programs and fosters transnational cooperation in digital upskilling.

The project's implementation plan is structured around four interrelated Work Packages:

- WP1: Project Management and Coordination

- WP2: Courses DesignWP3: Course Delivery
- WP4: Communication and Dissemination

After successfully completing the design phase, the project has entered its course delivery phase, where pilot courses are being implemented and monitored. One of the most mature and impactful actions is the Industrial Robotics Course developed under WP2 and delivered in multiple contexts within WP3 [10]. The dissemination of project activities is carried out through the official website and social media channels [11].

#### 3 Industrial Robotics course

The Industrial Robotics Course was designed to address the practical training needs of SME technicians and professionals, aiming to provide them with the competencies needed to work with industrial robotic systems in both virtual and real environments. The course is structured to combine theoretical concepts, practical applications, and problem-solving tasks, thereby offering a holistic training experience.

The course follows a blended learning model, with 8 hours of in-person sessions and 8 hours of autonomous work. The theoretical content is supported by instructional videos, while the practical activities are centered around the use of simulation tools (notably ABB RobotStudio) and, when available, physical robots. The in-person sessions focus on hands-on tasks using real robot manipulators and teach pendants, whereas the autonomous portion emphasizes self-paced learning and simulation-based exercises. The pilot course included 36 participants. Table 1 summarizes the participant profiles.

Attribute Categories Count Percentage (%) Age group 20 - 35/36 - 50/51 +18/12/6 50/33/17 Gender Male/Female 28/8 78/22Experience in Robotics None/Basic/Advanced 10/20/6 28/56/16 Technician/Engineer/Manager 20/12/4 56/33/11 Role

Table 1. Participant Demographics Summary

The course is built around the acquisition of both specific and transversal competences:

## **Specific Competences:**

- Identification and classification of industrial robots by structure, control mode, and application domain.
- Selection and use of robotic components including controllers, manipulators, end-effectors, and sensors.

- 4 Mario Peñacoba et al.
  - Programming and execution of robotic tasks using teach pendants and simulation tools.
  - Implementation of safety measures and risk mitigation strategies according to ISO standards.

#### Transversal Competences:

- Logical reasoning and troubleshooting skills.
- Effective information search and management.
- Application of problem-solving strategies in realistic industrial scenarios.

#### 3.1 Course Content

The course content is organized into three progressive blocks: Transversal Concepts, Core Content and Advanced Content. Each block has a different number of theoretical and practical training hours. The first number in the bracket denotes the theoretical hours and the second one the hours dedicated to practical content.

- Transversal Concepts (1h/0.5h): Introduction to robotics, etymology and evolution of the term, classifications, applications, and success cases.
- Core Content (3.5h/3h): Robot components, controller interfaces, manipulators, mobile bases, end-effectors, sensors. Practical training in robot selection, basic motion commands, and RAPID programming in RobotStudio.
- Advanced Content (1.5h/1.5h): Kinematic modeling, workspace analysis, integration of safety devices, and compliance with ISO 10218-1/2, ISO/TS 15066.

Each block combines theory with guided practice to ensure the applicability of acquired skills.

#### 3.2 Evaluation Methodology

Competence acquisition is assessed through several complementary mechanisms:

- A practical challenge, where students must develop and simulate a robotized sealing station for parcels using an IRB120 robot. It is evaluated with a testtype questionnaire designed to measure the understanding of the challenge, the understanding of the robot's operating principles and the use of the ABB RobotStudio tool to develop the application.
- A technical multiple-choice questionnaire focused on the understanding of robotic operations, programming logic, and safety considerations.
- A multiple choice questionnaire to measure the level of satisfaction of the student.
- A pre-post test to measure the improvement in the level of technology acceptance. To do it, the Unified Theory of Acceptance and Use of Technology (UTAUT) has been used [12].

In the following section, we present the results obtained during the first implementations of the course, based on participant responses, performance data, and qualitative feedback.

#### 4 Results

This section presents the results gathered from the first iterations of the Industrial Robotics Course, focusing on the evaluation of participant performance, task completion, and knowledge acquisition. The data are based on the practical exercise involving the simulation of a robotic sealing station using RobotStudio and on the answers to a technical questionnaire. The analysis also includes qualitative feedback to assess the perceived usefulness and applicability of the training.

Figure 1 displays a violin plot that simultaneously illustrates the density distribution and individual dispersion of the students' final exam grades. The highest concentration of students lies within the 8 to 9.5 grade range, indicating a generally positive performance trend.

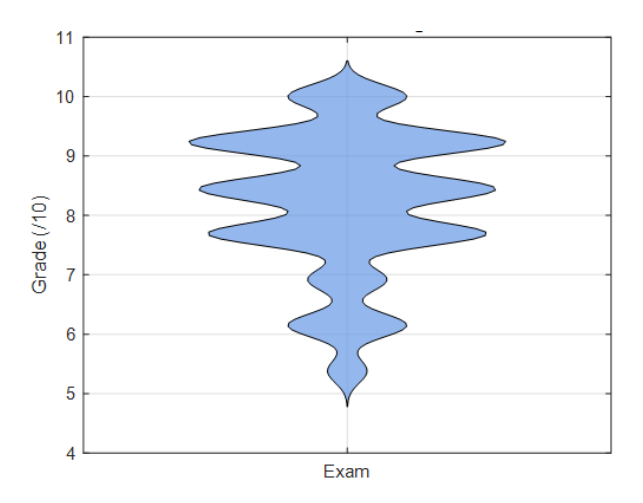
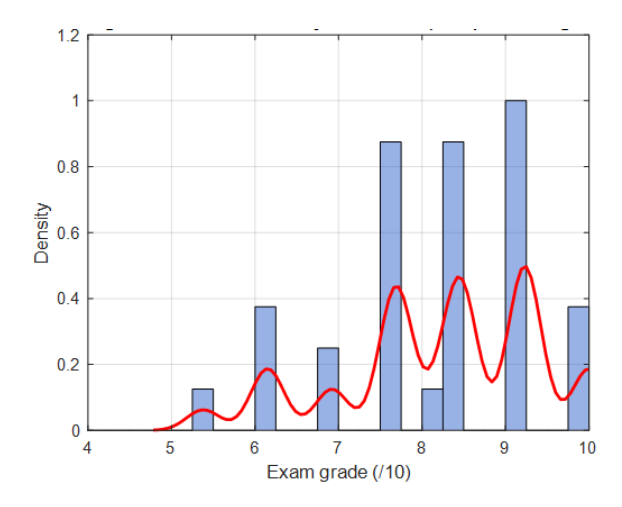


Fig. 1. Distribution of exam grades using a violin plot.

Figure 2 complements the analysis with a normalized density histogram overlaid with a kernel density estimation (KDE) curve. This visualization confirms the presence of several density peaks around higher grade values, suggesting that a significant portion of students achieved a satisfactory level of mastery in the evaluated content.

In addition to the technical assessment, the level of general satisfaction has been also evaluated. Table 2 shows the items of the questionary. A stacked bar chart illustrating the distribution of student responses for each evaluation item, rated on a Likert scale from 1 ("strongly disagree") to 5 ("strongly agree"), is presented in Figure 3. The labels on the x-axis correspond to the summary names of the evaluation dimensions, which are described in full in Table 2. The results reveal a clear predominance of positive ratings (4 and 5) across all categories, with 'Applicability', 'Method', and 'Tech impact' showing particularly high pro-



 ${\bf Fig.\,2.}$  Histogram with kernel density estimation (KDE) of exam grades.

 ${\bf Table~2.~Correspondence~between~chart~labels~and~full~question naire~items.}$ 

| Label in Figure | Full Questionnaire Item  |
|-----------------|--|
| Accreditation   | What importance do you place on this type of course having an official university accreditation (or from another higher education institution) when enrolling? |
| Applicability   | Has this course helped you acquire new skills or knowledge that you can directly apply in your job or within your professional sector?                         |
| Quality         | Are you satisfied with the overall quality of the course?  |
| Recommendation  | Would you recommend this course to other prospective students?   |
| Tech Impact     | Has this course helped you better understand the impact of the<br>studied technology in your sector and how to use it more effec-<br>tively in your company?   |
| Content         | Did the course content meet your learning expectations?  |
| Method          | Are you satisfied with the teaching method (quality and clarity of explanations, balance between theory and practice, etc.) used in this course?               |

portions of scores in the upper range. Negative ratings (1 and 2) were minimal, suggesting a generally favorable perception of the course structure, content, and teaching approach.

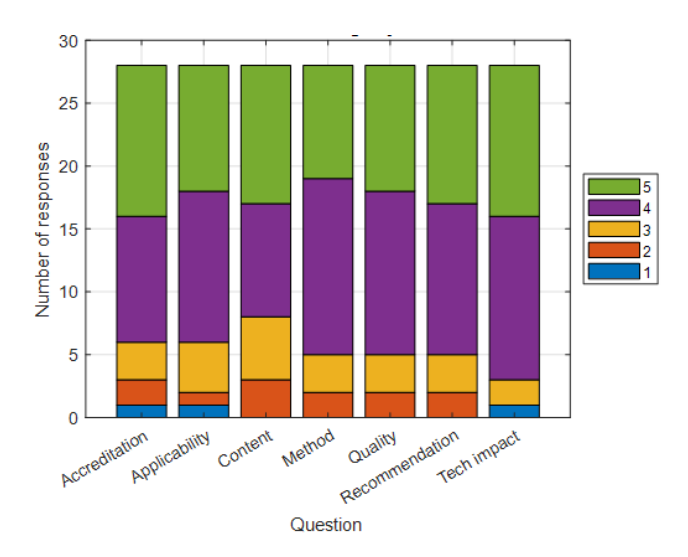


Fig. 3. Distribution of student ratings by evaluation item

Finally, the acceptance of robotics is measured before and after the course based on the UTAUT model. This point is evaluated with the questionnaire described in Table 3 divided into 9 categories. Figure 4 displays a radar chart comparing the average scores across nine analytical dimensions derived from the initial and final questionnaires (pre and post tests). These dimensions were constructed by grouping conceptually related items, as detailed in Table 3, which links each category with the specific questions used in both the pre- and post-course surveys.

Results show improvements in all categories after completing the course, with the most notable increases observed in "Support", "Habit", "Usefulness", and "Ease of Use". These findings suggest that the training program positively influenced participants' perceptions not only regarding the utility and enjoyment of the studied technology (robotics), but also in terms of their perceived competence, habitual integration, and access to support. The changes observed give some indication that the course contributes to both practical and attitudinal preparation for technology adoption in the workplace.

Cronbach's alpha has been used to evaluate the reliability of the UTAUT questionaries. It is possible to conclude that some categories are quite well represented as Economics ( $\alpha$  pre 0.47,  $\alpha$  post 0.31), Hedonic ( $\alpha$  pre 0.28,  $\alpha$  post 0.42) and Intention ( $\alpha$  pre 0.35,  $\alpha$  post 0.65). However, the values in other categories are low and the results should be taken with caution.

 ${\bf Table~3.~Question naire~items~associated~with~each~analytical~group.}$ 

| Group                   | Associated questionnaire items                                      |
|-------------------------|---|
| Intention to use        | I intend to use the studied technology (robotics) at work.          |
|                         | I will try to use the studied technology (robotics) at work.        |
|                         | I plan to frequently use the studied technology at work.            |
| Social influence        | People important to me at work think I should use the studied       |
|                         | technology.   |
|                         | People who influence my behavior at work think I should use         |
|                         | the studied technology.   |
|                         | People whose professional opinions I value think I should use       |
|                         | the studied technology.   |
| Perceived ease of use   | Learning to use the studied technology for my job is easy.          |
|                         | It is easy for me to use the studied technology for my job.         |
|                         | It is easy for me to become skilled in using the studied technology |
|                         | at work.  |
|                         | I have the resources needed to use the studied technology.          |
| D                       | I have the knowledge needed to use the studied technology at        |
| Resources and knowledge | work.   |
|                         | The studied technology is compatible with other technologies I      |
|                         | use at work.  |
| External support        | I can get help from others when I have difficulties using the       |
|                         | studied technology at work.   |
| Hedonic value           | Using the studied technology at work is fun.                        |
|                         | Using the studied technology at work is pleasant.                   |
|                         | Using the studied technology at work is very entertaining.          |
| Habit                   | Using the studied technology at work has become a habit for         |
|                         | me.   |
|                         | I am used to using the studied technology at work.                  |
|                         | Using the studied technology is a routine part of my workflow.      |
|                         | I find the studied technology useful for my job.                    |
| Perceived               | Using the studied technology helps me get things done at work       |
| usefulness              | more quickly.   |
|                         | Using the studied technology increases my productivity at work.     |
|                         | The studied technology offers good value for money.                 |
| Economic                | At its current price, the studied technology offers good value for  |
| evaluation              | money.  |
|                         | The studied technology is reasonably priced.                        |

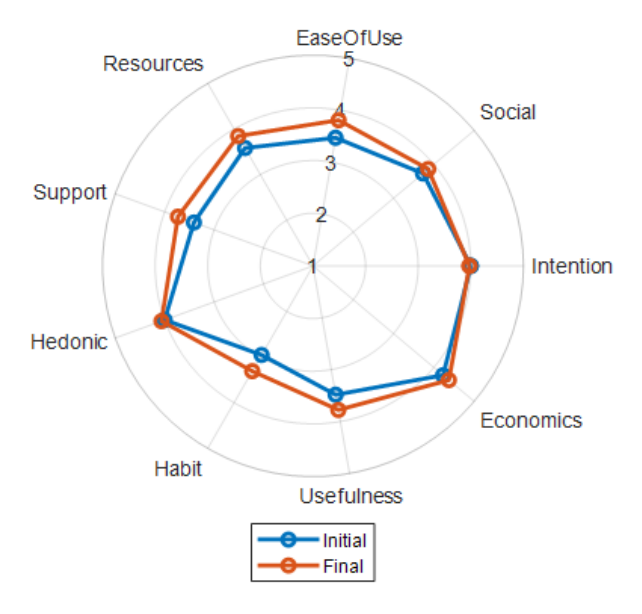


Fig. 4. Group-level comparison: Initial vs Final Questionnaire

#### 5 Conclusions

The implementation of the Industrial Robotics Course within the EAGLE project confirms the effectiveness of a hands-on, SME-oriented training model. Participants demonstrated solid acquisition of key competencies, particularly in simulation-based programming, trajectory control, and safety integration. The combination of practical and conceptual evaluation proved to be a reliable method for assessing outcomes.

The successful completion of the practical task and the high performance on conceptual questions indicate that the training approach was well-received and impactful. Feedback highlighted the value of real-world scenarios, simulation environments, and the accessibility of materials.

These findings support the broader application of the course and its potential for adaptation in other contexts. Future work will focus on scaling its implementation, refining content, and evaluating long-term impact.

Future work will focus on expanding the delivery of the course across partner institutions, adapting it to specific industrial sectors, and conducting longitudinal studies to assess the long-term impact on workforce capabilities and SME digitalization. In addition, statistical studies will be developed with a larger population sample to improve the statistical reliability of the results.

In pedagogical terms, this work offers a transferable model that integrates theory, simulation, and real-world interaction in a balanced structure. Its scalability, low infrastructure requirements, and modular assessment mechanisms make it highly applicable across SME contexts and regions. Next editions of

the course will include follow-up studies to evaluate knowledge retention and mid-term adoption in work environments.

## Acknowledgements

This work was partially supported by the European Union's Digital Europe Programme (DIGITAL) under grant agreement No 101100660.

#### References

- 1. M. Javaid, A. Haleem, R. P. Singh, and R. Suman. Substantial capabilities of robotics in enhancing industry 4.0 implementation. *Cognitive Robotics*, 1(1–2):58–75, 2021.
- 2. A. et al. Buerkle. Towards industrial robots as a service (iraas): Flexibility, usability, safety and business models. *Robotics and Computer-Integrated Manufacturing*, 81:102484, 2023.
- A. Telukdarie, T. Dube, P. Matjuta, and S. Philbin. The opportunities and challenges of digitalization for sme's. Procedia Computer Science, 217:689–698, 2023.
- 4. P. Jennes and A. D. Minin. Cobots in smes: Implementation processes, challenges, and success factors. In 2023 IEEE International Conference on Technology and Entrepreneurship (ICTE). IEEE, 2023.
- 5. A. Thrassou, N. Uzunboylu, D. Vrontis, and M. Christofi. Digitalization of smes: A review of opportunities and challenges. In *The Changing Role of SMEs in Global Business: Volume II*, pages 179–200. 2020.
- M. Hulla, P. Herstätter, M. Wolf, and C. Ramsauer. Towards digitalization in production in smes a qualitative study of challenges, competencies and requirements for trainings. *Procedia CIRP*, 104:887–892, 2021.
- 7. N. Shmatko and G. Volkova. Bridging the skill gap in robotics: Global and national environment. *SAGE Open*, 10(3), 2020.
- K. et al. Warnhoff. Learning factories as innovative training locations for smes: Qualitative analysis of concepts and cooperations. *Industry 4.0 Science*, 40(4):32–41, 2024.
- 9. C. Urrea and J. Kern. Recent advances and challenges in industrial robotics: A systematic review of technological trends and emerging applications. *Processes*, 13(3):832, 2025.
- 10. Eagle project official website. https://www.projecteagle.eu/, 2025.
- 11. Eagle news. https://www.projecteagle.eu/news/, 2025.
- 12. Michael D Williams, Nripendra P Rana, and Yogesh K Dwivedi. The unified theory of acceptance and use of technology (utaut): a literature review. *Journal of enterprise information management*, 28(3):443–488, 2015.

# WhoSQLWho: A Gamified Web Application for Learning SQL

Bernat Costa<sup>1</sup>, Juan M. Alberola<sup>2</sup>, and Victor Sánchez-Anguix<sup>3</sup>

<sup>1</sup> IES Antonio Machado,
 C. Arroyo, 80, 41008 Sevilla (Spain)

<sup>2</sup> Valencian Research Institute for Artificial Intelligence, Universitat Politècnica de València, Camino de Vera, s/n, 46022, Valencia (Spain)

<sup>3</sup> Instituto Tecnológico de Informática, Grupo de Sistemas de Optimización Aplicada, Ciudad Politécnica de la Innovación, Universitat Politècnica de València Camino de Vera s/n, 46022 Valencia (Spain)

bernatcosta@iesamachado.org, jalberola@dsic.upv.esvsanchez@eio.upv.es

Abstract. Learning Structured Query Language (SQL) remains a persistent challenge for students due to its abstract nature and syntactic complexity. Traditional pedagogical approaches often rely on generic business-oriented database examples, which may hinder student engagement and limit conceptual understanding. In this paper, we present WhoSQLWho, a web-based gamified application designed to make SQL learning more accessible, motivating, and interactive. An evaluation conducted with 97 students and 14 instructors revealed strong perceived effectiveness in supporting SQL learning. By combining playful mechanics with pedagogical rigor, WhoSQLWho offers a compelling alternative to traditional SQL instruction and demonstrates the potential of game-based learning environments in technical education.

**Keywords:** SQL learning, gamification, educational technology, web application

#### 1 Introduction

Learning database systems and Structured Query Language (SQL) presents significant challenges for students across a wide range of educational contexts. SQL is a declarative language used to interact with relational databases and represents a core component in most computer science and information systems curricula. However, mastering its syntax and logic is often difficult, especially for students with limited programming or data modeling experience [3]. In addition to these technical difficulties, the abstract nature of SQL may reduce student engagement and motivation [7]. Therefore, it is essential to design learning environments that are not only effective but also motivating [4].

In recent years, gamification has emerged as one of the most effective techniques to enhance motivation [11, 12, 9]. Its adoption in education has increased,

as an strategy to improve motivation and foster a more dynamic learning experience. By incorporating game-like elements such as competition, progress tracking, and rewards, educators aim to promote deeper engagement and active participation among learners. Several studies have shown that gamified environments can lead to increased student interest and improved academic outcomes. Notably, [2] reported that gamification significantly boosted both student involvement and performance, providing strong evidence of its pedagogical benefits in technical disciplines.

In the specific context of SQL instruction, various innovative approaches have been proposed to make learning more attractive through game-based mechanics. For example, [8] introduced a block-based learning tool designed to simplify SQL query writing for secondary school students. Similarly, [5] presented a gamified platform where students compete by solving SQL queries. [1] proposed a gamification framework for teaching NoSQL concepts, while [10] highlighted the positive impact of game elements on student performance in database-related topics. More recently, [6] developed SQLValidator, an interactive web-based tool focused on SQL query practice, aimed at improving learner proficiency through hands-on engagement.

In this work, we present a web-based application designed to support SQL learning through a gamified experience inspired by the classic game *Guess Who?*. In this application, students formulate SQL queries to identify a hidden character based on database attributes, thereby reinforcing their understanding of SQL syntax and logic through an engaging and iterative process. The tool is intended for use both in the classroom (encouraging competition based on accuracy and speed) and for independent study, enabling students to review and practice content at their own pace.

Beyond its primary learning purpose, the application was developed with three complementary educational goals: to provide students with a playful and engaging alternative to traditional instructional methods; to foster motivation through the integration of core database concepts into a game-based environment; and to serve as a support tool for reviewing course material at home. Additionally, by publishing the complete development process—including source code, database diagrams, and deployment instructions—the tool offers students a real-world example of a software project, encouraging technical skills and promoting a deeper understanding of software engineering practices.

The remainder of this paper is structured as follows: Section 2 describes the proposed application and its implementation. Section 3 presents the results of an evaluation conducted with both students and instructors. Finally, Section 4 offers conclusions and outlines possible directions for future work.

## 2 Description of the Proposal

This project  $WhoSQLWho^4$  is a gamified web application inspired by the classic game "Guess Who?", reimagined to facilitate the learning of SQL query lan-

<sup>4</sup> https://whosqlwho.org/

guage. The core objective is to transform the abstract and often demotivating experience of learning database concepts into an engaging and interactive process.

Traditional teaching approaches in database courses often rely on generic business examples (e.g., invoices, orders), which may feel distant or irrelevant to students. By leveraging a well-known cultural game and integrating it with core SQL learning objectives, this proposal seeks to foster active engagement and deeper understanding.

The main learning goals supported by this application include:

- Understanding the construction and execution of SQL queries.
- Applying SQL syntax in a game-based context.
- Practicing critical thinking using real-time database interaction.
- Exploring SQL queries in a non-traditional, motivating environment.

The project has been developed as a web application using two separate components to reflect the backend–frontend architecture commonly adopted in web development. This separation allows the backend to serve different types of interfaces (web, mobile, desktop) while maintaining a single shared database and consistent business logic. The backend, implemented as a RESTful API using Node.js, handles core functionalities such as user authentication and game session management. The frontend, built with ReactJS, provides a user-friendly interface that enables seamless interaction with the system.

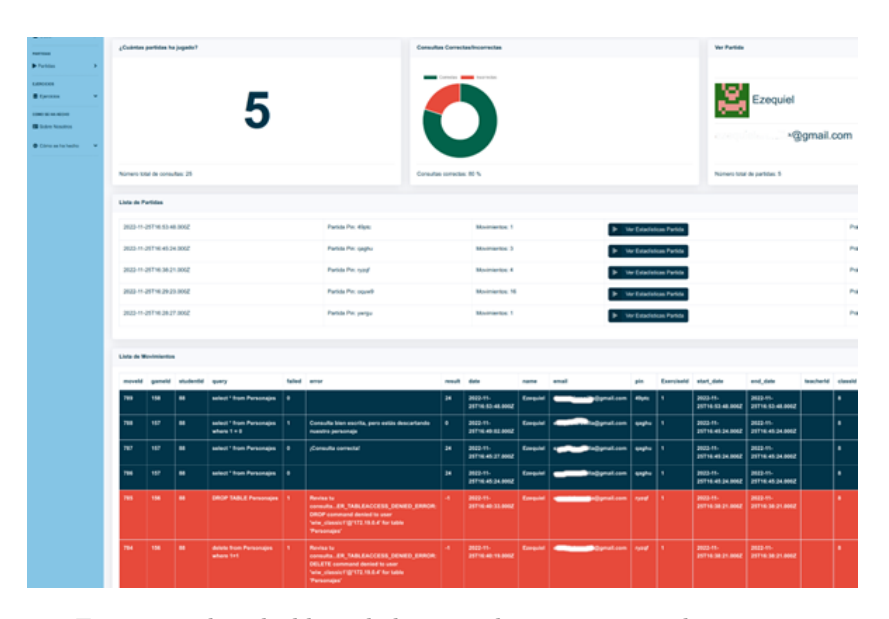


Fig. 1: Teacher dashboard showing class creation and statistics.

#### 2.1 User Profiles

The application offers two distinct user profiles. The first is the **Teacher** profile, which allows instructors to create sessions across different game modes. This profile is designed to support the preparation of exercises aligned with curricular objectives and to facilitate student monitoring through access to detailed analytics on activity, errors, and performance (Figure 1).

The available analytics include exercise-level reports, class-wide performance summaries, and individual student progress tracking. This data enables instructors to identify specific areas of student misunderstanding and to tailor their instruction accordingly, reinforcing the most challenging concepts for each particular group of students.

The second profile is the **Student** profile, which enables learners to join sessions, whether live games or assigned practice activities by means of a PIN provided by the instructor, without requiring prior registration. This lightweight access model allows students to participate during in-class activities or engage in independent practice at home, reviewing content at their own pace.

#### 2.2 Game Modes

The application offers two distinct game modes tailored to different teaching scenarios. On the one hand, the **Live** game mode allows the instructor to launch a real-time session using a PIN code, which is shared with students so they can join without the need for registration. Once connected, students compete to identify the hidden character by writing SQL queries. The instructor can monitor a real-time leaderboard, which may be projected in the classroom to provide immediate feedback and enhance the competitive dynamic (Figure 2).

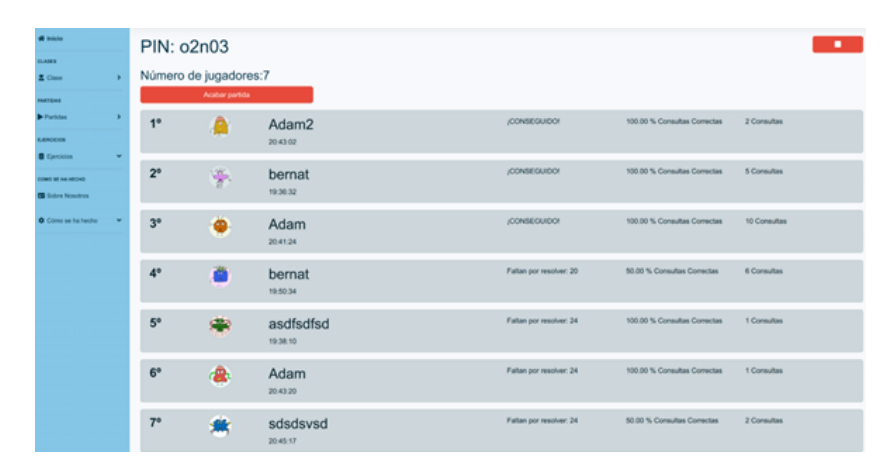


Fig. 2: Live classroom leaderboard interface.

On the other hand, the **Practice** game mode is focused for asynchronous use. In this mode, instructors can create virtual class groups (Figure 3). Students join using a class PIN and receive personalized exercises to complete at their own pace. This mode enables individual practice outside the classroom while still tracking progress.

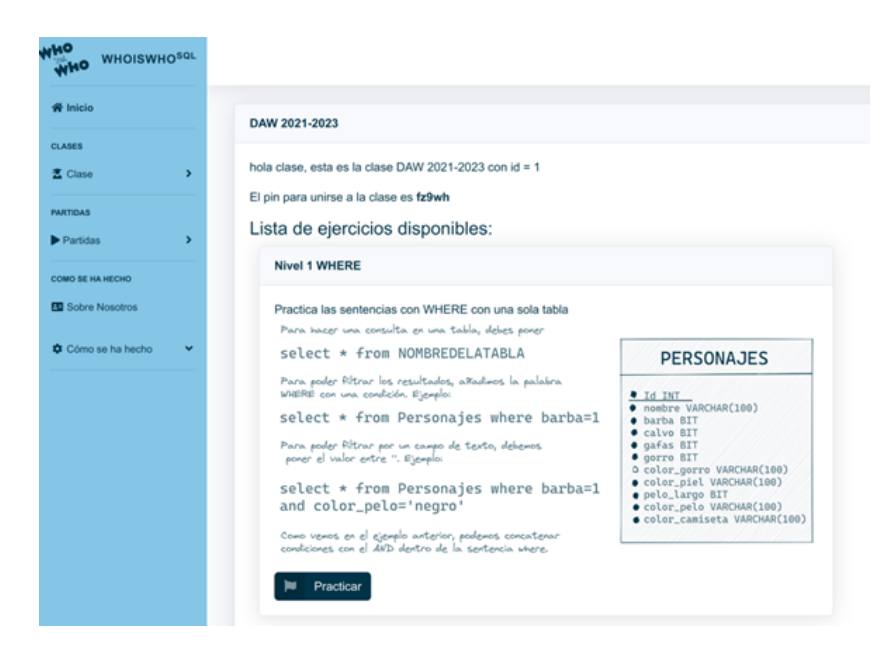


Fig. 3: Interface displaying assigned exercises for home practice.

#### 2.3 Game Mechanics

The game interface displays 24 character avatars with various attributes (e.g., beard, glasses, shirt color) as shown in Figure 4. A hidden character is selected at random, and the student must write SQL queries to narrow down the possibilities. For example:

#### SELECT \* FROM Characters WHERE hat = 1;

The system provides immediate feedback based on the query result:

- Green: Correct syntax and relevant condition; non-matching characters are eliminated.
- Yellow: Correct syntax but incorrect condition; the hidden character would be excluded.
- Red: Syntax error; an error message is returned to guide correction.

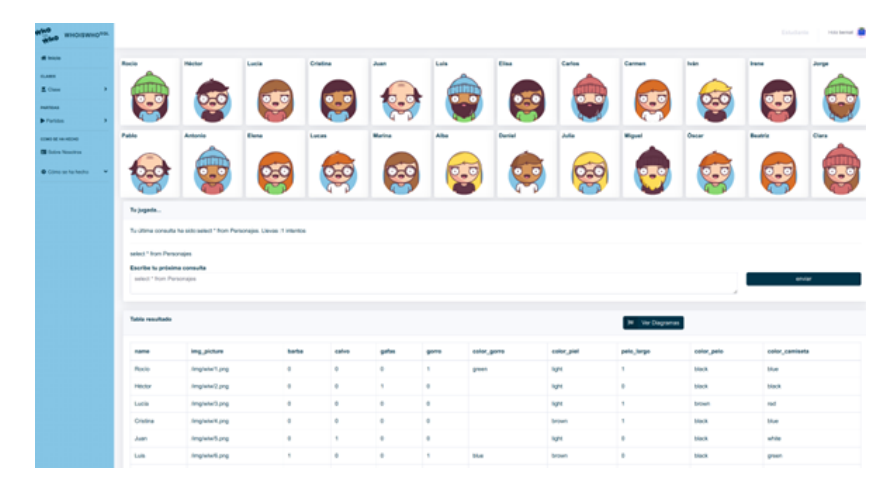


Fig. 4: Game interface.

The game ends when the student successfully identifies the hidden character, with a celebratory message displayed on both the student and classroom screens.

The current version of the application includes two levels of gameplay aligned with different assessment criteria. The first, more basic level focuses on simple SQL statements, allowing students to practice queries on single tables. The more advanced level introduces exercises involving multiple tables and more complex query structures. This structure enables instructors to select the appropriate level of difficulty based on the learning objectives of their course. In this way, students can play independently at home while practicing SQL, the language used to interact with relational databases.

Overall, the application not only promotes learning through play but also serves as a scalable, secure, and pedagogically aligned platform. It empowers teachers with actionable data while offering students a highly interactive and meaningful way to practice SQL.

#### 3 Evaluation

Below is an evaluation of the tool based on various questionnaires completed by both students and instructors involved in database-related courses. First, we aimed to assess whether students found the activities proposed by the tool to be engaging and effective for learning and practicing SQL queries. In this context, 97 computer science vocational training students participated in the evaluation. As shown in Figure 5a, the vast majority of students surveyed believe that the tool can support the learning of SQL, while only four respondents disagreed or remained neutral on this point.

Figure 5b presents students' views on the competitive aspect of the tool. Although most students responded positively, a larger proportion expressed some

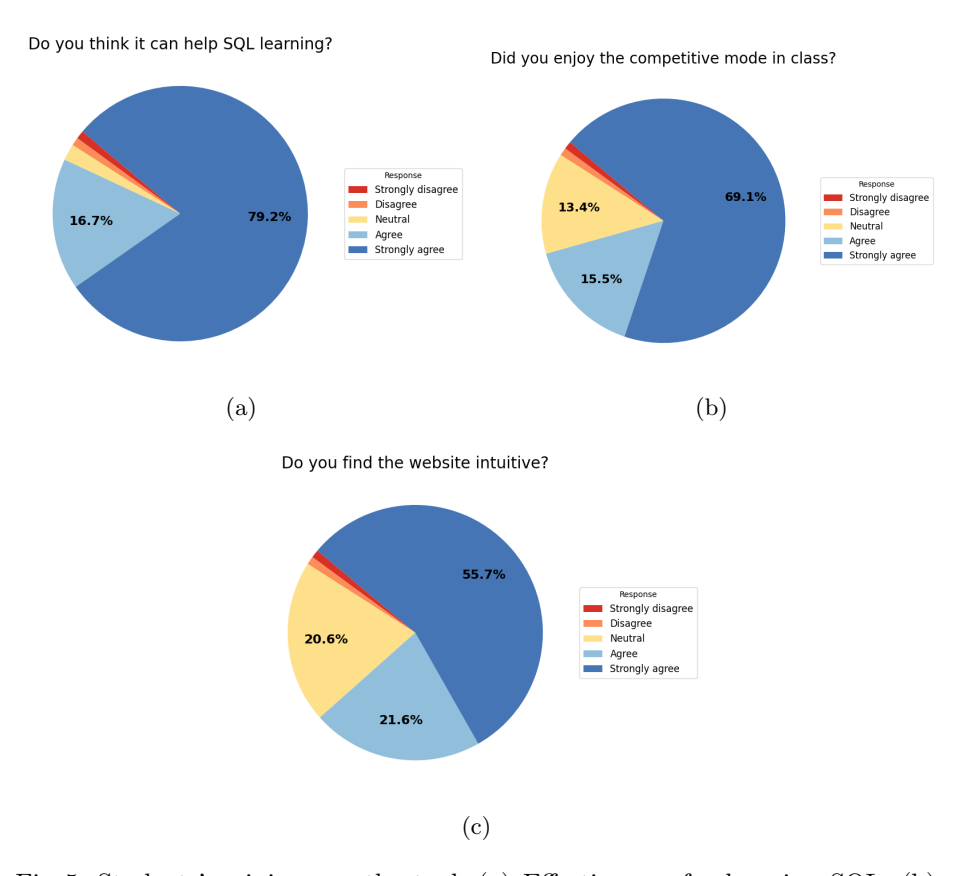


Fig. 5: Students' opinions on the tool: (a) Effectiveness for learning SQL; (b) Appeal of the competitive mode; (c) Intuitiveness of the interface.

level of disagreement compared to the previous question. This may be due to the pressure associated with competition, such as having to display answers publicly and compare performance with peers.

The aspect with the lowest rating among students was usability. Figure 5c shows responses to a question regarding this topic, where a smaller percentage of students considered the application to be very or fairly intuitive. We therefore identify usability as a key area for improvement in future iterations.

In addition to the students, a survey was conducted among 14 instructors teaching database-related subjects. Overall, as shown in Figure 6a, instructors viewed the tool positively as a resource for helping students understand the WHERE clause syntax. Notably, none of the respondents disagreed with this statement. Furthermore, instructors also responded favorably when asked whether students would use the tool independently to practice at home (Figure 6b).

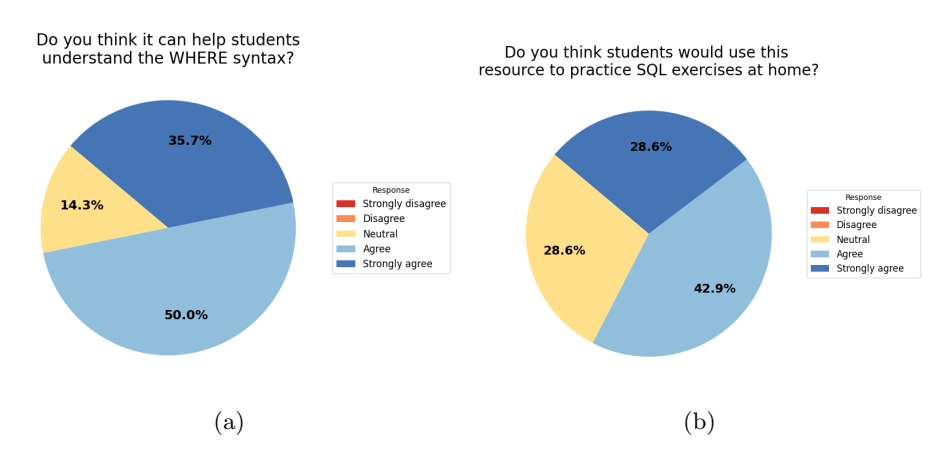


Fig. 6: Instructors' opinions on the tool: (a) Effectiveness in understanding the 'WHERE' syntax; (b) Likelihood that students would use the tool for self-directed practice.

As it can be observed, the results show that both students and instructors perceive the tool as an effective resource for learning SQL. While students responded particularly positively regarding its educational value and the gamified features, there is room for improvement in terms of usability and accessibility.

# 4 Conclusions

SQL is a fundamental component of database education, yet it often presents significant challenges for students due to its abstract and syntactic complexity. Recent pedagogical approaches have increasingly explored the use of gamification

to enhance student motivation, engagement, and learning outcomes. By incorporating game-like elements into instructional design, educators aim to create more dynamic and participatory learning environments that address the motivational and cognitive barriers commonly associated with technical subjects like SQL.

In this context, we have presented WhoSQLWho, a web-based application that integrates gamified mechanics inspired by the classic game Guess Who? to support SQL learning. The tool invites students to write SQL queries in order to uncover a hidden character, thereby reinforcing core SQL concepts through iterative practice and immediate feedback. The application includes features tailored for both classroom use (via real-time competitive sessions) and individual study through asynchronous practice modes. Additionally, a teacher dashboard provides analytics for monitoring student progress and identifying common errors

The evaluation of the tool, based on responses from both students and instructors, indicates that *WhoSQLWho* is perceived as an effective and engaging resource for practicing SQL. Students reported high levels of motivation and perceived learning benefits, particularly in the classroom-based game mode. Instructors highlighted the usefulness of the tool for reinforcing syntactic understanding and facilitating targeted instruction based on class performance data. However, usability was identified as an area for improvement, suggesting the need for further refinement of the user interface and interaction design.

Future work will focus on addressing the usability issues raised during the evaluation, as well as expanding the pedagogical scope of the tool. Planned improvements include the incorporation of additional SQL topics such as JOIN, GROUP BY, and nested queries, as well as the development of adaptive difficulty mechanisms to tailor exercises to individual learner profiles. Furthermore, we aim to explore the integration of the tool within existing learning management systems (LMS) to facilitate broader adoption and streamline usage in formal educational settings.

#### Acknowledgements.

This work is partially supported by Innovation and Educative Improvement project PIME-1951 from Universitat Politècnica de València, MINECO/FEDER RTI2018-095390-B-C31 project of the Spanish government, project TED2021-131295B-C32 from the State Research Agency, DIGITAL2022 CLOUDAI02/S8760000 from the European Commission, project PID2021-123673OB-C31 COSASS and project OPRES PID2021-124975OB-I00 partially funded by the Spanish Ministry of Science and Innovation and FEDER funds.

#### References

Laurie Butgereit. Four nosqls in four fun fortnights: Exploring nosqls in a corporate
it environment. In Proceedings of the Annual Conference of the South African
Institute of Computer Scientists and Information Technologists, pages 1–6, 2016.

- Francisco González-Alonso. La gamificación como estrategia de aprendizaje en educación secundaria: un estudio de caso. Revista de Educación a Distancia (RED), 54:1–25, 2017.
- Jalal Kawash, Levi Meston, H Chad Lane, Susan Zvacek, and James Uhomoibhi. Challenges with teaching and learning theoretical query languages. In CSEDU (2), pages 382–389, 2020.
- 4. Pauli PY Lai. Engaging students in sql learning by challenging peer during the pandemic. In 2020 IEEE International Conference on Teaching, Assessment, and Learning for Engineering (TALE), pages 205–212. IEEE, 2020.
- Miguel Ehécatl Morales-Trujillo and Gabriel Alberto García-Mireles. Gamification and sql: an empirical study on student performance in a database course. ACM Transactions on Computing Education (TOCE), 21(1):1–29, 2020.
- Victor Obionwu, David Broneske, Anja Hawlitschek, Veit Köppen, and Gunter Saake. Sqlvalidator—an online student playground to learn sql. *Datenbank-Spektrum*, 21:73–81, 2021.
- Sunitha Prabhu and Sapna Jaidka. Sql and pl-sql: Analysing teaching methods. In CITRENZ Conference, 2019.
- 8. Jorge Rodríguez, Natalia Ginez, Rodolfo Martinez, Martin Salazar, and Laura Cecchi. Enfoque didáctico para la ensenanza de base de datos en la escuela secundaria. In XIV Congreso Nacional de Tecnología en Educación y Educación en Tecnología (TE&ET 2019), (Universidad Nacional de San Luis, 1 y 2 de julio de 2019)., 2019.
- 9. Victor Sánchez-Anguix, Juan M Alberola, and Vicente Julián. Towards adaptive gamification in small online communities. In 16th International Conference on Soft Computing Models in Industrial and Environmental Applications (SOCO 2021), pages 48–57. Springer, 2022.
- 10. Mario Soflano, Thomas M Connolly, and Thomas Hainey. An application of adaptive games-based learning based on learning style to teach sql. *Computers & Education*, 86:192–211, 2015.
- 11. Kevin Werbach and Dan Hunter. For the win, revised and updated edition: The power of gamification and game thinking in business, education, government, and social impact. University of Pennsylvania Press, 2020.
- 12. Gabe Zichermann and Christopher Cunningham. Gamification by design: Implementing game mechanics in web and mobile apps. " O'Reilly Media, Inc.", 2011.

# Mixed Reality training in University courses

Alberto Martínez-Gutiérrez<sup>1\*6</sup>, Pablo Alonso-Diez <sup>26</sup>, Rubén Ferrero-Guillén<sup>16</sup>, Iván Sánchez-Calleja<sup>16</sup>, Jesús Pérez-González<sup>16</sup>, Madalena Araújo<sup>36</sup> and Javier Díez-González<sup>16</sup>

Department of Mechanical, Computer and Aerospace Engineering, Universidad de León, 24071 León, Spain.<sup>2</sup> Department of General Didactics, Subject-Specific Didactics, and Theory of Education, Universidad de León, 24071 León, Spain.<sup>3</sup> ALGORITMI, Universidade do Minho, Escola de Engenharia, Campus Azurem, Guimaraes, 4800-058, Braga, Portugal \*Corresponding author: Alberto Martínez-Gutiérrez (amartg@unileon.es)

**Abstract.** Education plays a fundamental role in the development of individuals and societies by transmitting knowledge, skills, and values. With the rise of digital technologies, new opportunities have emerged to enhance how people learn and interact with content. However, many digital platforms still face challenges when it comes to creating meaningful, immersive learning experiences. In this context, mixed reality (MR) offers a promising alternative by combining physical and virtual elements in real time. In this work, a practical training activity supported by MR headsets was developed and applied with engineering students. The experience was structured in phases to evaluate performance indicators under controlled conditions. Additionally, students' perceptions were collected through surveys to assess motivation, usability, and potential limitations. The results show improvements in task execution with repeated exposure and high acceptance of the MR methodology. These findings support the idea that MR can be a useful tool for improving engagement and learning in higher education environments. Keywords: Digital Training; Immersive Learning; Digital Twin; Mixed Reality; Education 5.0.

#### 1 Introduction

The transmission of knowledge across generations has always been central to human development and societal advancement. From oral traditions to institutionalized education, humanity has relied on pedagogical structures to disseminate values, skills, and competencies essential for survival and progress [1].

However, in recent years, the educational paradigm has undergone a profound transformation catalyzed by digital technologies. This shift has not only facilitated greater access to information but has also reshaped how knowledge is acquired and applied [2].

Within this broader context of digital transition, the concept of immersive learning environments has gained traction, propelled by innovations such as virtual reality (VR), augmented reality (AR), and more recently, mixed reality (MR). These technologies enable the creation of virtual spaces that blend physical and digital elements to enrich the learning process [3]. Compared to traditional 2D simulators and fully immersive VR systems, MR offers a more balanced approach by allowing

users to remain aware of their physical environment while interacting with virtual elements in real time.

According to Martínez-Gutiérrez et al., the use of digital platforms and educational metaverses introduces a new dimension of interaction where both human agents and virtual elements coexist and co-construct knowledge in real time. This model fosters not only the transmission of factual information but also the cultivation of critical thinking, creativity, and collaboration—competencies aligned with the principles of Education 5.0 and the ambitions of Industry 5.0 [1].

While VR has already demonstrated significant potential in educational settings—particularly in enhancing engagement and conceptual understanding [4], [5]—it is not without limitations. Fully virtual environments may isolate learners from real-world referents, leading to challenges in long-term retention and applicability [6].

Mixed reality, in contrast, aims to address these concerns by merging the tangible and intangible: it retains the immersive affordances of VR while anchoring experiences within physical contexts, thereby enhancing cognitive association and user agency [7].

Evidence suggests that MR fosters active learning, multisensory engagement, and higher-order thinking. For instance, Huang et al.'s meta-analysis reports a moderate effect size (0.56) in learning effectiveness when MR is integrated into instructional settings, with significant improvement in both motivation and knowledge retention [3]. These results corroborate earlier findings that underscore MR's value in supporting constructivist approaches and experiential learning [8].

Similarly, empirical data highlight that VR and MR environments substantially increase learner motivation and engagement. According to Díaz-García et al., 85% of students reported heightened interest in subject matter through VR use, while 92% described their experience as more immersive and participatory than traditional methods [9]. Nevertheless, current scholarship has primarily focused on isolated use cases or discipline-specific implementations, with few studies exploring MR's integration across diverse educational contexts or assessing its impact through longitudinal methodologies.

As highlighted by Martínez-Gutiérrez et al., the current state of MR in education calls for scalable, inclusive platforms that not only incorporate technological innovations but also respect pedagogical integrity and human-centered design principles [2]. Additionally, the integration of MR within Industry 5.0 frameworks emphasizes the need for systems that foster hybrid intelligence—where human creativity is amplified through machine precision [1].

In this light, the present study seeks to examine the educational applications of mixed reality from a cross-disciplinary and methodological standpoint. By synthesizing insights from existing literature and experimental studies, this paper aims to contribute to the ongoing dialogue on how MR can be leveraged to enhance learning outcomes, overcome pedagogical limitations, and meet the evolving demands of both learners and institutions.

Though the findings to date are promising, substantial work remains to fully realize the transformative potential of MR in education—particularly in terms of accessibility, scalability, and instructional design. This study emerges as a timely intervention that seeks to address these gaps and offer empirical guidance for the future integration of mixed reality in educational settings.

Therefore, the main educational and technological contributions of this work are:

Design and implementation of a mixed reality-based educational platform to support practical training in engineering contexts.

- Experimental evaluation of performance metrics (task time and failures) across sequential training phases to assess learning progression.
- Analysis of student perceptions regarding motivation, usability, and physical interaction using MR headsets through structured survey data.

## 2 Case study

This educational innovation has been implemented within the course Theory of Machines and Mechanisms, part of the third-year curriculum of the Bachelor's Degree in Mechanical Engineering at the University of León (Spain). The course focuses on the analysis and modeling of machine kinematics (i.e., mobility), with the aim of enabling students to understand mechanical systems' responses to known inputs.

Traditionally, after attending lecture-based theoretical sessions, students participate in practical classes involving computer-based simulations. However, these activities often suffer from perceptual limitations due to the constraints of two-dimensional interfaces such as computer screens.

To address this limitation and foster experiential learning, a new practical activity has been introduced in which students interact with a real mobile robot to explore and internalize its kinematic behavior. The underlying pedagogical hypothesis is that enhanced control over the physical system promotes deeper understanding of its mobility characteristics.

Nevertheless, due to the large number of enrolled students, the time required for individual hands-on training, and the high cost of the robotic platform (which limits the availability to a single unit), it becomes necessary to incorporate complementary instructional strategies. In this context, MR technologies offer an effective and scalable solution for skill development and concept reinforcement.

The objective of this educational intervention is to evaluate the effectiveness of mixed reality in the transfer of procedural knowledge and skills. To this end, students are presented with a challenge-based learning activity in which they must navigate the mobile robot through a predefined path with physical obstacles. The learning outcomes are assessed based on two key performance indicators: task completion time (i.e., agility) and number of errors committed (i.e., precision).

#### 3 Technological implementation

The successful execution of this case study requires the development of a MR platform specifically designed for educational purposes [10]. This platform must integrate a wide array of technological components—including Digital Twins (DTs), Graphical User Interfaces (GUIs), real-time rendering engines, mixed reality headsets, and physical robotic systems—as illustrated in Figure 1. The convergence of these diverse technologies presents a significant technical challenge due to the heterogeneity of the underlying architectures and interaction protocols [11].

At the core of the system is a DT [12], which accurately replicates the behavior of the mobile robot in response to both environmental conditions and user-generated inputs. The DT is implemented within the Robot Operating System (ROS) framework, where the robot's kinematic behavior is mathematically modeled and simulated with high fidelity.

#### 4 Alberto Martínez-Gutiérrez et al.

The output data generated by the DT is processed by a real-time graphics engine. This engine is responsible not only for rendering a high-fidelity 3D model of the robot but also for simulating physical interactions consistent with the model dynamics. Furthermore, the engine continuously updates the robot's virtual position based on the user's control actions, thereby enhancing realism and immersion and attaining an effective human-machine interaction.

# **Educational Mixed Reality Platform**

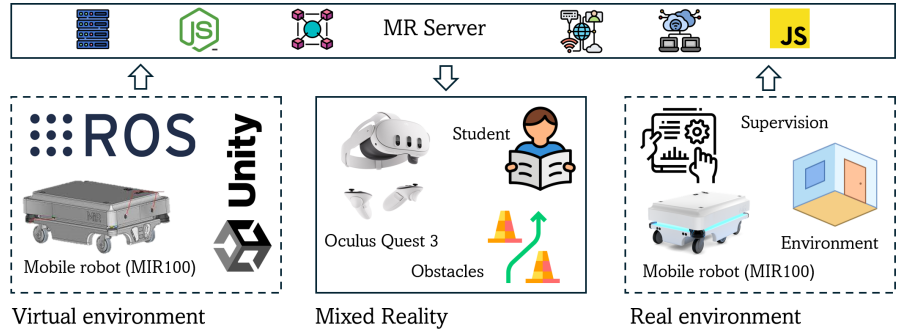


Fig. 1. Educational Mixed Reality platform integrating virtual, mixed, and real environments for robotics training

Mixed reality headsets (MR devices) play a crucial role in bridging the virtual and physical worlds. These devices convert digital outputs into multisensory stimuli—visual, auditory, and haptic—which are perceived by the learner in real time. This immersive experience allows students to interact with a virtual robot while simultaneously perceiving and navigating the physical environment surrounding them.

An additional feature of the MR-based training platform is the implementation of visualization interfaces for real-time performance monitoring. These interfaces provide key Performance Indicators (KPIs) that track student progress throughout the activity, supporting adaptive learning and enabling personalized instructional feedback. Instructors can also use these interfaces to view the virtual environment and deliver guidance or clarification during the exercise.

It is also critical to consider the integration with the physical mobile robot. This connection enables the assessment of skills transfer from the virtual simulation to any real-world application. Through the same graphical interface, all user interactions and performance data are logged and visualized, facilitating a comprehensive evaluation of the educational methodology.

## 4 Experiments

To rigorously assess the transfer of procedural skills and conceptual understanding related to machine kinematics through the use of MR technologies, a structured experimental protocol was implemented. The study was conducted with a sample

population of 63 undergraduate students enrolled in the Theory of Machines and Mechanisms course of the Mechanical Engineering degree program at the University of León.

The experimental procedure, summarized in Figure 2, was structured into three sequential phases designed to collect KPIs under controlled and replicable conditions.

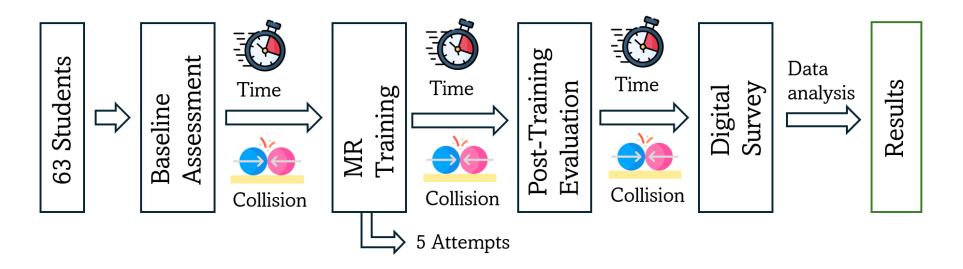


**Fig. 2.** Experimental protocol for assessing MR-based training through baseline, training, and post-training evaluations.

- A) Baseline Assessment: Each participant performed a driving task with a physical mobile robot for the first time, without prior hands-on experience. This initial trial was designed to evaluate baseline motor and cognitive skills, as well as to account for interindividual variability in the sample [13]. Performance metrics—including task completion time and number of execution errors—were recorded to establish each student's initial proficiency level.
- B) Training Phase with MR Simulation: Subsequently, all participants engaged in a structured MR-based training session replicating the same robot control conditions. The virtual environment maintained the kinematic and dynamic fidelity of the real system, allowing immersive interaction via mixed reality headsets. Each student completed five consecutive simulation attempts, with KPIs (execution time and errors) recorded for every trial to evaluate learning progression and adaptation within the virtual environment.
- C) Post-Training Evaluation: Upon completing the MR training, each participant performed a final trial with the physical robot. The objective of this stage was to measure the extent of skill transfer from the virtual to the real-world context, comparing final performance metrics against those obtained during the initial real-world attempt.

Following the practical sessions, participants were asked to complete an anonymous digital survey designed to capture qualitative insights regarding their perceived learning outcomes, usability of the MR system, and overall training experience. The survey included both closed-ended and open-ended items aimed at evaluating cognitive engagement, perceived realism, and motivational aspects of the MR-based learning process.

To better understand the students' perception, Figure 3 presents a frame illustrating the superimposition of virtual objects onto the real environment during the experimental sessions. This visualization highlights one of the key advantages of mixed reality systems: the seamless integration of digital content within the

#### 6 Alberto Martínez-Gutiérrez et al.

learner's physical context. Such an approach enhances spatial awareness and interaction fidelity, allowing students to engage more intuitively and effectively with the learning materials. Moreover, by maintaining a direct view of the real environment, mixed reality minimizes disorientation and physical discomfort often associated with fully immersive virtual reality systems, thereby promoting longer engagement and improved knowledge retention.

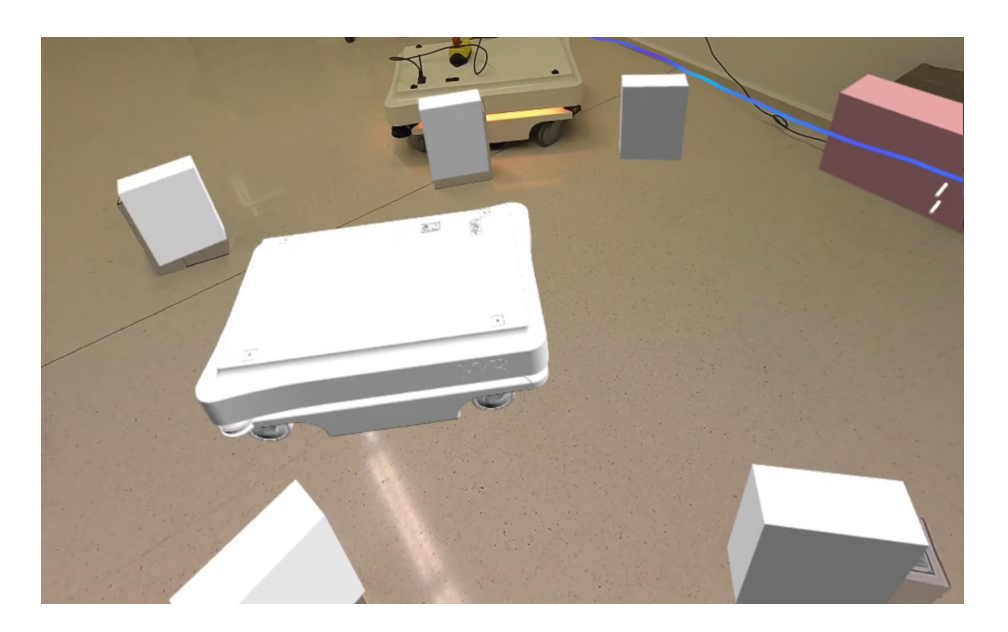


**Fig. 3.** Visual depiction of the mixed reality environment as perceived by students, showing the seamless integration of virtual objects within the physical space during the experimental activities.

#### 5 Results

The KPIs collected in this study are categorized into two main domains: performance metrics (i.e., task completion time and number of errors) and learning experience indicators, the latter derived from the post-activity survey designed to assess students' subjective perceptions.

**Performance Metrics and Relative Improvement** To ensure a fair evaluation of performance gains, it is essential to account for participants' initial skill levels. For this purpose, we introduce the metric Relative Improvement (RI), defined as the percentage change in performance between the first and final trials with the physical robot. This approach allows normalization across individuals with different prior abilities.

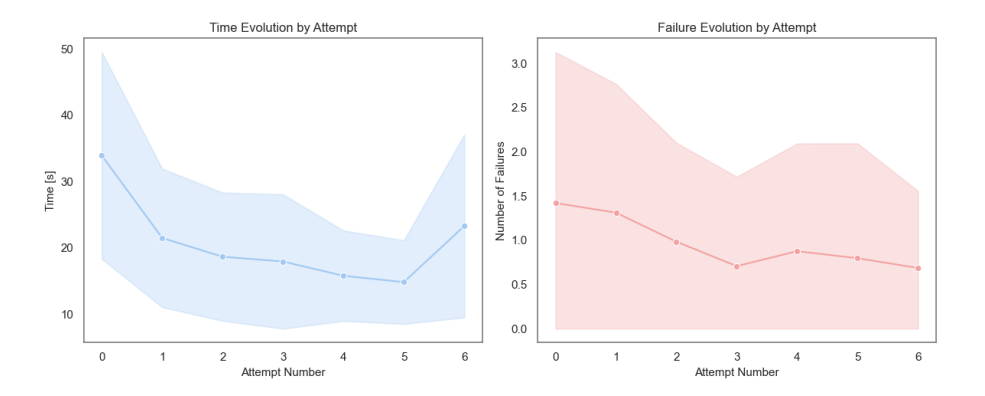


**Fig. 4.** Mean time (left) and failures (right) per training attempt with standard deviation bands. Both metrics decrease over attempts, indicating improved performance and accuracy.

Figure 4 presents the evolution of performance metrics across the different stages of the training protocol, including the baseline assessment (T0), five mixed reality (MR) training attempts (T1–T5), and the final post-training evaluation (T6) with the physical system.

A clear downward trend was observed in task completion time throughout the MR training phase. The average time decreased from 33.92 seconds at baseline (T0) to 14.83 seconds by the fifth MR attempt (T5), representing a 56.3% reduction. This suggests progressive motor and cognitive adaptation to the task. The time increased slightly to 23.28 seconds in the post-training evaluation (T6), indicating a partial transfer of acquired skills from the virtual to the real environment. While not matching the final MR performance, this value was still significantly lower than the baseline.

The number of execution errors, measured as failures (e.g., collisions), followed a similar pattern. The mean number of failures decreased from 1.42 at T0 to 0.80 at T5, reaching 0.69 in the final physical trial (T6). This reduction indicates improved control and task understanding. The slight increase in errors from T3 to T4 may reflect a greater tendency to take more risks to reduce times due to a sense of control after overcoming the first attempts with MR.

Overall, the performance trends suggest effective learning during MR training and a measurable transfer of skills to the real-world context, albeit with a moderate decrease in efficiency and precision, which is consistent with the change in interaction medium.

**Student Experience and Perception of MR Training** To complement the quantitative analysis, a digital survey was administered to gather qualitative insights into the learners' experience with the MR platform. The survey included the following Likert-scale questions:

- Have you been motivated by the use of mixed reality glasses?
- Would you consider using this methodology in future practical sessions across other courses?
- Did you consciously slow down your body movements while wearing the mixed reality headset due to fear of colliding with real-world obstacles?

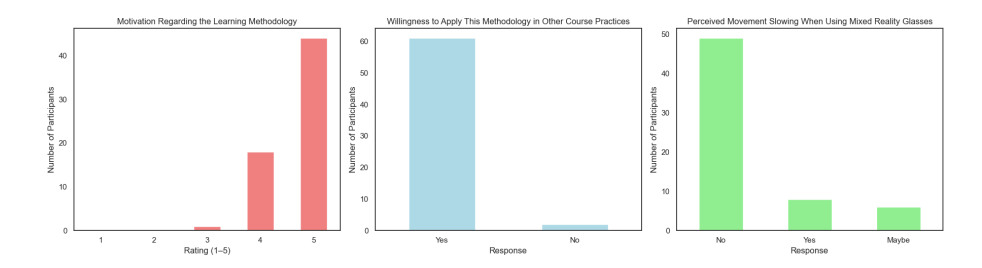


**Fig. 5.** Participant ratings of motivation, willingness to reuse the methodology, and self-reported movement slowing with mixed reality glasses. Data reflect unique respondents' answers.

The analysis of participant feedback reveals distinct trends in the perception and impact of the applied learning methodology utilizing MR headsets, as illustrated in Figure 5.

Firstly, motivation levels toward the employed methodology were notably high. Specifically, 69.84% of respondents assigned the highest possible rating of 5 out of 5, while an additional 28.57% rated it 4 out of 5. This overwhelmingly positive reception underscores the methodology's effectiveness in capturing learners' attention and fostering intrinsic motivation—an essential driver for successful educational interventions and sustained engagement [14].

Secondly, regarding the willingness to reutilize this pedagogical approach across different academic courses, the response was similarly affirmative. A remarkable 96.83% of participants expressed openness to adopting this technology-enhanced instructional strategy in other educational contexts. This finding highlights the perceived value, scalability, and transferability of the methodology, emphasizing its potential for broad implementation across diverse curricula. Therefore, this research reinforces other studies highlighting the users' willingness for learning in MR environments [15].

Lastly, participants were queried about whether they experienced any deceleration in their physical movements due to apprehension about potential collisions while wearing the MR headsets. Responses were more heterogeneous in this regard: the majority (77.78%) reported no perceptible slowing of movement, whereas 22.22% acknowledged some degree of deceleration ("Yes" 12.70%) or uncertainty ("Maybe" 9.52%). These results suggest that, while the MR setup is generally comfortable and does not significantly hinder physical interaction for most users, a subset of participants may experience cautious behavior. This phenomenon likely stems from the MR system's preservation of real-world environmental cues, as opposed to Virtual Reality (VR) platforms that fully occlude physical surroundings, thus limiting spatial awareness. In fact, the results of this study objectively show an improvement in physical mobility with regard to one of our previous studies conducted in a fully virtual environment [16].

In sum, these findings contribute valuable insights into the integration of mixed reality technologies in higher education settings, demonstrating their capacity to enhance learner motivation, engagement, and adaptability while maintaining physical comfort and spatial orientation. The results advocate for further exploration of MR-based pedagogies within the framework of immersive and active learning paradigms.

#### 6 Conclusions

This study contributes to the growing body of evidence supporting the integration of MR technologies into educational practice. By examining both performance metrics and user feedback across controlled experimental phases, the results demonstrate that MR environments can enhance learning effectiveness while maintaining physical comfort and user engagement. Notably, improvements in task performance were observed with repeated exposure, suggesting a learning curve that stabilizes over time and supports skill acquisition in an immersive setting.

Participants feedback further underscores the pedagogical viability of MR. High levels of motivation and willingness to reuse the methodology across other academic contexts reflect its perceived value and adaptability. While some users expressed caution regarding physical movement, the majority reported no hindrance, affirming the ergonomic and perceptual advantages of MR systems over fully immersive VR platforms. These insights are consistent with previous findings on the role of MR in promoting multisensory learning and fostering student agency.

Taken together, the results highlight MR's potential as a scalable and effective tool within higher education, particularly in the context of Education 5.0 and Industry 5.0 goals. However, the study also points to the need for continued research into long-term outcomes, cross-disciplinary applications, and inclusive design principles. Future work should focus on refining instructional strategies, ensuring accessibility, and expanding the evidence base through larger, more diverse samples and longitudinal designs.

# 7 Acknowledgements

This work has been funded by the project of the Spanish Ministry of Science and Innovation grant number PID2023-153047OBI00, by the Consejería de Educación de la Junta de Castilla y León and by the Universidad de León and the teaching innovation group MECACOM of the Universidad de León. The author Iván Sánchez-Calleja acknowledges funding for doctoral studies of the University of León. This work has been supported by FCT – Fundação para a Ciência e Tecnologia within the R&D Unit Project Scope UID/00319/Centro ALGORITMI (ALGORITMI/UM)

## References

- A. Martínez-Gutiérrez, J. Díez-González, H. Perez, and M. Araújo, "Towards industry 5.0 through metaverse," *Robotics and Computer-Integrated Manufacturing*, vol. 89, p. 102764, 2024.
- A. Martínez-Gutiérrez, J. Díez-González, R. Ferrero-Guillén, I. Sánchez-Calleja, P. Alonso-Diez, M. Araújo, and H. Perez, "Educational metaverse," in *International Conference on EUropean Transnational Education*, pp. 279–287, Springer, 2024.
- 3. T.-C. Huang, C.-H. Chen, and C.-Y. Tseng, "Exploring learning effectiveness of integrating mixed reality in educational settings: A systematic review and meta-analysis," *Computers & Education*, p. 105327, 2025.

- X. P. Lin, B. B. Li, Z. N. Yao, Z. Yang, and M. Zhang, "The impact of virtual reality on student engagement in the classroom—a critical review of the literature," *Frontiers in Psychology*, vol. 15, p. 1360574, 2024.
- D. Zapatero Guillén, "La realidad virtual como recurso y herramienta útil para la docencia y la investigación," TE & ET, 2011.
- E. Campos, I. Hidrogo, and G. Zavala, "Impact of virtual reality use on the teaching and learning of vectors," in *Frontiers in Education*, vol. 7, p. 965640, Frontiers Media SA, 2022.
- P. G. Pérez and J. M. M. Lema, "La realidad virtual para la enseñanza y aprendizaje de la perspectiva en el dibujo," *Edutec, Revista Electrónica de Tecnología Educativa*, no. 83, pp. 188–207, 2023.
- J. Díez-González, P. Verde, R. Ferrero-Guillén, R. Álvarez, N. Juan-González, and A. Martínez-Gutiérrez, "Evaluation of the skills' transfer through digital teaching methodologies," in *Computational Intelligence in Security for Information Systems Conference*, pp. 340–349, Springer, 2023.
- V. D. García, O. C. Márquez, and F. García-Chamizo, "Impacto del uso de gafas de realidad virtual en el aprendizaje de los alumnos: estudio empírico," European Public & Social Innovation Review, vol. 10, pp. 1–20, 2025.
- G. Kostov and J. Wolfartsberger, "Designing a framework for collaborative mixed reality training," *Procedia Computer Science*, vol. 200, pp. 896–903, 2022.
- A. Martínez-Gutiérrez, J. Díez-González, P. Verde, R. Ferrero-Guillén, and H. Perez, "Hyperconnectivity proposal for smart manufacturing," *IEEE Access*, vol. 11, pp. 70947–70959, 2023.
- A. Martínez-Gutiérrez, J. Díez-González, R. Ferrero-Guillén, P. Verde, R. Álvarez, and H. Perez, "Digital twin for automatic transportation in industry 4.0," Sensors, vol. 21, no. 10, p. 3344, 2021.
- 13. A. Martínez-Gutiérrez, J. Díez-González, P. Verde, and H. Perez, "Convergence of virtual reality and digital twin technologies to enhance digital operators' training in industry 4.0," *International Journal of Human-Computer Studies*, vol. 180, p. 103136, 2023.
- D. A. Cook and A. R. Artino Jr, "Motivation to learn: an overview of contemporary theories," *Medical education*, vol. 50, no. 10, pp. 997–1014, 2016.
- L.-K. Lee, X. Wei, K. T. Chui, S. K. Cheung, F. L. Wang, Y.-C. Fung, A. Lu, Y. K. Hui, T. Hao, L. H. U, et al., "A systematic review of the design of serious games for innovative learning: augmented reality, virtual reality, or mixed reality?," *Electronics*, vol. 13, no. 5, p. 890, 2024.
- A. Martínez-Gutiérrez, J. Díez-González, R. F. Guillén, I. Sánchez-Calleja, G. Arampatzis, and M. Araújo, "Impact of the metaverse on humans: Physical exertion and perception shifts.," 2024.